# Factors Influencing the Processing of VDE-induced DNA Double-Strand Breaks during Meiosis

**Tzu-Ling Tseng**

**A thesis submitted for the degree of:**

**Doctor of Philosophy**

**March 2015**

**University of Sheffield**

**Department of Molecular Biology and Biotechnology**

# *Summary*

During meiosis, repair of programmed Spo11-induced DNA double-strand breaks (DSBs) is essential to achieve the formation of crossovers, which contribute to the correct disjunction of homologous chromosomes. Much attention has been paid to the mechanisms and significance of 5' to 3' resection of DNA at the DSB end, which is an intermediate step during DSB repair. Multiple proteins participate in this process, leading to the formation of 3' single-strand DNA (ssDNA) that invades a donor homologous template. We have analysed resection during meiosis at a DSB created by the site-specific endonuclease VDE, which does not bind covalently to the DSB ends, thus allowing us to model the role of nucleases after Spo11 would be removed. Our data have shown that *mre11-H125N* nuclease dead mutants became delayed in VDE-DSB resection and repair, and only a small fraction of repair used long resection tracts. Moreover, *exo1*Δ mutants accumulated even more unrepaired VDE-DSBs early in meiosis, until 6 hour when VDE-DSB repair was rapid, supporting the view that different nucleases are dominant at different times. Furthermore, we also found that when Spo11 lost the function to make Spo11-DSBs within *exo1*Δ mutants, the delay of VDE-DSB was rescued, but long resection repair remained low. This could be because Mre11 is sequestered at the multiple Spo11-DSBs during early meiosis, but later becomes free for VDE-DSB repair, or perhaps in the absence of Spo11-DSBs the regulation of nuclease activities is altered. We also provide evidence that the DNA damage checkpoint kinase Tel1 has a role in processing meiotic resection that is related to the Mre11 nuclease function, and Tel1 might also have an impact on the repair of ssDNA.

# *Acknowledgements*

I am using this opportunity to express my gratitude to all the people that I have met in Sheffield, including my colleagues Bin Hu, who gave me good advice about my thesis; Emad, who supported me a lot during the preparation for my viva; a lovely girl, Emily, who always gave me a lot of support and has sent me a box of happy hippos to cheer me up during my hard times; a sweet girl, Laura, who helped me a lot in correcting my English grammar to allow the thesis to become more complete; an adorable girl, Selina, who gave me lots of encouragement and support; Inam, who always gave me sweeties to make me happy; and my best partner here, Ta-Chung, who always accompanied me and reminded me of my health. Many thanks to my previous lab members, Adam, Janet, Slava, Thibaut and Yinka; and friends met in the department, Bernado, David, Eileen, Iliyana, Jamie, Jude, Lina, Nicolas, Shler, Tacita, Taib and Simon. Especially, I would like to thank my supervisor Alastair as a boss and a good tutor to make me become a better scientist.

Further, much appreciation to my close friends here, Audrey Tan, Erica Lin, Fang Yang, Hsin-Hui Wu, Manlu Wang, Tzu-Pei Yeh, Vivian Yang, Wei-Ning Yang, Wen Qiu and Xueyan Zhao. They are just like my sisters! I cannot image being without you girls for my PhD life!

In the end, I really want to thank my lovely family, especially my parents, who have given me lots of unconditional support, whether financial or mental. Without them, I could not have finished this thesis. Thanks my dear Mom and Dad! I would like to devote this thesis to both of you.

# *Abbreviations*

| | |
|---|---|
| ABC-ATPase | ATP-binding cassette type ATPase |
| AE | axial element |
| ATM | ataxia telangiectasia mutated |
| ATR | ataxia telangiectasia and Rad3-related protein |
| CCD | the conserved C-terminal domain |
| CE | central element |
| ChIP | chromatin immunoprecipitation |
| CTAB | hexadecyltrimethylammonium brimoide |
| dAG | diploid Alastair Goldman |
| DAPI | 4', 6'-diamidino-2-phenylindoline |
| dHJ | double Holliday junction |
| $dH_2O$ | deionised water |
| $d_2H_2O$ | distilled and deionised water |
| D-loop | displacement loop |
| DNA | deoxyribonucleic acid |
| dNTP | deoxynucleotide triphosphate |
| DSB | DNA double-strand break |
| DSBR | double-strand-break repair |
| dsDNA | double-stranded DNA |
| EDTA | ethylene diamide tertacetate |
| FHA | forkhead-associated |
| G418 | geneticin |
| GC | gene conversion |

| | |
|---|---|
| hAG | haploid Alastair Goldman |
| HJ | Holliday junction |
| HLH | helix-loop-helix |
| HR | homologous recombination |
| Hyg | Hygromycin B |
| IR | ionizing radiation |
| JM | joint molecule |
| LB | Luria-Broth |
| LE | lateral element |
| MMS | methyl methane-sulfonate |
| MR | Mre11, Rad50 complex |
| *mre11-nd* | *mre11-nuclease defective* |
| MRN | Mre11, Rad50, Nbs1 complex |
| MRX | Mre11, Rad50, Xrs2 complex |
| NBD | nucleotide-binding domain |
| NHEJ | nonhomologous recombination or end joining |
| OB-fold | oligonucleotide/oligosaccharide-binding-fold |
| pAG | plasmid Alastair Goldman |
| PCR | polymerase chain reaction |
| qPCR | quantitative polymerase chain reaction |
| RE | restriction endonuclease |
| RMM | Rec114, Mer2/Rec107, Mei4 subcomplex |
| RPA | replication protein A |
| SC | synaptonemal complex |
| SC- | dropout media |

| | |
|---|---|
| SDS | sodium dodecyl sulfate |
| SDSA | synthesis-dependent strand-annealing |
| SEI | single-end invasion intermediate |
| SGD | *Saccharomyces* Genome Database |
| SMC | structural maintenance of chromosomes |
| SPB | Spindle pole body (microtubule organising centre) |
| SSA | single-strand annealing |
| SSBs | the single-stranded DNA binding protein family |
| ssDNA | single-strand(ed?) DNA |
| TF | transverse element |
| UV | ultraviolet light |
| VDE | *VMA1*-derived endonuclease |
| YPAD | Yeast extract, peptone, adenine and D-glucose |
| ZMM | Zip1/2/3/4, Msh4/5 and Mer3 |

# *Contents*

# *Contents of Figures and Tables*

***Chapter 4***



***Chapter 5***



***Appendix***

# *Chapter 1*

# General Introduction

## 1.1 *Saccharomyces cerevisiae*

Yeasts are tiny, single-celled fungi, approximately 5 µm in diameter; moreover, many of the genes in them are conserved in higher eukaryotes and a lot of their molecular mechanisms are remarkably similar to our own (Adams et al., 1997; Alberts et al., 2008). Today, yeasts are widely recognized as an ideal eukaryotic microorganism for genetic and molecular biology research. This can be traced back to substantial contributions from two major groups during the 1930s to 1940s (Adams et al., 1997). Winge and his co-workers initiated the first genetic investigation of yeast in the mid-1930s, and approximately ten years later Lindegren and his colleagues also began extensive studies. They have taken significant responsibility for unveiling the general principles and establishing much of the basic methodology of yeast genetics (Adams et al., 1997). Since yeasts such as *Saccharomyces cerevisiae* possess many features that are extremely suitable and useful for genetic studies, they have been successfully employed for all areas of genetic research, such as mutagenesis, recombination, chromosome segregation, gene action and regulation, as well as aspects distinct to eukaryotic systems, like mitochondrial genetics (Adams et al., 1997). These properties include rapid growth, the small genome size (less than 1% that of mammals), clonability, the ease of replica planting and mutant isolation (Adams et al., 1997; Alberts et al., 2008). Most importantly, using yeasts provides the ability to isolate each haploid product of meiosis (spores) by microdissection of a tetrad ascus, and both haploid and diploid

cells can stably exist (Adams et al., 1997; Alberts et al., 2008). The last two features are amenable to rapid molecular genetic manipulation, because it avoids the complication of having a second copy of the gene in the cell (Adams et al., 1997; Alberts et al., 2008). Furthermore, in 1996 the whole genome sequencing of *S. cerevisiae*, which contains 16 chromosomes with 12 Mb nucleotides and 6,000 genes, was fully completed with the involvement of 92 laboratories (National Human Genome Research Institute/NHGRI, last reviewed: May 16$^{th}$, 2010). This achievement has provided more detailed analysis of cellular functions and genome organization in eukaryotes, and the sequence database can be accessed conveniently through Internet websites, such as *Saccharomyces* Genome Database (SGD) (Adams et al., 1997).

In this study, we used the budding yeast *Saccharomyces cerevisiae*, SK1-background, as a model organism to investigate the resection of double-strand breaks (DSBs) in DNA during meiosis. It is relatively easy in SK1 cells to induce meiotic cell division by starvation and the meiotic cultures of these cells are relatively synchronous (Kane and Roth, 1974). Here, the indications of the physiological state in WILD-TYPE *S. cerevisiae*, briefly described below, are helpful in making strains and setting up good meiosis time courses:

## Growth Properties summarized from (Adams et al., 1997)

*Saccharomyces cerevisiae* is an oval cell that grows by forming a bud, and the doubling time in SK1 is 150 minutes (Kane and Roth, 1974). A cell that gives rise to a bud is called a mother cell, and the bud is referred to as the daughter cell, which first emerges during the G1 phase and continues to grow until it separates from the mother cell after mitosis. This bud formation is essentially related to progressing

through the cell cycle and is prioritized during the yeast growth. Thus, the size of the bud and the frequency of budded cells become approximate indicators for the growth state, and can be simply determined under the microscope. There are approximately one-third unbudded cells, one-third cells with a small bud and one-third cells with a large bud in an exponentially growing culture of yeast cells. However, when cells in a growing culture use up the available nutrients or are under starvation, they stop growing by arresting in the cell cycle, resulting in the formation of unbudded cells, and diploid cells start to sporulate and progress throughout meiosis. Then, this characteristic has been utilized in synchronizing cells for induction of meiosis time course **(Chapter 2.4)**.

## Haploids vs. Diploids summarized from (Adams et al., 1997)

Although haploid and diploid yeast cells have morphological similarity, there are still several differences between them. First, diploids are larger than haploids with the diameter roughly 1.3 times that of haploid cells. Second, the shape of diploids is more elongated or ovoid, whereas haploids are often almost round. Third, they don't share one budding pattern. In diploids, the buds emerge from either end of the elongated mother cells leading to a polar pattern. However, haploids bud in an axial pattern in which each bud emerges adjacent to the site of the previous bud. Lastly, in SK1 background, due to the different composition of the cell wall, haploids appear to be much stickier to each other so that aggregation of haploid cells can be observed under the microscope, whereas there is more separation among diploid cells.

## Mating cells summarized from (Adams et al., 1997)

Yeast cells have three mating types: *MAT*a and *MAT*α; these two are able to

mate with each other to produce a *MAT*a/α cell. Generally speaking, *MAT*a and *MAT*α cells are haploid, and *MAT*a/α cells are diploid which cannot mate with cells of either mating type. We can use this feature to construct strains with desired genotypes by the genetic methods **(Chapter 2.3.1)**.

**Mitochondria** summarized from (Adams et al., 1997)

The yeast mitochondrial genome is essential to encode several proteins involved in oxidative phosphorylation, one ribosomal protein, and the rRNAs and tRNAs required for the mitochondrial translation apparatus, although most mitochondrial proteins are encoded from nuclear genes. Yeast cells with mitochondrial mutations are called petite strains. Such mutants grow more slowly than wild-type cells and form small milky-white colonies. Moreover, since they have lost the ability to carry out oxidative phosphorylation, the source of energy is obtained from fermentation. Thus, petite strains are unable to grow on nonfermentable carbon sources such as lactate, glycerol or ethanol. Also, petite mutants in diploids cannot sporulate. Therefore, to select diploid cells harboring healthy mitochondria before inducing to progress through meiosis, it is important to grow cells on a nonfermentable carbon source first **(Chapter 2.4)**.

## 1.2 Meiosis

Sex is not absolutely necessary, and it is simple and direct that asexual reproduction propagates offspring with the same genotypes as that of parents (Alberts et al., 2008). However, although sexual reproduction is much more elaborate and spends a large quantity of energy and resources, still the vast majority

of organisms have adopted it. It seems to be because this mechanism provides organisms great advantages to survive in an unpredictably variable environment (Alberts et al., 2008). It can efficiently eliminate deleterious genes from a population due to the choice for fitness in mates; the major advantage in sexual reproduction is genes reshuffling between two individuals that gives rise to offspring that genetically differ from one another and from their parents (Alberts et al., 2008; Longhese et al., 2008). Thus, through this wide variety of gene combinations, the chance for survival in a changing environment is increased (Alberts et al., 2008). Since sexual reproduction occurs in diploid organisms, which inherit two full sets of chromosomes from each parent, and in order to maintain the genetic content in the offspring, a specialized type of cell division called meiosis is required **(Figure 1.1)**. In meiosis, diploid cells divide to form haploid gametes that receive one full set of chromosomes, and the haploid gametes from two individuals fuse in pairs to form new diploid zygotes, in which the maternal and paternal versions of each chromosomes are known as homologous chromosomes or homologs (Alberts et al., 2008; Zickler and Kleckner, 1998). However, in many higher eukaryotes haploid gametes, such as eggs and sperms, do not proliferate themselves, unlike diploid cells that propagate through mitosis to develop a multicellular organism (Alberts et al., 2008). They only exist briefly and are highly specialized for sexual fusion. By contrast, both haploids and diploids in some simple eukaryotes like *Saccharomyces cerevisiae* are able to proliferate by mitosis, and haploid cells have a long existence (Alberts et al., 2008).

Different from mitosis, meiosis is developed to precisely halve the number of cellular chromosomes from diploid cells to generate haploid gametes **(Figure 1.1)**. Although much of the same molecular machinery and control systems are shared

*Picture source: Alberts et al., 2008.*

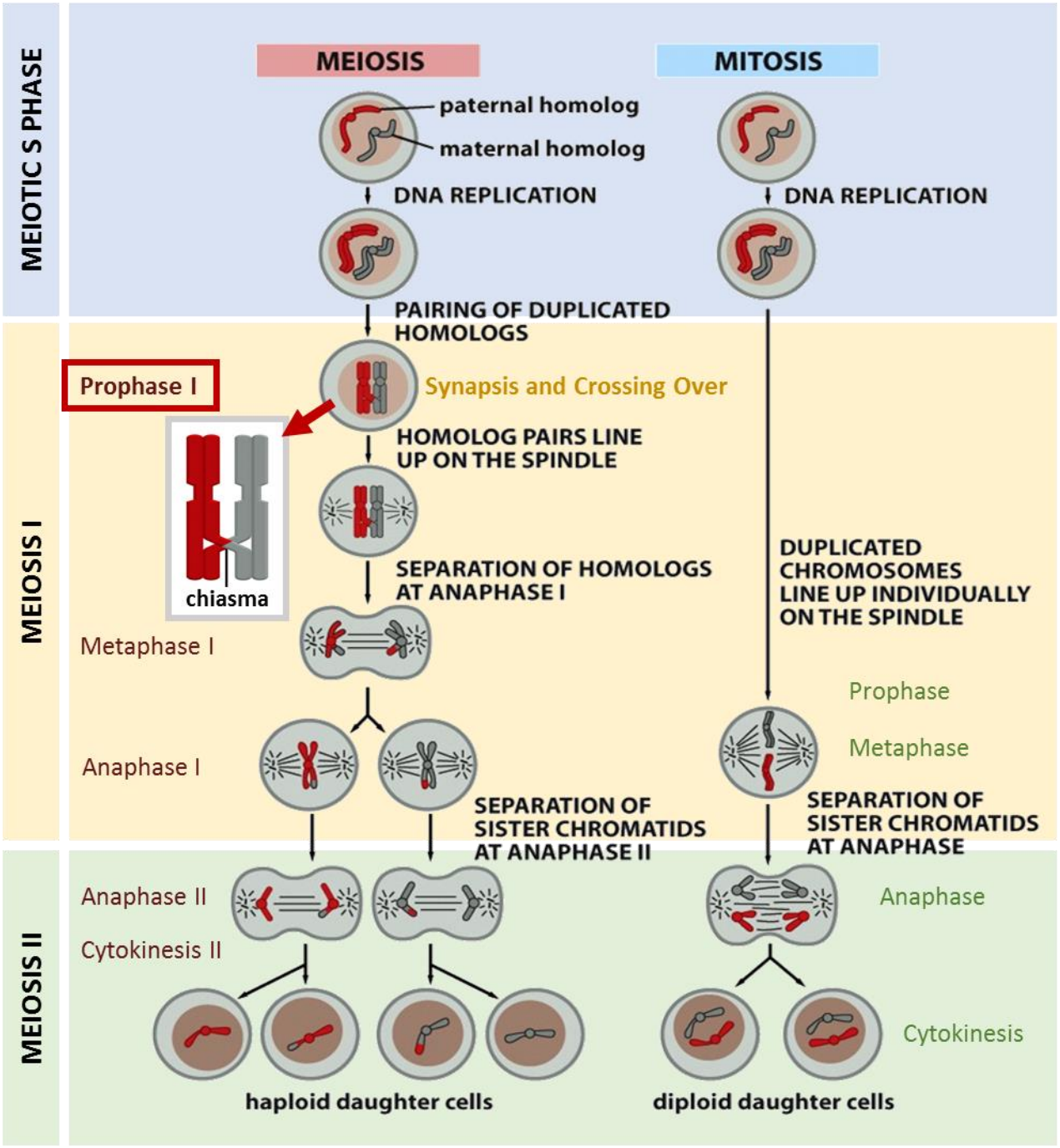


**Figure 1.1 Meiosis versus mitosis.** Meiosis is important in producing haploid gametes. Different from mitosis, which contains only one round of cell division following one DNA replication, meiosis includes one DNA replication and two cell divisions, meiosis I and meiosis II, thus causing the reduction of chromosome content from diploid to haploid. Meiosis I is also called reductional division, which separates homologous chromosomes, whereas meiosis II is named equational division, in which sister chromatids are pulled apart. Synapsis and crossing over occur at Prophase I and is essential to establish the correct alignment and disjunction of homologous chromosomes into two daughter cells.

between meiosis and mitosis, the mechanism used in meiosis is much more complicated than that in operating ordinary mitosis, and many meiotic-specific proteins have been uncovered and studied (Alberts et al., 2008). Moreover, instead of one cell division in mitosis, meiosis involves two consecutive cell divisions, meiosis I (segregation of homologous chromosomes) and meiosis II (separation of sister chromatids), following a single round of DNA synthesis **(Figure 1.1)** (Alberts et al., 2008; Zickler and Kleckner, 1998).

Before cells are going to proceed to mitosis or meiosis, the DNA of each chromosome is replicated in a semi-conservative way during S phase to generate two identical DNA copies called sister chromatids, each pair of which is tightly glued together along their entire length by cohesin complexes consisting of four core subunits **(Figure 1.2 A)** (Alberts et al., 2008; Peters et al., 2008). Both of the mitotic and meiotic cohesin complexes contain a pair of structural maintenance of chromosomes (SMC) subunits, Smc1 and Smc3, which are large ATPases with an unusual domain organization; and two non-SMC subunits, Scc3 (whose structure has not yet been determined) and one of the kleisin family proteins, Scc1 and Rec8 in mitotic and meiotic cohesin complexes, respectively, which interacts with two heads of the SMC subunits to thereby form a closed ring **(Figure 1.2 A)** (Peters et al., 2008; Wood et al., 2010). Once replicated, sister chromatids are tightly glued together during mitosis, and the further condensation and shortening of chromosomes is initiated, conducted through condensin complexes (Alberts et al., 2008; Hirano, 2012; Wood et al., 2010). The architecture of condensin complexes is similar to that of cohesin complexes with a pair of SMC subunits and ancillary non-SMC subunits **(Figure 1.2 B)**. It is currently known that there are (at least) two different types of condensin complexes existing in eukaryotes, known as condesins I and II **(Figure 1.2**

*Picture source: Wood et al., 2010.*

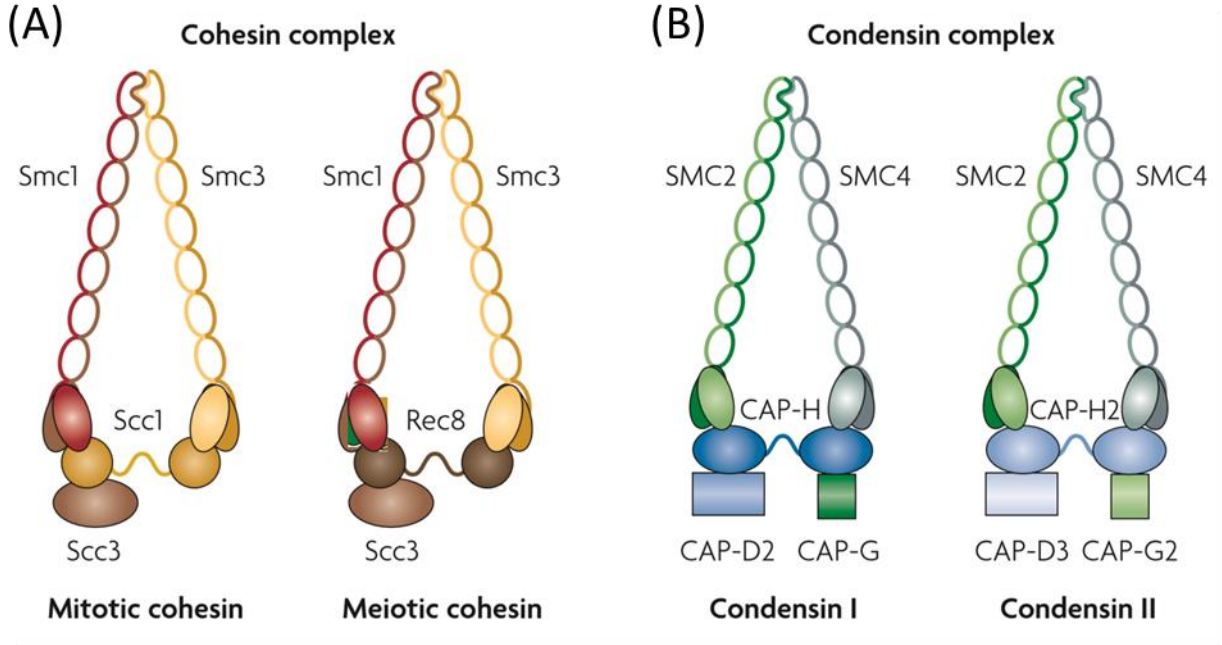


**Figure 1.2 Cohesin and condensin complexes.** Cohesin and condensin complexes are conserved from bacteria to humans. Both of these complexes contain a pair of structural maintenance of chromosome (SMC) subunits and ancillary non-SMC subunits. All SMC proteins share five domains: two nucleotide-binding domains (NBDs), the Walker A and B motifs, which are located at the N- and C-terminus, respectively, and two long coiled coils, linking the NBDs, which are separated by a hinge domain that is related to dimerization with another SMC protein. Each SMC protein folds back on itself to form a large globular ATPase region and a antiparallel coiled-coil region with a hinge domain at the apex. **(A)** Both of the mitotic and meiotic cohesins contain a pair of SMC subunits, Smc1 and Smc3, and two non-SMC subunits, Scc3 and Scc1/Rec8 (mitotic/meiotic), the later of which can interact with two heads of SMC subunits thereby forming a closed ring. **(B)** There are (at least) two different types of condensin complexes that exist in eukaryotes, condensins I and II. These two complexes share the same pair of SMC subunits, SMC2 and SMC4, and each complex contains a unique set of three non-SMC subunits, CAP-D2, CAP-G and CAP-H for condensin I, and CAP-D3, CAP-G2 and CAP-H2 for condensin II.

**B)** (Hirano, 2012; Wood et al., 2010). These two complexes share the same pair of SMC subunits, SMC2 and SMC4, and each complex contains a unique set of three non-SMC subunits, CAP-D2, CAP-G and CAP-H for condensin I, and CAP-D3, CAP-G2 and CAP-H2 for condensin II. CAP-D2/D3 and CAP-G/G2 have HEAT repeats, and CAP-H/H2 are members of the kleisin family of SMC-interacting proteins. In mammals, condensin II localizes to the nucleus from interphase through prophase and primarily contributes to an early stage of axial shortening of chromatids within the prophase nucleus, whereas condensin I is sequestered in the cytoplasm during interphase and gains access to chromosomes during prometaphase, in which the nuclear envelope breaks down, and then participates in lateral compaction of chromosomes (Hirano, 2012). Through the collaboration of these two complexes, this proper assembly of chromosomes promotes the complete separation of sister chromatids in metaphase, during which the duplicated chromosomes line up randomly at the equator of the mitotic spindles, and the faithful segregation of the separated chromatids to the opposite poles during anaphase (Hirano, 2012). Therefore, mitotic division ensures that each diploid cell produces two genetically identical diploid daughter cells.

However, from the perspective of meiosis, each chromosome must communicate with its unique homologous partner by physically pairing and undergoing genetic recombination during the first cell division, meiosis I. This communication is essential to establish the correct disjunction of homologous chromosomes into different daughter cells (Alberts et al., 2008; Krogh and Symington, 2004; Longhese et al., 2008). Thus, after sister chromatids forms and are tightly glued together by meiotic cohesin complexes, each pair of duplicated homologous chromosomes begins to tightly associate together along their axes via

the assembly of a synaptonemal complex (SC) to form a four-chromatid structure called a bivalent in a very prolonged meiotic prophase I, which can take hours in yeast, days in mice, and weeks in higher plants (Alberts et al., 2008; Krogh and Symington, 2004; Zickler and Kleckner, 1998, 1999). This process of SC assembly to form a tight association between homologous chromosomes is called synapsis. Homologous recombination occurs between synapsed chromosomes, and some of these recombination events will later resolve into crossovers resulting in the formation of a physical link between non-sister chromatids called chiasmata, where a fragment of a maternal chromatid is exchanged for a corresponding fragment of a homologous paternal chromatid (Alberts et al., 2008; Krogh and Symington, 2004). The mechanisms of synapsis and recombination are highly complicated and involve many proteins, and are discussed later in the following sections. Moreover, it is chromosome movements within the nucleus that are required for homologous pairing at the early stage of meiotic prophase I **(leptotene and zygotene, see Section 1.3 for details)** via the SUN/KASH bridge formation, which makes the ends of the chromosomes attach to the inner surface of the nuclear envelope and also provides a connection to various cytoskeletal forces in the cytoplasm (Baudrimont et al., 2010). Then, the telomeres will shuffle inside the envelope so that they come together transiently at one spot on the envelope and coalesce to form the chromosomal bouquet, and then disperse again **(see Section 1.3 for details)**. When homologous chromosomes are found by each other, synapsis overcomes the cytoplasmic forces and synapsis can be established (Baudrimont et al., 2010).

After synapsis, the SC is disassembled **(see Section 1.3 for details)** and chromosomes become more condensed and compacted (by condensin complexes) as a preparation for entering meiotic metaphase I (Alberts et al., 2008). Although

during this period from desynapsis to metaphase I there is no more SC to hold homologous chromosomes together, the bivalent still exists via a strong physical linkage between homologs; that is, the cooperation of the chiasmata formed between non-sister chromatids and the cohesin complexes between sister-chromatids arms holds the homologous chromosomes together (Alberts et al., 2008). Therefore, each pair of replicated homologs (bivalent) rather than an individual duplicated chromosome lines up in a random order at the equator of the cell in meiotic metaphase I, and then homologous chromosomes instead of sister chromatids segregate into the two daughter cells during meiotic anaphase I, leading to the halving of chromosome content in meiosis I (Alberts et al., 2008; Zickler and Kleckner, 1998). This is one fundamental difference of meiosis I from mitosis and meiosis II which do not reduce chromosome number, and thus it is named reductional division (Alberts et al., 2008; Zickler and Kleckner, 1998). Besides synapsis, two other features of chromosome behavior in meiosis I are distinct from mitosis and meiosis II (Alberts et al., 2008; Zickler and Kleckner, 1998): The first is each homolog contains two sister kinetochores which are located side-by-side at sister centromeres and are attached to microtubules emanating from the same spindle pole. The second is the sister chromatids within each homolog are still glued together due to the residual cohesin complexes at the centromeres although the cohesin complexes along the arms are degraded. Thus, these features of meiosis I allow the successful disjunction of homologous chromosomes into two daughter cells. On the contrary, meiosis II occurs rapidly with a quick succession of following phases and closely resembles the mitotic cell division (Alberts et al., 2008). Then, during meiosis II, the cohesin complexes at the centromeres are destroyed, and sister chromatids are permitted to pull to the opposite poles and finally four haploid cells are generated (Alberts et al., 2008; Zickler and Kleckner, 1998). Because the

chromosome content doesn't change in this time, meiosis II is also named equational division (Alberts et al., 2008; Zickler and Kleckner, 1998).

Many mutation studies have demonstrated that abnormalities in any of the three major events of meiotic prophase I, cohesion of sister chromatids, pairing and synapsis of homologs, and reciprocal recombination (crossovers), can lead to errors in chromosome segregation that results in yielding aneuploid gametes (Hassold et al., 2007; Longhese et al., 2008; Zickler and Kleckner, 1999). Moreover, aneuploidy is astonishingly common with no fewer than 5% of all clinically recognized pregnancies being trisomic or monosomic (Hassold et al., 2007). The vast majority of aneuploidy terminate *in utero*, but a small portion of trisomies are compatible with live birth and are usually accompanied with congenital birth defects and mental retardation. These include Trisomy 13 (Patau syndrome), Trisomy 18 (Edwards syndrome), Trisomy 21 (Down syndrome), the 47,XXX syndrome and 47,XXY (Kleinfelter syndrome) (Hassold et al., 2007) . In addition, non-disjunction of homologous chromosomes more commonly results from maternal meiosis I errors than maternal meiosis II errors (Hassold et al., 2007). Thus, during meiosis I homologs pairing, synapsis and recombination play substantial roles in establishing the faithful disjunction of homologous chromosomes, in order to prohibit anueploid gamete formation, which would otherwise contribute to reduced fertility and abnormal progeny.

## 1.3 Culmination of Homolog Pairing and Synapsis in the Formation of a Synaptonemal Complex (SC)

The synaptonemal complex (SC), a tripartite zipper-like protein ribbon **(Figure 1.3 B)**, plays an important role in promoting functional crossovers and contributing to the faithful disjunction of homologous chromosomes during meiosis I division (Alberts et al., 2008; Krogh and Symington, 2004; Zickler and Kleckner, 1998, 1999). The assembly and disassembly of the SC occurs in meiotic prophase I **(Figure 1.3 A)**, which is divided into five sequential stages, namely leptotene, zygotene, pachytene, diplotene, and diakinesis, depending on the chromosome morphology (Alberts et al., 2008; Zickler and Kleckner, 1998). To bring the homologs into closer juxtaposition and preceding the appearance of the SC, the paired sister chromatids of each chromosome condenses firstly along a rod about 50 nm in diameter termed the axial element (AE) at the leptotene stage, where recombination begins and is initiated via the programmed double-strand DNA breaks (DSBs) formation **(Figure 1.4 and see Section 1.4 for more details)**. Next comes the zygotene stage, at which synapsis begins with assembling the central region of the SC that makes homologous chromosomes closely associated and bridges the only 100 nm gap between them; in addition, recombination events are occurring and double Holliday junctions start forming **(Figure 1.4 and see Section 1.5 for more details)**. The central region of the SC is composed of central elements (CE), transverse elements (TF) and the dense structures named nodules **(Figure 1.3 B)**, which contain two types: early nodules presenting at zygotene are generally small and irregular, whereas recombination nodules (or late nodules) presenting at pachytene and often located above the central region are larger and make the SC become completely mature (Zickler and Kleckner, 1999). Now within the SC, the axial elements at the leptotene stage are termed lateral elements (LE) **(Figure 1.3 B)**. This mature SC is completely formed at the pachytene stage, which can persist for days or longer, and keeps homologous chromosomes synapsed along their entire length throughout this stage,

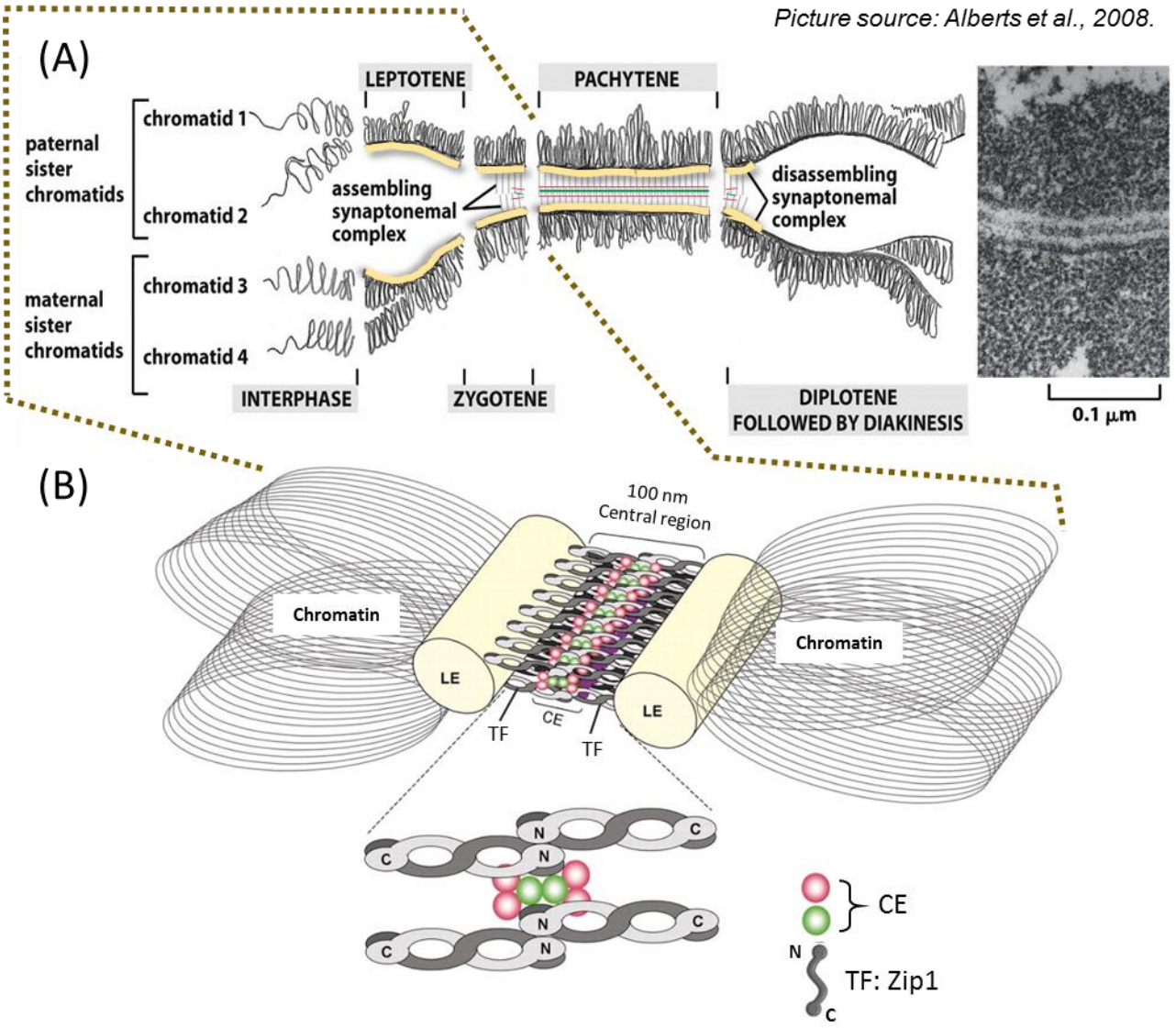


**Figure 1.3 The synaptonemal complex (SC).** The SC plays an important role in promoting functional crossovers and contributing to the correct segregation of homologous chromosomes in meiosis I. **(A)** A single bivalent is shown schematically. Each pair of sister chromatids coalesces together, and the chromatid loops extend out from a common axial core at leptotene. Then, the SC begins to assemble focally in early zygotene. Assembly continues throughout zygotene and the SC becomes mature and complete in pachytene stage. In the end, the mature SC is disassembled in diplotene. **Right of (A)** is an electron micrograph of a SC from a lily flower. **(B)** A mature SC is composed of homologous chromatids and several proteins, that is, lateral elements (LE), central elements (CE), transverse filaments (TF) and recombination modules (not shown). The last three compose the central region. Zip1 is a central region component of the yeast SC and is a building block of TFs, which contain a central extensive α-helical coiled coil domain flanked by two globular domains at the N- and C-termini. The interaction between Zip1 monomers occurs strongly through the N-terminal domains, causing them to be located in the middle of the central region, while the C-terminal domain is anchored into the LEs.

*Picture source: Zickler and Kleckner, 1998.*

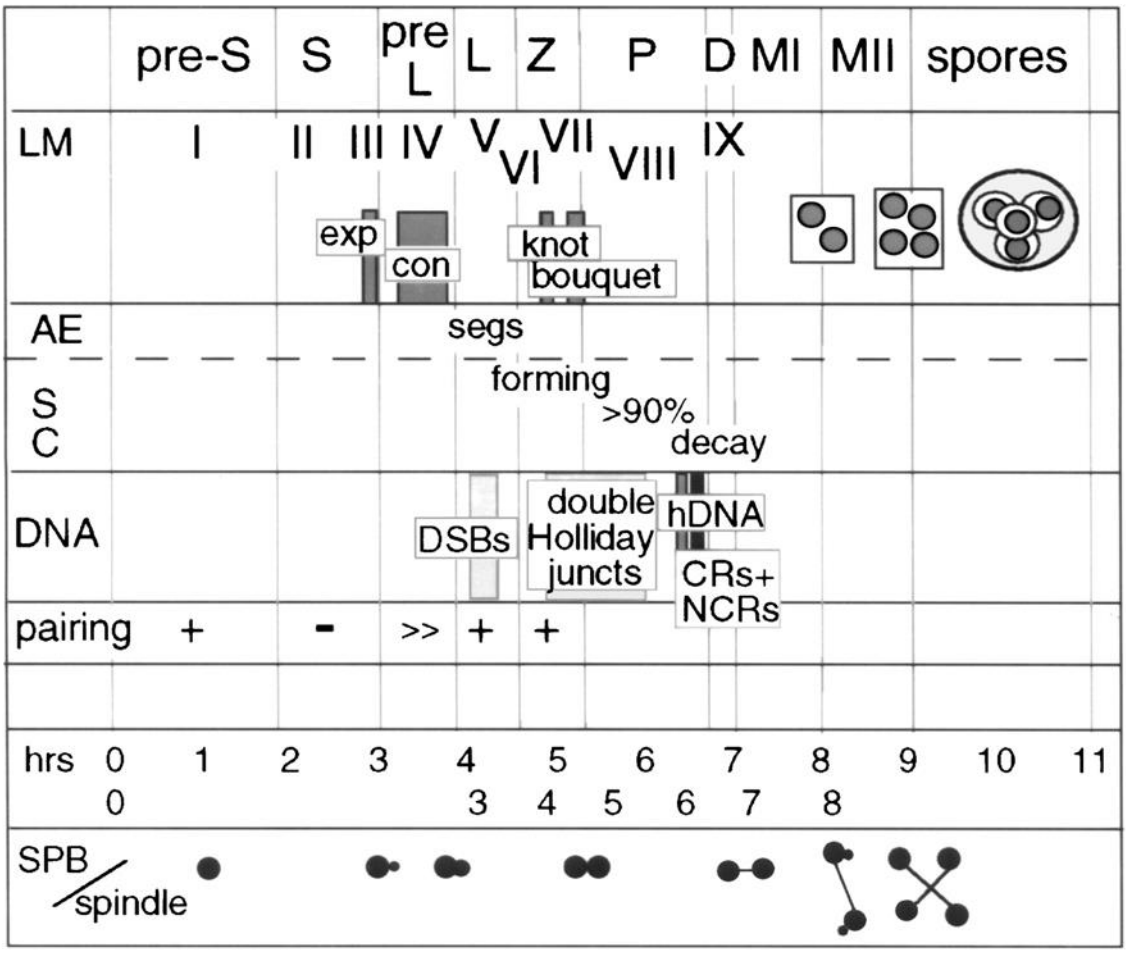


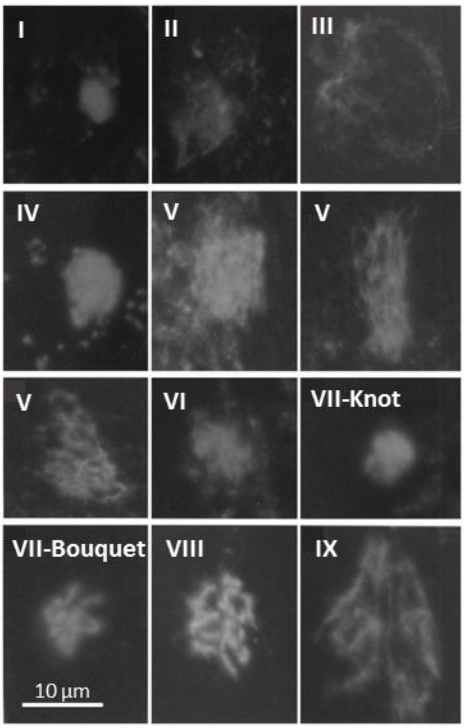


**Figure 1.4 Events of meiosis in *Saccharomyces cerevisiae*.** In leptotene (L), programmed DSBs are formed and start to initiate homologous recombination. Meanwhile, each pair of sister chromatids is condensing along AEs, and the SC begins to assemble. During zygotene (Z), synapsis begins with formation of the SC, recombination events occur, and double Holliday junctions begin forming. The assembly of the SC is complete and mature during pachytene (P). In late pachytene, crossovers (CRs) and noncrossovers (NCRs) occur, and the SC start to decay. LM (light microscopy) of stages I to IX are shown below from fluorescence microscopy of squashed, DAPI-stained nuclei. AE, axial elements; SPB, spindle pole bodies; S, S phase; D, diplotene followed by diakinesis; MI, metaphase I; MII, metaphase II.

leading to the occurrences of homologous recombination and crossovers between the homologs (Alberts et al., 2008). Then comes the diplotene stage, where the SC disassembles and homologous chromosomes separate along their length but are still linked at the sites of crossovers (chiasmata) that are critical for their correct alignment in metaphase. In the meantime, the condensation and shortening of bivalents begins as preparation for entering into metaphase I. At the final stage of meiotic prophase I, diakinesis, homologous chromosomes are fully compacted and ready to progress into metaphase I.

The chromosomal bouquet, which describes the grouping of one or both ends (telomeres) of the thread-like meiotic prophase I chromosomes together within a limited sector of the nuclear periphery, is essentially concomitant with the onset of SC formation that promotes the pairing of homologous chromosomes at the leptotene/zygotene transition **(Figure 1.4)** (Scherthan, 2001; Zickler and Kleckner, 1998, 1999). A model has been proposed that (Scherthan, 2001): at the leptotene stage, chromosome ends are attached randomly over the inner surface of the nuclear envelope, and then move to congregate near the centrosome, probably by motor proteins and intact microtubules or via nucleus rotations that could position telomeres near the centrosome. These movements, contemporaneous with the DSBs formation, contribute to homology testing and recognition leading to the homology pairing. The bouquet persists throughout the zygotene stage until mid-pachytene, where the chromosome ends disperse again evenly around the nuclear periphery and then release from their nuclear envelope attachments (Zickler and Kleckner, 1999).

Many component proteins of the SC structure **(Figure 1.3 B)**, the central region

proteins and the axis-associated proteins, have been unveiled and identified in yeast and in mammals through biochemical and genetic approaches, although it is not straightforward and some difficulties exist in the precise mapping of particular proteins onto the SC structure. One of the best characterized proteins is the *Saccharomyces cerevisiae* Zip1 protein **(Figure 1.3 B)**, which is a central region component of the yeast SC and has been verified as a building block of the transverse filaments within the SC (Dong and Roeder, 2000; Zickler and Kleckner, 1999). The sequence of the Zip1 protein is also predicted to form a central extensive α-helical coiled coil domain, flanked by two globular domains at the $NH_2$ and COOH termini **(Figure 1.3 B)**. This protein structure is similar to that of myosin and intermediate filament proteins (Dong and Roeder, 2000; Zickler and Kleckner, 1999). Moreover, the mammalian central region protein of the SC, SCP1/Syn1, has also been revealed, and harbors a similar protein conformation as well as exhibiting strong functional homology to Zip1 despite the lack of significant sequence homologues between them (Dong and Roeder, 2000; Zickler and Kleckner, 1999). The mapping of different domains of the protein by immunoelectron microscopy using gold-labeled antibodies has demonstrated that the organization of Zip1 within the SC is similar to that of SCP1/Syn1; that is, the $NH_2$-terminal domain of Zip1/SCP1/Syn1 is located in the middle of the central region of the SC, whereas the COOH-terminal domain is embedded and anchored into the lateral elements of the complex **(Figure 1.3 B)** (Dong and Roeder, 2000). This is consistent with the phenomena of the two globular domains that have been discovered in SCP1 protein (Zickler and Kleckner, 1999), where the COOH-terminal domain is capable of binding to DNA *in vitro* and possesses several potential phosphorylation sites proposed to be related to the SC (dis)assembly (Meuwissen et al., 1992), whereas the $NH_2$-terminal domain interacts strongly with itself, but not with other regions of

proteins through the yeast two-hybrid analysis (Liu et al., 1996). In addition, like myosin and most intermediate filament proteins, two Zip1 monomers associate with each other through the $NH_2$-terminal domains to form a homodimer, and the estimated length of a Zip1 tail-to-tail dimer is around 100 nm, which is similar to the distance between the LEs of the SC **(Figure 1.3 B)** (Sym et al., 1993). Thus, when the length of coiled coil domain changes, the width of the SC is correspondingly altered (Sym and Roeder, 1995; Tung and Roeder, 1998). Furthermore, two Zip1 homodimers form a tetramer, which is regarded as the basic building block of the SC, and line up side-by-side in parallel and in register to span the width of the SC (Dong and Roeder, 2000). In *zip1* mutants, the morphogenesis of the AE is apparently normal, and sisters usually segregate together in meiosis I, even if the separation of homologs is aberrant; however, the synapsis cannot be formed and meiotic recombination is affected (Zickler and Kleckner, 1999).

The polymerization of Zip1 requires the recruitment of meiosis-specific Zip2 to axial associations dependent on Zip3 that colocalizes with Zip2, and both Zip2 and Zip3 proteins are implied to mark the sites of axial association (Agarwal and Roeder, 2000; Chua and Roeder, 1998; Zickler and Kleckner, 1999). The cytological phenotype of *zip2* mutants displays similarly to that of *zip1* mutants, and the colocalization of Zip2 with the proteins involved in meiotic DSB formation (Rad50, Mre11 and Xrs2) has also been shown (Zickler and Kleckner, 1999). In addition, the localization of Zip2 to the axial associations in *zip1* mutants requires the recombination function of Dmc1 and Rad51(Schmekel et al., 1993). These suggest that Zip2 (and thus Zip3) are not only required for the initiation of synapsis, but also may play a key role in the linkage between the initiation of recombination and synapsis (Zickler and Kleckner, 1999). Moreover, prior or during Zip1 polymerization,

the meiosis-specific protein, Hop2, localizes on chromosomes independently of the DSBs formation, and helps homologous chromosomes synapse by constraining SC formation to occur between homologs (Leu et al., 1998).

Besides the parts of the axis-associated proteins (Zip2, Zip3 and Hop2) that have been introduced above, the Red1, Hop1 and Mek1 proteins are components of the axial element protein cores in the yeast SC. They are not only important for effective chromosome segregation and for the meiotic recombination checkpoints, but are also necessary for normal levels of DSB formation and for ensuring crossovers occur between homologous chromosomes (interhomologs) instead of between sister chromatids (intersisters) (Prieler et al., 2005; Wan et al., 2004). Red1 is a multifunctional protein, which is required for the maximum activity of Mek1, the interaction between Mek1 and Hop1, sister chromatid cohesion, the establishment of interhomolog bias at double Holliday junctions, and for the proper timing of the first meiotic division (Malone et al., 2004; Wan et al., 2004; Woltering et al., 2000; Zierhut et al., 2004). Although there is a minor transcript of *RED1* present in mitotic cells, no effect of the *red1* mutation in nonmeiotic cells has been discerned; whereas, Hop1 and Mek1 are meiosis-specific proteins, and Mek1 contains homology to serine/threonine protein kinases as well as being able to phosphorylate Red1, Hop1 and itself *in vitro* (Zickler and Kleckner, 1999). The model of the relationship among these three proteins has been described that (Zickler and Kleckner, 1999): Red1 is induced early in meiosis, and associates first on chromosomes then recruits Hop1 to the chromosomes during zygotene stage; following the dissociation of Hop1 by the presence of Mek1 on the chromosomes at early/mid-pachytene, Red1 still remains on the chromosomes until late-pachytene or early diplotene. According to the review paper by Zickler and Kleckner in 1999

(Zickler and Kleckner, 1999): *red1* mutants cause the failure of the assembly of any AE or SC structure although chromosome compaction exhibits normally. And, in *hop1* mutants, long fragments of AE are formed, but no SCs are shown and axial chromosome compaction is defected. However, in *mek1* mutants, the SCs are discontinuous and less than a full complement. Basing on these phenotypes, it is suggested that the Red1, Hop1, and Mek1 proteins are crucial in organizing chromosomes for all of their important meiotic prophase functions (Zickler and Kleckner, 1999). Moreover, mutations of any one of these genes results in the reduction of meiotic recombination, and can suppress the prophase arrest observed in several mutants (such as *rad50S*, *dmc1* null and *sae2* null), which block the metabolism of prophase chromosomes at the DSB-to-double Holliday junction transition (AE to SC), implying that it is probably via a mitosis-like intersister exchange pathway independent of the meiosis-specific repair machinery that the lack of Red1/Hop1/Mek1 allows DSB repair to proceed (Zickler and Kleckner, 1999; Zierhut et al., 2004).

Rec8 is a meiosis-specific homolog of the Rad21/Mcd1(Scc1) cohesin, and is found in foci that are axis-associated at mid-prophase and remain on centromeres until anaphase II (Zickler and Kleckner, 1999). When *REC8* is mutated, there is no trace of AE shown in budding yeasts, and the linear elements in fission yeasts become abnormal; in addition, the separation of premature sister chromatids appears at metaphase I and during/before prophase in both yeasts (Klein et al., 1999; Molnar et al., 1995). Moreover, *rec8* mutations in both organisms also show a strong defect in meiotic recombination (Klein et al., 1999).

## 1.4 Meiotic Double-Strand Breaks (DSBs) Formation and Processing

Genomes of living organisms can suffer from either spontaneous or induced DNA damages, and it is double-strand breaks (DSBs) that are the most deleterious for genome integrity among the various kinds of DNA lesions, because failure in repairing them can lead to genome rearrangements or chromosome loss (Alberts et al., 2008; Krogh and Symington, 2004; Longhese et al., 2008). However, DSBs not only arise accidentally by either DNA replication problems or exposure to environmental factors, such as ionizing radiations or genotoxic drugs, in both mitotic and meiotic cells, but also are introduced into the genome in a programmed manner to initiate meiotic recombination in germ cells (Longhese et al., 2008). This meiotic programmed DSBs formation is then important to establish the correct disjunction of homologous chromosomes into two daughter cells (Alberts et al., 2008; Krogh and Symington, 2004; Longhese et al., 2008). During the leptotene stage, the formation of DSBs to initiate meiotic recombination requires the meiosis-specific protein, Spo11, which is an evolutionarily conserved topoisomerase-like protein (Krogh and Symington, 2004; Zickler and Kleckner, 1998). The MRX complex, composed of Mre11, Rad50 and Xrs2 in budding yeasts, belonging to the *RAD52* epistasis group, is also necessary for meiotic DSB formation, and it might take this responsibility together with Sae2 (Krogh and Symington, 2004). Moreover, eight other genes, *MEI4*, *MER2/REC107*, *REC102*, *REC103/SKI8*, *REC104*, *REC114*, *MER1* and *MRE2* (the last two produce meiosis-specific RNA splicing factors) in yeasts, are also required for DSB formation in meiosis, where they form a stable complex at DSB hot-spot sites and act as a scaffold to load Spo11 onto these hot-spot sites (Keeney, 2001; Krogh and Symington, 2004).

Topoisomerases are enzymes that catalyze unwinding and winding of DNA, and are classified into two classical types, type I and type II topoisomerases (Champoux, 2001; Wang, 1991). The type I topoisomerase acts as a monomer and transiently cuts one strand of a DNA double helix by forming a covalent bond between topoisomerases and 5' or 3' ends of breaks (5' ends for type IA; 3' ends for type IB), whereas the type II topoisomerase forms a dimer that makes both strands of one DNA double helix cut transiently through the formation of covalent 5' phosphotyrosyl enzyme-DNA intermediates (for both type IIA and IIB). After the DNA topoisomerization, these two types of topoisomerases resolve the covalent linkages, and then reanneal the transient breaks (Champoux, 2001; Wang, 1991). Spo11, one of the meiosis-specific proteins, belongs to the classical type II topoisomerase group with sequence similarity to the small subunit (Top6A) of a type IIB topoisomerase in *Sulfolobus shibatae* (Krogh and Symington, 2004). However, differently from the classical types of topoisomerases, Spo11 appears to catalyze only the formation of Spo11-DNA covalent intermediates by a topoisomerase-like transesterification reaction (Krogh and Symington, 2004). In addition, Spo11 harbors two identified domains, the 5Y-CAP motif and the Toprim domain (Diaz et al., 2002). The 5Y-CAP motif contains the catalytic tyrosine residue, which is Tyr-135 within *S. cerevisiae* Spo11 (Diaz et al., 2002). During meiosis, Spo11 proteins act as a dimer, together with several other factors, to break double strands of a DNA molecule, and each catalytic tyrosine residue of Spo11 covalently joins to each of the newly created 5' ends **(Figure 1.5)** (De Massy et al., 1994; Keeney et al., 1997). When this catalytic tyrosine residue (Tyr-135) is mutated, there is no DSB formed *in vivo* (Bergerat et al., 1997; Diaz et al., 2002). Moreover, Spo11 proteins catalyze DSB formation nonrandomly at 150-200 sites within the yeast genome to initiate a high

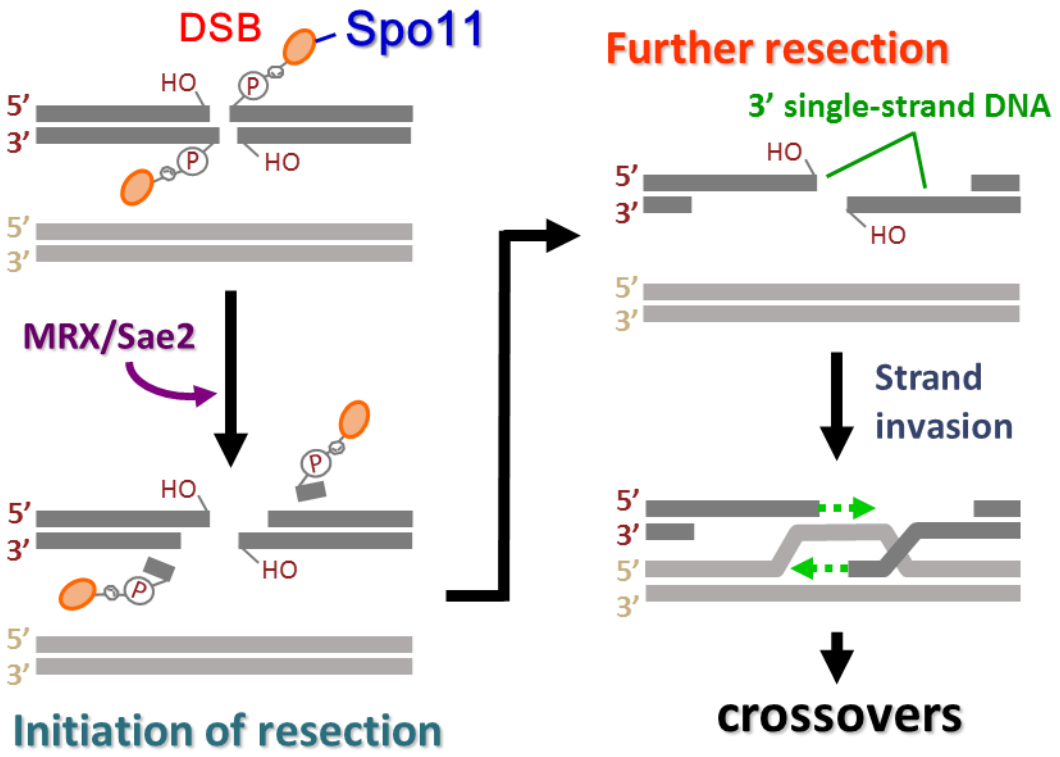


**Figure 1.5 Crossovers are made from induced DSBs.** A meiotic-specific-protein, Spo11, acts as a dimer to catalyze DSB formation and covalently bind to the ends of the DSB. During the initiation of resection, the MRX complex together with Sae2, removes Spo11 from the ends of the DSB. Then, further resection proceeds, leading to the exposure of 3′ single-strand DNA (3′ ssDNA). This ssDNA can then invade the homologous donor template to repair the DSB, leading to the occurrence of crossovers.

frequency of recombination (Keeney, 2001). However, unlike in the initiation of mitotic recombination, where the long nonpalindromic recognition sequences are cleaved by endonucleases HO or I-*Sce*I, Spo11 does not exhibit sequence-specific cleavage sites, but the DSB hot-spot sites are generally in the 5' noncoding regions of genes and coincide with DNaseI hypersensitive sites (Krogh and Symington, 2004).

Following the formation of Spo11-DNA covalent intermediates, each MRX complex is required to remove each Spo11 protein from the 5' ends of a DSB by using its endonuclease activity to nick a few bases away from the break site, which then frees this single-strand oligonucleotide, together with a covalently bound Spo11, and makes the 5' ends become available for resection, which causes the exposure of 3' single-strand DNA for the initiation of meiotic recombination **(Figure 1.5 and see Section 1.5 and 1.6 for more details)** (Neale et al., 2005). Moreover, Sae2 is likely responsible for this activity accompanied by the MRX complex, and it might be a possible fourth member of the MRX complex that modulates and enhances its full function (Krogh and Symington, 2004; Longhese et al., 2008). Therefore, in *rad50S*, *sae2*Δ, *mre11-S* and *mre11-58* single mutants, Spo11 still stably covalently binds to the 5' ends of break sites (Alani et al., 1989; Keeney et al., 1997; McKee and Kleckner, 1997; Nairz and Klein, 1997; Prinz et al., 1997; Tsubouchi and Ogawa, 1998). However, based on recent studies, a new model for bidirectional processing of DSBs has been proposed, and is different from the previous proposal that resection traverses unidirectionally. This new mechanism indicates that, during meiosis, the ends of DSBs are terminally blocked by covalently bound Spo11 proteins and may be protected from Mre11-dependent exonuclease degradation by a large metastable multisubunit complex. Therefore, instead of using the

exonuclease activity, Mre11 proteins make asymmetrically spaced nicks up to 300 bases away from DSBs using the endonuclease function together with Sae2 (Neale et al., 2005), and these nicks then enable resection in a bidirectional manner, using Exo1 in the 5'-3' direction away from the DSBs leading to the further resection, and the exonuclease function of Mre11 in the 3'-5' direction towards the DSBs resulting in the removal of Spo11 (Garcia et al., 2011). (Mre11 contains both endonuclease and 3'-5' exonuclease function; Sae2 is an endonuclease; Exo1 is a 5'-3' exonuclease) The stoichiometry of an MRX complex is composed of two Mre11, two Rad50 and one Xrs2 to form a $M_2R_2X_1$ heteropentamer (Anderson et al., 2001; Chen et al., 2001; Usui et al., 1998). However, a recent review shows the composition of an Mre11 complex in mammals to be an $M_2R_2N_2$ heterohexamer **(Figure 1.6)** (Stracker and Petrini, 2011).

Rad50 belongs to a member of the structural maintenance of chromosomes (SMC) family of proteins that contain N-terminal Walker A and C-terminal Walker B motifs, linked by a 600-900 residue α-helical coiled-coil domain **(Figure 1.6)** (Aravind et al., 1999; Krogh and Symington, 2004). The Walker A and B motifs assemble into a single globular intramolecular ATP-binding cassette (ABC) type ATPase domain [also named nucleotide-binding domain/NBD (Lammens et al., 2011)], whereas the α-helical region folds up as a protruding antiparallel coiled-coil (Krogh and Symington, 2004). Each coiled-coil of Rad50 in *Saccharomyces cerevisiae* (*Sc*) extends approximately 60 nm away from the globular ABC-ATPase domain or NBD (Anderson et al., 2001). The apex of the Rad50 coiled-coil contains a dimerization interface, which is a conserved Cys-X-X-Cys motif in a hook-shaped domain, and allows it to dimerize with a second Rad50 hook domain via cysteine-mediated zinc ion coordination, thereby leading to the intermolecular dimerization of two

*Picture source: Stracker and Petrini, 2011.*

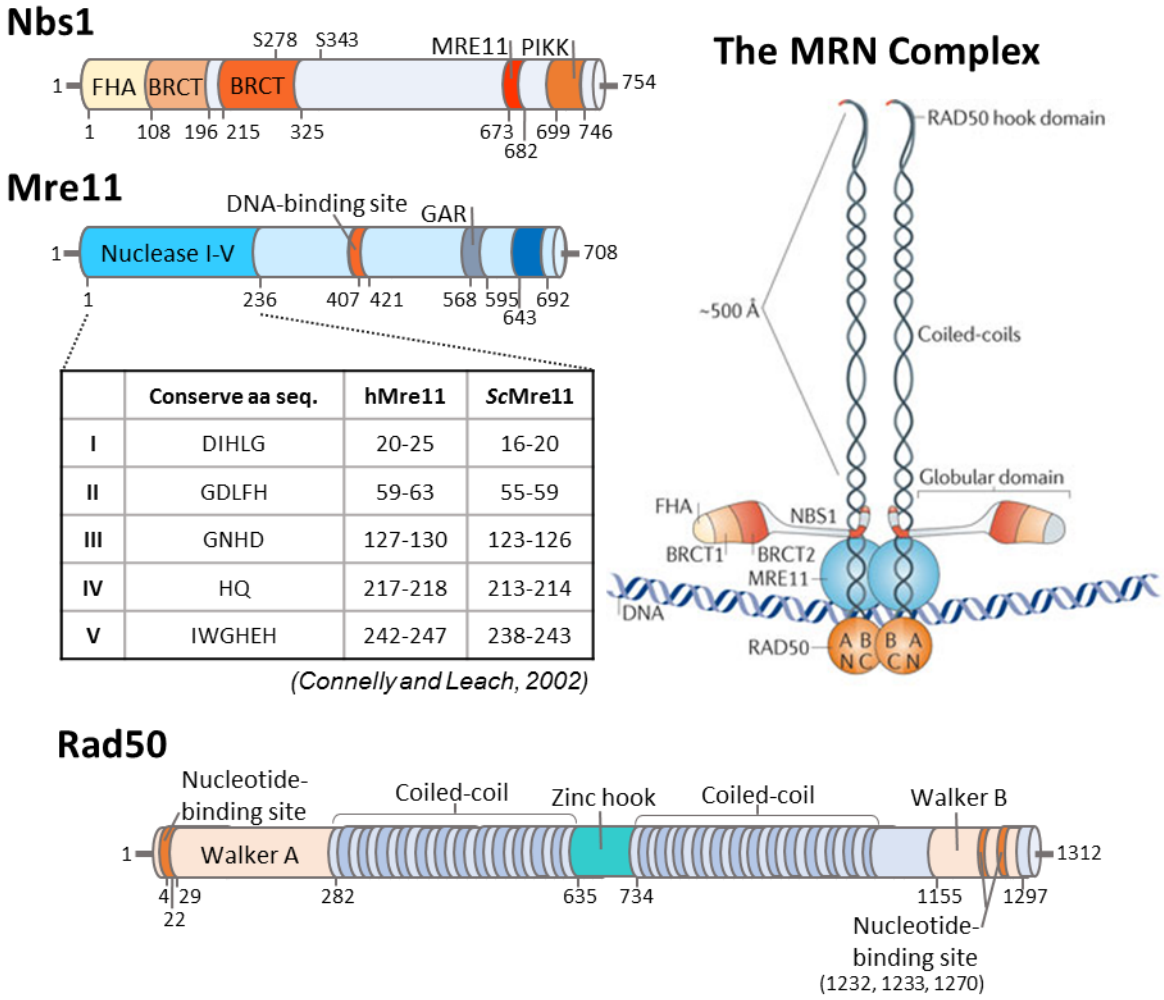


| | Conserve aa seq. | hMre11 | *Sc*Mre11 |
|---|---|---|---|
| I | DIHLG | 20-25 | 16-20 |
| II | GDLFH | 59-63 | 55-59 |
| III | GNHD | 127-130 | 123-126 |
| IV | HQ | 217-218 | 213-214 |
| V | IWGHEH | 242-247 | 238-243 |

*(Connelly and Leach, 2002)*

**Figure 1.6 Components of the MRX/MRN complex. The MRN complex** consists of a large globular domain, in which two Mre11 and two Nbs1 associate with two Rad50 and DNA, and the extended coiled-coil domains of Rad50, and plays an important role in the formation of DSBs and the initiation of resection during meiosis. **Mre11** contains five conserved phosphoesterase motifs at the N-terminal region, which are related to 3' to 5' exonuclease and endonuclease activities. The conserved amino-acid sequences of these five motifs and their corresponding amino acid sites are listed above in humans and *Saccharomyces cerevisiae*. **Rad50** is one of the SMC family that contains N-terminal Walker A and C-terminal Walker B motifs, linked by a long α-helical coiled-coil domain with a Zink hook in the middle. Rad50 folds back on itself, making the Walker A and B motifs form an ABC type ATPase domain, and the α-helical region become a protruding antiparallel coiled-coil. **Nbs1** shares a common motif with yeast, the forkhead-associated (FHA) motif at the N-terminus, and has a conserved C-terminal domain, which is involved in the interaction with Mre11, and has phosphorylation sites (PIKK) for ATM/Tel1. All figures are drawn to scale.

individual MRX complexes to transiently tether broken DNA ends together or perhaps tether and align sister chromatids together (Krogh and Symington, 2004; Stracker and Petrini, 2011). The *rad50*-hook mutants show a defect in meiotic DSB formation similar to that in *rad50*-null mutant cells, and this phenotype can be suppressed by artificially restoring the dimerization of Rad50-hook mutant variants, therefore suggesting that the activity of the MRX complex mediated by the Rad50 coiled-coil might bridge sister chromatids in order to establish a proper architecture of the sisters to be cleaved (Mimitou and Symington, 2009; Wiltzius et al., 2005).

Structural and functional homologues for Mre11 and Rad50, but not Xrs2 (Nbs1 in vertebrates), are found in all domains of life, and are also known as SbcC (Rad50 homolog) and SbcD (Mre11 homolog) in bacteria (Sharples and Leach, 1995). Based on the crystallographic studies from *Thermotoga maritima* (*Tm*), Mre11 shows an extended structure composed of two functional modules, the nuclease module and the Rad50-binding domain (Lammens et al., 2011). In the nuclease module, there are the phosphodiesterase and the accessory DNA-binding capping domains, whereas the Rad50-binding domain contains a helix-loop-helix (HLH) domain that anchors Mre11 to the root of the Rad50 coiled-coil (Lammens et al., 2011). Thus, two Mre11 and two Rad50 form a large MR complex **(Figure 1.6)** that comprises a catalytic head, which is the Mre11 dimer binding to the two Rad50 ABC-ATPase domains (NBDs) and contains ATP-stimulated nuclease and DNA-binding activity (Hopfner et al., 2001; Lammens et al., 2011), and two long Rad50 coiled-coil domains that protrude from the head for dimierizing with other MR complexes (de Jager et al., 2001; Hopfner et al., 2002). This prokaryotic MR complex shares similar enzymatic activities and morphological features with the eukaryotic MRX.

Consistent with the homology to the nuclease subunit of SbcD, human and yeast Mre11 have manganese-dependent nuclease activities *in vitro*, including 3'-5' dsDNA exonuclease activity on blunt and 3' recessed ends, and ssDNA endonuclease activity that acts on 5' overhangs, 3' flaps and 3' branches; in addition, they also harbor DNA unwinding and DNA annealing activities (Krogh and Symington, 2004). The observation that ssDNA homopolymers are resistant to cleavage implies that Mre11 is structure specific and cleaves ssDNA by trapping transient secondary structures that allow the enzyme to cut at the preferred single/double-stranded transition (Krogh and Symington, 2004). Mre11 contains five conserved phosphoesterase motifs in the N-terminal region found in the superfamily of phosphodiesterases **(Figure 1.6)**, and several conserved residues within these phosphoesterase motifs, for instance, Asp 16, Asp 56, His 125 and His 213, are required for Mre11 endo- and exonuclease functions *in vitro* (Connelly and Leach, 2002; Mimitou and Symington, 2009; Symington, 2002). Once these conserved residues become mutated, D16A, D56N, H125N and H213Y (mre11-58S), the nuclease activity of Mre11 is eliminated and these kinds of mutations are generally referred to as *mre11-nd* (nuclease defective) alleles (Connelly and Leach, 2002; Krogh and Symington, 2004; Mimitou and Symington, 2009; Symington, 2002). Based on chromatin immunoprecipitation studies, it is suggested that the transient association of Mre11 with DSB specific regions does not depend on the DSB formation (Borde et al., 2004). Moreover, in the defective resection strains Mre11 remains bound to DSB sites, but it still dissociates from chromatin in the defective strand invasion strains. This implies that it is resection not repair that is the signal for removal of Mre11 (Borde et al., 2004; Krogh and Symington, 2004). A recently proposed model for ATP-dependent DSB processing and DNA tethering by MR demonstrates that the engagement of two ATPs to each of the two Rad50 NBDs

drives the extensive conformational changes of the MR complex from open to closed form. The MR catalytic head could then be responsible for the unwinding of dsDNA and promote endonucleolytic cleavage of ssDNA or hairpins, and the Rad50 DNA-binding groove could tether two DNA ends in close proximity to each other by Rad50 coiled-coil dimerizing with a second MR complex (Lammens et al., 2011; Mockel et al., 2012). Moreover, the switch of Mre11 nuclease activities between exonuclease and endonuclease functions is dependent on this butterfly-like opening and closing model, where the endonuclease function appears more dominant than the exonuclease function in the closed form of MR, and vice versa (Majka et al., 2012).

Xrs2 in yeast (MRX) and Nbs1 (MRN) in vertebrates are only found in eukaryotic cells and they share some common motifs. These include the N-terminal forkhead-associated (FHA) domain that is a phosphorylation-dependent protein-protein interaction motif found in a variety of eukaryotic proteins and is verified to bind to phosphorylated H2A, and the conserved C-terminal domain (CCD), which is involved in the interaction with Mre11 and contains phosphorylation sites for the DNA damage checkpoint protein ATM/Tel1 **(Figure 1.6)** (Stracker and Petrini, 2011; Symington, 2002). When cells are exposed to DNA damage, the *Sc*MRX and *Hs*MRN complexes are important in the initiation of the intra S-phase checkpoint and both Xrs2 and Nbs1 can be phosphorylated by the ATM family kinases (Krogh and Symington, 2004). Moreover, the association of Mre11 with DSB sites requires Xrs2 not Rad50 (Borde et al., 2004), and the interaction between Mre11 and Xrs2 is crucial to all functions of the MRX complex (Tsukamoto et al., 2005).

Sae2 is an endonuclease involved in processing hairpin DNA structures, and is

thought to be the fourth member of the MRX complex although it is without known homologues (Krogh and Symington, 2004). Both *sae2*Δ and *rad50S* mutants show the same phenotype, where Spo11-mediated DSBs still form but the endonucleolytic removal of Spo11 from the 5' DSB ends is totally defective (McKee and Kleckner, 1997; Prinz et al., 1997). Based on crystal structure study in the narrow surface patch of Rad50, it is suggested that Rad50 could form a protein interaction site that raises the possibility of *rad50S* mutants affecting the interaction between Sae2 and Rad50 (Hopfner et al., 2000; Rattray et al., 2001). Moreover, the *mre11-nd* mutants show DSBs can form but Spo11 proteins still covalently join to the ends of breaks (Longhese et al., 2008). Taking the above phenomena together, it implies that the removal of Spo11 from 5' DSB ends requires Mre11 nuclease activity that is enhanced by Tel1- and Mec1-mediated phosphorylation of Sae2 which then forms a transient interaction with Rad50 (Cartagena-Lirola et al., 2006; Longhese et al., 2008).

During meiosis, DSB formation not only depends on Spo11 itself, but also requires a number of Spo11-accessory proteins, which have been largely identified in *S. cerevisiae*, but the functions of whom are just partially uncovered; and these accessory proteins interact with each other to form the pre-DSB recombinosome prior or during DSB formation (Keeney, 2001). Among these proteins, Rec102, Rec103/Ski8 and Rec104 are necessary for Spo11 dimerization, DNA binding and nuclear retention (Arora et al., 2004; Kee et al., 2004; Prieler et al., 2005; Sasanuma et al., 2007), whereas three other factors, Rec114, Mer2/Rec107 and Mei4, are quite separate from Spo11-acessory proteins and have been shown to form a RMM subcomplex required for Spo11 binding to sites of DNA cleavage (Li et al., 2006; Sasanuma et al., 2007). From cytological studies in many organisms, where

recombination complexes are already associated with chromosome axes before synapsis, and from the mapping of budding yeast DSB hotspots, which have been shown to localize on the loop regions that are between the axial sites, it implies that the interaction between hotspot sequences and the recombinosome is required for tethering loop and axis regions together (Panizza et al., 2011). Moreover, it has been shown that Mer2 recruits Rec114 and Mei4 upon phosphorylation of its S30 by S-Cdk, and the RMM subcomplex then stably binds to chromosome axis association sites rather than to the loop regions (Henderson et al., 2006; Panizza et al., 2011). This localization of RMM to the chromosome axis requires axial elements Red1 and Hop1 and cohesin proteins. After tethering these proteins together at axial sites, the linear arrays of loops emerge, and the Spo11-containing pre-DSB recombinosome anchored at the axis interacts with one of these surrounding hotspots to form a DSB; thus, it is prior to DSB formation that hotspot sequences become tethered to the axis sites (Panizza et al., 2011). On the other hand, this also could illustrate how the long distance of crossover interference occurs **(see the last paragraph in Section 1.5 for details)**.

## 1.5 Recombination and Crossover Formation

Due to DSBs leaving no intact template strand to enable accurate repair itself, the mechanism of recombination has evolved to solve this situation. The phenomenon of the exchange, or transfer, of information between, or within, DNA molecules is referred to as recombination, and it is found in all organisms and mainly includes homologous recombination (HR) and nonhomologous recombination or end joining (NHEJ) (Alberts et al., 2008; Krogh and Symington,

2004). It is HR that involves the interaction between DNA sequences using perfect, or near-perfect homology over several hundreds of base pairs, and restores the genetic information much more accurately although it is more difficult to accomplish; whereas NHEJ is thought to be a “quick and dirty” solution to repairing DSBs utilizing little or no sequence homology to simply rejoin broken ends together mediated the Ku70/80 heterodimer together with the MRX complex and the Ligase IV complex (Dnl4-Lif1), and can cause either deletion or short insertion of DNA sequences (Alberts et al., 2008; Krogh and Symington, 2004). HR plays essential roles in the maintenance of genome stability and integrity in both prokaryotic and eukaryotic cells. Once mitotic cells are exposed to DNA-damaging agents or have some spontaneous mutations that cause the formation of DSBs or single-strand gaps leading to the collapse of DNA replication forks, HR repairs these DNA lesions and restarts the replication forks (Alberts et al., 2008; Krogh and Symington, 2004; Longhese et al., 2008; Moynahan and Jasin, 2010). HR is also important in telomere maintenance (Alberts et al., 2008; Krogh and Symington, 2004; Lydeard et al., 2007). Moreover, during meiosis, HR is required for the establishment of physical connections between homologous chromosomes to ensure their correct disjunction at meiosis I, and this high frequency of meiotic recombination then contributes to the creation of new linkage arrangements between genes or parts of genes causing the wide diversity of gene combinations (Alberts et al., 2008; Krogh and Symington, 2004; Longhese et al., 2008; Zickler and Kleckner, 1999). On the other hand, NHEJ is a predominant pathway for the repair of DSBs in higher eukaryotic somatic cells (Jeggo, 1998), and is commonly used in V(D)J recombination at the early stages of the production of immunoglobulin and T cell receptors in the immune system (Krogh and Symington, 2004; Moynahan and Jasin, 2010).

Meiotic Spo11-induced DSBs are repaired by HR, and are thought to form two four-way DNA intermediate structures called double Holliday junctions (dHJs) or joint molecules (JMs) according to the double-strand-break repair (DSBR) model **(see Section 1.6 for details)**. Through the alternate resolution of a dHJ intermediate, which is either asymmetric or symmetric resolution **(see Section 1.6 for details)**, two types of meiotic recombinants are ultimately yielded respectively (Krogh and Symington, 2004; Petes et al., 1991): (1) Crossovers associated with gene conversions. A crossover is a reciprocal exchange between homologue pairs, and is required for homologous chromosome segregation (Blat et al., 2002). (2) Non-crossover gene conversions, in which no reciprocal exchange occurs. Before the formation of dHJ intermediates, the presynaptic Rad51 and Dmc1 nucleoprotein filament assembles and engages in the search for a homologous template, with a strong preference towards the homologous chromosome rather than the sister chromatid, thus leading to the crossover formation **(Figure 1.5 and 1.7)** (Krogh and Symington, 2004; Sung and Klein, 2006). It is the *RAD52* group genes (*RAD50*, *RAD51*, *RAD52*, *RAD54*, *RDH54/TID1*, *RAD55*, *RAD57*, *RAD59*, *MRE11* and *XRS2*) that play direct roles in homologous recombination (Krogh and Symington, 2004).

Upon resecting 5’ strands from both ends of a DSB by MRX complexes and 5’-3’ exonucleases, 3’ single-stranded DNA (3’ ssDNA) stretches are rapidly coated by RPA (replication protein A) proteins **(Figure 1.7 a and b)**, which belong to the single-stranded DNA binding protein family (SSBs) that contains an evolutionarily conserved single-stranded DNA-binding domain, the oligonucleotide/ oligosaccharide-binding (OB)-fold, and is essential for sequestering ssDNA from chemical or enzymatic degradation, as well as for the processing of ssDNA (Alberts et al., 2008; Ashton et al., 2013). The secondary structures within 3’ ssDNA are then

*Picture source: Krogh and Symington, 2004.*

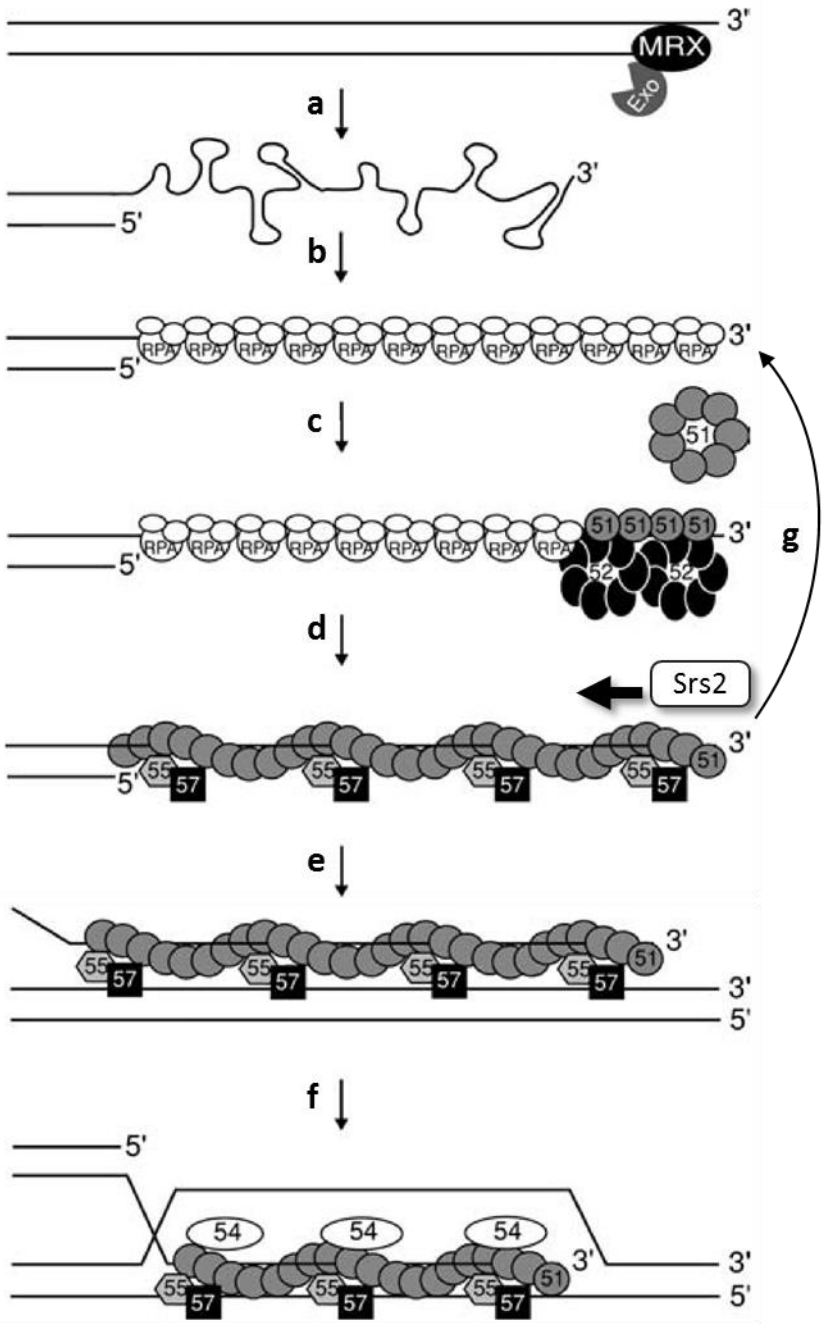


**Figure 1.7 Model for the Rad51 nucleoprotein filament formation and strand invasion.** Only one side of the DNA is shown. **(a and b)** Once 3' ssDNA is generated by the MRX complex and/or a 5'-3' resection exonuclease, the 3' ssDNA tail is rapidly coated by RPA to eliminate secondary structures. **(c)** Then, Rad52 recruits Rad51 to the RPA-ssDNA complex to displace RPA. **(d)** The Rad51 nucleoprotein filament extends and is stabilized by the mediators, Rad55 and Rad57. **(e)** The Rad55-Rad57 heterodimer promotes Rad51 nucleoprotein filament localising on a homologous DNA donor sequence and leads to Rad51-mediated strand invasion. **(f)** Then, the mediator protein, Rad54, interacts with Rad51 and promotes chromatin remodeling, DNA unwinding, and strand annealing between donor DNA and the incoming Rad51 nucleoprotein filament. **(g)** To prevent unwanted HR events from occurring, Srs2 is thought to remove Rad51 from the nucleoprotein filament in 3'-5' direction, and the ssDNA is immediately recoated with RPA.

eliminated by RPA proteins **(Figure 1.7 b)** (Krogh and Symington, 2004), and Rad52 multimeric rings, which are observed in both yeast and humans as heptameric rings (Shinohara et al., 1998; Stasiak et al., 2000), recruit Rad51 proteins to the RPA-ssDNA complex and displace RPA proteins by loading Rad51 to the 3' ssDNA tails **(Figure 1.7 c)** (Song and Sung, 2000; Sugiyama and Kowalczykowski, 2002). *RAD51* is a eukaryotic gene and highly conserved in most eukaryotes from yeast to humans. *Sc*Rad51 has 30% identity to bacterial RecA proteins, and the highest homology is with the catalytic domain of RecA composed of the Walker A and B motifs for nucleotide binding and/or hydrolysis (Krogh and Symington, 2004; Symington, 2002). In addition, there is an extension of 100 amino acids at the N-termini of Rad51 that is absent in RecA (Shinohara et al., 1993), and this N-terminal domain is well conserved among eukaryotes and thought to be important in DNA binding and protein-protein interactions (Aravind et al., 1999; Krejci et al., 2001). Moreover, the crystal structures of *Pyrococcus furiosus* Rad51 reveals that Rad51 proteins assemble a double heptameric ring, and this ring structure is proposed to be the inactive or storage form of Rad51, which is recruited to the ssDNA by Rad52, where it disassembles, and then binds to 3' ssDNA to form right-handed filaments similar to those formed by RecA **(Figure 1.7)** (Krogh and Symington, 2004). Rad52 is one of the mediator proteins for Rad51 filament assembly. It has been shown that Rad52 interacts directly with both RPA and Rad51 and is required for the localization of Rad51 to DSB sites, which has been verified *in vivo* using chromatin immunoprecipitation (ChIP) (Krogh and Symington, 2004). In addition, the C-terminal region, residues 409-412, of Rad52 takes responsibility for the Rad51/Rad52 interaction (Krejci et al., 2002). All of these findings imply that Rad52 is indispensable for Rad51 filament formation by replacing RPA with Rad51 on ssDNA. Following the delivery of Rad51 onto ssDNA with Rad52, the Rad51

nucleoprotein filament extends and is stabilized by the mediators, Rad55 and Rad57 **(Figure 1.7 d)**, which are referred to as Rad51 paralogs and form a stable heterodimer that binds to ssDNA and exhibits a weak ATPase activity. At the same time, RPA displaces from the ssDNA, and Rad55 mediates by interacting with Rad51 not RPA to stabilize Rad51 proteofilaments that the mediatory regulation is different from Rad52 exerting. (Krogh and Symington, 2004). In addition, the Rad55-Rad57 heterodimer promotes the Rad51 nucleoprotein filament locating a homologous DNA donor sequence, leading to Rad51-mediated strand exchange **(Figure 1.7 e)** (Krogh and Symington, 2004). Then, the mediator protein Rad54, which belongs to the Swi2/Snf2 chromatin remodeling protein family, interacts with Rad51 and promotes chromatin remodeling, DNA unwinding, and strand annealing between donor DNA and the incoming Rad51 nucleoprotein filament **(Figure 1.7 f)** (Krogh and Symington, 2004), where Rad54 stimulates the extension of the heteroduplex for strand exchange and disassociates Rad51 from the nucleoprotein filament formed on dsDNA to uncover the 3’ end of paired intermediates to initiate DNA repair synthesis (Solinger and Heyer, 2001; Solinger et al., 2002). However, in order to prevent unwanted HR events occurring, one of the mechanisms is through Srs2, which is a DNA helicase and DNA-dependent ATPase, removing Rad51 proteins away from the presynaptic nucleoprotein filament in a 3’-5’ direction; as well as the immediate occupation of ssDNA by RPA proteins to avoid reloading of Rad51 **(Figure 1.7 g)** (Krogh and Symington, 2004; Sung and Klein, 2006).

From the perspective of meiosis, it is important to direct DSB repair between homologous nonsister chromatids, and this is achieved by the formation of presynaptic nucleoprotein filaments with Rad51 as well as the meiosis-specific protein Dmc1, which has significant sequence and functional similarity to RecA and

Rad51, and has been observed to form octameric rings or helical filaments on DNA (Sung and Klein, 2006). Although both Rad51 and Dmc1 are necessary for meiotic recombination and harbor partial redundancy, their functions are still not completely identical with each other, according to the partial suppression of the *dmc1*Δ phenotype by overexpression of Rad51 (Tsubouchi and Roeder, 2003). The *dmc1*Δ mutants show defects in reciprocal recombination, accumulation of DSBs with around 200 resecting Spo11-DSBs and hundreds of kilobases of ssDNA intermediates, the failure to form a normal SC, and the arrest of late meiotic prophase (Bishop et al., 1992).

During meiosis, all Spo11-DSBs in eukaryotic individuals are able to be repaired as either crossovers or noncrossovers (Allers and Lichten, 2001a; Hunter and Kleckner, 2001). However, only a subset of these precursors can be repaired as crossovers, while the remaining is repaired as noncrossovers (Alberts et al., 2008; Thacker and Keeney, 2009). Taking the situation in a single *S. cerevisiae* cell for consideration, approximately 60% of the 140-170 Spo11-DSBs are processed into crossovers during meiosis; in other words, there are approximately 90 crossovers formed in *S. cerevisiae* meiosis to distribute over 16 homolog pairs (Nishant et al., 2010). In addition, the occurrence of crossovers and noncrossovers is not simply by chance, instead there is a sophisticated mechanism to regulate meiotic recombination (Thacker and Keeney, 2009). This ensures that each homolog pair obtains at least one crossover, regarded as the obligate crossover, and also controls the spatial distribution of crossovers along chromosomes, where a crossover in one interval decreases the possibility of additional crossovers occurring nearby, referred to as crossover interference; the inhibitory distance of which could be up to 60 kb according to the model proposed by Panizza et.al **(see the last paragraph in Section**

**1.4)**. It is ZMM proteins (Zip1/2/3/4, Msh4/5 and Mer3) and the recently mentioned pachytene checkpoint protein Pch2 that have been observed to be involved in the regulation of crossover interference (Thacker and Keeney, 2009). Furthermore, the phenomenon of crossover homeostasis maintains the crossover numbers at the expense of non-crossovers when the total number of DSB is reduced (Longhese et al., 2008; Thacker and Keeney, 2009). Several studies also imply that it is before Holliday junction resolution, prior to or during the formation of the first stable strand exchange intermediate, that the generation of crossovers or noncrossovers has been decided (Allers and Lichten, 2001b; Bishop and Zickler, 2004; Borner et al., 2004; Longhese et al., 2008).

## 1.6 Models for the Repair of DSBs in Meiotic Recombination

During meiosis, the occurrence of the programmed Spo11-induced DSB formation initiates DNA resection from the 5' to 3' ends of the DSBs **(Figure 1.5)**, and thus exposes 3' single-stranded DNA (3' ssDNA) tails **(Figure 1.8 a)**. Then, these ssDNA tails assemble as the presynaptic nucleoprotein filaments **(Figure 1.7)** that are active in strand invasion and prefer using homologous nonsister chromatids as the donor templates to form homologous heteroduplexes, or D-loops (displacement loops, which refers to all the DNA structures formed between a main double-stranded DNA and a third strand of DNA containing the complementary sequence to one strand of the main dsDNA pairing with it by displacing the other main strand in the region), and are extended by DNA synthesis within the D-loops **(Figure 1.8 a)**. If the displaced strand of the D-loop cannot pair with the other 3' ssDNA tail of the DSB, the 3' ssDNA tail with nascent DNA will be channeled into the

*Picture source: Chen et al., 2007.*

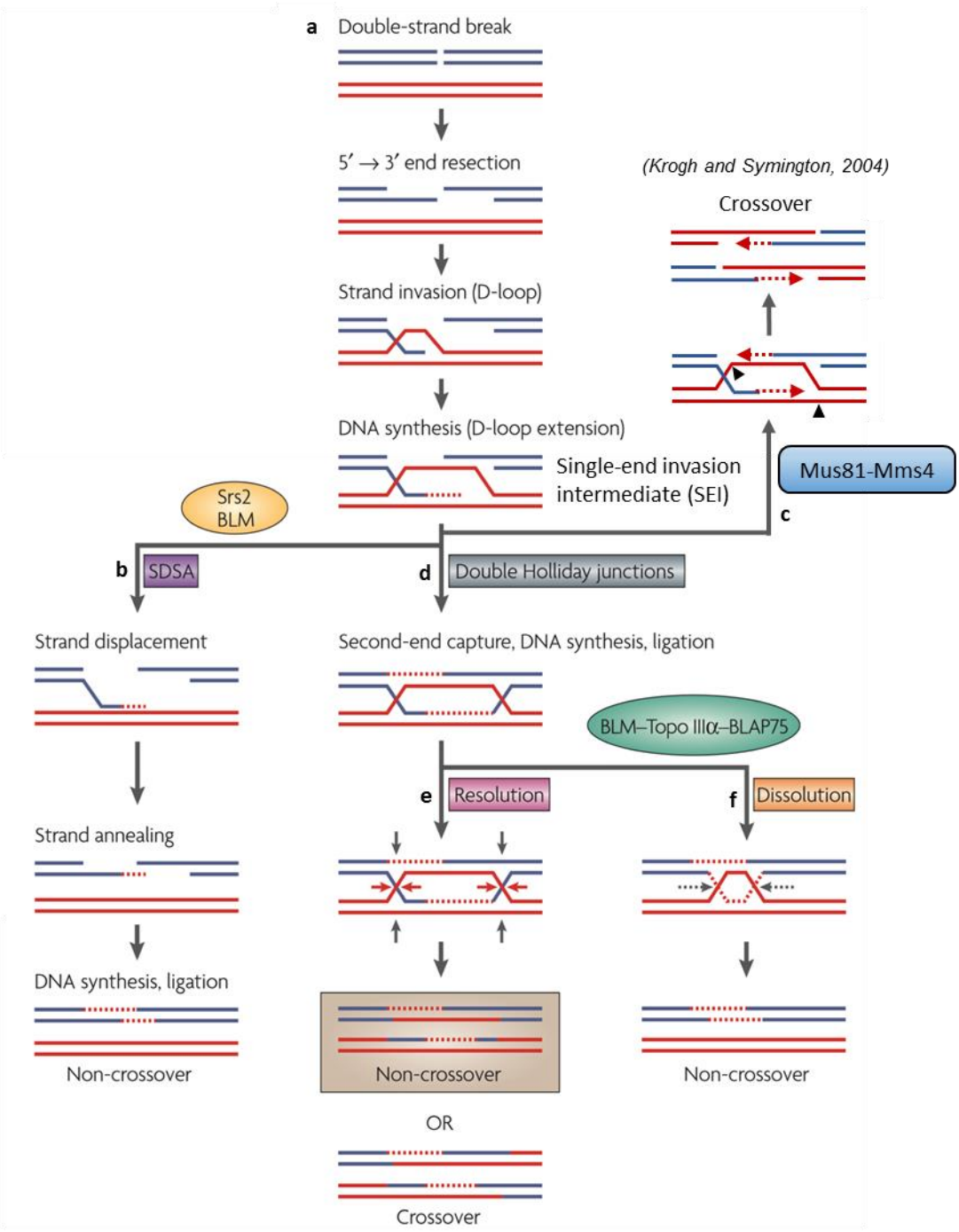


**Figure 1.8 Models for the repair of double-strand breaks (DSBs). (a)** When a DSB occurs, it initiates resection from the 5' to 3' end of the DSB that generates 3' ssDNA tails. These ssDNA are active in strand invasion, thus forming the D-loop. **(b)** In SDSA, the nascent DNA displaces from the homologous sequence and anneals to the other end of the DSB to produce non-crossover products. **(c)** Or, the unligated SEI can be resolved by the Mus81-Mms4/Eme1 endonuclease to result in crossover. **(d)** When second-end capture occurs, dHJs are formed. **(e)** Resolution of a dHJ leads to the double-strand break repair pathway (DSBR) with cleavage of these HJs in either the same or the opposite direction, thereby resulting in non-crossover and crossover, respectively. **(f)** Alternatively, instead of resolving a dHJ, branch migration can address the dHJ to yield non-crossover products, via the double Holliday junction dissolution pathway.

synthesis-dependent strand-annealing pathway (SDSA) **(Figure 1.8 b)**, where the nascent DNA displaces from the homologous donor sequence and anneals back to the other end of the DSB, using DNA synthesis and ligation to fill the gaps, thus producing noncrossovers (Chen et al., 2007; Krogh and Symington, 2004; Longhese et al., 2008). If, the displaced strand captures the other side of the DSB, second-end capture, it forms a single-end invasion intermediate (SEI) prior to dHJ formation and can be resolved by the Mus81-Mms (Eme1) endonuclease to produce crossover products **(Figure 1.8 c)** (Krogh and Symington, 2004). On the other hand, if second-end capture occurs and results in formation of the dHJ intermediate **(Figure 1.8 d)**, this dHJ can be channeled into the double-strand break repair pathway (DSBR) and be resolved in either the same or opposing directions to repair the DSB, resulting in noncrossover and crossover products, respectively **(Figure 1.8 e)** (Chen et al., 2007; Krogh and Symington, 2004; Longhese et al., 2008). Alternatively, instead of resolution of the dHJ, branch migration addresses the dHJ intermediate by BLM (Sgs1 in *S. cerevisiae*), a helicase of the RecQ family, and TOP IIIα to yield noncrossovers, via the double Holliday junction dissolution pathway **(Figure 1.8 f)** (Chen et al., 2007; Krogh and Symington, 2004). Gene conversion events are associated with these models, but it is in the DSBR pathway or via the Mus81-Mms (Eme1) endonuclease that crossover products are generated. Moreover, the DSBR model adequately explains several features of meiotic recombination, while many mitotic gene conversion events are not related to crossovers and are led from the SDSA pathway (Krogh and Symington, 2004; Longhese et al., 2008).

Another repair model is single-strand annealing (SSA), which is restricted to DSBs occurring between direct repeats **(Figure 1.9)** (Krogh and Symington, 2004). When resection is sufficient to reveal complementary single-stranded regions, these

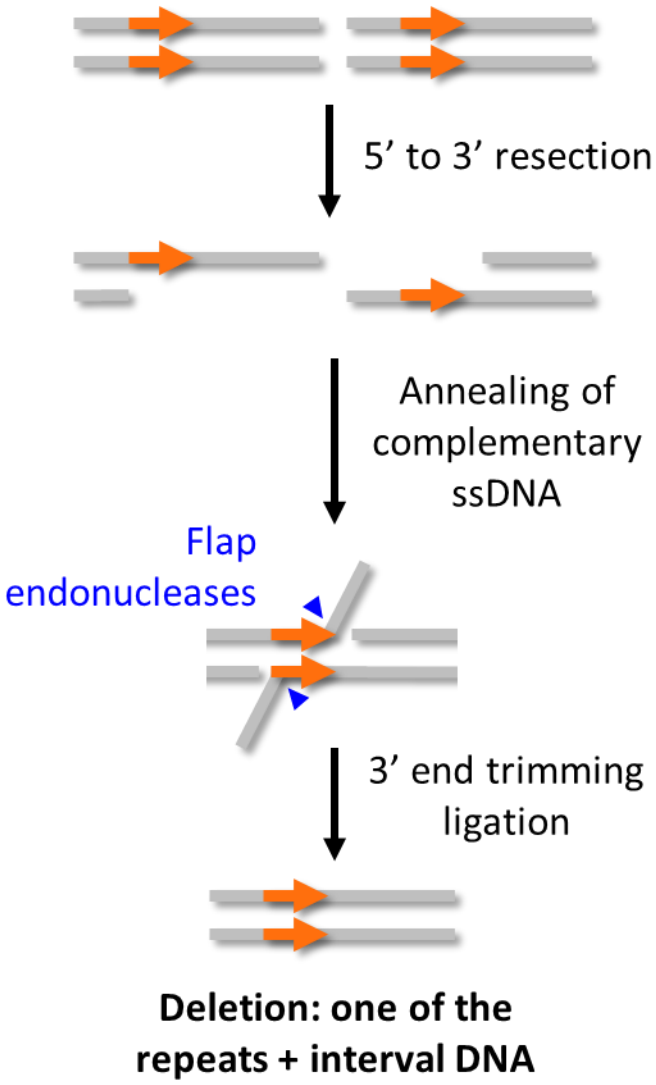


**Figure 1.9 Model of the single-strand annealing (SSA).** In SSA model, the resection is sufficient to reveal complementary single-stranded regions that can anneal together to generate 3’ ssDNA overhangs and these can be removed by flap endonucleases. This process is accompanied by deleting one of the repeats and the interval DNA between the direct repeats.

regions then pair together to expose the 3’ ssDNA overhangs that are removed by flap endonucleases, and the gaps are filled in by DNA synthesis and ligation. This process is accompanied by deleting one of the repeats and the interval DNA between the direct repeats. This could conceivably be important for repairing genomes in higher eukaryotes that contain many repeated sequences (Fishman-Lobell et al., 1992; Lin et al., 1984; Maryon and Carroll, 1991).

## 1.7 Mechanisms and Regulation of DSB End Resection in Detail

The first process for all HR pathways is DNA resection **(Figure 1.5)**, in which mitotic and meiotic DSBs undergo nucleolytic degradation of their 5’-ending strands and thus the resulting 3’ single-stranded DNA can be exposed and form nucleoprotein filaments to invade homologous templates and repair the DSBs (Sun et al., 1991; White and Haber, 1990). The average resection tract in nature of meiotic Spo11-DSBs is 800 nucleotides (Mimitou and Symington, 2011). Moreover, because the failure to perform and regulate ssDNA production at DSB ends results in a threat to genome stability and contributes to the development of human diseases, such as cancers, the mechanisms and regulation of DSB end resection play very important and essential roles in preventing aberrant DSB repair events from occurring and thus maintains genetic integrity (Longhese et al., 2010). In addition, most proteins involved in resection have been well uncovered and studied in mitosis, but are less known in meiosis. Therefore, the mechanisms and regulation of resection introduced here are basically according to that which occurs during mitosis.

## Mechanisms of DSB End Resection

Once a DSB occurs in mitotic cells, the first group of proteins recruited to the DSB ends is the highly conserved MRX/MRN complex (Lisby et al., 2004), and the Ku70/80 heterodimer is also loaded onto the DSB ends at almost the same time (Longhese et al., 2010). In addition, the decision of which DSB repair mechanisms to be used is dependent on the nature of the DSB and the cell cycle phase in which the damage has occurred (Longhese et al., 2010). If a DSB is detected in the G1 phase, resection is normally prohibited by the Ku proteins, which together with the MRX/MRN complex recruit the downstream NHEJ factors (Lif1, Dnl4 and Nej1) to religate the DSB ends (Chen et al., 2001; Clerici et al., 2008; Lee et al., 1998; Palmbos et al., 2008; Zhang et al., 2007), and thus the DSB is repaired through the NHEJ pathway; conversely, if a DSB is detected in the S or G2 phase, resection is activated to generate 3’ ssDNA tails that inhibit NHEJ and target DSB repair to HR (Longhese et al., 2010). It is thought that the MRX complex together with Sae2 promote the initial processing of resection by making an endonucleolytic cleavage at each 5’ strand, which reduces the ability of Ku protein binding on the ends of DSBs; and the 3’-5’ exonuclease function of Mre11 within the MRX complex catalyzes the removal of oligonucleotides from the nicks of the 5’ strands to generate short 3’ ssDNA tails (Longhese et al., 2010). Then, the resulting partially resected 5’ strands can be further processed by either Exo1 or Sgs1 and Dna2. However, in the absence of either Mre11 or Sae2, this metabolism of initial resection could be compensated for Exo1, which is a member of the Rad2/XPG family of nucleases and contains both 5’-3’ dsDNA exonuclease and flap-endonuclease activities (Longhese et al., 2010). This is according to the partial suppression of the DSB repair and resection defects in the *mrx* null mutants by overproduction of Exo1 (Lewis et al., 2002; Mantiero et

al., 2007; Moreau et al., 2001; Tsubouchi and Ogawa, 2000), as well as the synergistic resection impairment shown in *exo1*Δ *sae2*Δ and *exo1*Δ *mre11*Δ double mutants compared to each single mutant (Clerici et al., 2006; Nakada et al., 2004). Also, the lacking nuclease function of Mre11 and Sae2 single mutants shows partial defects in the processing of DSB ends (Clerici et al., 2005; Furuse et al., 1998; Llorente and Symington, 2004; Moreau et al., 1999; Tsubouchi and Ogawa, 1998). All these phenotypes are observed under the production of DSBs with clean ends; therefore, it also indicates that the resection of 5' strands from clean DSB ends does not necessarily require the MRX-Sae2 activity, and these clean DSB ends can be substrates not only to the MRX-Sae2 but also directly to Exo1 for resection (Longhese et al., 2010). Nevertheless, MRX-Sae2 is crucial for processing the initial resection of modified/blocked DSB ends, such as those formed by Spo11 in meiosis **(see Section 1.4 for details)** or after exposure to ionizing radiation (IR), bleomycin or methylating agents (Krogh and Symington, 2004; Longhese et al., 2010). Moreover, the nuclease function of Mre11 and Sae2 are necessary for the removal of modified terminal nucleotides or protein-DNA products from DSB ends and the start of resection. In fact, both *mre11-nd* and *sae2*Δ mutants display marked hypersensitivity to camptothecin that traps covalent topoisomerase I-DNA complexes in mitotic cells (Adams et al., 1997; Deng et al., 2005; Liu et al., 2002; Longhese et al., 2010), and also show no resection in meiotic DSBs where Spo11 proteins still covalently bind on the breaks **(see Section 1.4 for more details)**.

Not only Exo1 but also the Sgs1-Dna2 proteins have been indicated as being able to directly resect clean DSB ends in the absence of the initial processing step by the MRX-Sae2, as well as taking responsibility for the long-range 5'-strand resection, also known as the further resection **(Figure 1.5)**. In fact, in the *sgs1*Δ *exo1*Δ double

mutant strains, it has been shown that the long-range resection of an HO-induced DSB is abolished, and only some minimal processing can be detected, which depends on both Mre11 and Sae2 and generates only a few hundred nucleotides of 3' ssDNA from the break site; suggesting that the MRX-Sae2 initiates the resection that is then extended by Exo1 and/or Sgs1 (Gravel et al., 2008; Longhese et al., 2010; Mimitou and Symington, 2008; Zhu et al., 2008). Moreover, according to the more severe resection impairment shown under the *mre11*Δ than the *mre11-nd* mutant background (Clerici et al., 2005; Llorente and Symington, 2004; Moreau et al., 1999), it suggests that the integrity of the MRX complex is more important than the nuclease activity of Mre11 in fully exerting the functions of Exo1, Sgs1, and/or Dna2, which can even so process the clean DSB ends without the MRX-Sae2 (Longhese et al., 2010). Sgs1 is a nucleolar DNA helicase of the RecQ family and is homologous to the human BLM and WRN helicases, whereas Dna2 seems to be a Sgs1-associated protein and is a tripartite DNA replication factor with one potential regulatory domain at the N-terminus and two catalytic domains for ATP-dependent nuclease and single-stranded DNA-dependent ATPase/helicase activity located at the middle and C-terminal regions respectively (Bae et al., 2001; Longhese et al., 2010). In addition, Dna2 has also been shown to function in the processing of Okazaki fragments during DNA replication (Bae et al., 2001). However, it is only the nuclease function of Dna2 that is required for DSB resection despite harboring both nuclease and helicase activities (Zhu et al., 2008). This is consistent with the helicase-nuclease coupling model that seems to be a general mechanism for catalyzing DSB resection, in which Sgs1 unwinds DSB ends first and then lets Dna2 remove the 5' strands by its nuclease activity (Longhese et al., 2010). Depletion of *SGS1* or *DNA2* results in a delay of the resection progress of an HO-induced DSB and reduction of SSA repair, while the remaining processing of long-range resection depends on Exo1 proteins

(Zhu et al., 2008). Moreover, although the function of Dna2 is unclear in vertebrates, BLM and hExo1 have been shown to be involved in the DSB resection of human beings, where BLM physically interacts with hExo1 and enhances the efficiency of hExo1-mediated degradation of 5’ strands to generate 3’ ssDNA tails that are the substrates to hRad51 for the processing of strand invasion and HR (Nimonkar et al., 2008). Then, these observations suggest that Sgs1 can provide unwound DSB ends as substrates for Exo1, not only for Dna2.

During meiosis, Exo1, Sgs1 and Dna2 have also been verified to be involved in the lengthening of resection tracts at Spo11-induced DSBs, while they are not required for the removal of Spo11 from the 5’ ends of DSBs, suggesting that the initiation and elongation steps of meiotic DSB resection depend on distinct sets of nucleases and their associated proteins (Longhese et al., 2010; Manfrini et al., 2010). Under the *dmc1*Δ background that ensures visualization of the resected intermediates, simultaneous inactivation of Sgs1 and Exo1 causes the severest reduction of DSB resection among the set of mutants, but while there is no significant defect under the Sgs1 repression alone there is impairment in the *EXO1* deletion, implying that the further resection of meiotic DSBs is controlled by two different mechanisms involving Sgs1 and Exo1 but with Exo1 having the major function (Manfrini et al., 2010). Due to the defects in the generation of the longest 3’ ssDNA tails in *dna2*Δ cells under the *dmc1*Δ and *pif1-M2* mutant background, Dna2 is also suggested to contribute to meiotic DSB resection and mainly to the long-range resection (Manfrini et al., 2010).

According to the severe meiotic phenotype of *mre11-nd* mutants, which show an accumulation of unresected meiotic DSBs and a failure to sporulate *in vivo*, the

nuclease function of Mre11 is also considered to play an important role in the further resection as well as the 5’ to 3’ exonucleases, even though the directionality of resection is greatly odds with its 3’ to 5’ exonuclease function (Krogh and Symington, 2004). However, this shows only mild to intermediate sensitivity to IR, mating-type switching and the resection of HO-induced DSBs in mitosis (Bressan et al., 1998; Furuse et al., 1998; Lee et al., 2002; Moreau et al., 1999). In addition, for meiotic DSB formation, it is the integrity of the MRX complex rather than its nuclease activity that have been shown to be required (Longhese et al., 2010).

## Regulation of DSB End Resection

It has been revealed that when DSBs occur during mitosis, the choice of repair of DSBs between NHEJ and HR is controlled by the activity of a cyclin-dependent protein kinase (CDK; Cdk1 or Cdc28 in budding yeast), which promotes the progression of resection to generate 3’ ssDNA tails that are required for HR and concomitantly inhibits NHEJ pathway due to its poor binding to ssDNA (Longhese et al., 2010). In addition, during the progression of the cell cycle, in different phases distinct combinations of cyclins (the regulatory subunits) and CDKs (the catalytic subunits) are needed to form the activated cyclin-CDK complexes that are required for cell cycle events to occur at the precise time and in the correct order; Cdk1 activity is low in the G1 phase but is high during the S and G2 phases (Alberts et al., 2008; Longhese et al., 2010). Therefore, Cdk1 activation in the S and G2 phases leads to the generation of 3’ ssDNA tails and subsequent HR, whereas only NHEJ occurs in the G1 phase (Longhese et al., 2010). The binding of Ku and the MRX complex to DSB ends occurs independently and almost at the same time (Wu et al., 2008), thus a lack of MRX increases the amount of DSB-bound Ku that can act as a blocker to prevent Exo1-mediated resection (Longhese et al., 2010).

The initiation of resection at both mitotic and meiotic DSB sites has been verified to rely on the phosphorylation of Sae2 Ser267 by Cdk1 (Huertas et al., 2008). In fact, the *sae2-S267A* mutants, which lack the phosphorylatable Ser267 because of replacement with an alanine residue, severely impair both mitotic and meiotic DSB resection, as well as damage the removal of Spo11 from meiotic DSB ends (Huertas et al., 2008). And, it is also shown that the same processes take place quite efficiently in both mitotic and meiotic mutants with the *sae2-S267E* allele, which contains a glutamic residue mimicking a constitutively phosphorylated Ser267 (Huertas et al., 2008). Moreover, the full activation of Sae2's meiotic function is thought to require Cdk1-dependent phosphorylation of additional residues, Ser134 and Ser179 (Manfrini et al., 2010). However, in the absence of phosphorylation events, the nuclease function of Sae2 is still detected *in vitro* (Longhese et al., 2010). Therefore, according to these different phenomena between *in vivo* and *in vitro*, it is implied that *in vivo* some unknown proteins inhibit Sae2 function, which can be released through Cdk1-dependent phosphorylation; alternatively, Sae2 may interact with some positive regulators of DSB resection to enhance its activity by Cdk1-mediated phosphorylation (Longhese et al., 2010). According to Henderson et al. (Henderson et al., 2006) and Wan et al. (Wan et al., 2008), Cdk1 activity is not only required for the processing of DSB resection, but also necessary to generate Spo11-induced DSBs in meiosis by phosphorylating the Mer2/Rec107 protein, that is one of the Spo11 accessory proteins, thereby modulating the interactions of Mer2 with other proteins required for DSB formation, such as Rec114, Mei4 and Xrs2. Thus, Cdk1 activity coordinates the DSB formation and resection with meiotic progression.

In order to ensure the cell cycle progresses in an exact and precise way, the checkpoint mechanisms are evolved to act as the surveillance for monitoring ongoing cell cycle events and relaying this information to other processes, thus causing the cell cycle arrest (through the deactivation of cyclin-Cdk functions by modification or degradation of cyclins, or inactivating Cdks by inhibitory phosphorylation or CKIs/Cdk inhibitory proteins) and activation of repair systems, if necessary, to resolve damage errors and then proceed to the cell cycle events (Alberts et al., 2008; Cheng et al., 2013). The major players which are involved in the DNA damage checkpoint mechanism during mitosis and meiosis are ATM (ataxia telangiectasia mutated) and ATR (ataxia telangiectasia and Rad3-related protein) in mammals and their respective homologs Tel1 and Mec1 in *S. cerevisiae* (Longhese et al., 2006). During the mitotic cell cycle, ATM/Tel1 appears to bind unprocessed DSBs via the MRX/MRN complex, and its signaling activity is disrupted when the ends of DSBs are resected (Mantiero et al., 2007; Nakada et al., 2003), whereas, ATR/Mec1 is thought to recognize ssDNA that arise after DSB processing (Zou and Elledge, 2003). These four proteins belong to serine/threonine-specific protein kinases and preferentially phosphorylate their substrates at serine (S) and threonine (T) residues that precede glutamine (Q) residues, so called the SQ/TQ motifs (Carballo et al., 2008). Once a mitotic DSB occurs, at each side of the break the MRX/MRN complex recruits Tel1/ATM and its binding partner Tel2 to these unresected DSB ends (Falck et al., 2005; Nakada et al., 2003; Usui et al., 2001; You et al., 2005). The activation of Sae2 has been shown to be mediated by Cdk1- and Tel1/ATM-dependent phosphorylation events, in which Sae2 Ser134, 179 and 267 are the targets for Cdk1 (Manfrini et al., 2010) while the SQ/TQ motifs are preferred for Tel1/ATM (and Mec1/ATR later) (Baroni et al., 2004), to initiate the DSB resection and thereby detach Ku proteins from the DSB ends, promoting further resection by Exo1, Sgs1

and Dna2 (Longhese et al., 2010). The 3’ ssDNA tails coated with RPA proteins then allow the recruitment of Mec1/ATR via its binding partner Ddc2 (Navadgi-Patil and Burgers, 2009), and Sae2 is subsequently phosphorylated by Mec1/ATR to contribute to potentiating resection (Longhese et al., 2010). Thus, it is implied that DSB resection regulates not only the transition from NHEJ to HR, but also from the Tel1/ATM- to Mec1/ATR-controlled checkpoints (Longhese et al., 2010).

In meiosis, Tel1/ATM and Mec1/ATR also participate in the pachytene checkpoint (also named the chromosome synapsis checkpoint or the meiotic recombination checkpoint) (Lydall et al., 1996; Roeder, 1997; Roeder and Bailis, 2000), which is activated by incomplete assembly of the SC or inadequate repair of Spo11-induced DSBs, to cause the pachytene arrest that prevents the failure of meiotic recombination and synapsis to occur. However, some studies have revealed that pachytene checkpoint mainly monitors the leptotene-zygotene transition, not the pachytene stage (Borner et al., 2004; Zickler and Kleckner, 1998). On the other hand, the cell cycle progression at the pachytene stage is also achieved by the regulation of Cdc28 function, and the loss of Cdc28 activity has been shown to result in pachytene arrest (Shuster and Byers, 1989), suggesting that during the pachytene stage Tel1/ATM and Mec1/ATR are activated to inhibit the Cdc28 function that promotes pachytene arrest to ensure the formation of synapsis is completely achieved. In addition, Sae2 has also shown that its meiotic resection function still requires the Tel1/ATM and Mec1/ATR phosphorylation (Baroni et al., 2004).

## 1.8 Project Summary

The aim of this thesis was to characterize the relative roles of Mre11, Exo1 and Tel1 in the process of resection during meiosis. To accomplish this, we have created a system that generates a DSB by the site-specific endonuclease VDE, which does not bind covalently to the DSB ends, thus allowing us to model the role of our proteins of interest after Spo11 would have been removed. In addition, this DSB is only allowed to repair through single strand annealing (SSA), which requires resection to uncover sequence repeats located on the two sides of the break to produce deletion products. We have used Southern blotting and have also developed the loss of RE site assay with qPCR, which is able to accurately quantify ssDNA levels at regular intervals on both side of VDE-DSB, to analyze the repair ability and monitor the processive resection of different genetic mutant backgrounds.

# *Chapter 2*

# Materials and Methods

## 2.1 *Saccharomyces cerevisiae* Strains Used in this Study

All of the strains used in this study are listed below and based on SK1 cells:

| **Diploid strains** | | | |
|---|---|---|---|
| **Name**<br>**Description** | **Haploid cross** | **Genotype** | **Source** |
| dAG630<br>**Wild-type** | hAG416<br>x<br>hAG684 | *MATα lys2 ho::LSY2 leu2 arg4-nsp,bgl ura3*<br>*MATa lys2 ho::LYS2 leu2 ARG4 ura3 ade2Δ nuc1::LEU2*<br>*ade2::ura3-[arg4-vde]-URA3 nuc1::LEU2 TFP1::VDE*<br>*TFP1* | Anna E Bishop-Bailey |
| dAG1201<br>***sae2Δ*** | hAG1156<br>x<br>hAG1159 | *MATa lys2 ho::LSY2 LEU2 ARG4*<br>*MATα lys2 ho::LYS2 leu2-R arg4-nsp,bgl ura3 ade2::ura3-[arg4-vde]-URA3*<br>*ura3 ade2Δ TFP1 sae2Δ::KanMX*<br>*TFP1::VDE sae2Δ::KanMX* | Anna E Bishop-Bailey |
| dAG1305<br>***exo1Δ*** | hAG1253<br>x<br>hAG1257 | *MATa lys2 ho::LSY2 leu2 arg4-nsp,bgl ura3*<br>*MATα lys2 ho::LYS2 leu2 ARG4 ura3 ade2Δ nuc1::LEU2*<br>*ade2::ura3-[arg4-vde]-URA3 nuc1::LEU2 TRP1 TFP1::VDE exo1Δ::KanMX*<br>*Trp1::hisG TFP1 exo1Δ::KanMX* | Anna E Bishop-Bailey |
| dAG1589<br>***mre11-58S*** | hAG929<br>x<br>hAG944 | *MATa lys2 ho::LYS2 leu2-R/-K/::hisG?*<br>*MATα lys2 ho::LYS2 leu2-R/-K/::hisG? arg4-bgl/-nsp,bgl ura3*<br>*arg4-bgl/-nsp,bgl ura3 ade2Δ*<br>*ade2::ura3-[arg4-vde]-URA3* | This study |

| | | | |
|---|---|---|---|
| | | *his4::LEU2 TRP1 TFP1::VDE mre11-58S*<br>*HIS4 trp1::hisG TFP1 mre11-58S* | |
| dAG1592<br>***mre11-H125N*** | hAG1320<br>x<br>hAG1670 | *MATa lys2 ho::LYS2 LEU2 arg4-nsp,bgl*<br>*MATα lys2 ho::LYS2 leu2-R? arg4-nsp,bgl*<br>*URA3 ade2::ura3-[arg4-vde]-URA3*<br>*ura3 ade2Δ*<br>*TFP1 mre11-H125N*<br>*TFP1::VDE mre11-H125N* | This study |
| dAG1593<br>***mre11-H125N*, *exo1Δ*** | hAG1673<br>x<br>hAG1674 | *MATa lys2 ho::LSY2 leu2-*<br>*MATα lys2 ho::LYS2(VMA1-201?) LEU2*<br>*arg4-nsp,bgl ura3*<br>*arg4-nsp,bgl ura3?*<br>*ade2Δ TFP1::VDE*<br>*ade2::ura3-[arg4-vde]-URA3 TFP1*<br>*mre11-H125N exo1Δ::KanMX*<br>*mre11-H125N exo1Δ::KanMX* | This study |
| dAG1624<br>***spo11-Y135F*, *exo1Δ*** | hAG1728<br>x<br>hAG1729 | *MATα lys2 ho::LSY2 leu2?*<br>*MATa lys2 ho::LYS2(VMA1-201?) LEU2*<br>*arg4-nsp,bgl ura3*<br>*ARG4 ura3/ura3::URA3-[arg4-vde]?*<br>*ade2Δ nuc1::LEU2?*<br>*ade2::ura3-[arg4-vde]-URA3 NUC1*<br>*TRP1 TFP1::VDE*<br>*trp1::hisG? TFP1*<br>*spo11-Y135F-HA3His6::KanMX*<br>*spo11-Y135F-HA3His6::KanMX*<br>*exo1Δ::KanMX*<br>*exo1Δ::KanMX* | This study |
| dAG1629<br>***tel1Δ*, *exo1Δ*** | hAG1750<br>x<br>hAG1751 | *MATa lys2 ho::LSY2 leu2-R/::hisG?*<br>*MATα lys2 ho::LYS2 leu2::hisG*<br>*arg4-nsp/nsp,bgl? ura3*<br>*ARG4 ura3*<br>*ade2Δ nuc1::LEU2*<br>*ade2::ura3-[arg4-vde]-URA3 NUC1*<br>*his4::LEU2? TRP1 TFP1::VDE*<br>*HIS4 trp1::hisG? TFP1* | This study |

| | | | |
|---|---|---|---|
| | | *tel1Δ::HphMX exo1Δ::KanMX*<br>*tel1Δ::HphMX exo1Δ::KanMX* | |
| dAG1636<br>***tel1Δ*** | hAG1768<br>x<br>hAG1769 | *MATa lys2 ho::LSY2 leu2::hisG?*<br>*MATα lys2 ho::LYS2 leu2::hisG?*<br>*arg4-nsp/nsp,bgl? ura3*<br>*arg4-nsp? ura3*<br>*ade2Δ nuc1::LEU2*<br>*ade2::ura3-[arg4-vde]-URA3 nuc1::LEU2?*<br>*his4::LEU2? TRP1 TFP1::VDE*<br>*his4::LEU2? trp1::hisG? TFP1*<br>*tel1Δ::HphMX*<br>*tel1Δ::HphMX* | This study |
| dAG1638<br>***tel1Δ, sae2Δ*** | hAG1778<br>x<br>hAG1780 | *MATα lys2 ho::LSY2 leu2::hisG?*<br>*MATa lys2 ho::LYS2 leu2::hisG?*<br>*arg4-nsp/nsp,bgl? ura3*<br>*arg4-nsp? ura3*<br>*ade2Δ nuc1::LEU2?*<br>*ade2::ura3-[arg4-vde]-URA3 nuc1::LEU2?*<br>*his4::LEU2 TFP1::VDE tel1Δ::HphMX*<br>*HIS4 TFP1 tel1Δ::HphMX*<br>*sae2Δ::KanMX*<br>*sae2Δ::KanMX* | This study |
| dAG1639<br>***sae2Δ, exo1Δ*** | hAG1782<br>x<br>hAG1785 | *MATα lys2 ho::LSY2 leu2-R/::hisG?*<br>*MATa lys2 ho::LYS2 leu2-R/-K/::hisG?*<br>*arg4-nsp,bgl ura3*<br>*arg4-nsp/nsp,bgl? ura3*<br>*ade2::ura3-[arg4-vde]-URA3 TFP1*<br>*ade2Δ TFP1::VDE*<br>*sae2Δ::KanMX exo1Δ::KanMX*<br>*sae2Δ::KanMX exo1Δ::KanMX* | This study |
| dAG1649<br>***pCLB2-MEC1, tel1Δ, exo1Δ*** | hAG1804<br>x<br>hAG1807 | *MATα lys2 ho::LSY2 leu2-R/::hisG?*<br>*MATa lys2 ho::LYS2 leu2::hisG?*<br>*arg4-nsp,bgl ura3*<br>*ARG4 ura3*<br>*ade2Δ nuc1Δ::LEU2?*<br>*ade2::ura3-[arg4-vde]-URA3 NUC1* | This study |

| | | | |
|---|---|---|---|
| | | *his3::TRP1? trp1::hisG? SCC3-C-TAP?*<br>*his3::TRP1? trp1::hisG? SCC3-C-TAP? Clb2KanMX-6HA3mec1 tel1Δ::HphMX*<br>*Clb2KanMX-6HA3mec1 tel1Δ::HphMX exo1Δ::KanMX*<br>*exo1Δ::KanMX* | |

**Haploid strains**

| **Name** | **Genotype** | **Source** |
|---|---|---|
| hAG55 | *MATa ura2 (ura2 tester)* | Lab resource |
| hAG56 | *MATα ura2 (ura2 tester)* | Lab resource |

## 2.2 Growth and Culture of Yeast Strains

### 2.2.1 Media and Growth Conditions

All media were made up with $dH_2O$ and autoclaved on a standard program: no free steam and 15 minutes sterilization. The stocks of amino acid for supplements were prepared with $dH_2O$ and sterilized by filtering through 0.20 μm filters (sartorius stedim biotech). The growth condition for yeast strains in liquid cultures was normally at 30$^oC$ with 200 rpm shaking overnight and it normally took 1~2 days for yeast cell growth on solid media plates.

**YPAD Media**

It is the standard yeast growth medium, which contains 1% Bacto™ yeast extract (BD), 2% Bacto™ peptone (BD), 2% D-glucose (Fisher chemical), 40 mg/L adenine (Sigma) and 2% Bacto™ agar (BD) for solid media. Yeast strains with *KanMX* or *HphMX4* genes were selected on YPAD plates containing 200 μg/ml geneticin (G418) (MELFORD) and 300 μg/ml hygromycin B (Hyg) (Duchefa) respectively. Both G418 and Hyg were added to autoclaved YPAD when the medium became cooled to

55°C. For selection of *mre11* mutants, YPAD plates with 0.01% to 0.1% methyl methane-sulfonate (MMS) (Sigma) were used. MMS was added to autoclaved YPAD cooled to 55°C. These plates need to be used within 12 hours after pouring them and after 2 days the unused plates have to be discarded due to the degradation of MMS. Because MMS is volatile and hazardous, all the operations using MMS need to be under laminar flow hoods.

## Amino Acid and Base Stock Solutions

The stock solutions of amino acid were given as weight/volume (g/100 ml) and were made in $dH_2O$. Most of the stock solutions can be either autoclaved or filter sterilized, whereas arginine, aspartic acid, histidine, threonine, tryptophan and tyrosine solutions should be filter sterilized rather than autoclaved. All stock solutions were stored in the refrigerator except adenine, aspartic acid, glutamic acid, phenylalanine, threonine and uracil solutions, which should be stored at room temperature. Histidine and tryptophan solutions were kept in the dark. The amino acid reagents were obtained predominately from Sigma. The recipes for stocks of amino acid are shown in **Table 2.1**.

## Supplement Mixtures of Amino Acids

There are many compositions of amino acids to make supplement mixtures for preparing dropout media. To make a supplement mixture, the different desired components of amino acids were simply weighed out and mixed very well by shaking each time of addition. The weights of mixture components are shown in **Table 2.2**.

**Table 2.1 Stock solutions of amino acid for supplements.**

| Constituent | Stock conc. (g/100ml) | Volume of stock for 1 liter of medium (ml) | Final conc. in medium (mg/liter) | Volume of stock to spread on plate (ml) | Volume of stock for meiosis time course in 250 ml K-Acet medium (µl) |
|---|---|---|---|---|---|
| **Adenine sulfate** | 0.2[a] | 10 | 20 | 0.2 | 625 |
| **Uracil** | 0.2[a] | 10 | 20 | 0.2 | 625 |
| **L-Tryptophan** | 1 | 2 | 20 | 0.1 | 125 |
| **L-Histidine HCl** | 1 | 2 | 20 | 0.1 | 125 |
| **L-Arginine HCl** | 1 | 2 | 20 | 0.1 | 125 |
| **L-Methionine** | 1 | 2 | 20 | 0.1 | 125 |
| **L-Tyrosine** | 0.2 | 15 | 30 | 0.2 | 937.5 |
| **L-Leucine** | 1 | 10 | 100 | 0.1 | 625 |
| **L-Isoleucine** | 1 | 3 | 30 | 0.1 | 187.5 |
| **L-Lysine HCl** | 1 | 3 | 30 | 0.1 | 187.5 |
| **L-Phenylalanine** | 1[a] | 5 | 50 | 0.1 | 312.5 |
| **L-Glutamic acid** | 1[a] | 10 | 100 | 0.2 | 625 |
| **L-Aspartic acid** | 1[a,b] | 10 | 100 | 0.2 | 625 |
| **L-Valine** | 3 | 5 | 150 | 0.1 | 312.5 |
| **L-Threonine** | 4[a,b] | 5 | 200 | 0.1 | 312.5 |
| **L-Serine** | 8 | 5 | 400 | 0.1 | 312.5 |

**[a]Store at room temperature. [b]Add after autoclaving the medium. Conc. is abbreviated from concentration.**

| Constituent | “mg” in supplement mixture |
|---|---|
| **Adenine** | 800 |
| **Arginine** | 800 |
| **Aspartic acid** | 4000 |
| **Histidine** | 800 |
| **Leucine** | 2400 |
| **Lysine** | 1200 |
| **Methionine** | 800 |
| **Phenylalanine** | 2000 |
| **Threonine** | 8000 |
| **Tryptophan** | 800 |
| **Tyrosine** | 1200 |
| **Uracil** | 800 |

**Table 2.2 Weights of amino acids for making supplement mixtures.**

## Dropout Media (SC-)

One liter of dropout medium contained 6.8 g Difco™ Yeast nitrogen base without amino acid (BD), 20 g D-glucose (Fisher Chemical), 0.87 g supplement mixture of amino acids mentioned above (for preparing SC-THR and SC-ASP media, 0.54 g of supplement mixture was used instead), 200 µl of 10 N NaOH (Fisher Chemical) for the medium to become pH 5.5 and 20 g Bacto™ agar (BD) for solid plates. The selection markers test took one overnight growth at 30°C after replicating the cell patches, which were already grown on YPAD plates, to dropout plates.

## Minimal Plates

For identification of diploid cells and the mating type test of haploid cells with hAG55a and hAG56α **(Section 2.1)**, minimal plates were used. There were made up of 0.67% Difco™ Yeast nitrogen base without amino acid (BD), 2% D-glucose (Fisher Chemical) and 2% Bacto™ agar (BD). The growth conditions for identification of diploid cells and mating type test of haploid cells were 30°C overnight after replicating the cell patches, which were already grown on YPAD plates together with hAG55a and hAG56α respectively, to minimal plates.

## Potassium-Acetate Plates (K-Acet Plates)

For dissection to receive haploid tetrads, sporulation media, K-Acet plates, were used. There included 1% potassium-acetate (Sigma-Aldrich), 0.1% Bacto™ Yeast extract (BD), 0.05% D-glucose (Fisher Chemical) and 2% Bacto™ agar (BD). After diploid cell patches already grown on YPAD plates were replicated to K-Acet plates, they needed to be incubated at 30°C for 2 days to sporulate.

### 2.2.2 Production of Single Yeast Colony

Stocks of cells were streaked out from -80$^{o}$C glycerol stocks or from cell patches on solid media, onto fresh YPAD plates **(Section 2.2.1)** by using sterilized flat-bladed toothpicks or loops (COPAN). Then, single colonies were allowed to grow at 30$^{o}$C for 48 hours. To receive single colonies of diploid strains, cells were always streaked out from -80$^{o}$C glycerol stocks instead of from solid media to reduce the probability of spontaneous sporulation or papillation, especially in the strains containing VDE-DSB2 system cassettes **(Figure 3.2)**.

### 2.2.3 Standard 5 ml Yeast Cultures

After receiving single colonies shown in the previous step, a single colony was picked up by a sterilized loop (COPAN) and inoculated into 5 ml fresh YPAD medium **(Section 2.2.1)** in a sterile glass culture tube. Then, the culture was grown at 30$^{o}$C for 16-17 hours overnight using a rotor drum (New Brunswick). These standard 5 ml yeast cultures were used for yeast genomic DNA preparation, synchronous sporulation, transformation of haploid strains and making -80$^{o}$C glycerol stocks for storage of yeast strains.

## 2.3 Construction of Yeast Strains with Desired Genotypes

There are two major strategies for making yeast strains with desired genotypes, one is using general genetic methods and the other is by transformation of haploid yeast strains with DNA cassettes containing selectable markers (or) together with epitope tags (like GFP, His or Myc tags et al.) or the desired genetic manipulation (such as *arg4-vde* or *arg4-vde-VRS* et al.), which are flanked by partial homologous

regions for integrating into a specific gene locus. The steps of procedures are followed.

### 2.3.1 General Genetic Methods

#### 2.3.1.1 Mating Haploid Yeast Strains

The haploid strains with opposite mating type (*MAT*a/α) for constructing a new clone were streaked out on YPAD plates and incubated at 30°C for 2 days to receive single colonies **(Section 2.2.2)**. Then, colonies with similar size of each mating type cells were mixed together in a small area of approximately 0.5-1 $cm^2$ on an YPAD plate to make a mating patch. Haploid cells were allowed to mate for 1 to 2 days at 30°C. After which, cells were streaked out from the mating patch and allowed to grow at 30°C for another 2 days. Then, 8 single candidate colonies were selected and patched on an YPAD plate at 30°C overnight for further diploid test or tetrad dissection **(Section 2.3.1.2 and 2.3.1.3)**.

#### 2.3.1.2 Identification of Diploid Cells by Replicas

Before proceeding with this method, YPAD plates containing the lawns of haploid tester strains, hAG55a and hAG56α **(Section 2.1)**, were prepared respectively in advance by simply spreading out 150-200 µl of 5 ml standard overnight cultures per YPAD plate. Here, these YPAD plates with the lawns of hAG55a and hAG56α were abbreviated to YPAD55a and YPAD56α respectively. Because the auxotrophic requirements of haploid strains can be complemented by haploid tester strains with the opposite mating type, the absence of growth on minimal plates **(Section 2.2.1)** can distinguish diploid from haploid cells by mixing candidate strains resulting from a cross with haploid tester strains. The patches of

candidate diploid strains **(Section 2.3.1.1)** were crossed respectively with hAG55a and hAG56α from YPAD55a and YPAD56α plates by replicating cells on fresh YPAD plates. After one day growth at 30$^{o}$C, the cells were replicated to minimal plates and incubated at 30$^{o}$C overnight. Then, the diploid strains were identified and stored at -80$^{o}$C **(Section 2.3.1.12)**.

### 2.3.1.3 Sporulation of Diploid Strains and Tetrad Dissection

The patches of candidate strains on YPAD plates **(Section 2.3.1.1)** were replicated to K-Acet plates **(Section 2.2.1)** to allow diploid cells to sporulate at 30$^{o}$C for 2 days. After that, the candidate strains were checked for tetrads under the microscope and the diploid strains could be isolated to do tetrad dissection. A small amount of diploid cells on K-Acet plates were scraped out by a sterilized loop (COPAN) filling the hole of loop. Then, the cells were transferred to 20 µl of a 1 in 10 dilution of β-glucuronidase (Roche) and incubated at 30$^{o}$C for 20 minutes to release spores from the ascus. After treatment with β-glucuronidase, the density of cells was diluted by adding 500 µl of autoclaved water and 20 µl of the diluted cells was taken out and dropped down along a line at the bottom of a flat YPAD plate (remembering to always keep the cells at the bottom of a plate). Then, the plate was placed under a laminar flow hood to dry the liquid and tetrad dissection was ready to proceed. The spores from 20 tetrads were arranged in order on a YPAD plate by using a micromanipulator (Singer) and were allowed to grow at 30$^{o}$C for 2 days.

### 2.3.1.4 Selection Markers and Mating Type Test of Haploid Yeast Strains by Replicas

After tetrad dissection and 2 days growth, the arrays of haploid colonies on

the YPAD plate were replicated to one YPAD plate for conservation, one YPAD55a plate and one YPAD56α plate **(Section 2.3.1.2)** for mating type test, and a set of dropout solid media **(Section 2.2.1)** or selective plates such as YPAD plates with G418 or Hyg **(Section 2.2.1)** to determine genotypes of temporary haploid strains. These replica plates were then incubated at 30°C overnight. Next day, the haploid colony arrays together with hAG55a and hAG56α were replicated to minimal plates **(Section 2.2.1)** and after another overnight growth at 30°C the mating type of the haploid strains were revealed. Through checking the selection markers and mating types, the haploid strains with desired genotypes and opposite mating types (*MAT*a and *MAT*α) were selected to form diploid strains **(Section 2.3.1.1 and 2.3.1.2)** and were made into -80°C glycerol stocks **(Section 2.3.1.12)**. However, when there was no available auxotrophic/prototrophic or antibiotic resistance markers that could be used, diagnoses of PCR, yeast colony PCR and DNA sequencing of PCR products **(Section 2.3.1.8, 2.3.1.9 and 2.3.1.11 respectively)** were used to determine genotypes. For example, the insertion of *VDE* into *TFP1* promoter to create *TFP1::VDE* can be revealed by PCR or yeast colony PCR and the point mutation of *MRE11*, *mre11-58S* and *mre11-H125N* can be unveiled by DNA sequencing.

For constructing a diploid strain with the desired genotype, multiple crosses were often necessary to bring the desired allelic combination together in a single haploid strain. In addition, during strain construction there is an important consideration to be paid attention to; that is, in order to prevent the loss of the *VDE* cutting site within *AGR4* gene by intra-chromosomal repair or gene conversion with the other *ARG4* allele during meiosis, the mating between haploid strains containing *arg4-vde* allele and *TFP1::VDE* allele should be avoided until the final

diploid strains are formed.

### 2.3.1.5 Yeast Mini Preparation of Genomic DNA

In order to determine genotypes without available selection markers by PCR, yeast colony PCR or DNA sequencing of PCR products **(Section 2.3.1.8, 2.3.1.9 and 2.3.1.11 respectively)**, genomic DNA was prepared in this method.

## Solutions Used in this Method

**NOTE:** Normally all the stocks of buffers used in this study were made up with $dH_2O$ and can be autoclaved on a standard program: no free steam and 15 minutes sterilization except buffers containing volatile organic compounds, detergents (such as SDS) or heat sensitive chemicals.

- **Zymolyase Buffer:** 1.2 M D-sorbitol (Sigma), 10 mM Tris-HCl (pH 8.0) (Sigma) and 10 mM $CaCl_2$ (AnalaR).
- **Zymolyase 100T Solution:** Each ml of zymolyase buffer contained 0.7 mg zymolyase 100T (MP Biomedicals) and 1 % β-mercaptoethanol (Sigma), **prepared freshly**.
- **Lysis Buffer:** 50 mM Tris-HCl (pH 8.0) (Sigma), 50 mM disodium ethylene diamide tertacetate $2H_2O$ (EDTA) (Fisher Chemical) and 1.2 % sodium dodecyl sulfate (SDS) (Fisher Chemical).
- **Potassium-Acetate (K-Acet) Buffer:** 60 ml of 5 M K-Acet (Sigma-Aldrich), 11.5 ml of acetic acid (Fisher Chemical) and 28.5 ml of $dH_2O$.
- **3 M Sodium-Acetate (Na-Acet), pH 5.5.** (AnalaR)
- **RNase A, DNase free:** 10 mg/ml RNase A (Sigma) in 10 mM Tris-HCl (pH 7.5) (Sigma) and 22.5 mM NaCl (Fisher Chemical) was heated to 100$^{o}$C for 15 minutes and cooled slowly to room temperature, then stored at -20$^{o}$C.

- **100 % Isopropanol.** (Fisher Chemical)
- **70 % Ethanol.** (Fisher Chemical)
- **10x TE Buffer:** 100 mM Tris-HCl (pH 7.5) (Sigma) and 10 mM EDTA (pH 8.0) (Fisher Chemical).

1.5 ml of a standard yeast culture **(Section 2.2.3)** was used and was spun down in a microcentrifuge at 4,000 rpm for 1 minute. Most of the supernatant was drained off and the cell pellet was resuspended with the remaining supernatant by vortex or pipetting. Then, yeast cell walls were digested to produce protoplasts or spheroplasts by incubating with 250 µl of zymolyase 100T solution at 37$^{o}$C for 10-20 minutes (cells were checked regularly for producing protoplasts or spheroplats under the microscope). After which, 200 µl of lysis buffer was added and mixed by inverting the tube several times, making a thick gloopy mass. Then, 100 µl of K-Acet buffer was immediately added and mixed by inverting the tube several times again. To separate nucleic acids from cell debris and proteins, the thick sticky mass was spun down in a cooled (10$^{o}$C) microcentrifuge at 13,200 rpm for 10 minutes. Then, the supernatant was poured into a new 1.5 ml microcentrifuge tube and the white precipitate must be removed. To precipitate nucleic acids, 700 µl of 100 % isopropanol was added and mixed gently by inverting the tube, and then the pellet of nucleic acids was centrifuged at 13,200 rpm for 5-10 minutes. The supernatant was removed and the pellet was resuspended properly in 300 µl of 1x TE with 2 µl of 10 mg/ml RNase A to digest RNA at 37$^{o}$C for 15-30 minutes. The optional step of standard phenol chloroform extraction could be performed to further deproteinize the nucleic acid solution **(Section 2.3.1.7)**. Then, the DNA pellet was precipitated again by standard ethanol precipitation **(Section 2.3.1.6)** and was resuspended in 30-50 µl of 1x TE buffer

depending on the size of the DNA pellet.

### 2.3.1.6 Standard Ethanol DNA Precipitation

**Solutions Used in this Method**

**(See Section 2.3.1.5 NOTE)**

- **70 % Ethanol.** (Fisher Chemical)
- **100 % Ethanol or 100 % Isopropanol.** (Fisher Chemical)
- **3 M Sodium-Acetate (Na-Acet), pH5.5.** (AnalaR)
- **10x TE Buffer:** 100 mM Tris-HCl (pH 7.5) (Sigma) and 10 mM EDTA (pH 8.0) (Fisher Chemical).

In order to precipitate DNA, the nucleic acid solution was mixed in 1/10 volume of 3 M Na-Acet, pH5.5 followed by adding 2 volume of 100 % ethanol or isopropanol. Then, DNA was precipitated at -80$^{o}$C for 1 hour or -20$^{o}$C for overnight and harvested by centrifugation at 13,200 rpm for 10 minutes. The DNA pellet was washed at least twice in 70 % ethanol that was subsequently removed by aspiration. Then, normally within 5-10 minutes the white DNA pellet became transparent, which is an indicator to distinguish whether the DNA pellets were dry or not. After drying (not too dry), the DNA pellet was resuspended in an appropriate volume of 1x TE buffer.

### 2.3.1.7 Standard Deproteinisation of Nucleic Acid Solution and Cell Lysate Suspensions

**Solutions Used in this Method**

**(See Section 2.3.1.5 NOTE)**

- **Phenol : Chloroform : Isoamyl Alcohol (IAA) (25 : 24 : 1) Solution.** (Sigma,

Fisher Chemical and Sigma respectively)

- **Chloroform : IAA (24 : 1) Solution.** (Fisher Chemical and Sigma)

To denature and precipitate protein out of an aqueous sample, an equal volume of phenol : chloroform : IAA (25 : 24 : 1) solution was added and mixed well by agitation or inverting the tubes several times. Then, the aqueous phase containing nucleic acids was separated from the organic phase in which mainly phenol and proteins were by centrifugation at 13,200 rpm for 10 minutes. The upper aqueous phase was transferred to a new 1.5 ml microcentrifuge tube and mixed with one volume of chloroform : IAA (24 : 1) solution to ensure complete deproteinisation of the sample and to remove residual phenol. Then, the aqueous phase and the organic phase were separated again by centrifugation at 13,200 rpm for 10 minutes and nucleic acids were harvested from the upper aqueous phase by standard ethanol DNA precipitation **(Section 2.3.1.6)**.

### 2.3.1.8 Polymerase Chain Reaction (PCR)

For amplification of specific DNA regions or genetic loci, 30-100 ng of genomic or plasmid DNA was used for a 25 µl or 50 µl PCR reaction. One PCR reaction was also contained 1x Mango *Taq* reaction buffer (BIOLINE), 0.4 mM dNTP Mix (BIOLINE), 0.5 µM each of forward and reverse primers, 4 mM $MgCl_2$ solution (BIOLINE) and 5 units of Mango *Taq* DNA polymerase (BIOLINE). For a typical thermal cycle, DNA was denatured at 95$^{o}$C for 2 or 5 minutes followed by 30 cycles of 95$^{o}$C for 30 seconds, x$^{o}$C for 30 seconds and 72$^{o}$C for y seconds (x represents the primer specific annealing temperature and the extension time y is dependent on the amplicon length, namely 60 seconds per 1 kb), and then the reaction was terminated by a final extension step at 72$^{o}$C for 7 or 10 minutes. The primers and

the PCR programs used in this study were listed in **Table 2.3**.

### 2.3.1.9 Yeast Colony PCR

In order to select yeast strains with desired genotypes quickly and easily, yeast colony PCR could also be used instead of doing an extraction of genomic DNA first and then running PCR. A single colony or a small area of the candidate yeast patch was picked or scraped out with a 200 µl microtip, was resuspended in 30 µl of 0.1% NaOH (Fisher Chemical) and mixed well by pipetting up and down several times. Then, the cells were lysed at 95-100$^{o}$C for 15 minutes and were immediately chilled on ice. Most of the cell debris was roughly isolated with quick spin for 4-5 seconds and 5 µl of the supernatant near the pellet of cell debris was taken out as a crude DNA template to run PCR **(Section 2.3.1.8)**. Sometimes the annealing temperature of primers should be decreased 3-5$^{o}$C due to using the crude DNA as templates.

### 2.3.1.10 DNA Electrophoresis

#### Solutions and Chemicals Used in this Method

**(See Section 2.3.1.5 NOTE)**

- **Agarose.** (biogene.com)
- **6x DNA Loading Dye:** 30 % (v/v) glycerol (Fisher Chemical), 0.25 % (w/v) bromophenol blue (Sigma) and 0.25 % (w/v) xylene cyanol FF (Sigma). Store at 4$^{o}$C.
- **Ethidium Bromide Solution, 10 mg/ml in $H_2O$.** (Sigma-Aldrich)
- **50x Tris/Ac Electrophoresis (TAE) Buffer:** 242 g of Tris-Base (Sigma), 57.1 ml of acetic acid (Fisher Chemical) and 37.2 g of EDTA (Fisher Chemical) for 1 liter.

**Table 2.3 Synthetic oligonucleotide primers and PCR programs used in this study.**

| Name | Sequence | PCR program | Product size |
|---|---|---|---|
| **MNO3_VDE_For** | GGT ACA ATC ACT TGG ATT GCT CC | 94°C 2', (94°C 30", 55°C 30", 72°C 45") × 30 cycles, 72°C 7' | 1800 bp for *TFP1::VDE* and 460 bp for *TFP1* |
| **MNO4_VDE_Rev** | AAG CTT CTC TGG CTG CAA CCG GC | | |
| **MRE11_For** | GAG ATT ATG TTG CAT GGG TGA CAA G | 94°C 2', (94°C 30", 55°C 30", 72°C 2') × 30 cycles, 72°C 10' | ~600 bp |
| **MRE11_Rev** | AGC TAC AGA TGA ACC TGG TTG TAA TAC | | |
| **Primers for qPCR** | | | |
| **DSB_For** | CGT CAT CCA AAC GAC GAG GA | 95°C 15', (95°C 15", 60°C 30") × 45 cycles | 100-200 bp |
| **DSB_Rev_Latest** | CTG ACG CCA TTA TCT ATG TCG GG | | |
| **rDNA_For** | CTG ATG TCT TCG GAT GGA TTT GAG | 95°C 15', (95°C 15", 60°C 30") × 45 cycles | 100-200 bp |
| **rDNA_Rev** | TTT CCT CTG GCT TCA CCC TAT TC | | |
| **5' 0.2_For_VD2** | GAT GTA TAA GGC AGA TTT AGA AGG | 95°C 15', (95°C 15", 60°C 30") × 45 cycles | 100-200 bp |
| **5' 0.2_Rev** | CTT CAT GGA TCT TTG CCA ATT C | | |
| **5' 1.0_For** | TGG ACG AAC TAA TGG CAG GGT | 95°C 15', (95°C 15", 60°C 30") × 45 cycles | 100-200 bp |
| **5' 1.0_Rev** | GGC AAG TAC CGT ATT TTC TTT GGT | | |
| **5' 2.0_For** | GCT AAC GCA GTC AGG CAC CGT G | 95°C 15', (95°C 15", 60°C 30") × 45 cycles | 100-200 bp |
| **5' 2.0_Rev** | ATA TCC CGC AAG AGG CCC GGC A | | |
| **3' 0.2_For** | TAA TTG GCC GCG AGA TTG CTG G | 95°C 15', (95°C 15", 60°C 30") × 45 cycles | 100-200 bp |
| **3' 0.2_Rev** | TTG TAA ATG TGT GTA GCC TGG C | | |
| **3' 1.0_For** | TAT GCT AGC TAC CGA CTT GGC | 95°C 15', (95°C 15", 60°C 30") × 45 cycles | 100-200 bp |
| **3' 1.0_Rev** | CGC TTA GAC CAA GTC TTT CAG C | | |

| | | | |
|---|---|---|---|
| **3’ 2.0_For** | TTC GTC ACT GGT CCC GCC ACC | 95°C 15’, (95°C 15”, 60°C 30”) × 45 cycles | 100-200 bp |
| **3’ 2.0_Rev_VD2** | TCG CGT CGC GAA CGC CAG C | | |
| **3’ 4.0_For** | ACA CGA CTT ATC GCC ACT GGC | 95°C 15’, (95°C 15”, 60°C 30”) × 45 cycles | 100-200 bp |
| **3’ 4.0_Rev** | AAC TGG CTT CAG CAG AGC GC | | |

For routine analysis, DNA fragments were separated in 1% agarose gel with 1x TAE buffer as an electrolyte. To prepare agarose gel with 1x TAE buffer, the desired weight of agarose powder was poured into the corresponding amount of 1x TAE buffer and was soaked into 1x TAE buffer by a brief swirl. Before heating the gel solution by microwave, the weight of gel solution was recorded. Then, the gel solution was heated in the microwave oven on high power until it boiled gently swirling from time to time between every 30 seconds or 1 minute interval. When the gel solution reached boiling point, it was held for 1 minute until all of the particles were dissolved well. After that, the gel solution was weighed again and sufficient hot $dH_2O$ was added to obtain the initial weight. The gel solution and hot $dH_2O$ were mixed thoroughly and cooled to 50-60$^oC$ before casting. After the gel was cast, DNA samples with DNA loading dye, diluted to 1x concentration using $dH_2O$, were loaded into wells of the gel. Generally, DNA fragments were separated in 15 cm x 10 cm 1% TAE agarose gel by using the sub-cell systems (Bio-Rad), running at 80-100 voltage for 0.5-1 hour depending on the size of DNA fragments. To visualize DNA fragments after electrophoresis, ethidium bromide was added at 200 µg/L to 1x TAE buffer.

### 2.3.1.11 Sending for DNA Sequencing

After checking the size of amplicon by DNA electrophoresis, PCR products together with primers for DNA sequencing were sent to the medical school, core genomic facility, the University of Sheffield to be analyzed. For each DNA sequencing reaction, the requirements of templates and primers were 10 µl at 50 ng/µl of purified PCR product and 10 µl of 1 µM primer. Primers used in this study for sequencing the point mutation of *MRE11* alleles, *mre11-58S* and *mre11-H125N*,

are listed in **Table 2.3**.

### 2.3.1.12 Storage of Yeast Clones at -80°C

**Solutions Used in this Method**

**(See Section 2.3.1.5 NOTE)**

- **50% Glycerol:** To be convenient, each 1 ml of 50% glycerol (Fisher Chemical) was directly aliquoted into each glass screw cap tube first, and then sterilized by autoclave.

After confirming genotypes, yeast clones were stored in 25% glycerol at -80°C. Cells from standard 5 ml cultures **(Section 2.2.3)** were harvested by centrifugation at 4,000 rpm for 5 minutes. Then, most of supernatant was removed to reserve 2 ml of it for resuspending the cell pellet. After resuspending the cell pellet by pipetting, 1 ml of cells was mixed with 1 ml of 50% glycerol in a glass screw cap tube and the other 1 ml of cells was treated in the same manner to be a duplicate. After mixing well with glycerol, the duplicates of cell suspensions were immediately stored in -80°C freezers separately.

## 2.3.2 Yeast Transformation of Haploid Strains with DNA Cassettes Flanked with Partial Homology Regions

### 2.3.2.1 Plasmid DNA and Escherichia coli Strain Used in this Study

| Name of plasmid | Description | PCR Product Size | Source |
|---|---|---|---|
| pFA6a-KanMX6 | Selection marker *kanMX6* is included in this plasmid that acts as the module for PCR | 1559 bp | (Longtine et al., 1998) |

| | | | |
|---|---|---|---|
| | templates to generate fragments for gene manipulation. | | |
| pFA6a-TRP1 | Selection marker *S. cerevisiae TRP1* is included in this plasmid that acts as the module for PCR templates to generate fragments for gene manipulation. | 1036 bp | (Longtine et al., 1998) |
| **Name of *E. coli* Strain** | **Genotype** | | **Source** |
| DH5α | *supE*44 Δ*lacU*169(ϕ80 *lacZ*ΔM15) *hsdR*17 *recA*1 *endA*1 *gyrA*96 *thi*-1 *relA*1 | | Lab resource |

### 2.3.2.2 Preparation of Escherichia coli Rubidium Chloride Chemically Competent Cells

**Media and Solutions Used in this Method**

**(See Section 2.3.1.5 NOTE)**

- **LB (Luria-Broth):** Bacterial growth medium: 1.1% Bacto™ tryptone (BD), 1% Bacto™ yeast extract (BD), 0.5% NaCl (Fisher Chemical), adjusted pH to 7.4.
- **300 mM KAC:** 2.49 g / 100 ml. (Sigma-Aldrich)
- **1000 mM $RbCl_2$:** 12.09 g / 100 ml. (Sigma)
- **100 mM $CaCl_2$:** 1.47 g /100 ml. (AnalaR)
- **500 mM $MnCl_2$:** 9.85 g /100 ml. (FISONS)
- **100 mM MOPS:** 2.093 g / 100 ml. (Sigma)

- **750 mM $CaCl_2$:** 11.025 g / 100 ml. (AnalaR)
- **TFB1:** For 50 ml, 5 ml of 300 mM KAC, 5 ml of 1000 mM $RbCl_2$, 5 ml of 100 mM $CaCl_2$, 5 ml of 500 mM $MnCl_2$ and 7.5 ml of 100% glycerol were included. pH was adjusted to 5.8 with 0.2 M acetic acid (DON'T OVERSHOOT!) and the volume of 50 ml was made up with $dH_2O$, and then filter sterilized.
- **TFB2:** For 10 ml, 1 ml of 100 mM MOPS, 1 ml of 750 mM $CaCl_2$, 1ml of 100 mM $RbCl_2$ and 1.5 ml of 100% glycerol were included. pH was adjusted to 6.5 with KOH (DON'T OVERSHOOT!) and the volume of 10 ml was made up with $dH_2O$, and then filter sterilized.

*E. coli* DH5α or other *E. coli* strains like BL21 depending on experimental requirements were streaked out on LB agar plates from -80$^oC$ stocks and were incubated at 37$^oC$ overnight for single colonies. Then, one of the single colonies was selected and inoculated in 5 or 10 ml of LB, and then grown at 37$^oC$ for overnight as one starter culture. Next day, a small fraction of the starter culture (~1.5 ml) was transferred into 100 ml of LB and grown at 37$^oC$ until the value of cell density measured by the spectrometer (GENEFLOW) with a wavelength of 550 nm reached 0.4~0.6 ($OD_{550}$=0.4~0.6). This normally took around 4 hours. After this point, it is important to keep everything cold. Cells were collected by centrifugation at 4,000 rpm and 4$^oC$ for 10 minutes and the supernatant was discarded. Then, cells were resuspended in 40 ml of ice-cold filter sterilized TFB1 and incubated in wet ice for 5 to 10 minutes. After that, cells were harvested again by centrifugation at 4,000 rpm and 4$^oC$ for 10 minutes and resuspended in 5 ml of ice-cold filter sterilized TFB2. Cells were then stood in wet ice for 15 minutes and eppendorf tubes were chilled at the same time. Next, 100 µl aliquots of cells were dispensed into pre-chilled tubes and were snap frozen in liquid nitrogen or put

quickly in a -80°C freezer. Finally, cells were stored at -80°C for up to 6 months.

### 2.3.2.3 Transformation of *E. coli* $RbCl_2$ Chemically Competent Cells

**Media Used in this Method**

**(See Section 2.3.1.5 NOTE)**

- **LB (Luria-Broth):** Bacterial growth medium: 1.1% Bacto™ tryptone (BD), 1% Bacto™ yeast extract (BD), 0.5% NaCl (Fisher Chemical) and adjusted pH to 7.4. Solid media included 1.5% Bacto™ agar (BD).
- **LB + Ampicillin Plates or LB + Kanamycin Plates:** *E. coli* strains harboring plasmids with ampicillin or kanamycin antibiotic resistant markers were selected on LB agar plates containing 50~100 μg/ml ampicillin (Sigma) or 25~50 μg/ml kanamycin (Sigma) respectively. Both of ampicillin and kanamycin were added to autoclaved LB when the medium became cooled to 55°C.

For transforming a DNA construct, 50 μl of *E. coli* $RbCl_2$ chemically competent cells **(Section 2.3.2.2)** were used. For transforming a DNA ligation, 100 μl of competent cells was used. The more or less competent cells needed were dependent on how competent cells they were. *E. coli* $RbCl_2$ chemically competent cells **(Section 2.3.2.2)** were taken out from -80°C and put on ice until slightly melted but not all melted. Then, 1~5 μl (1~50 ng) of DNA was added to competent cells and the sample was incubated in wet ice for 30 minutes. After that, the sample was heat shocked in 42°C water bath for 1.5 minutes and put immediately on wet ice for 2 minutes. 900 μl of LB was added to the sample and the sample was incubated at 37°C for 1 hour to let cells recover. Finally, the cells were collected by spinning down at 3,000~4,000 rpm for 5 minutes and most of the

supernatant was discarded, retaining 100~200 µl of which to resuspend the cells. Then the cells were plated out on LB + Ampicillin plates or LB + Kanamycin plates, depending on which antibiotic resistant markers were contained in the plasmid DNA, and were grown at 37°C for 12~16 hours. To more easily get single colonies from transformation of a DNA construct, it is not necessary to spin down the cells for concentration after the 1 hour recovering at 37°C. Instead, 100~200 µl of the sample could be directly taken out after the recovery or a serial dilution maybe needed after spinning down, cells plated out on selection plates, and then the cells grown at 37°C for 12~16 hours.

### 2.3.2.4 Minimal Preparation of Plasmid DNA

#### Media and Solutions Used in this Method

**(See Section 2.3.1.5 NOTE)**

- **LB + Ampicillin Medium or LB + Kanamycin Medium:** *E. coli* strains harboring plasmids with ampicillin or kanamycin antibiotic resistant markers were cultured in LB liquid medium containing 50~100 µg/ml ampicillin (Sigma) or 25~50 µg/ml kanamycin (Sigma) respectively. Both ampicillin and kanamycin were added to autoclaved LB freshly.
- **TEG Buffer:** 0.9% glucose (Fisher Chemical), 25 mM Tris-HCl (pH 7.5) (Sigma) and 10 mM EDTA (pH 8.0) (Fisher Chemical), stored at 4°C.
- **Alkaline SDS Buffer:** 200 mM NaOH (Fisher Chemical) and 1% SDS (Fisher Chemical), prepared freshly.
- **K-Acetate Solution:** 3 M potassium acetate (Fisher Chemical) and 11.5% glacial acetic acid (Fisher Chemical).
- **100% Isopropanol.** (Fisher Chemical)
- **70 % Ethanol.** (Fisher Chemical)

- **TE-RNase Buffer:** 10 µg/ml RNase A (Sigma) in 1x TE buffer, which contained 10 mM Tris-HCl (pH 7.5) (Sigma) and 1 mM EDTA (pH 8.0) (Fisher Chemical).

After *E. coli* transformation **(Section 2.3.2.3)**, single colonies of *E. coli* antibiotic resistant clones were inoculated into 2~5 ml of LB + ampicillin medium or LB + Kanamycin medium, depending on which selectable markers were contained in the plasmid DNA, and were grown at 37$^{o}$C for 12~16 hours. Then, cells were harvested by centrifugation at 4,000 rpm for 5 minutes, resuspended in 100 µl of ice-cold TEG buffer and incubated at room temperature for 5 minutes. After which, the cells were lysed by addition of 200 µl freshly prepared alkaline SDS buffer with incubation on ice for 5 minutes. To precipitate unwanted cellular components, 150 µl of K-Acetate solution was added and the sample was incubated on ice for 5 minutes. Then, the pellet of cell debris was discarded after centrifugation at 13,200 rpm for 10 minutes and the DNA-containing supernatant was transferred into a new 1.5 ml microcentrifuge tube. The DNA was precipitated by mixing with 300 µl of isopropanol with gentle inversion and incubation at room temperature for 5 minutes. Then, the DNA pellet was harvested by centrifugation at 14,000 rpm for 5 minutes and washed in 500 µl of 70% Ethanol twice. After washes, the DNA pellet was dried but not dried out and resuspended in 40 to 100 µl of TE-RNase buffer depending on the size of the DNA pellet.

#### 2.3.2.5 Production of DNA Cassettes Flanked with Partial Homology Regions

In *Saccharomyces cerevisiase*, a PCR-mediated technique has been developed and as a standard method that allows single-step deletion or tagging of chromosomal genes by homologous recombination (Longtine et al., 1998). In order

to specifically and precisely modify chromosomal genes, not only selectable markers or together with epitope tags but also the short-flanking homology regions (SFH regions) are necessary to be contained in DNA cassettes for yeast transformation. To produce this kind of DNA cassettes, the PCR primers were designed to have 60~100 nucleotides at 5' ends that corresponded to the desired target gene sequences for amplifying the SFH regions and 20~24 nucleotides at 3' ends that annealed to and allowed amplification of the selectable marker gene or together with the epitope tag if included in the template. After that, the DNA cassettes were amplified by two-step PCR and, as the size of the DNA amplicon was less than 1.5 kb, Mango *Taq* DNA polymerase (BIOLINE) was used in this study. However, if the size of DNA amplicon is above 1.5 kb, *Pfu* DNA polymerase is better used instead. In the first step of PCR, 5 reaction cycles were set up with the annealing temperature suitable for the 3' ends of primers that can anneal to the templates and amplify the selection markers or together with the epitope tags. Then, the annealing temperature was increased to 65$^{o}$C in the second step of PCR to enhance the specificity for producing the DNA cassettes flanked with SFH regions and the reaction cycle here was repeated 30 times. After PCR, the fragments of DNA amplicons were separated and purified by DNA electrophoresis **(Section 2.3.1.10)** and gel extraction kit (Sigma-Aldrich) respectively, or could be purified by standard ethanol precipitation if there were no nonspecific DNA products **(Section 2.3.1.6)**.

Another way to produce the DNA cassettes with partial flanking homology regions was directly from restriction enzyme digested plasmids, which already harbored the desired target gene sequences, such as the *URA3* gene in pMJ113_115. After restriction enzyme digestion, the fragments of DNA cassettes

were separated through DNA electrophoresis **(Section 2.3.1.10)** and purified by gel extraction kit (Sigma-Aldrich) or by standard ethanol precipitation **(Section 2.3.1.6)**.

### 2.3.2.6 Lithium Acetate (LiAc) Yeast Transformation

**Media and Solutions Used in this Method**

**(See Section 2.3.1.5 NOTE)**

- **YPAD Agar Plates and Medium: See Section 2.2.1.**
- **Dropout Agar Plates (SC-) or YPAD with G418 or Hyg Plates: Section 2.2.1.**
- **10x TE Buffer:** 100 mM Tris-HCl (pH 7.5) (Sigma) and 10 mM EDTA (pH 8.0) (Fisher Chemical).
- **10x LiAc:** 1 M LiAc (Sigma-Aldrich), adjusted pH to 7.5.
- **50% PEG3350.** (Sigma)
- **10 mg/ml Salmon Sperm DNA (Sigma D1626):** $dH_2O$ was added to 10 mg/ml, autoclaved first, then dispensed into eppendorf tubes and stored at -20$^oC$.

Haploid yeast strains desired for genetic manipulation were streaked out on YPAD agar plates from -80$^oC$ stocks and were incubated at 37$^oC$ for two days to let single colonies grow. Then, one of the single colonies was selected and inoculated into 2 or 5 ml of liquid YPAD and grown at 37$^oC$ overnight as one starter culture. Because the efficiency of transformation becomes constant for 3 to 4 cell divisions, it is important to allow yeast cells to complete at least two cell divisions. Therefore, 1~2 ml of the overnight starter culture was transferred into 50 ml of warm liquid YPAD and grown at 37$^oC$ until the value of cell density measured by the spectrometer (GENEFLOW) with a wavelength of 600 nm reached to 0.6~0.8 ($OD_{600}$=0.6~0.8). This normally took around 3 to 5 hours and the culture was

sufficient for 10 transformations. After that, the cells were harvested by centrifugation at 4,000 rpm for 5 minutes and the medium was removed. The cells were then washed with 10 ml of sterilized $dH_2O$ and collected again by centrifugation at 4,000 rpm for 5 minutes. At the same time, salmon sperm DNA (10 mg/ml) was boiled for 5 minutes and chilled quickly on ice for 5 minutes. 1 ml of 1x TE/LiAc (100 µl of 10x TE buffer, 100 µl of 10x LiAc buffer and 800 µl of $dH_2O$) was prepared to resuspend the washed cells and every 100 µl of the resuspended cells was transferred to a new 1.5 ml eppendorf tube as one transformant competent cells. For one transformant, 1~5 µg of DNA **(Section 2.3.2.5)** and 5 or 10 µl of boiled salmon sperm DNA (10 mg/ml) were first added and mixed well with cells. Then, 600 µl of 40% PEG3350/ 1x TE buffer/ 1x LiAc (480 µl of 50% PEG3350, 60 µl of 10x TE buffer and 60 µl of 10x LiAc) was also prepared and added to cells. (It is important to premix the solution of 40% PEG3350/ 1x TE buffer/ 1x LiAc well before adding to transformant competent cells, or the PEG3350 should go in first, which can shield the cells from the detrimental effects of the high concentration of LiAc.) After which, the transformant cells with solutions were mixed well by vigorous vortex and incubated at 30°C for 30 minutes, and then were heat shocked in 42°C water bath for 15 minutes. Finally, the cells were collected by quick spin for 5 seconds at 13,200 rpm twice, resuspended with 100~200 µl of sterilized water, plated out on dropout agar plates or YPAD with G418 or Hyg plates depending on auxotrophic or antibiotic resistant selectable markers and incubated at 30°C for 2~4 days to recover the transformants .

After further confirming the genotypes of transfromants by yeast colony PCR **(Section 2.3.1.9)** or DNA sequencing **(Section 2.3.1.11)**, haploid yeast clones were stored at -80°C **(Section 2.3.1.12)**. In order to construct the diploid yeast clones

with desired genotypes, sometimes more than once DNA manipulation should be conducted. Therefore, the general genetic methods **(Section 2.3.1)** or yeast transformation of haploid strains with flanked homology regions **(Section 2.3.2)** could proceed again. When the desired diploid yeast strains were acquired, cells were then to progress through a meiosis time course **(Section 2.4)**.

## 2.4 Induction of Meiosis Time Course

Briefly, in order to guide yeast strains to progress through a meiosis time course, cells were synchronized with PSP2 medium first, and then were transferred into 1% potassium-acetate to lead to sporulation **(see Chapter 1.1)**. The detailed procedures are described below.

### Appliances, Media and Chemicals used in this Method

**(See Section 2.3.1.5 NOTE)**

For each meiosis time course, the following were needed:

- **4 of 2 L Flasks (autoclaved):** Stored at 30°C.
- **2 of 250 ml Measuring Cylinders (autoclaved):** Stored at 30°C.
- **2 of 250 ml Centrifuge Bottles (autoclaved):** Stored at 30°C.
- **2 of 2.8 L Baffled Flasks (autoclaved):** Stored at 30°C. (BELLCO)

---

- **1 of YPG Plate:** Yeast growth medium for selection against petite mutants: 15% glycerol (Fisher Chemical), 1% Bacto™ yeast extract (BD), 2% Bacto™ peptone (BD) and 2% Bacto™ agar (BD).
- **1 of YPAD Plate and 15 ml of YPAD Medium: Section 2.2.1.**
- **1 L of PSP2 Medium:** 6.7 g Bacto™ yeast nitrogen base without amino acids &

ammonium sulfate (BD), 2.0 g Bacto™ yeast extract (BD), 10.0 g K-Acet (Fisher Chemical), 10.2 g potassium hydrogen phthalate (Sigma-Aldrich) and supplements of amino acid stock solutions depending on auxotrophic requirements **(Table 2.2)**. Stored at 30°C.

- **1 L of 1% Potassium-Acetate (K-Acet):** Stored at 30°C. **(See Section 2.2.1)**.

---

- **10 of Eppendorf Tubes (for time point 0-8 and 24 hour):** Each tube contained 0.75 ml 100% ethanol and was stored at -20°C.
- **9 of Falcon Tubes (for time point 0-8 hour):** Each tube contained 6 ml of 50% glycerol (Fisher Chemical) and 300 µl of 10% NaAzide (Merk) (filter sterilized) and was stored at 4°C.
- **Time Course Spheroplasting Solution:** 1 M D-sorbitol (Sigma), 50 mM $KPO_4$ buffer (pH 7.5), 10 mM EDTA (pH 7.5) (Fisher Chemical) and 20% glycerol (Fisher Chemical).
- **1 M $KPO_4$ Buffer, pH 7.5:** Each 100 ml of 1 M $KPO_4$ buffer (pH 7.5) was composed of 83.4 ml of 1 M $K_2HPO_4$ (Fisher Chemical) and 16.6 ml of 1 M $KH_2PO_4$ (AnalaR).

### Day 1 (Morning): Patched Cells on YPG Plates

Cells of one yeast strain were patched from the -80°C glycerol stock onto an YPG plate to select cells with healthy mitochondria **(see Chapter 1.1 Mitochondria)**.

### Day 2 (Morning): Growth of Single Colonies on YPAD Plates

Cells were then streaked out from the YPG plate to a fresh YPAD plate for single colonies and were allowed to grow at 30°C for 2 days.

### Day 4 (Morning to Afternoon): Setting up 10-15 ml YPAD Cultures

After 2 days growth, a single colony was selected and inoculated into 10-15 ml YPAD medium to set up an overnight culture. Before inoculation, a tiny amount of cells were scraped out from the single colony and were checked whether they were diploid cells under the microscopy. Normally, for strains with the VDE-DSB1 system (Matt's system) and the VDE-DSB2 system (Anna's system) **(see Chapter 3.1)**, 15 ml of YPAD overnight culture was set up around 11:30 am.

***Day before Meiosis Time Course***

PSP2 medium and 1% K-Acet were prepared **(see the above section of appliances, media and chemicals used in this method)**, sterilized by autoclaving and stored at 30$^{o}$C before setting up the PSP2 cultures and the meiosis time course. Moreover, 2 L flasks, 250 ml measuring cylinders, 250 ml centrifuge bottles and 2.8 L baffled flasks were cleaned and sterilized by autoclaving **(see the above section of appliances, media and chemicals used in this method)**. Eppendorf tubes with ethanol for DAPI and falcon tubes contained 50% glycerol and 0.5% NaAzide **(see the above section of appliances, media and chemicals used in this method)** were also prepared in advance of the meiosis time course.

## Day 5 (Morning to Afternoon): Synchronous Sporulation with PSP2 Cultures

Time for setting up PSP2 cultures was entirely dependent on the growth characteristics of strains, so first time try inoculating cells at 2-3 pm. For strains with the VDE-DSB1 system (Matt's system) and the VDE-DSB2 system (Anna's system) **(Figure 3.2)** PSP2 cultures were set up around 11:30 am. 250 ml of PSP2 medium was aliquoted to four 2 L flasks and were inoculated with 0.5 ml, 1.5 ml, 2 ml and 3 ml of overnight YPAD cultures respectively. Then, these PSP2 cultures were incubated shaking vigorously at 270 rpm in a 30$^{o}$C incubator overnight.

## Day 6 (Morning 9-10 am): Meiosis Time Course

Next day, small fractions of the four PSP2 overnight cultures were respectively diluted 1 in 2 with water and the values of cell density were measured through the spectrometer with a wavelength of 600 nm (GENEFLOW). It was important to select the PSP2 culture with a cell density that had reached 3.2-3.6 x $10^7$ cells/ml, namely the value of 1 in 2 diluted $OD_{600}$ was between 0.8 and 0.9 (1 $OD_{600}$=2 x $10^7$cells/ml). However, sometimes it was the PSP2 culture with low cell density, which was $OD_{600}$=0.5-0.7 or even lower to $OD_{600}$=0.4-0.5, needed to be selected for induction of a fine meiosis time course, depending on the characteristic of strains. Cells were harvested in a 250 ml centrifuge bottle at room temperature, 4,500 rpm for 2 minutes and washed with 250 ml of 1% K-Acet. After washing, the cells were collected again by centrifugation at room temperature, 4,500 rpm for 2 minutes and rapidly placed into a 2.8 L baffled flask to maintain aerobic condition by resuspension with 250 ml of 1% K-Acet plus amino acids supplements (a quarter of the usual amounts used for dropout media) **(see Section 2.2.1 and Table 2.1)**. Then, cells were incubated at 30$^o$C and 25 ml of the culture was taken out at each time point, normally from 0 to 8 hour, and mixed well with 6 ml of 50% glycerol and 300 µl of 10% NaAzide, stood on ice for 5 minutes, collected by centrifugation at room temperature, 4,000 rpm for 5 minutes, washed with 6 ml of time course spheroplastiong solution, collected again by centrifugation, then snap frozen in liquid nitrogen and stored at -80$^o$C for extraction of genomic DNA by the CTAB method **(Section 2.6)**. At the same time, a small fraction of cells was topped up in an eppendorf tube containing 0.75 ml ethanol and stored at -20$^o$C for DAPI staining **(Section 2.5)**.

## 2.5 Analysis of Meiotic Nuclear Division by DAPI Staining

### Solutions Used in this Method

**(See Section 2.3.1.5 NOTE)**

- **0.5 mg/ml DAPI Stock Solution.** (Sigma)
- **50% Glycerol.** (Fisher Chemical)

In order to reveal the quality of the meiosis time course, the proportion of 1, 2, 3 and 4 nuclei in cells of each meiosis time point already fixed with 100% ethanol **(Section 2.4)** was visualized and counted by DAPI staining. 1 µl of 0.5 mg/ml DAPI stock solution was added to each cell sample and left to incubate at room temperature for 5 minutes. Then, cells were pelleted by centrifugation at 14,000 rpm for 2 minutes. The supernatant was removed and the cell pellet was resuspended in 150 µl of 50% glycerol. To destroy possible cell clumps affected analysis, cells were subsequently sonicated for 10 seconds with an amplitude of 4 microns by using the Soniprep 150 (SANYO). After that, 5 µl of the cell sample was deposited on slides for microscopy and the number of nuclei per cell was assessed with excitation light sources at 358 nm and emission at 461 nm. For each meiosis time point, 100 random cells were analyzed.

## 2.6 Extraction of Genomic DNA by CTAB (Hexadecyltrimethylammonium Bromide)

### Solutions Used in this Method

**(See Section 2.3.1.5 NOTE)**

- **CTAB Spheroplasting Solution:** 36.43 g of sorbitol (Sigma), 10 ml of 1 M $KPO_4$ buffer (pH 7.5) **(see Section 2.4)** and 4 ml of 0.5 M EDTA (pH 7.5) (Fisher Chemical) adding $dH_2O$ to 200 ml, then filter sterilized and stored at 4°C.
- **CTAB Spheroplasting Solution with Zymolyase 100T:** Each 100 µl of ice cold CTAB spheroplasting solution (see above) contained 0.25 mg zymolyase 100T (MP Biomedicals) and 5 µl β-mercaptoethanol (Sigma) and was for one cell pellet of 25 mL meiosis time course culture **(see Section 2.4)**, **prepared freshly.**
- **CTAB Extraction Solution:** The method of preparation is critical, as 2 M NaCl (Fisher Chemical) and 3% CTAB (Sigma) is too viscous to be filtered. For 100 ml of CTAB extraction solution, 50 ml of NaCl/Tris/EDTA solution was first made by mixing 11.69 g NaCl (Fisher Chemical), 10 ml 1 M Tris-HCl (pH 7.5) (Sigma) and 5 ml 0.5 M EDTA (pH 8.0) (Fisher Chemical) with $dH_2O$. Then, 20 ml of 10% PVP40 (Sigma) and 30 ml of 10% CTAB (Sigma) were prepared with $dH_2O$. After that, these three solutions were filter sterilized in the order of NaCl/Tris/EDTA, 10% PVP40 and 10% CTAB **(the order for filter sterilization is very important)** and stored at 37°C.
- **CTAB Dilution Solution:** 20 ml of 10% CTAB (Sigma), 10 ml of 1 M Tris-HCl (pH 7.5) (Sigma) and 4 ml of 0.5 M EDTA (pH 8.0) (Fisher Chemical) adding $dH_2O$ to 200 ml, filter sterilized and stored at room temperature.
- **0.4 M NaCl/TE Wash Buffer:** 16 ml of 5 M NaCl (Fisher Chemical), 2 ml of 1 M Tris-HCl (pH 7.5) (Sigma) and 400 µl of 0.5 M EDTA (pH 8.0) (Fisher Chemical) adding $dH_2O$ to 200 ml, filter sterilized and stored at 4°C.
- **1.42 M NaCl/TE Resuspending Buffer:** 28.4 ml of 5 M NaCl (Fisher Chemical), 1 ml of 1 M Tris-HCl (pH7.5) (Sigma) and 200 µl of 0.5 M EDTA (pH 8.0) (Fisher Chemical) adding $dH_2O$ to 100ml, filter sterilized and stored at 4°C.
- **Proteinase K (20 mg/ml):** 20 mg of proteinase K (Sigma) was dissolved in 1 ml

of filter sterilized solution, which contained 10 µl of 1 M Tris-HCl (pH 7.5) (Fisher Chemical), 20 µl of 1 M $CaCl_2$ (AnalaR), 500 µl of glycerol (Fisher Chemical) and 470 µl of $dH_2O$, and stored at -20°C.

- **RNase A, DNase free:** 10 mg/ml RNase A (Sigma) in 10 mM Tris-HCl (pH 7.5) (Sigma) and 22.5 mM NaCl (Fisher Chemical) was heated to 100°C for 15 minutes and cooled slowly to room temperature, then stored at -20°C.
- **Chloroform : IAA (24 : 1) Solution.** (Fisher Chemical and Sigma)
- **100% Ethanol.** (Fisher Chemical)
- **70% Ethanol.** (Fisher Chemical)
- **10x TE Buffer:** 100 mM Tris-HCl (pH 7.5) (Sigma) and 10 mM EDTA (pH 8.0) (Fisher Chemical).

In order to obtain a high quality of yeast genomic DNA, nucleic acids were separated from polysaccharides and proteins by exploiting the insolubility of cetyltrimethylammonium-nucleic acid complexes at low salt concentration and here is modified version of the published protocol (Allers and Lichten, 2000). One standard 5 ml yeast culture **(Section 2.2.3)** or each time point of cell pellets from 25 ml meiosis time course culture **(Section 2.4)** was washed in 1 or 1.5 ml of CTAB spheroplasting solution and collected gently at 4,000 rpm for 1 minute. Then, most of the supernatant was poured off and cells were resuspended in the remaining supernatant. 100 µl of ice-cold CTAB spheroplasting solution with zymolyase 100T was added and cells were resuspended completely. (If doing multiple samples, each were kept on ice until all were resuspended to avoid some of the samples being over treated.) After that, the sample was incubated in a 37°C water bath and inverted twice with 3 minutes incubation – invert – 3 minutes incubation – invert (maybe one more minute incubation and invert) to digest yeast cell walls and

produce spheroplasts. For mitotic cells, it took a longer time, 10 to 15 minutes, for incubation. 200 µl of CTAB extraction solution was added and the sample was mixed well by pipetting and vortexing gently (Well-zymolyased cells should be stringy when pipetted, not bitty). Then, 5 µl of proteinase K (20 mg/ml) was added and the sample was vortexed well gently. After that, the sample was incubated in a 37$^{o}$C water bath for 15 minutes mixing by inversion or vortexed, 3 times with 5 minutes incubation – invert/vortex – 5 minutes incubation – invert/vortex – 5 minutes incubation – invert/vortex to lyse the spheroplasts. (Solution of samples should go a bit translucent, as the detergent solubilizes the cells during the incubation.) The sample was deproteinised by adding 100 µl of ice-cold chloroform : IAA (24 : 1) solution and the phases of samples were mixed by inversion to avoid shearing of single-strand DNA, rested for 2 minutes and inverted thoroughly again. (Samples must be white after inversion well.) Then, the aqueous phase containing nucleic acids was separated from the denatured protein and the organic phases by centrifugation at room temperature, 14,000 rpm for 5 to 10 minutes. After centrifugation, the upper phase with nucleic acids (~300 µl) was immediately removed to a new 1.5 ml microcentrifuge tube without disrupting the denatured protein interphase carefully. RNA was digested with 2 µl of 10 mg/ml RNase A at 37$^{o}$C for 30 minutes. Then, three volumes of CTAB dilution solution (~900 µl) was gently layered on top of the sample. To precipitate DNA, these two layers were mixed thoroughly by inverting the tube gently 5 times, left undisturbed at room temperature for 10 minutes, inverted 20 more times until a precipitate was observed, and left at room temperature for 2 more minutes. (If no DNA clumps appear, the sample could be centrifugated at 14,000 rpm for 1 or 2 minutes. It is not ideal but still can receive plenty of DNA.) After the appearance of CTAB-DNA complexes, the liquid was removed carefully from the tube (the CTAB-DNA is STICKY!

Try to get it to the side of the tube NOT to the end of the pipette tip) and the CTAB-DNA pellet was washed with ice-cold 0.6 ml of 0.4 M NaCl/TE wash buffer twice (during these two washes, do not let the CTAB-DNA pellet dry out and it should become considerably smaller, DON'T PANIC). Then, the CTAB-DNA pellet was resuspended in 300 µl of ice-cold 1.42 M NaCl/TE resuspending buffer and the DNA pellet was precipitated by mixing with 600 µl of 100% ethanol with gentle inversion, stood at room temperature for 5 to 20 minutes and spun down at 14,000 rpm for 5 minutes. Finally, the DNA pellet was washed with 600 µl of 70% ethanol twice, dried but not dried out and resuspended in 30 to 100 µl of ice-cold 1x TE buffer depending on the size of the DNA pellet.

## 2.7 Southern Blotting

### 2.7.1 Digestion of Genomic DNA

After CTAB extraction **(Section 2.6)**, 1 µl of yeast genomic DNA for each meiosis time point was used to measure the concentration through image density analysis by Quantity One software (Bio-Rad) after DNA electrophoresis **(Section 2.3.1.10)** and 0.5 µl of lambda DNA/*Hind*III Marker (238.4 ng/µl) (Fermentas) was used as a standard. All DNA samples and the marker were mixed well with such DNA loading dye **(Section 2.3.1.10)** as was needed to dilute to 1x concentration using $dH_2O$ in a 12 µl volume before loading into wells of a gel. Then, for quantification of VDE DSB formation, turnover, repair as well as Spo11 induced DSB formation by Southern blot analysis, 0.5~1 µg of genomic DNA was digested with 5~10 units of *Spe*I (NEB) in a 20 µl reaction volume and this reaction was incubated in 37$^{o}$C water bath for 3~4 hours or overnight.

## 2.7.2 Agarose Gel Construction and DNA Electrophoresis

In order to separate restriction enzyme digested DNA fragments **(see the above)**, 25 cm x 15 cm 0.5% 1x TAE agarose gel (250 ml) was prepared **(see Section 2.3.1.10)**. After boiling and mixing well with sufficient hot $dH_2O$ to regain the initial weight, the gel solution was cooled in 55~60$^oC$ water bath for 30minutes. Then, the molten agarose was poured in the 25 x 15 cm gel tray and casted for 1 hour before being soaked in 1x TAE buffer. After gel casting, the digested DNA fragments and 1 µl of *Bst*EII-digested lambda DNA (NEB) were separated in the gel by using the sub-cell system (Bio-Rad). Before loading into wells of the gel, all DNA samples and the marker were mixed well with as much DNA loading dye **(Section 2.3.1.10)** as was needed to dilute to 1x concentration using $dH_2O$ in a 24 µl volume. For strains containing the VDE-DSB1 system (Matt's system) **(Figure 3.2)**, DNA fragments were run at 70V for 13~14 hours. However, for strains containing the VDE-DSB2 system (Anna's system) **(Figure 3.2)**, DNA fragments were run at 70V for 16~17 hours. To visualize DNA fragments after electrophoresis, ethidium bromide was added to 200 µg/L of 1x TAE buffer. **(See Section 2.3.1.10 for more details)**.

## 2.7.3 Vacuum Blotting

### Solutions Used in this Method

**(See Section 2.3.1.5 NOTE)**

For each vacuum blot, the following were needed:

- **1 L of 0.25 M HCl:** 25 ml of 37% HCl (Fisher Chemical) and 975 ml $dH_2O$, prepared freshly, without being autoclaved.
- **2 L of 0.4 M NaOH:** 32 g NaOH (Fisher Chemical) pellets in 2 L $dH_2O$, prepared freshly, without being autoclaved.

- **20x SSPE:** Each liter contained 175.3 g NaCl (Fisher Chemical), 31.2 g $NaH_2PO_4 \cdot 2H_2O$ (Fisher Chemical) and 7.4 g EDTA (Fisher Chemical), with added water to 800 ml first, then adjusted pH to 7.4 and autoclaved.

## Gel Washes:

After DNA electrophoresis **(Section 2.7.2)**, the DNA fragments were visualized on the ultraviolet transilluminator and a photo was taken by a gel doc system (keeping UV to minimum). Then, the gel was washed with $dH_2O$ for 10~15 minutes twice on a shaking platform to remove the electrophoresis buffer. After that, DNA fragments were depurinated by rinsing the gel in 1 L of 0.25 M HCl for 15 minutes and were then denatured by rinsing the gel in 1 L of 0.4 M NaOH for 45 minutes. Before denaturation of DNA fragments, the gel was washed with $dH_2O$ for 10 minutes twice to remove excess HCl.

## Setting of Vacuum Blot:

After gel washes, DNA fragments were transferred onto a 25 cm x 15 cm Amersham Hybond-N+ nylon membrane (GE Healthcare) by setting up the VacuGene XL vacuum blotting system (GE Healthcare) in the order of a support screen (shiny side up) and a rubber gasket inserted into the well around the inner rim of the base unit first, one Whatman 3MM paper (the size of the paper should be between the support screen and the membrane), one nylon membrane, one plastic mask with an open window that can let the gel attach to the membrane but the range of the open window should allow the gel and plastic mask to have 1~1.5 cm overlap, and finally the gel (avoid trapping bubbles between the gel and the membrane). Before setting up this vacuum blotting, the support screen, Whatman 3MM paper, nylon membrance and plastic mask were pre-wetted with $dH_2O$. Then,

the top frame was fitted and secured by tightening the four clamps and to immobilize the gel, the vacuum pump was switch on but not to reach the working level. 1 L of 0.4 M NaOH was poured gently to cover the gel and the vacuum was applied at 50~100 mbar for 2 hours.

### Post-Transfer:

Following transfer, the gel was removed and the membrane was washed in 200 ml of 2x SSPE for 10 minutes to neutralize residual NaOH. Then, the membrane was blotted onto Whatman 3MM papers and dried under the fume hood, and then the DNA fragments were covalently cross-linked onto the nylon membrane by using UV light.

## 2.7.4 Pre-Hybridization

### Appliance and Solution used in this Method

**(See Section 2.3.1.5 NOTE)**

For each blot, the following were needed:

- **1 Cleaned and Siliconized Techne$^{TM}$ Hybridization Tube:** This glass tube was cleaned with Decon 90 detergent first, rinsed with 100% Ethanol, dried under the fume hood, and then was siliconized by 1~2 ml of sigmacote (Sigma), dried again under the fume hood, washed again to removed the HCl by-products, finally dried under the 65$^{o}$C incubator to expand the rubber ring on the lids that make them tightly attached to the glass tube and avoid buffer leakage. Residual sigmacote was reused.
- **40 ml of Pre-Hybridization Buffer:** 200 mg of non-fat dry milk was dissolved in 31.5 ml of hot $dH_2O$ (the water was microwaved with full power for 30 seconds to 1 minutes but not to be boiled) first. Then, 4 ml of 20x SSPE **(see Section**

**2.7.3)**, 4 ml of 10% SDS and 0.5 ml of 5~10 minutes pre-boiled salmon sperm DNA (10 mg/ml) (Sigma) were added and mixed well by vigorous vortex and this kept in the 65°C incubator. Prepared freshly and not autoclaved.

The membrane with DNA side was slid up into the cleaned and siliconized Techne™ hybridization tube. Then, 40 ml of pre-hybridization buffer was poured into it to blot the membrane in the 65°C incubator with rolling for at least 3~4 hours or overnight.

### 2.7.5 Generating Double-Stranded $^{32}$P-Labelled DNA Probes

**Materials used in this Method**

- **DNA Probe Templates:** These templates were prepared by PCR of yeast genomic DNA **(see Section 2.3.1.8)** and then separated from contaminating genomic DNA and nonspecific amplicons by the gel extraction kit (Sigma-Aldrich). The templates could be concentrated by standard ethanol DNA precipitation **(Section 2.3.1.6)**.
- **0.5 ng/µl *Bst*EII-Digested Lambda DNA (NEB):** 1 µl of *Bst*EII-Digested Lambda DNA (0.5 µg/µl) in 999 µl of $dH_2O$.
- **HighPrime Random Primer Labeling Kit (Roche).**
- **$\alpha^{32}$P-dCTP (Perkin Elmer):** 3000 Ci/mmol or 6000 Ci/mmol.
- **G30 BioSpin Columns (Bio-Rad).**

For each Southern blot, to generate double-stranded $^{32}$P-labelled DNA probes, 50~100 ng of DNA probe templates and 0.5 ng of *Bst*EII-digested lambda DNA were denatured at 100°C dry bath for 5 minutes in one 11 µl volume (made up to this volume with MilliQ water) and cooled down immediately on ice for 5 minutes. Then

4 µl of HighPrime and 5 µl of $\alpha^{32}$P-dCTP were added and mixed well to incorporate $^{32}$P into DNA probes in 37$^{o}$C water bath for 20~30 minutes. After that, a G30 BioSpin column was prepared by snapping off the bottom of the spin column and inserting this column into a collection tube provided, and then centrifuging at 4,000 rpm for 2 minutes to remove the resin storage buffer and replacing the collection tube with a screw cap one. Then, all 20 µl of the reaction at 37$^{o}$C was added into the resin of the spin column and the $^{32}$P-labelled probes were purified from unincorporated nucleotides by centrifugation at 4,000 rpm for 4 minutes. The incorporation of $^{32}$P was then revealed by detecting both the signals of the elution and the resin using a radiation monitor after centrifugation. If the $^{32}$P incorporation is above 50/50 (the elution/the resin), the hybridization step **(Section 2.7.6)** can proceed. Otherwise, the $^{32}$P-lablled DNA probes have to be prepared all over again.

### 2.7.6 Hybridization

#### Solution used in this Method

**(See Section 2.3.1.5 NOTE)**

For each blot, the following was needed:

- **20 ml of Hybridization Buffer:** 100 mg of non-fat dry milk and 1 g of dextran sulphate stored at 4$^{o}$C (Sigma) were dissolved in 15.75 ml of very hot d$H_2O$ (the water was microwaved with full power for 30 seconds to 1 minute but not to be boiled) by vortexed hard first. Then, 2 ml of 20x SSPE **(Section 2.7.3)** was added and mixed well by vigorous vortex. After the solution was dissolved, 2 ml of 10% SDS and 0.25 ml of 5~10 minutes pre-boiled salmon sperm DNA (10 mg/ml) (Sigma) were added and mixed well by vigorous vortex and kept in the 65$^{o}$C incubator. Prepared freshly and not autoclaved.

After pre-hybridization, the double-stranded $^{32}$P-labelled DNA probes **(Section 2.7.5)** were mixed with 300 µl denatured salmon sperm DNA (10 mg/ml) and boiled for 5 minutes. Then, all 320 µl of the boiled mixture was added to 20 ml of the hybridization buffer and replaced pre-hybridization buffer to hybridize the blot in the 65$^{o}$C incubator with rolling overnight.

## 2.7.7 Scanning Densitometry

### Solutions used in this Method

**(See Section 2.3.1.5 NOTE)**

For each blot, 200 ml of each following washing buffers were needed and prepared freshly:

- **Washing Buffer 1:** 2x SSPE **(see Section 2.7.3)** and 0.1% SDS.
- **Washing Buffer 2:** 0.5% SSPE and 0.1% SDS.
- **Washing Buffer 3:** 0.1% SSPE and 0.1% SDS.

After hybridization, three washes of a blot were performed by using washing buffer 1, 2 and 3 respectively to wash away the nonspecific hybridization. The washing time was dependent on the intensity of radioactive $^{32}$P signal residual on the blot and normally took 10~15 minutes for each wash to receive 5~10 counts/second of radioactive signal in the end. Then, the blot was dried under the fume hood, wrapped in cling film, removing air bubbles, and fixed in a cassette together with a phosphor imaging image screen (Bio-Rad). The time for imaging was according to the strength of radioactive signal. Then, the radiation-emitted image was visualized by scanning with a Personal FX Phosphoimager (Bio-Rad) and the density of radiation emitted was measured and quantified by using Quantity One software (Bio-Rad). Generally speaking, frame lanes were created first with the

desired number and the anchors of lanes were adjusted to let lines lie down in the middle of lanes, and then the signals of lanes were normalized to lane background. Next, the bands of each lane were created and the range of radiation-emitted peaks adjusted. Therefore, all lanes signals can be reported on a clipboard and subsequently calculated in an Excel file **(Section 2.8)**.

### 2.7.8 Stripping Southern Blot for Re-Probing

**Solutions used in this Method**

**(See Section 2.3.1.5 NOTE)**

For each blot, the following were needed:

- **0.1% SDS:** has to be boiling hot.
- **200 ml of 2x SSPE: (see Section 2.7.3)**.

For re-probing, a Southern blot was washed with 500 ml of boiled hot 0.1% SDS for 10~15 minutes by shaking vigorously, repeating two times more until the signal of radioactive $^{32}P$ has been removed. Then, the blot was rinsed in 200 ml of 2x SSPE and can be pre-hybridized and re-probed as normal **(Section 2.7.4 to 2.7.7)**.

## 2.8 Quantification and Calculation for Southern Blot Analysis

### 2.8.1 The VDE-DSB1 System (Matt's System)

In the VDE-DSB1 system, the proportion of *arg4-vde* chromatids visible as DSBs and repaired by single-strand annealing (SSA) or gene conversion (GC) was calculated with *Spe*I digestion from which three bands appeared **(Figure 3.2)**. The 11.5 kb fragment contains DNA from each of parental *arg4-vde* chromatids (P),

*arg4-vde* chromatids that have been gene converted to either *arg4-bgl* or *ARG4* (GC) and the donor homologue *arg4-bgl* allele (D). This band is referred to as (P + GC + D). The 7.8 kb fragment contains broken *arg4-vde* chromatids (VDE-DSB1). The 2.3 kb fragment contains the SSA deletion products by using parts of homologue *URA3* repeats (SSAΔ). Then,

- Total signal in lane:

  $T_L$ = (P + GC + D) + VDE-DSB1 + SSAΔ.

- Lane signal attributable to parental *ura3::arg4-vde* chromatids:

  $T_V = T_L / 2$.

- Lane signal attributable to donor *ura3::arg4-bgl* chromatids:

  $D = T_L / 2$.

- Proportion of *ura3::arg4-vde* chromatids in a broken state:

  $B = (\text{VDE-DSB1} / T_V)\ \% = [(\text{VDE-DSB1} \times 2) / T_L]\ \%$.

- Proportion of *ura3::arg4-vde* chromatids in SSA repaired:

  $R_{SSA} = (\text{SSA}\Delta / T_V)\ \% = [(\text{SSA}\Delta \times 2) / T_L]\ \%$.

- Proportion of *ura3::arg4-vde* chromatids repaired in gene conversion:

  $R_{GC} = \{ [ (P + GC + D) – D ] / T_V \}\ \% – Pr_t$.

  ($Pr_t$ = proportion of parental *ura3::arg4-vde* chromatids remaining at time point t; **see Section 2.10**)

- Proportion of *ura3::arg4-vde* chromatids remaining unrepaired

  $= [B / (100 – Pr_t)]\ \%$.

- Proportion of SSA repaired over total amount of VDE-induced breaks

  $= [R_{SSA} / (100 – Pr_t)]\ \%$.

- Proportion of GC repaired over total amount of VDE-induced breaks

  $= [R_{GC} / (100 – Pr_t)]\ \%$.

### 2.8.2 The VDE-DSB2 System (Anna's System)

In the VDE-DSB2 system, the proportion of *arg4-vde* chromatids that was visible as DSBs and repaired by either short or long resected tract of single-strand annealing was calculated within a *Spe*I digest from which five bands appeared **(Figure 3.2)**. The 15 kb and 3 kb fragments contain DNA from each of parental *ade2::ura3-[arg4-vde]-URA3* chromatids (P) and the other allele of *ade2*Δ(*Eco*RV, *Stu*I) ($P_{ade2\Delta}$) respectively. The 5.5 kb fragment contains broken *arg4-vde* chromatids (VDE-DSB2). The 10 kb fragment contains the SSA proximal deletion products (Δproximal) using exposed homologue *URA3* repeats resulting from short resection. However, the 4.2 kb fragment contains the SSA distal deletion products (Δdistal) using the exposed homologue *ADE2* repeats caused by long resection. Then,

- Total signal in lane:

  $T_L$ = P + VDE-DSB2 + Δproximal + Δdistal + $P_{ade2\Delta}$.

- Lane signal attributed to *ade2::ura3-[arg4-vde]-URA3* chromatids:

  $T_V = T_L /2$ = P + VDE-DSB2 + Δproximal + Δdistal.

- Lane signal attributed to *ade2*Δ(*Eco*RV-*Stu*I) chromatids:

  $T_{ade2\Delta} = T_L /2 = P_{ade2\Delta}$.

- Proportion of *ade2::ura3-[arg4-vde]-URA3* chromatids in a broken state:

  B = (VDE-DSB2 / $T_V$) %.

- Proportion of *ade2::ura3-[arg4-vde]-URA3* chromatids in Δproximal:

  $R_{\Delta proximal}$ = (Δproximal / $T_V$) %.

- Proportion of *ade2::ura3-[arg4-vde]-URA3* chromatids in Δdistal:

  $R_{\Delta distal}$ = (Δdistal / $T_V$) %.

- Proportion of *ade2::ura3-[arg4-vde]-URA3* chromatids remaining unrepaired

  = [B / (100 – P)] %.

- Proportion of Δproximal products over total amount of VDE-induced breaks

  = $[R_{\Delta proximal} / (100 – P)]$ %.

- Proportion of Δdistal products over total amount of VDE-induced breaks

  = $[R_{\Delta distal} / (100 – P)]$ %.

## 2.9 Quantitative PCR (qPCR)

In order to detect and measure the amount of target in the sample efficiently and without running out much of the sample, quantitative PCR (qPCR) has been established, from which a measurable signal has to be generated that is proportional to the amount of amplified products, and all current signal detection systems are based on fluorescent technologies (EUROGENTEC). There are several detection methods has been developed, such as using high resolution melting dyes (HRM dyes), TaqMan® probes (=double-dye probes), LNA® double-dye probes and so on. In this study, we used SYBR® Green I to do the detection assay. SYBR® Green I is a double-strand DNA intercalating dye and once it binds to DNA it fluoresces, emitting at 520 nm. Therefore, the amount of dye incorporated is proportional to the amount of generated amplicons and the emitting beam can be detected and related to the amount of target. However, because of the disadvantage that SYBR® Green I is non-specific to the target, a pair of specific primers is required to be designed. Then, the design guideline of primers and amplicon were listed below (EUROGENTEC):

## Primers

- Length: 18~30 bases.
- GC content: 30~80 % (ideally 40~60 %).
- Tm: 50~60$^{o}$C, ΔTm difference between forward and reverse primer should be ≤ 4$^{o}$C.
- Avoid 3’ end T and runs of identical nucleotides, especially of 3 or more Gs or Cs at the 3’ end, to prohibit mismatches between primers and target.
- Avoid complementarities within the primers to prohibit hairpin formation.
- Avoid complementarities between the primers to prohibit primer dimer formation.
- Check whether primers are unique and specific by using BLAST.

## Amplicon

- Length: 100~200 bp.
- GC content: 30~80 % (ideally 40~60 %).
- Avoid secondary structures in the amplicon.

In order to control for DNA concentration, qPCR was undertaken simultaneously using test primer pair and rDNA primer pair. To also ensure that the data was not influenced by variable PCR efficiency due to the variation of primer pairing, standard curves for both of the rDNA primers and test primers were generated for all experiments. Therefore, each set of qPCR reactions contained samples for diagnosis with test primer pair and rDNA primer pair (the latter was as rDNA loading controls), negative controls (= no template controls) with both test and rDNA primer pair and standards with both test and rDNA primer pair, and all qPCR reactions were undertaken in duplicate 20 µl reactions and performed by the

Corbett Rotor-Gene 6000 (Qiagen). All primer sets flanking VDE-DSB2, restriction enzyme sites and rDNA were listed in Table 2.3. To construct standard curves, 8 iterations of 1 in 3 serial dilutions of pre-meiotic DNA starting from ~3 ng/µl were formed. Each 20 or 25 µl of qPCR reaction was catalyzed by 1x SensiMix *Taq* polymerase (BioLine), 10 nM forward and reverse primers and 1-2 ng of genomic DNA. All qPCR reactions can be mixed and prepared by the Corbett CAS1200 (Corbett Robotics). Then, PCR was initiated by heat activation of *Taq* DNA polymerase at 95$^{o}$C for 10 minutes followed by 40 or 45 amplification cycles of 95$^{o}$C for 15 seconds, 60$^{o}$C for 15 seconds and 72$^{o}$C for 30 seconds. The formations of single product amplification and primer dimer were examined by melt curve analysis, and the primer pair efficiency was calculated by standard curve analysis. Moreover, the take-off Ct value for each reaction was determined by using Rotor-Gene 6000 series software. Then, DNA concentrations from Ct values were calculated through the equation of the standard curves.

## 2.10 Quantification of VDE cleavage by qPCR

To quantify the proportion of uncut chromatids at *ura3::arg4-vde* in the VDE-DSB1 system or at *ade2::URA3[arg4-vde, ura3]* in the VDE-DSB2 system, meiotic DNA after CTAB extraction **(Section 2.6)** was diluted to 0.1~0.2 ng/µl in PCR grade $H_2O$ first (typically 1 µl of meiotic genomic DNA in 1 ml of $H_2O$) and 5 µl of diluted DNA (0.5~1.0 ng of DNA) was subsequently taken out for one 20 µl qPCR reaction **(see Section 2.9)**. The test primers, DSB_For and DSB_Rev_Latest **(Table 2.3)**, were designed to anneal to unique hemizygous sequences on either sides of the DSB, one of which was within the VDE-recognition cut site and the other was on

the *ARG4* sequence **(Figure A1)**. Therefore, break formation and repair by either gene conversion or SSA destroyed template DNA for VDE-DSB amplification. The percentage of VDE cleavages at each meiosis time point can be represented by the proportion of parental *arg4-vde* chromatids remaining at time point t, $Pr_t$, which has been normalized to 0 hour. Then,

- $P_t$ = Parental *arg4-vde* concentration determined from qPCR standard curve using test primers at time point t.
- $RD_t$ = rDNA concentration determined from qPCR standard curve using rDNA primers at time point t.
- $Pr_t = [(P_t / RD_t) / (P_0 / RD_0)]$ %.

## 2.11 The Loss of Restriction Endonuclease (RE) Site Assay with Quantitative PCR

In order to monitor and detect the intermediate products of resection in meiosis, the qPCR assay for single-stranded DNA (ssDNA) was designed. Due to the innate characteristic of restriction endonucleases, most of which recognize and cleave double-stranded DNA not single-stranded DNA *in vitro*, we developed the assay to combine treating meiotic genomic DNA with restriction enzymes first and then with qPCR to allow the quantification of single-stranded DNA at different distances from VDE-DSB2. These RE sites are *Xmi*I (*Acc*I), *Mse*I and *Ban*I on the 5' side of the VDE-DSB, and *Age*I, *Hin*FI and *Eag*I on the 3' side of the VDE-DSB, which are located approximately 0.2 Kb, 1.0 Kb and 2.0 Kb away from each side of the VDE-DSB, respectively **(Figure 4.1)**. In addition, the *Scf*I RE site, which is 4.0 Kb away from the VDE-DSB site on the 3' side of the break, is selected for reporting on the

long tract of resection **(Figure 4.1)**. Forward and reverse primers for each target were designed to flank a RE site, and these corresponding primers are named 5'0.2, 5'1.0, 5'2.0, 3'0.2, 3'1.0, 3'2.0, 3'4.0 **(Table 2.3)**. Due to a small difference in the DNA sequences of the *ura3-[arg4-vde]-URA3* constructs between VDE-DSB systems (Bishop-Bailey, 2006; Neale, 2002), primers of 5'0.2_For_VD2 and 3'2.0_Rev_VD2 **(Table 2.3)** have replaced the originals (utilised in the VDE-DSB1 system) for analysing the VDE-DSB2 resection here. Because of the different efficiency among restriction enzymes, two control experiments were designed to determine whether ssDNA was lost due to enzyme activity on ssDNA and the proportion of dsDNA that was reliably digested. Then, raw data from each site of interest could be corrected by these controls, if necessary. The details of these two control experiments were shown below.

### 2.11.1 Control for ssDNA Degradation

After CTAB extraction **(Section 2.6)**, 100~200 ng of pre-meiotic yeast genomic DNA was denatured at 95$^{o}$C for 10 minutes to receive single-stranded DNA (ssDNA) and digested in parallel with native genomic DNA (dsDNA) by using 10 units of restriction enzyme in a 50 µl reaction volume. Before adding restriction enzyme, 2 µl aliquot of the restriction digest was diluted in 100 µl of ice-cold $d_2H_2O$. Then, further 2 µl aliquots were also sampled in the same way after 5, 10, 15 and 30 minutes of digestion. After which, 5 µl of each diluted sample containing 0.2~0.4 ng of DNA was taken out for one 25 µl qPCR reaction and qPCR reactions were undertaken to target the region of rDNA and the site of interest at the VDE-DSB locus **(Section 2.9)**. Then, the proportion of ssDNA degradation over the digest time course can be quantified by the following equations:

- $SS_t$ = ssDNA concentration determined from qPCR standard curve using primers flanking RE site at time point t.
- $RD_t$ = rDNA concentration determined from qPCR standard curve using rDNA primers at time point t.
- % ssDNA at each digest time point t = $(SS_t / RD_t) \times 100$.

Through this control experiment, the efficiencies of digestion among different restriction enzymes used in this study were also discovered, and can be represented by the proportion of dsDNA remaining uncut after RE digest, $DSr_t$, which was normalized to 0 minutes. Then,

- $DSr_t = [(SS_t / RD_t) / (SS_0 / RD_0)]$ %.
- The percentage of actual digested dsDNA at each digest time point t = $100 – DSr_t$.

### 2.11.2 Control for ssDNA Calibration

To obtain ssDNA, pre-meiotic genomic DNA extracted by the CTAB method **(Section 2.6)** was boiled for 10 minutes and snap chilled on ice. Mixtures of ssDNA (denatured genomic DNA) with dsDNA (native genomic DNA) were made in the following proportions, 1:0, 1:1, 1:3, 3:17, 1:10, 1:19, to generate 100, 50, 25, 15, 10 and 5% ssDNA respectively. Then, approximately 200 ng of each DNA mixture was digested with 10 units of restriction enzyme in a 50 µl reaction volume for the minutes that were determined by **Section 2.11.1** (10 minutes for the digestion were used in this study). After the digest, samples were snap chilled on ice and 20 µl of each sample was diluted in 80 µl of ice-cold $d_2H_2O$. Subsequently, 5 µl of each diluted sample containing ~4 ng of DNA was taken out for one 25 µl qPCR reaction and qPCR reactions were undertaken to target the region of rDNA and the site of

interest at the VDE-DSB locus **(Section 2.9)**. Then, the concentrations of ssDNA in different DNA mixtures were quantified using the equation in **Section 2.11.1**. And, these measured ssDNA concentrations were plotted against the expected values (y and x axis respectively) to generate an equation extrapolated from the line of best fit.

### 2.11.3 Sample Preparation for the Loss of RE Sites Assay

In order to measure the proportion of resected chromatids from VDE-DSB during meiosis, each pair of primers was designed to anneal and flank a corresponding RE site at the VDE-DSB locus **(Chapter 4 for more details and Figure 4.1)**. 100~200 ng of meiotic genomic DNA extracted by the CTAB method **(Section 2.6)** was digested with 10 units of restriction enzyme in a 50 µl reaction volume for the minutes that were determined by **Section 2.11.1** (10 minutes for the digest were used in this study). After digest, reactions were placed on ice immediately and 20 µl of each reaction was diluted in 80 µl of ice-cold $d_2H_2O$. Then, 5 µl of each diluted sample containing 2~4 ng of DNA was taken out for one 25 µl qPCR reaction to target the region of rDNA and the site of interest at the VDE-DSB locus **(see Section 2.9)**. Template DNA at the sites of interest was destroyed by restriction enzyme digestion, unless protected in single-stranded form. However, loading control template DNA (rDNA target) was preserved during the digest due to the absence of recognition sequences for the restriction enzymes used in this study.

### 2.11.4 Calculation of ssDNA as Proportion of VDE-DSB2

To receive accurate quantification of ssDNA at each site of interest during meiosis time courses, the raw data should be corrected by the equation of the line of best fit from the control for ssDNA calibration **(see Section 2.11.2)** rearranged in

terms of x. Then,

- $SD_t$ = ssDNA expressed as proportion of VDE-DSB2s present at time point t.
- $B_t$ = Proportion of *ade2::URA3[arg4-vde, ura3]* chromatids in a broken state **(see Section 2.8.2)**.
- $SD_t = (x / B_t)$ %.

# *Chapter 3*

## Analysing the Roles of Exo1 and Mre11 Nuclease Function on Short and Long Resection during Meiosis

## 3.1 Introduction of the VDE-DSB Systems

We used a meiotic double strand break (DSB) made by the homing endonuclease VDE (*VMA1*-derived endonuclease, also known as PI-*Sce*I) (Hirata et al., 1990; Kane et al., 1990; Nagai et al., 2003; Perler et al., 1994) to investigate the meiotic roles of Exo1 and Mre11 in meiotic DSB resection **(Figure 3.1)**. During meiosis VDE normally acts as a self-homing endonuclease that causes the conversion of an endonuclease$^-$ allele (*TFP1*) into an endonuclease$^+$ allele (*TFP1::VDE*) by creating a site-specific DSB within *TFP1* followed by HR using the *TFP1::VDE* allele as a repair template (Gimble and Thorner, 1992). The system used contains a reporter cassette harboring a VDE-cutsite sequence flanked by two sets of direct repeat sequences integrated at the *ADE2* locus **(Figure 3.2 B)**. A major advantage of analysing the VDE-induced DSB is that, unlike Spo11, the VDE recognises a long nonpalindromic cleavage sequence equivalent to at least 18bp in length, thus ensuring that the DSB formation is site-specific (Bremer et al., 1992; Gimble and Thorner, 1992). The homing endonuclease activity of VDE occurs only in meiosis, and more importantly, the creation of DSBs by VDE is almost at the same time as those formed by Spo11 (Gimble and Thorner, 1992). Another important feature of the VDE system is that the enzyme does not covalently bind to the DSB ends while catalyzing their formation (Gimble and Thorner, 1992), and thereby can

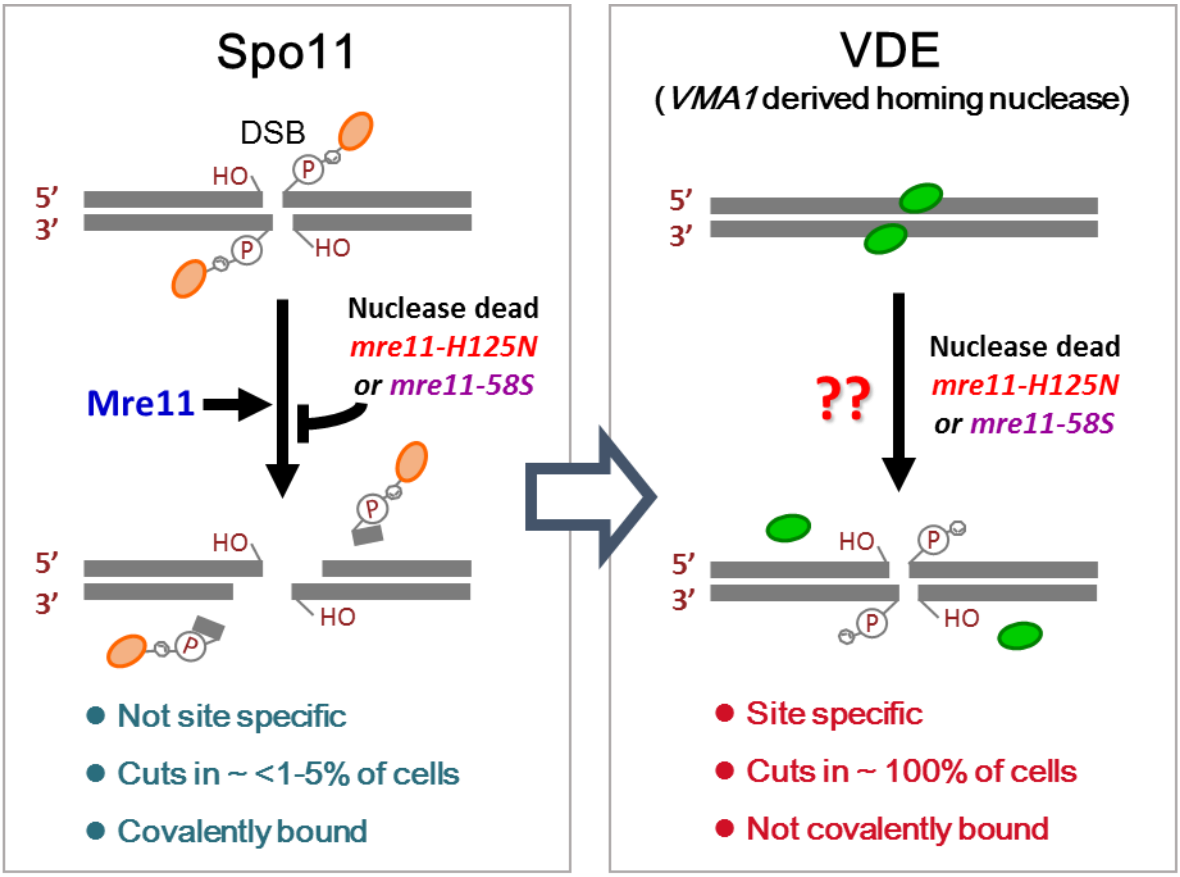


**Figure 3.1 Spo11-DSB versus VDE-DSB.** Several mutations fail to remove Spo11 from the ends of DSBs, such as nuclease dead mre11, thereby leading to difficulty for investigating the role of these genes in further resection. Therefore, we have analysed resection during meiosis at a DSB created by the site-specific endonuclease VDE, which does not bind covalently to the DSB ends, thus allowing us to model the role of nucleases or other regulatory proteins after Spo11 would be removed.

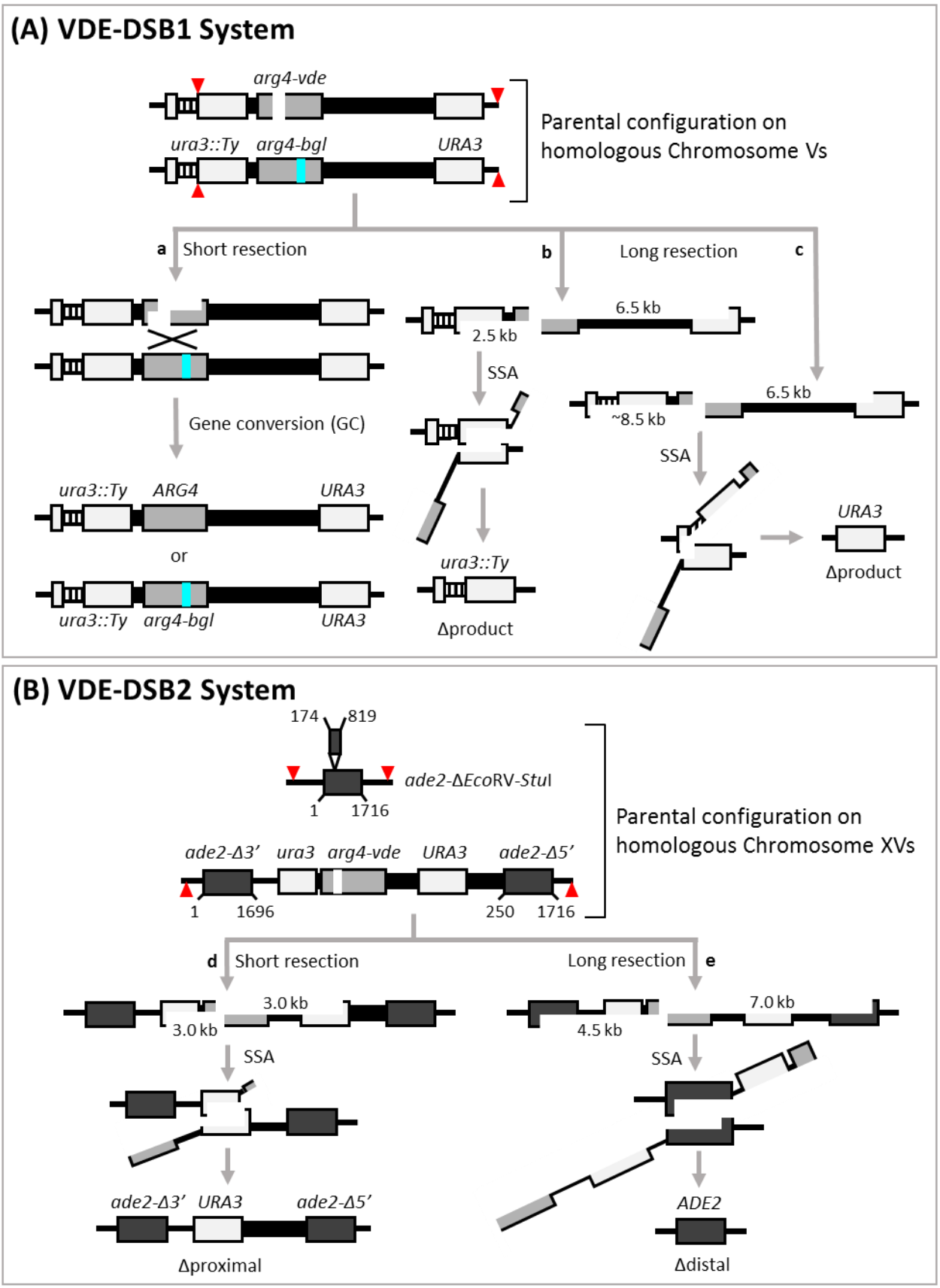


**Figure 3.2 The VDE-DSB systems.** During meiosis, the VDE endonuclease creates clean DSBs without forming covalent bounds. There are two VDE-DSB systems that have been established in our lab, the VDE-DSB1 **(A)** and the VDE-DSB2 **(B)**, where a VDE-DSB site was incorporated into *URA3* or *ADE2* loci on chromosomes V and XV, respectively. VDE-induced DSB1 can be repaired either by GC or SSA, while VDE-DSB2 can only be repaired by SSA due to the absence of homologous donor template, the *ade2*Δ(*Eco*RV-*Stu*I). Red arrows: *Spe*I RE sites.

solve the problems resulting from the failure of Spo11 removal for uncovering the mechanism of meiotic further resection **(Figure 3.1)**.

There are two VDE-DSB systems that have been established in our lab, the VDE-DSB1 and VDE-DSB2, by Matthew Neale (Johnson et al., 2007; Neale, 2002) and Anna Bishop-Bailey (Bishop-Bailey, 2006; Johnson et al., 2007) respectively **(Figure 3.2)**. In this study we utilised the system VDE-DSB2 in which one of the *ADE2* loci of chromosome XV is engineered to become an *ade2::ura3-[arg4-vde]-URA3* allele **(Figure 3.2 B)**. On the opposite chromosome XV a portion of the *ADE2* allele is deleted as an *ade2*Δ(*Eco*RV-*Stu*I), which is required to distinguish it by Southern analysis **(see Section 3.2.1)** from an *ADE2* locus generated during single-strand annealing (SSA) repair. Because the insertion is in a hemizygous configuration, repair by strand invasion with the homologue is inhibited. This forces repair to be by SSA using either of the flanking repeated sequences 3kb and 7kb away. The proximal flanking repeated sequences of *URA3* (the overlap between *ura3-3'*Δ and *URA3*) are approximately 2.5kb from each side of the VDE-DSB2, whereas the distal *ADE2* repeats (the overlap between *ade2-3'*Δ and *ade2-5'*Δ) are situated 3.9kb and 6.5kb from the left and right sides of VDE-DSB2 respectively. Therefore, the SSA repair of the VDE-DSB2 can be mediated either by the exposed proximal *URA3* repeats to generate the *ade2::URA3* allele (Δproximal) when the resection at both sites of the VDE-DSB2 reaches ~3kb **(Figure 3.2 B)**, or by the uncovering of distal *ADE2* repeats to become the *ADE2* allele (Δdistal) as the further resection reaches to 4.5kb and ~7.0kb to the left and right of the VDE-DSB2 **(Figure 3.2 B)**.

In this study, the majority of the work to elucidate the mechanism of meiotic resection is based on the VDE-DSB2 system mediated by Southern blot analysis and

the loss of RE sites assay with qPCR **(Chapter 4)**.

## 3.2 Results

### 3.2.1 Physical Analysis of DNA Events Occurring in Wild-type Cells within the VDE-DSB2 System during Meiosis

The VDE-DSB2 system has been established for unveiling the mechanism of meiotic resection, and several tests about this system have been evaluated by Anna Bishop-Bailey (Bishop-Bailey, 2006). Therefore, to continue this study, it was important to repeat the analysis of wild-type cells previously done to demonstrate their reproducibility as well as to understand the physical process of DNA events occurring within the VDE-DSB2 system throughout the meiotic progression that was induced by using the PSP2 method in this research **(Chapter 2.4)**.

The formation and repair of VDE-DSB2 can be monitored in a single Southern blot analysis that permits resolution of five bands within an *Spe*I digest: two parental bands, the *ade2::ura3-[arg4-vde]-URA3* **(P)** and the *ade2*Δ(*Eco*RV-*Stu*I) **($P_{ade2\Delta}$)** alleles, the latter of which is used as a loading control, one band representing a broken *ade2::ura3-[arg4-vde]-URA3* allele **(VDE-DSB2)**, and two different SSA repair products, **Δproximal** and **Δdistal** [see **Figure 3.3 A** and **Chapter 2.8.2** for quantification; (Hodgson et al., 2011)]. In wild-type cells (dAG630), the parental *ade2::ura3-[arg4-vde]-URA3* fragment gradually disappeared throughout the meiosis time course from 0 h to 8 h **(Figure 3.3 A)**, in which the signal reduced to an average of ~7.61% at 8 h **(Figure 3.3 B *Parent*)**. This loss of the parental band was then turned over to broken chromatids, which were repaired as proximal and

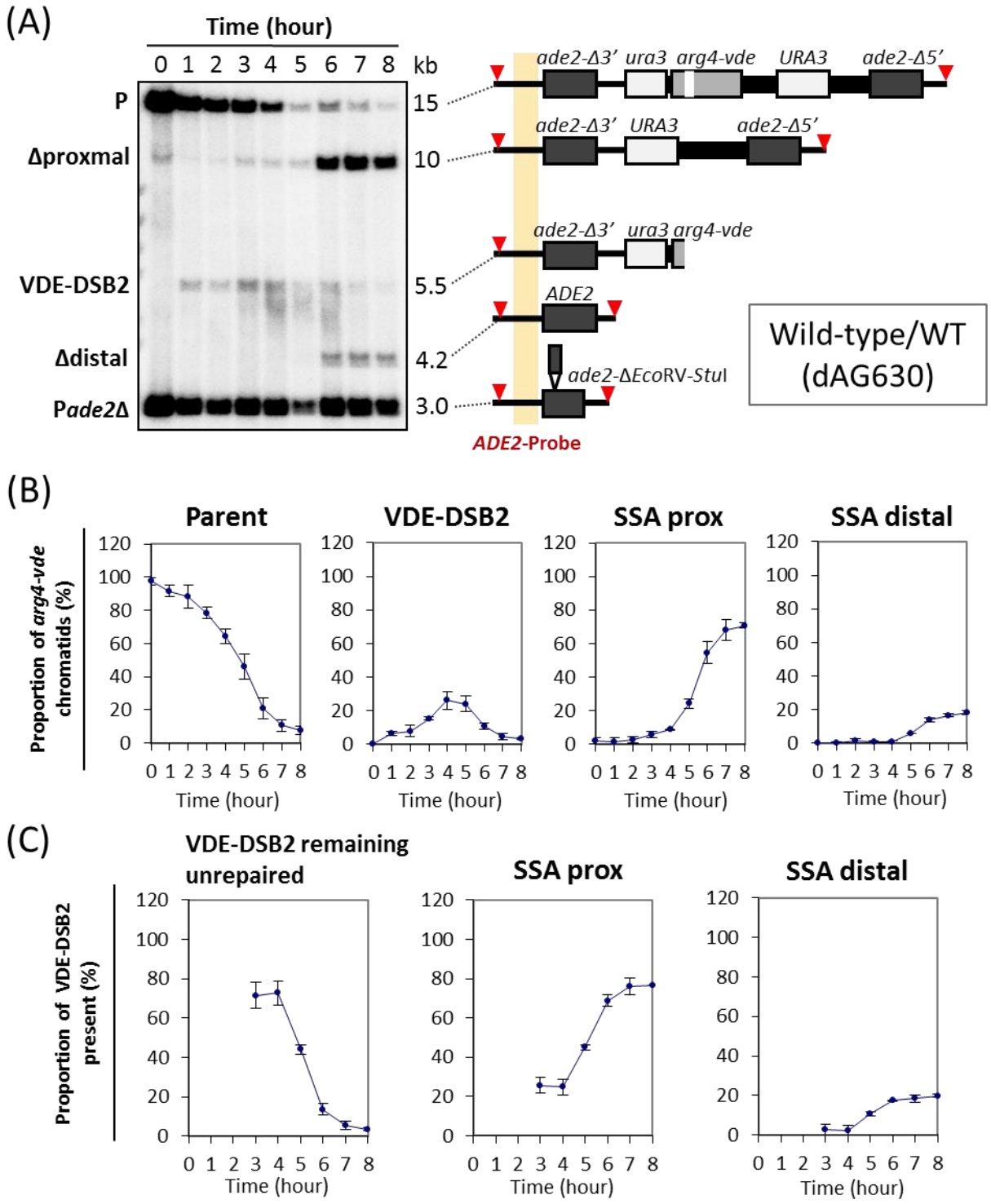


**Figure 3.3 Physical analysis of *arg4-vde* cleavage and SSA product formation within the VDE-DSB2 system. (A)** The DNA events of *arg4-vde* during meiosis was visualized by Southern blotting, with an *Spe*I digest (red arrows) and hybridizing with an *ADE2*-probe (yellow shadow), that showed five major fragments as expected. **(B)** are the proportion of *arg4-vde* chromatids in each fragment at each time point. **(C)** are the proportion of VDE-DSB2 remaining unrepaired, Δproximal and Δdistal over the total amount of VDE-DSB2 that have been made at each time point. Through these two calculations, it has shown that VDE-induced DSBs within the VDE-DSB2 system are able to be repaired efficiently by SSA repair, most mediated via shorter resection. P: parental band. Duplicated experiments have been done (n=2).

distal products, namely Δproximal and Δdistal, or still remained unrepaired as the VDE-DSB2 band. The VDE-DSB2 band peaked at 4 h after initiation of meiosis, with an average of ~26.11% of the total chromatids **(Figure 3.3 B *VDE-DSB2*)**. ("The total chromatids" here means the whole of the DNA fragments originating from the *ade2::ura3-[arg4-vde]-URA3* alleles, namely "$T_V$" shown in **Chapter 2.8.2**.) However, overall the published results and the data shown here, after 4 h of meiosis, show that the signal of the VDE-DSB2 band was fading away while both SSA proximal and SSA distal products arose and increased progressively **(Figure 3.3 A and B)**. When the meiosis time course reached 8 h, most of the VDE-induced DSB2s repaired either by short resection or via long resection SSA, where ~70.71% and ~18.36% of the total chromatids were respectively generated as Δproximal and Δdistal; and just a few breaks, around 3.33% of $T_V$, did not receive repair **(Figure 3.3 B)**.

Because there can be some variation in the timing of meiosis and break formation, we also calculated the proportion of VDE-DSB2, Δproximal and Δdistal normalised to the total amount of VDE-DSB2 that had been made at each time point **(Figure 3.3 C)**. For the wild-type strain, only ~3.61% of VDE-DSBs remained unrepaired by 8 h **(Figure 3.3 C *left*)**, and the proportion of VDE-DSB2s repaired to Δproximal and Δdistal were, respectively, ~76.53% and ~19.86% **(Figure 3.3 C *middle* and *right*, respectively)**. In other words, ~96.39% of the total broken *arg4-vde* chromatids were repaired, with most repair being mediated through shorter resection **(Figure 3.3 C)**.

### 3.2.2 Exo1 Has a Major Impact on the Repair of VDE-DSB2, Especially in the Longer Range of Resection

Next, we tested the impact of deleting *EXO1* on the VDE-DSB2 system [**Figure 3.4**; also reported in (Hodgson et al., 2011)]. The Southern blots of DNA from wild-type and *exo1*Δ (dAG1305) cells exhibited that the parental *ade2::ura3-[arg4-vde]-URA3* band was lost at the similar rate to wild-type cells **(Figure 3.4 B *Parent*)**, i.e. the timings of VDE-induced DSB formation in these two strains were similar to each other. However, deleting *EXO1* caused the continuous accumulation of the VDE-DSB2 to reach a maximum of ~73.36% at 5 h of meiosis **(Figure 3.4 B *VDE-DSB2*)**. In addition, consistent with the delay in VDE-DSB2 disappearance, the SSA proximal products appeared two hours later than in wild-type, at 6 h, after which repair of VDE-DSB2 appeared to accelerate **(Figure 3.4 B *SSA prox* and C *middle*)**. This phenomenon of delayed and then rapid repair in *exo1*Δ cells was also reported within the VDE-DSB1 system (dAG1319) **(Figure A2 D)** (Hodgson et al., 2011). Although in *exo1*Δ mutants within the VDE-DSB2 system there were still ~21.32% of the total broken *arg4-vde* chromatids remaining unrepaired at the end of the meiosis time course, the Δproximal products were generated in a similar amount as in wild-type cells **(Figure 3.4 C *middle*)**. Nevertheless, the signal of the SSA Δdistal was barely detected throughout the meiosis time course. By 8 h of meiosis only ~5.14% of the total *arg4-vde* chromatids or ~5.44% of the broken chromatids were repaired to Δdistal products, compared to ~20% in wild-type cells **(Figure 3.4 B *SSA distal* and C *right*)**. Taken together, these data suggest that after 6 hours of the meiotic induction, other proteins can substitute for Exo1 in repairing VDE-induced DSBs, but the SSA repair mediated through long resection (a sum of 10.4kb long from 3.9kb left and 6.5kb right of the VDE-DSB2 site) still requires the involvement of Exo1 proteins.

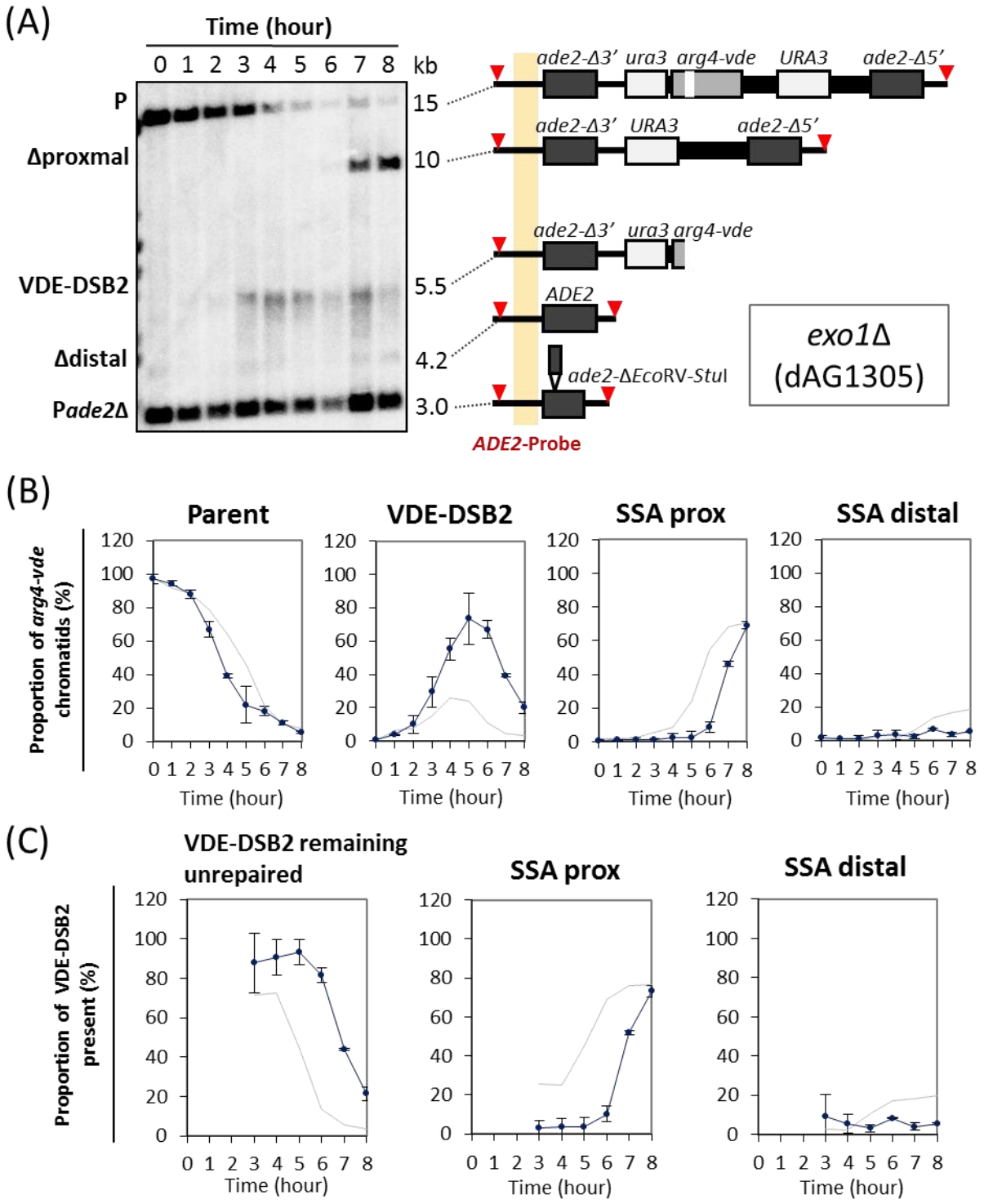


**Figure 3.4 VDE-DSB2 repair is delayed in *exo1*Δ cells. (A)** The Southern image of *exo1*Δ cells from a meiotic time course of 8 hours is shown on the left and a schematic of the corresponding bands after *Spe*I digest (red arrows) and hybridizing with an *ADE2*-probe (yellow shadow) is displayed on the right. **(B)** The graphs are quantification of the parental (P), the VDE-DSB2, the Δproximal and the Δdistal bands expressed as a proportion of *arg4-vde* chromatids in the population. **(C)** Normalizing with the parental bands calculated out the proportion of VDE-DSB2 that have been made up to the time point and remain unrepaired, and the proportion of SSA products expressed as proportion of broken *arg4-vde* chromatids. Comparing to WT (grey lines), Exo1 has a major impact on the repair of VDE-DSB2, especially in the long-range resection. Duplicated experiments have been done (n=2).

### 3.2.3 The Nuclease Function of Mre11 at H125 is Involved in the Resection and Repair of VDE-DSB2 while H213 Has Little Impact

In order to further characterise the involvement of Mre11 in meiotic resection, here the *mre11-H125N* and *mre11-58S* mutants were tested in the VDE-DSB2 system (strains dAG1592 and dAG1589, respectively).

The *mrell-H125N* allele has a mutation in the third phosphoesterase motif (Moreau et al., 1999). Although this mutation causes Mre11 to be nuclease dead, it still has been demonstrated that the Mre11-H125N protein harbors the ability to form the MRX complex, and has little impact on DSB repair in vegetative cells (Krogh et al., 2005; Moreau et al., 1999; Shim et al., 2010). This suggests that the third phosphoesterase motif of Mre11 is not important for processing damaged DNA. However, during meiosis, this allele does result in the accumulation of unresected Spo11-DSBs (Moreau et al., 1999). In addition, our previous results based on the meiotic VDE-DSB1 repair assays have indicated that the *mre11-H125N* allele has a significant impact on repair (similar to *mre11*Δ), where approximately 40% of the total amount of broken *arg4-vde* chromatids still persisted throughout the meiosis time course; the SSA repair was severely inhibited with very little SSA products found in the end (~5% of the total *arg4-vde* chromatids), as well as the GC repair also being reduced by a third compared with wild-type cells after 5 h **(Figure A2 B)** (Hodgson et al., 2011). From the perspective of the meiotic VDE-DSB2 analysis, it has shown that the rate of VDE-DSB2 formation in *mre11-H125N* mutants was similar to wild-type cells **(Figure 3.5 B *Parent*)**. At the 8 hour point of the meiosis time course, the signal of VDE-DSB2 remaining unrepaired over the total amount of broken *arg4-vde* chromatids in *mre11-H125N* mutants was ~21.17% **(Figure 3.5 C**

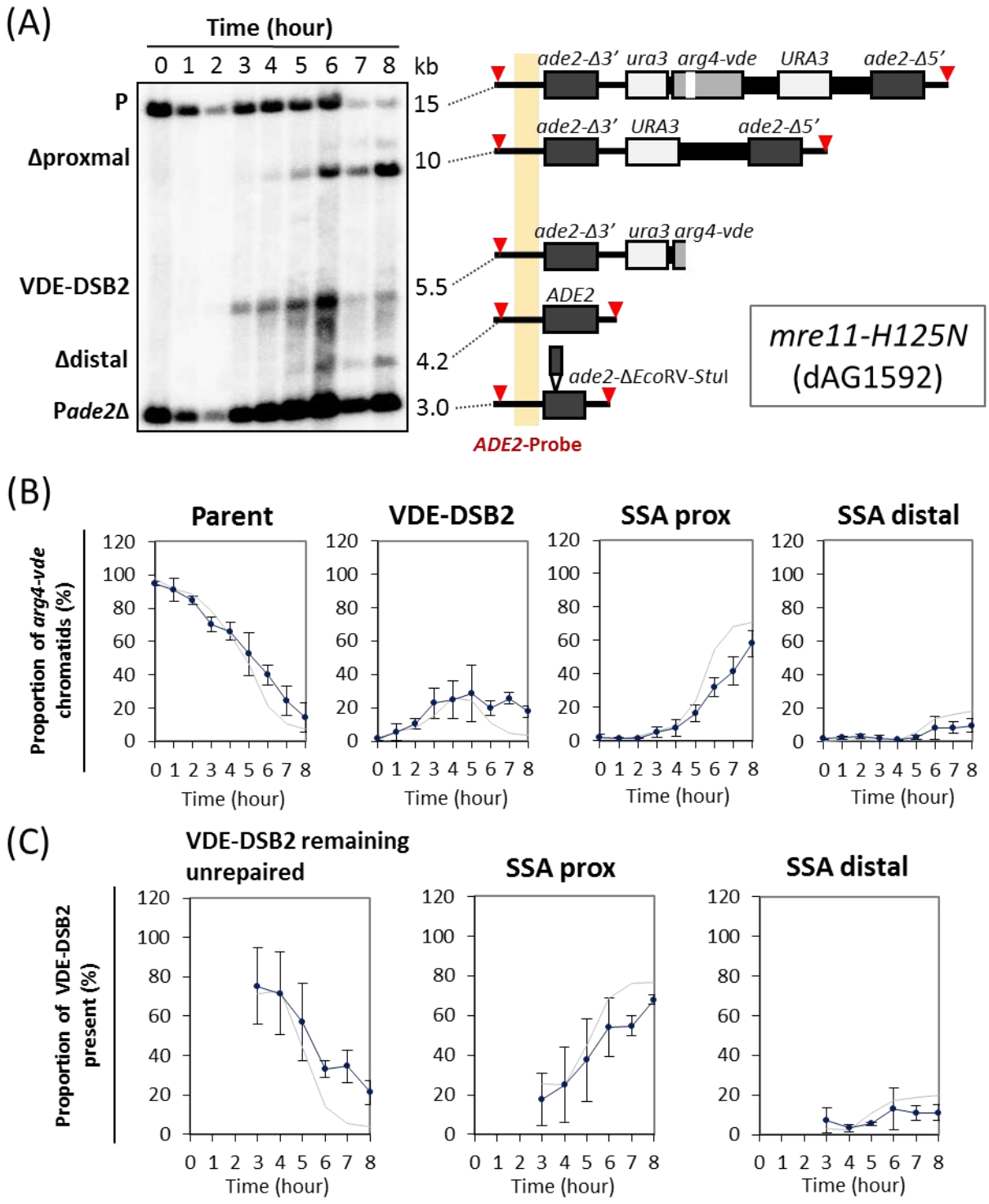


**Figure 3.5 The nuclease function of Mre11 at the third phosphoesterase motif is involved in resection and repair of the VDE-DSB2. (A)** DNA was extracted from *mre11-H125N* cells from each time point of a meiosis culture and the band pattern with *Spe*I digest (red arrows) was visualized by Southern blotting with *ADE2*-probe (yellow shadow). **(B)** Quantifications of the parental (P), the VDE-DSB2, the Δproximal and the Δdistal bands, expressed as a proportion of *arg4-vde* chromatids in the population, respectively. **(C)** Calculated proportions of VDE-DSB2 remaining unrepaired over the total amount of VDE-DSB2 that have been made at each time point, and the proportion of SSA products expressed as proportion of broken *arg4-vde* chromatids. Through this Southern analysis, it is verified that the nuclease function of Mre11 at H125 indeed has a role in VDE-DSB2 processing. Grey line: WT. n=2.

***left*)**, and at the end of the time course there was a ~50% decrease in the SSA distal products compared to the wild-type cells, while the SSA repair via short resection was not affected stringently **(Figure 3.5 C *middle* and *right*)**. Overall, these data raise the possibility of the third phosphoesterase motif of Mre11 is not only playing a role in the initiation of VDE-DSB resection, but also it is significantly affecting the process of the long-range resection of VDE-induced DSBs.

The *mre11-58S* has a substitution of a tyrosine residue for Mre11 His213 at the fourth phosphoesterase motif and thus is also called *mre11-H213Y* (Tsubouchi and Ogawa, 1998). The Mre11-58S protein then not only loses the nuclease function but also it has been reported that it might lose its affinity to form the MRX complex, neither in vegetative nor meiotic cells according to our previously published data by co-immunoprecipitation experiments using antibodies against Mre11 and Rad50 (Hodgson et al., 2011). Moreover, it has been proposed that the MRX being present as a complex is more important than the nuclease activity of Mre11 for processing mitotic DNA damages based on the phenotype of *mre11-4* (*H214L*, *H243Y*) and *mre11-58S* that fails to interact with Rad50 to form the MRX complex (Bressan et al., 1998; Tsubouchi and Ogawa, 1998; Usui et al., 1998). In meiosis, the *mre11-58S* allele also shows failure to process Spo11-DSB resection, but does not affect the formation of Spo11-DSBs (Tsubouchi and Ogawa, 1998). Since Mre11-58S might not form a complex, the repair phenotypes of *mre11-58S* in the VDE-DSB systems might be expected to be similar to or even worse than that seen in mitosis and in *mre11-H125N* cells. However, this was not the case. Compared to wild-type cells, the *mre11-58S* were shown to have weak but discernible phenotypes regarding repair of the VDE-DSB2 (similar to VDE-DSB1; see **Figure A2 C**). In the VDE-DSB2 system, the distribution of the signal of the VDE-DSB2 band throughout the meiosis

time course was similar to that of wild-type cells, though there was a slight delay in the disappearance of the VDE-DSB2 band in *mre11-58S* mutants **(Figure 3.6 B *VDE-DSB2*)**. In other words, there was a threefold increase of the VDE-DSB2 remaining unrepaired at 8 h (~11.19%) compared to wild-type cells (3.61%) **(Figure 3.6 C *left*)**. The mutation of *mre11-58S* also caused very little effect on the short and long resection repair **(Figure 3.6 B and C)**. Therefore, these data imply that the fourth phosphoesterase motif of Mre11 has a minor impact on the resection and repair of the VDE-induced DSBs, unlike with the action of the third phosphoesterase motif **(Table 3.1)**. Also, it suggests either that the complex formation of the MRX might not play an essential role in the meiotic resection, or the complex is actually formed *in vivo* with Mre11-58S **(Table 3.1)**.

The repair delay in *mre11-H125N* cells appears relatively late in the time course (after 5 hours of meiotic initiation; **Figure 3.5**), suggesting this might be because Mre11 does not act early in the VDE-DSB repair. This idea can be supported by the finding that in *exo1*Δ cells repair is delayed early and after 6 h becomes more rapid **(Figure 3.4)**. In other words, Mre11 may only be acting at VDE-DSBs after 6 h. One possible reason is Mre11 is too busy working on Spo11-DSBs to remove Spo11-oligonucleotide from the ends of the breaks. If this is true, then removing Spo11-DSBs should make Mre11 available to work earlier at VDE-DSBs. In that case, the lack of Spo11-DSBs should rescue the delayed repair of *exo1*Δ cells.

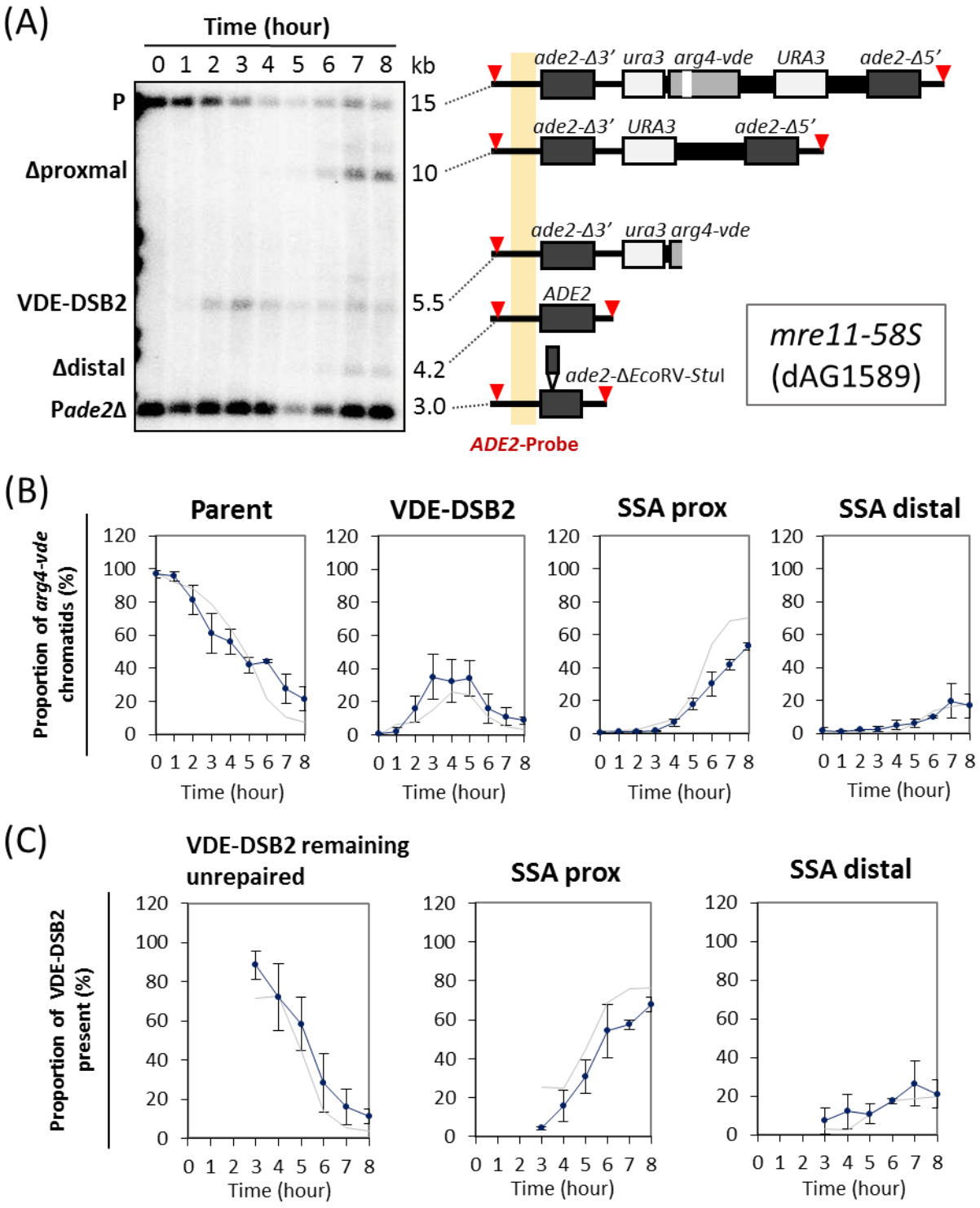


**Figure 3.6 The *mre11-58S* allele has little impact on resection and repair of the VDE-DSB2.** The legends of **(A)**, **(B)** and **(C)** here are same as the previous (Figure 3.3 to 3.5), except the DNA here is from the *mre11-58S* cells. The repair phenotype of *mre11-58S* is almost similar to that in WT, suggesting the fourth phosphoesterase motif of Mre11 does not play a significant role in VDE-DSB2 processing, which is different from the mutant of *mre11-H125N*. Grey line: WT. Duplicated experiments have been done (n=2).

| Schematic representation of *Sc*Mre11 | | |
|---|---|---|
| 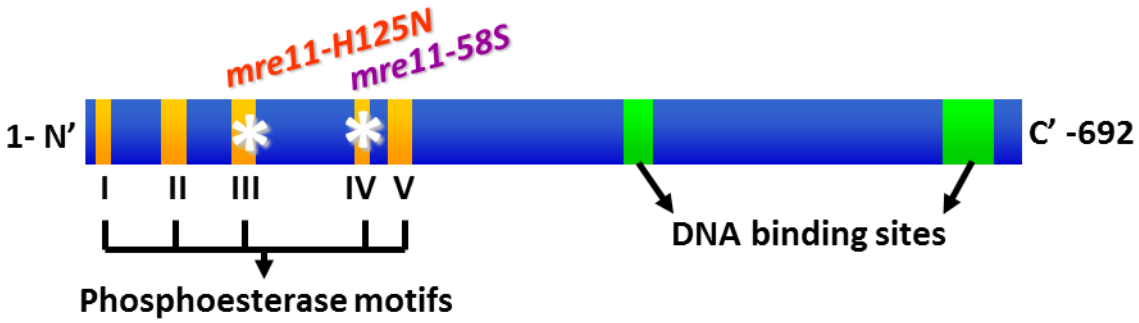 | | |
| **Name of mutants and the ability of MRX formation** | **Mitotic phenotype** | **Meiotic phenotype** |
| 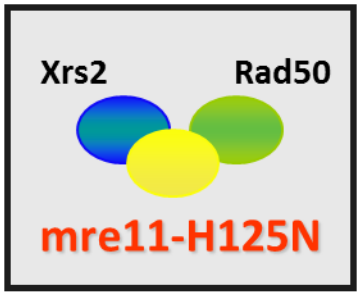 <br>MRX complex is able to form. | • Nuclease dead (neither exo- or endo-).<br>• No radiation sensitivity.<br>• Similar to WT mating type switching. | • Impeded Spo11 removal.<br>• Spo11-DSBs still form.<br>• SSA repair via short resection for VDE-DSB2 was affected in the late time of meiosis.<br>• A ~50% decrease in the SSA distal products compared to WT. |
| 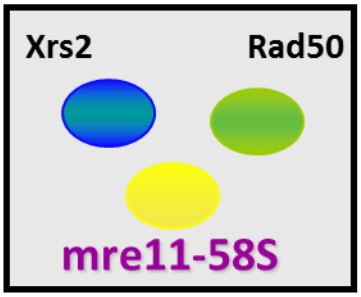 <br>Low affinity to form MRX complex. | • Nuclease dead (neither exo- or endo-).<br>• Radiation sensitivity.<br>• Impeded mating type switching. | • Impeded Spo11 removal.<br>• Spo11-DSBs still form.<br>• The repair phenotype of VDE-DSB2 was similar to WT. |

**Table 3.1 Summary of *mre11-H125N* and *mre11-58S* phenotypes in mitotic and meiotic cells.** The nuclease activity of Mre11 is not of major importance in repair of clean mitotic DSBs, and the integrity of the MRX complex is implied to have an major impact on mitotic DSBs repair. However, for the process of meiotic resection, the nuclease function of Mre11 at the third phosphoesterase motif is required, and the complex formation of the MRX might be dispensable.

### 3.2.4 Abolition of Spo11 Function Rescues the Delayed Repair Phenotype of *exo1*Δ, and to a Lesser Extent the Reduced Long-range Resection Repair

In order to validate the hypothesis mentioned above, the Spo11 function was abolished by replacing the catalytic tyrosine residue, Tyr135, with a phenylalanine to create a *spo11-Y135F*, *exo1*Δ double mutant strain (dAG1624). The idea is that with no Spo11-DSBs, the now plentiful MRX complexes can take over the Exo1 function for repairing the VDE-induced DSB2, thus suppressing the delayed repair phenotype of *exo1*Δ. The *spo11-Y135F*, *exo1*Δ double mutant cells revealed the appearance and disappearance of the VDE-DSB2 band, throughout the meiosis time course, was similar to that of wild-type cells **(Figure 3.7 B *VDE-DSB2* and C *left*)**. Also, the SSA repair mediated by short resection was restored to the same as that in wild-type cells **(Figure 3.7 B *SSA prox* and C *middle*)**. However, by 8 h the long resection of SSA was not completely recovered, but comparing to the *exo1*Δ mutants there was a 50~60% increase of Δdistal, as a proportion of total *arg4-vde* chromatids **(Figure 3.7 B *SSA distal*)**. In other words, the double mutants of *spo11-Y135F*, *exo1*Δ had ~95% and ~70% more SSA distal products than the single mutant of *exo1*Δ **(Figure 3.7 C *right*)**. These data raise the possibility that the accelerated SSA proximal repair in *exo1*Δ cells after 6 h of meiosis is caused from the Mre11 proteins which are released from the Spo11-DSBs after the initiation of Spo11-DSB resection and become available for dealing with the VDE-DSB2. Moreover, the partially rescued repair by the longer resection also implies that not only Exo1 can do long range of resection, but the nuclease function of Mre11 might also play a role in it, this view is also supported by the data in **Figure 3.5** and (Johnson et al., 2007).

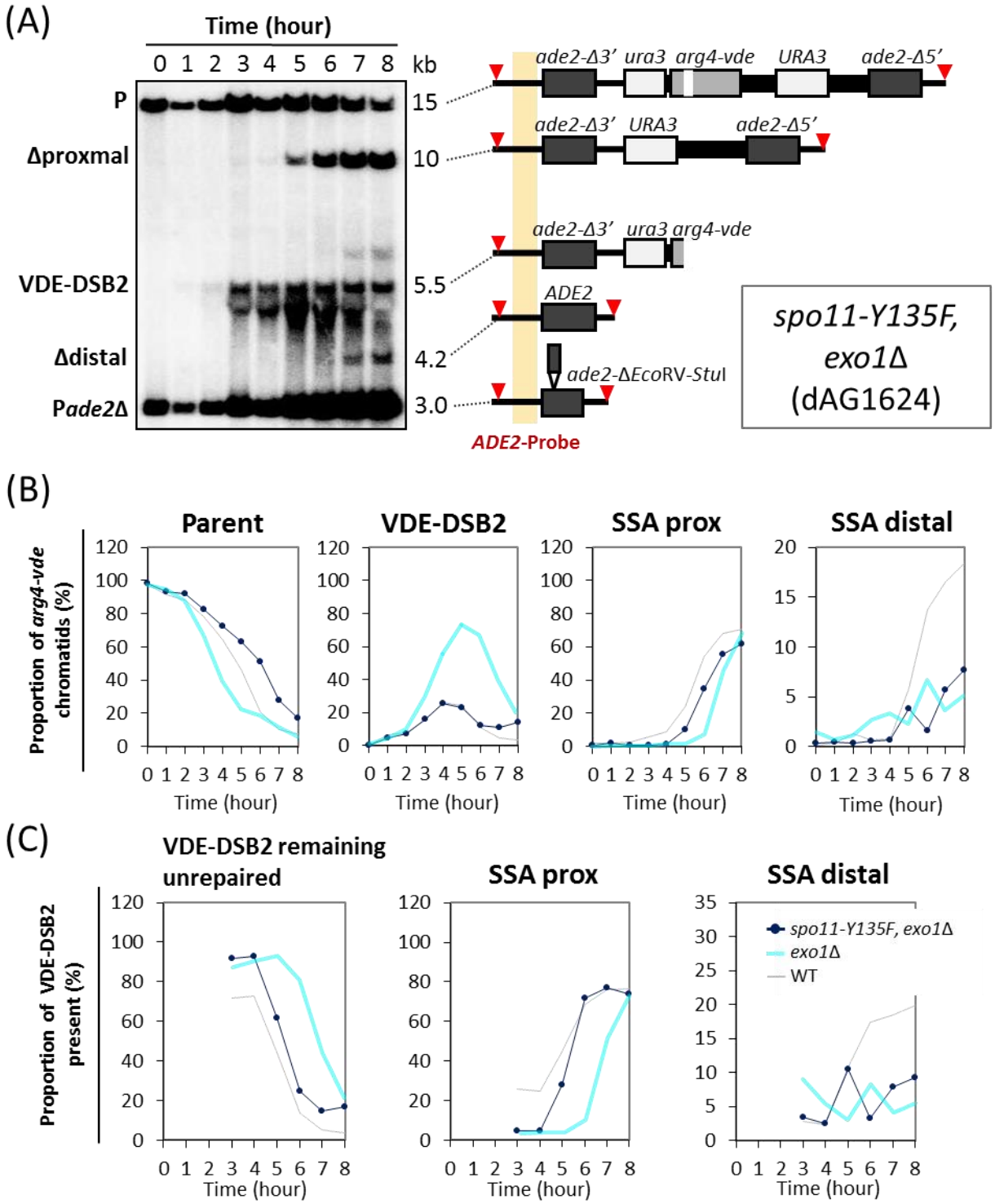


**Figure 3.7 Analysis of the VDE-DSB2 turnover in the double mutant strain of *spo11-Y135F* and *exo1Δ*.** The legends of **(A)**, **(B)** and **(C)** here are same as those previously mentioned in Figure 3.3 to 3.5, except the DNA here is from the *spo11-Y135F*, *exo1*Δ double mutant cells. When abolishing Spo11 function under the *exo1*Δ genetic background, the phenotype of VDE-DSB2 repair has been rescued slightly in the SSA distal repair. This is presumably because of the abundantly available Mre11 released from Spo11-DSB sites for the VDE-DSB2, and also raises the possibility of our model: that Mre11 is busy dealing with Spo11-DSBs at the beginning of meiosis, and later becomes available for VDE-DSB repair together with Exo1. One experiment has been done (n=1). **(B *SSA distal*)** and **(C *right*)** are in different scales to others.

### 3.2.5 The Repair and Resection of VDE-DSB2 Are Severely Impaired in *mre11-H125N*, *exo1*Δ Double Mutants

The *mre11-H125N* allele caused a decrease in the proportion of the broken VDE-DSB2 being repaired with long resection SSA by half compared to that in wild-type cells **(Figure 3.5)**. Furthermore, in *spo11-Y135F*, *exo1*Δ double mutants, the long resection repair was slightly restored with an increase of SSA distal products compared to *exo1*Δ single mutants **(Figure 3.7)**. These imply that the long range of resection within the meiotic VDE-induced DSB uses not only the Exo1 exonuclease activity but also the endonuclease function of Mre11. To further verify this, the double mutant strain of *mre11-H125N*, *exo1*Δ was constructed (dAG1593) and produced a much more severe phenotype than the single mutants **(Figure 3.8)**. The fragment of VDE-DSB2 continuously accumulated throughout 8 h of meiosis **(Figure 3.8 B *VDE-DSB2*)**, in the end of which 70.39% of the broken *arg4-vde* chromatids remained unrepaired **(Figure 3.8 C *left*)**. With the overall amounts of SSA repaired products being decreased there was almost no Δdistal product **(Figure 3.8 B and C)**, a nearly 93% drop at 8 h compared to wild-type cells **(Figure 3.9)**. This phenotype of *mre11-H125N*, *exo1*Δ cells supports the view that not only Exo1 but also the nuclease function of Mre11 is normally active for the long-range resection of the meiotic VDE-induced DSBs.

## 3.3 Discussion

Altogether, the data from our meiotic VDE-DSB2 assay with Southern blotting firstly validate that not only Exo1 but also the nuclease function of Mre11 are used for the long range of meiotic resection, and these two proteins might act on

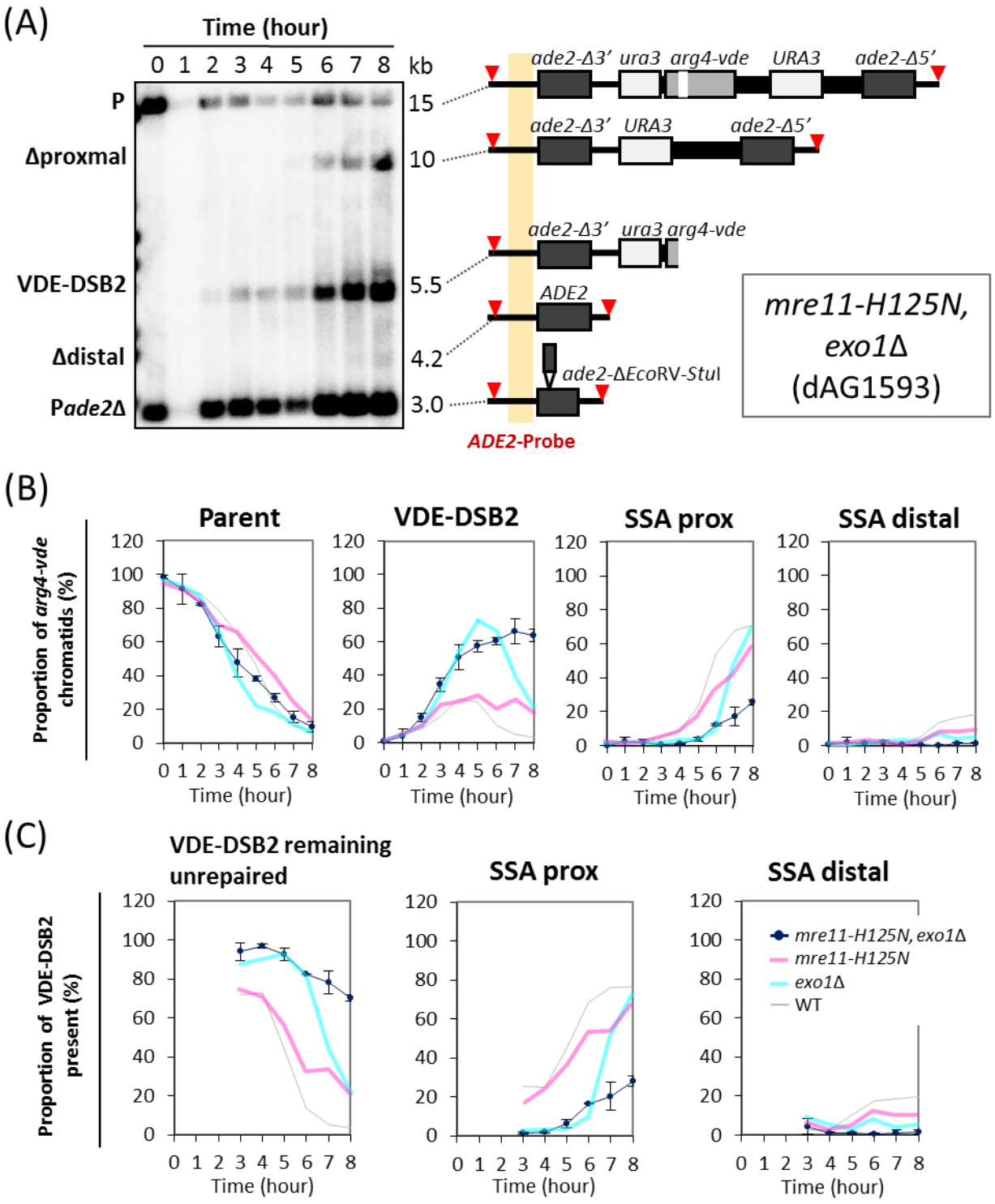


**Figure 3.8 Analysis of the VDE-DSB2 turnover in the *mre11-H125N, exo1*Δ double mutant strain.** The legends of **(A)**, **(B)** and **(C)** here are same as the previous graphs (Figure 3.3 to 3.5), except the DNA here is from the *mre11-H125N*, *exo1*Δ cells. Simultaneous mutation of *MRE11* to *mre11-H125N* and deletion of *EXO1* caused a severe defect in processing VDE-DSB2, suggesting that not only Exo1 but also the nuclease function of Mre11 are important in repair and resection of the VDE-induced DSB during meiosis. Duplicated experiments have been done (n=2).

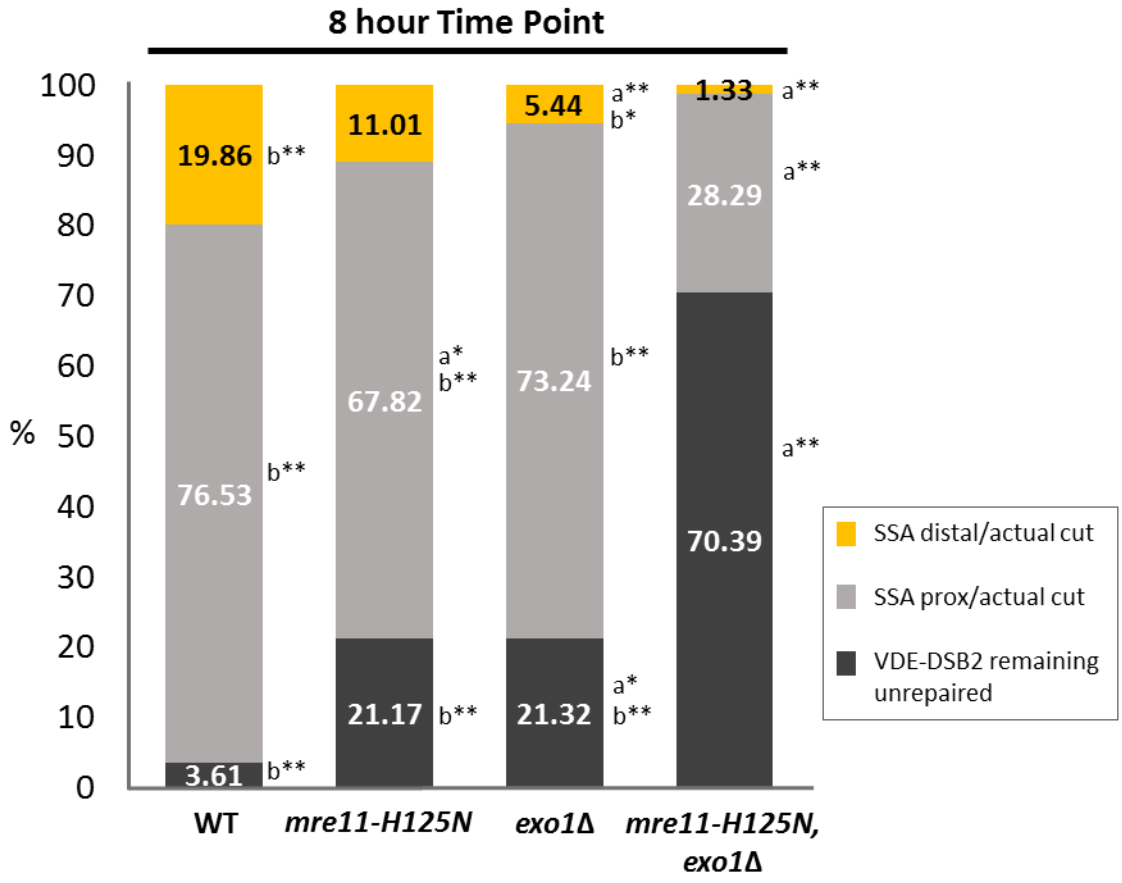


**Figure 3.9 Highlighting the VDE-DSB2-turnover phenotypes at the 8 hour meiosis time point in *mre11-H125N*- and *exo1*Δ-related mutant strains.** When mutating *MRE11* as *mre11-H125N* within the *exo1*Δ genetic background, it caused a significant decrease of both SSA repair products compared to *exo1*Δ single mutants, though only resulting in a significant drop in SSA proximal products compared to *mre11-H125N* cells, suggesting not only Exo1 but also Mre11 are required for processing the short and long resection of VDE-DSB2. *, $p<0.05$; **, $p<0.01$; a, compared to WT; b, compared to the *mre11-H125N*, *exo1*Δ double mutant cells. Duplicated experiments have been done for each strain (n=2).

different pathways. In addition, both of nuclease functions of Exo1 and Mre11 are able to compensate for each other for processing the short range of resection, but the major role for the long-range resection is considered to be Exo1.

These data also imply to us that **(Figure 3.10)**: at the beginning of meiosis, Mre11 proteins within the MRX complexes are busy dealing with the multiple Spo11-DSBs while Exo1 proteins are available and dominant for addressing the VDE-DSB2. According to Borde et al., the removal of Mre11 from DSB specific regions is dependent on resection rather than repair (Borde et al., 2004; Krogh and Symington, 2004), suggesting to us that after the initiation of Spo11-DSB resection the MRX complexes are thought to be still sequestered at numbers of Spo11-DSB sites until Exo1 proteins are recruited to commence further Spo11-DSB resection, and this association of MRX complexes with Spo11-DSBs probably acts as a signal for the recruitment of Exo1 to the Spo11-DSB sites. Subsequently, the released Mre11 proteins are available for the VDE-DSB2 resection, where the long-range resection of VDE-DSB2 presumably requires both the dismissed Mre11 and either the persisting Exo1 or one released from the Spo11-DSBs that have completed the further resection. Alternatively, this model could be illustrated in different way, because the rescue of the *exo1*Δ phenotype in SSA proximal repair by simultaneously abolishing Spo11 function is perhaps due to altering the regulation of nuclease activities in the absence of Spo11-DSB formation, rather than releasing an abundantly of Mre11 proteins.

The last interesting point is that when simultaneously mutating *MRE11* as *mre11-H125N* alleles and deleting *EXO1*, the SSA repair by short-range resection was not completely abolished. This small amount of SSA proximal products is

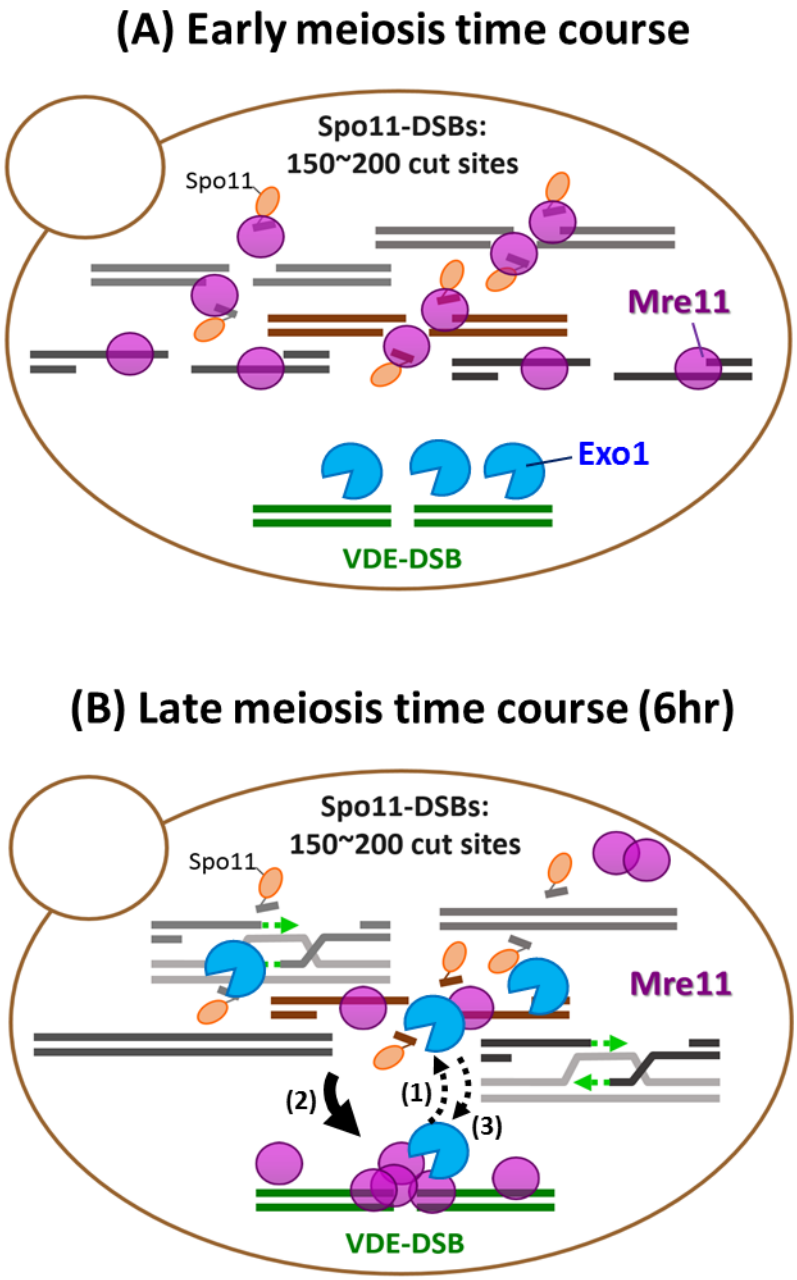


**Figure 3.10 The model for Mre11 and Exo1 in the VDE-DSB processing. (A)** At the beginning, Mre11 proteins within the MRX complexes are busy dealing with the multiple Spo11-DSBs while Exo1 proteins are available and play a major role in addressing the VDE-DSB repair. **(B1 and 2)** After the initiation of Spo11-DSB resection, the MRX complexes are thought to be still sequestered at numbers of Spo11-DSB sites until Exo1 proteins are recruited to commence further Spo11-DSB resection, which makes Mre11 become available for the VDE-DSB resection **(B2 and 3)** The long-range resection of VDE-DSB presumably requires both the dismissed Mre11 and either the persisting Exo1 or the one released from Spo11-DSBs in which resection has been completed.

suggested due to Sgs1/Dna2, Sae2 or other nuclease factors that is independent of Exo1 and Mre11 pathways.

# *Chapter 4*

## Monitoring the Resection Tracts in *exo1* and *mre11* Mutant Cells within the VDE-DSB2 System by the Loss of Restriction Endonuclease Site Assay with qPCR

## 4.1 Introduction of the Loss of Restriction Endonuclease (RE) Site Assay by Quantitative PCR

In order to directly quantify and analyse the intermediates of single-stranded DNA several methods have been established, including filter-binding, in gel hybridization, two-dimensional gel electrophoresis, sucrose gradient, monoclonal antibody and hydroxyapapatite chromatography, as well as the loss of restriction endonuclease (RE) site assay in denaturing gel electrophoresis and Southern blotting (Hodgson, 2009; Johnson et al., 2007; White and Haber, 1990). Several limitations and difficulties arise from using these methods, such as poor reproducibility of results, requirements of extensive experience for routinely producing reliable results, and radioactive dependence. A previous member, Adam J Hodgson, has developed a new method combining the loss of RE site assay with quantitative PCR, to accurately map the resection profiles at the VDE-DSB site throughout the progress of meiosis that is time-saving, non-radioactive dependence and just requires a tiny amount of genomic DNA (Hodgson et al., 2011; Hodgson, 2009).

Because most of restriction endonucleases act on double-stranded DNA rather

than the single-stranded, PCR target sites unveiled by resection are protected from being digested after incubation with a selected endonuclease. Therefore, primers will only amplify the DNA template that is single-stranded at the time of the digest, and the signal obtained from qPCR following RE digestion is proportional to the amount of ssDNA present. Seven distinct RE sites have been targeted with different distances from the VDE-DSB site on either side of the break for providing analysis of the initiation, extent and symmetry of DSB resection **(Figure 4.1)**. After normalising this fluorescence signal generated from the resection target at each meiosis time point to that from the loading control rDNA **(Figure 4.1 *right*; Chapter 2.10)**, which neither receives meiotic DSBs nor contains the relevant RE sites, the proportion of the *arg4-vde* that had been resected beyond a point of interest is then determined. Furthermore, the amount of ssDNA as a proportion of VDE-DSB present can also be calculated **(Chapter 2.11.4)**, meaning the state of the VDE-DSBs present at each time point can be reported, rather than just the proportion of chromosomes being single-stranded.

## 4.2 Results

In this thesis, to establish the loss of RE sites assay within the VDE-DSB2 system by qPCR, two controls were needed to validate first **(Section 4.2.1 and 4.2.2)**. Then, the resection profile at the VDE-DSB2 site can be mapped based on the same circumstance even undergoing different endonuclease treatments.

### 4.2.1 Validation of Rate of ssDNA Degradation under each RE Digest and Efficiency of each RE Activity for VDE-DSB2 System

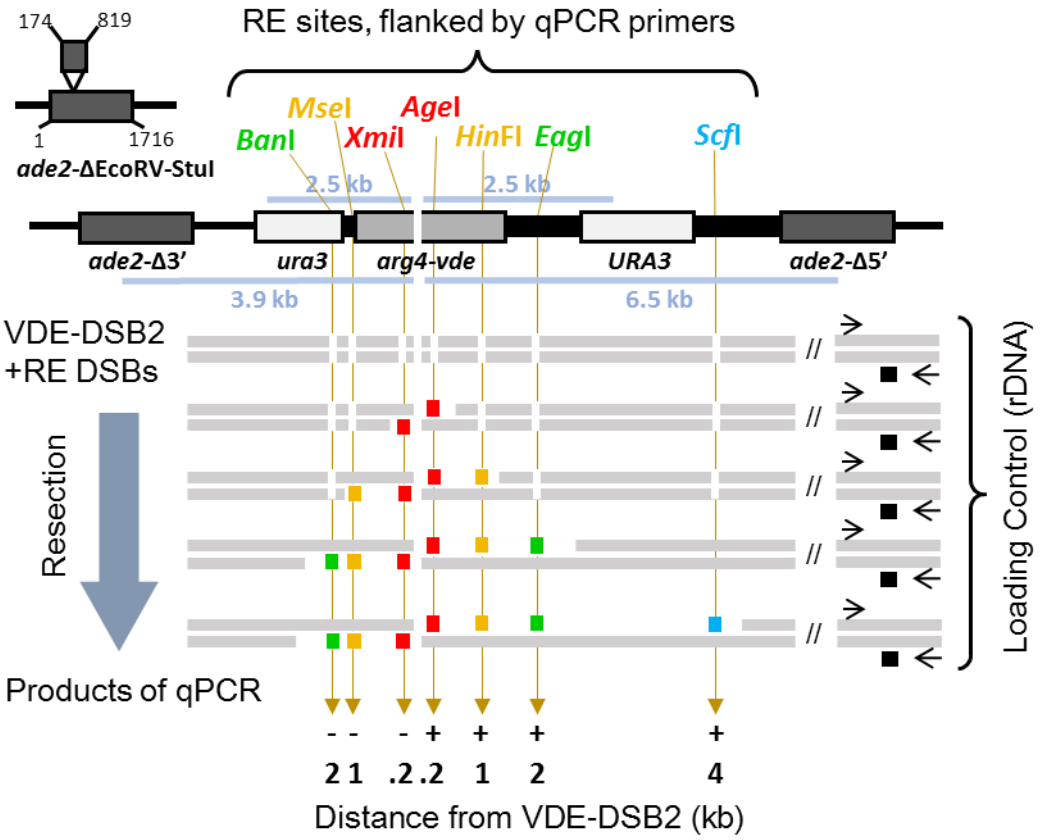


**Figure 4.1 Introduction of qPCR into the loss of RE site assay for the VDE-DSB2 system.** Schematic of the VDE-DSB2 reporter cassette showing relative positions of restriction endonuclease sites used in this assay, primers for qPCR flanking these RE sites and an rDNA site as a loading control. RE sites have been colour coded, the gaps interrupting the grey DNA represent DSBs resulting from VDE *in vivo* and REs *in vitro*. Once resection destroys a RE site, the qPCR products are obtained by the corresponding flanking-primers as indicted by the coloured squares, and always from the rDNA.

The accuracy of the loss of RE site assay depends on two assumptions: (1) 100% of endonuclease recognition sites are digested after incubation with the restriction enzyme, and (2) during the period of digestion 3' ssDNA tails stably exist (Hodgson, 2009). However, different restriction enzymes harbor their own characteristics causing a diversity of digest efficiencies and maybe accompanying different effects on ssDNA. Therefore, the rate of ssDNA degradation and the efficiency of RE digest under each RE treatment was determined first to find out the best reaction time suitable for all RE sites that we targeted. Through the control experiment we have designed **(Chapter 2.11.1)**, and according to the previous data shown in the VDE-DSB1 system (Hodgson, 2009), 10 minutes of RE digestion was selected to do the tests for the VDE-DSB2 system using mitotic genomic DNA from wild-type cells (dAG630) as the template resource. Most of the target RE sites showed less than 20% of denatured genomic DNA being degraded **(Figure 4.2 A)**. Only the *Xmi*I (*Acc*I) site was underestimated more after 10 minutes of digest, possibly due to the formation of secondary structures that can be recognized by *Xmi*I (*Acc*I); while there was approximately 25% more denatured genomic DNA overestimated in the *Hin*FI site after 10 minute digest **(Figure 4.2 A)**. Most of these selected restriction enzymes showed almost 100% digest efficiency with incubation of native genomic DNA with each RE for 10 minutes, *Scf*I displayed 75.15% digestion **(Figure 4.2 B)**.

### 4.2.2 Validation of ssDNA Calibration Controls for Analysis of the VDE-DSB2 Resection

After confirming the suitable reaction time for all target RE-sites within the VDE-DSB2 system (10 minutes of digestion), we further designed the control experiments for ssDNA calibration to receive an accurate quantification of ssDNA

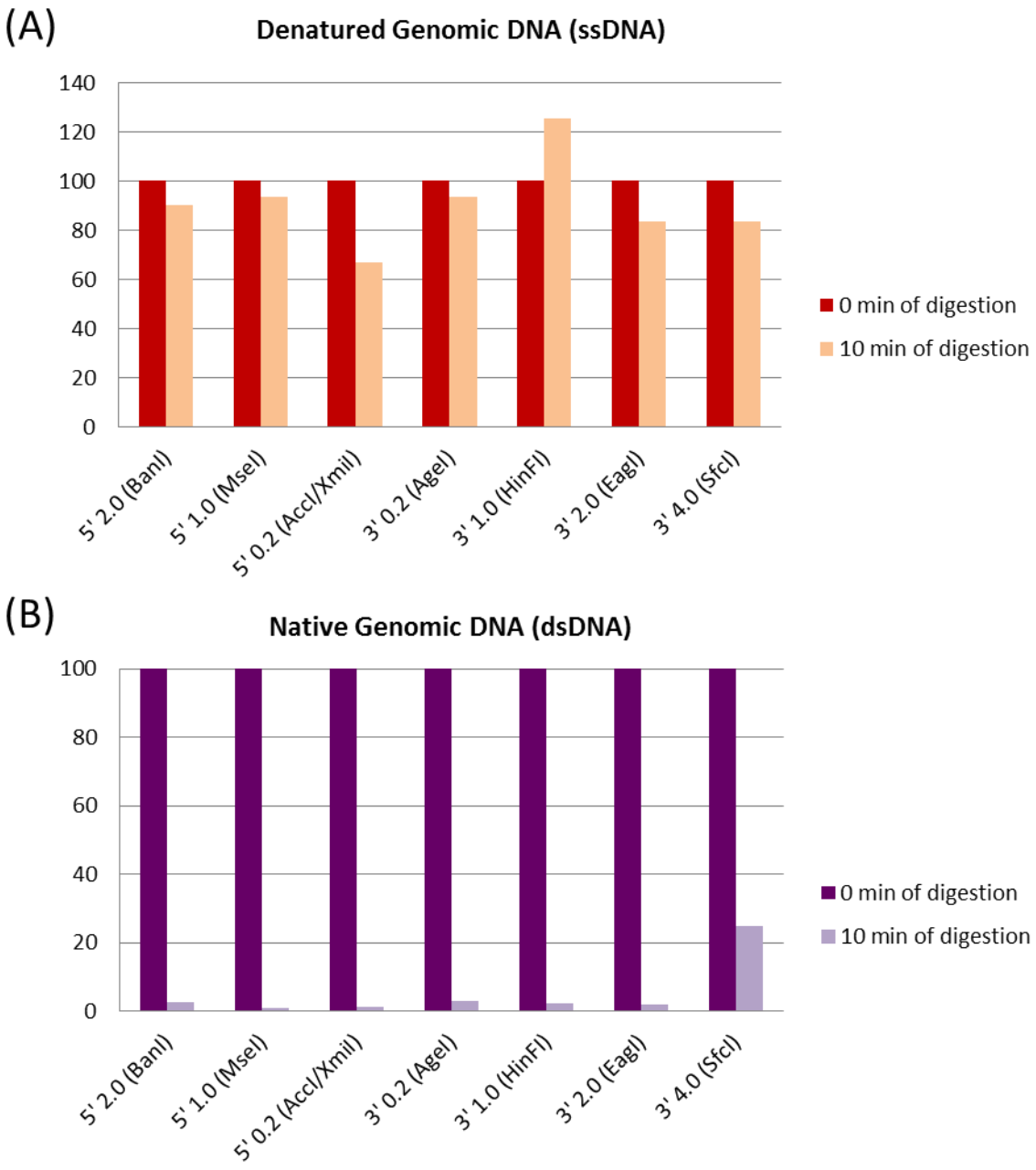


**Figure 4.2 Controls for the rate of ssDNA degradation and the RE activity for the VDE-DSB2 system.** Template DNA was extracted from mitotic wild-type cells (dAG630). **(A)** To validate the ssDNA degradation controls in each RE site, 100~200 ng of genomic DNA was boiled first to denature as ssDNA and digested with 10 units of the corresponding RE for 0 and 10 minutes. Then, after qPCR quantification, the value from each RE-digested treatment was compared to the value from the non-digested one that was regarded as 100% to determine the degradation rate of ssDNA in each RE site. **(B)** Same as for verifying the RE activity in each RE site, except template DNA was native without denaturation.

intermediates at each site of interest during the meiotic VDE-DSB2 resection **(Chapter 2.11.2)**. In brief, standard concentrations of ssDNA were generated as 5%, 10%, 15%, 25%, 50% and 100% by mixing native and denatured mitotic genomic DNA of wild-type cells (dAG630) in different proportions **(see Chapter 2.11.2 for more details)**. As standards were digested with each RE in turn and the template DNA remaining was quantified by qPCR, these measured ssDNA concentrations were plotted against the expected values to generate an equation extrapolated from the line of best fit (**Figure 4.3 A**, take 5' 0.2 VDE-DSB2 target RE site, *Acc*I/*Xmi*I, for example). Thus, data from each target site were joined by a line of best fit and were set to pass through the origin (x,y) = (0,0), that was described mathematically as y = ax, where y is the measured concentration of ssDNA at the test target, x is the actual percentage of ssDNA in the standard, and a is the slope. These equations were listed in **Figure 4.3 B**. The control experiments for ssDNA calibration already contain two factors mentioned in **Section 4.2.1**, namely the rate of ssDNA degradation and the efficiency of RE digest, hence we directly used the adjusted formulas to obtain the actual quantity of resected intermediates of the VDE-DSB2 at each target RE-site in this study.

### 4.2.3 Physical Analysis of the VDE-DSB2 Resection Event in Wild-type Cells via the Loss of RE Site Assay with qPCR

In wild-type cells (dAG630), the ssDNA levels at 0.2 kb, 1.0 kb, 2.0 kb and 4.0 kb-resected tracts peaked all at either 4 or 5 h after initiation of meiosis **(Figure 4.4 A)**. This is consistent with the Southern blot result that the proportion of VDE-DSB2s repaired increased after 4 h **(Figure 3.3)**. Throughout the meiosis time course signals of ssDNA with the shortest resected tract were stronger than others, but the ratio of them to the others changed **(Figure 4.4 A)**. Therefore, we highlighted the ratio of

(A)

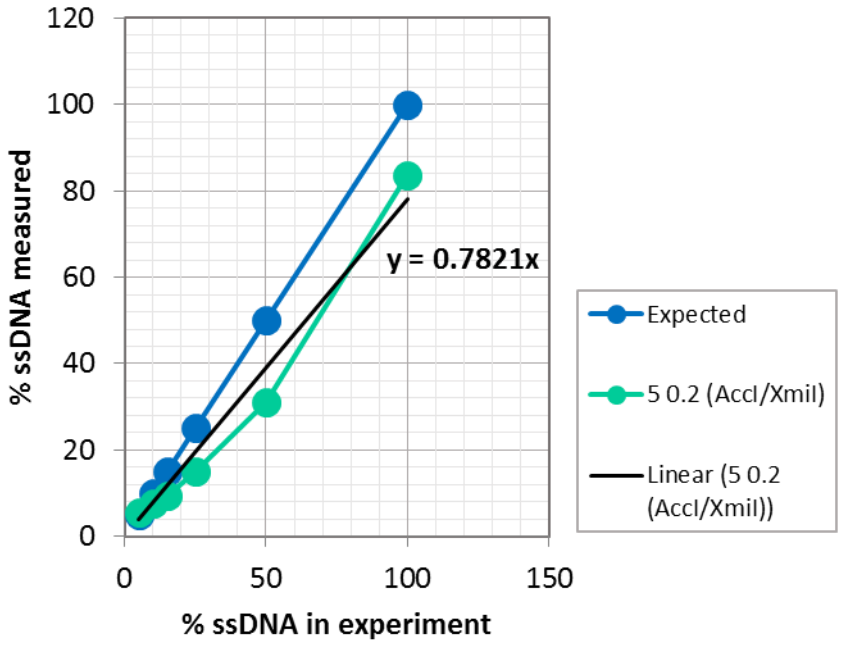


(B)

| Trend-line Linear Equation for ssDNA Calibration | |
|---|---|
| | **Intercept set at origin** |
| **5' 2.0 (*Ban*I)** | y = 0.3633x |
| **5' 1.0 (*Mse*I)** | y = 0.369x |
| **5' 0.2 (*Acc*I/*Xmi*I)** | y = 0.7821x |
| **3' 0.2 (*Age*I)** | y = 0.1279x |
| **3' 1.0 (*Hin*FI)** | y = 0.3048x |
| **3' 2.0 (*Eag*I)** | y = 0.6456x |
| **3' 4.0 (*Sfc*I)** | y = 0.2911x |

**Figure 4.3 ssDNA calibration controls for analyzing the VDE-DSB2 resection tract at each target RE site. (A)** Normalizing the qPCR data with the rDNA loading control showed the deviation of measured ssDNA levels from expected for 5' 0.2 VDE-DSB2 target RE site validation (green for the measured, blue for the expected). **(B)** The trendline linear equations for ssDNA calibration in each target RE site are shown with setting intercept at origin.

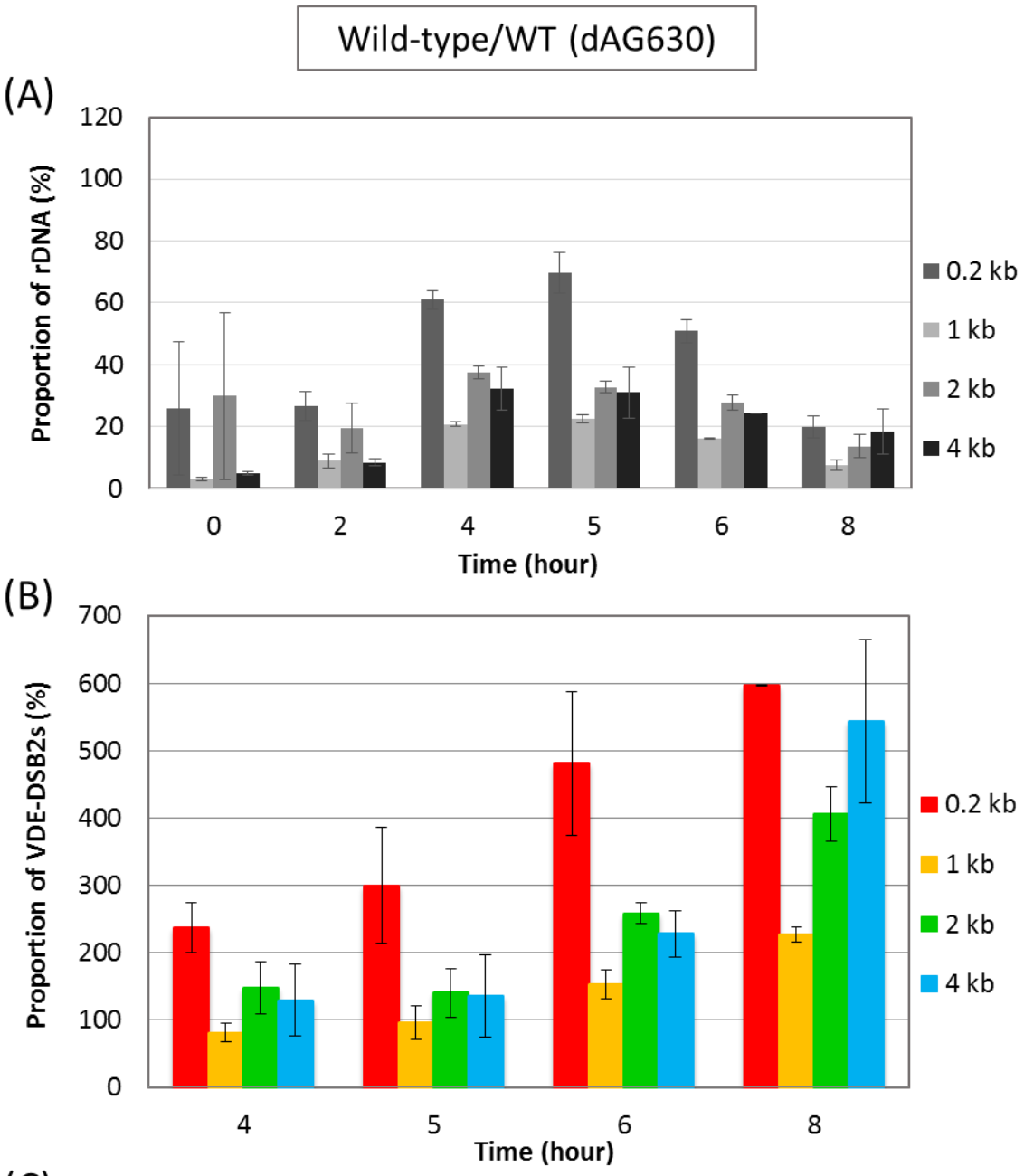


**Figure 4.4 Physical monitoring the resection tract of VDE-DSB2 in WT cells by our loss of RE site assay. (A)** Quantification of the qPCR expressed as a proportion of rDNA that turns into ssDNA intermediates at each target RE site during the meiosis time course. **(B)** Quantification of the qPCR expressed as a proportion of VDE-DSB2s in a single-stranded state at coloured-coded distances and time point shown. **(C)** The ratio of the longest ssDNA signal to the shortst ssDNA signal. Each bar is the average of data from two independent experiments and for sites of the same distance on each side of VDE-DSB2. The genomic DNA is from the same resource of Southern blot shown in Chapter 3.

the longest ssDNA molecules (4.0 kb) to the ssDNA with the exposure of the RE-sites that are nearest to the VDE-DSB2 (0.2 kb) during the period from 4 to 8 h. This indicates ~50% of ssDNA intermediates were processed to become long tract resection at all times (**Figure 4.4 C)**, and in the end of meiosis nearly 100% of the intermediates became long tract ssDNA, thus the ratio of the 4.0 kb to the 0.2 kb being almost 1:1 **(Figure 4.4 C)**. There was a gradual increase in the proportion of VDE-DSB2s in each resection state throughout the meiosis time course **(Figure 4.4 B)**, which is different from the VDE-DSB1 finding showing little fluctuation instead (Hodgson et al., 2011).

### 4.2.4 Direct Analysis of ssDNA Intermediates in *exo1*Δ Cells within the VDE-DSB2 Resection

According to the Southern analysis, we have realized that Exo1 plays a dominant role in catalyzing the VDE-DSB resection, especially in the long range of resection **(Figure 3.4)**. To further confirm this, we directly quantified the ssDNA intermediates with different resection tracts that we targeted by the loss of RE site assay with qPCR. In fact, deleting *EXO1* in the VDE-DSB2 system caused the severe reduction in producing ssDNA compared to wild-type cells **(Figure 4.5 *exo1*Δ)**. Before the meiosis time point of 6 h, the number of ssDNA with short resection tracts (0.2 kb and 1.0 kb away from the VDE-DSB2 site) were similar to those in wild-type cells, whereas the ssDNA levels with long resection tracts (2.0 kb and 4.0 kb) significantly ($p<0.05$) reduced compared to wild-type cells **(Figure 4.5 A *top left*)**. When normalising with the presence of VDE-DSB2 from Southern analysis, all of the ssDNA levels displayed much lower than wild-type cells, particularly at further distances from the VDE-DSB2 site **(Figure 4.5 A *top right*)**. This is consistent with the result shown in the VDE-DSB1 system (Hodgson et al., 2011), and agrees with the

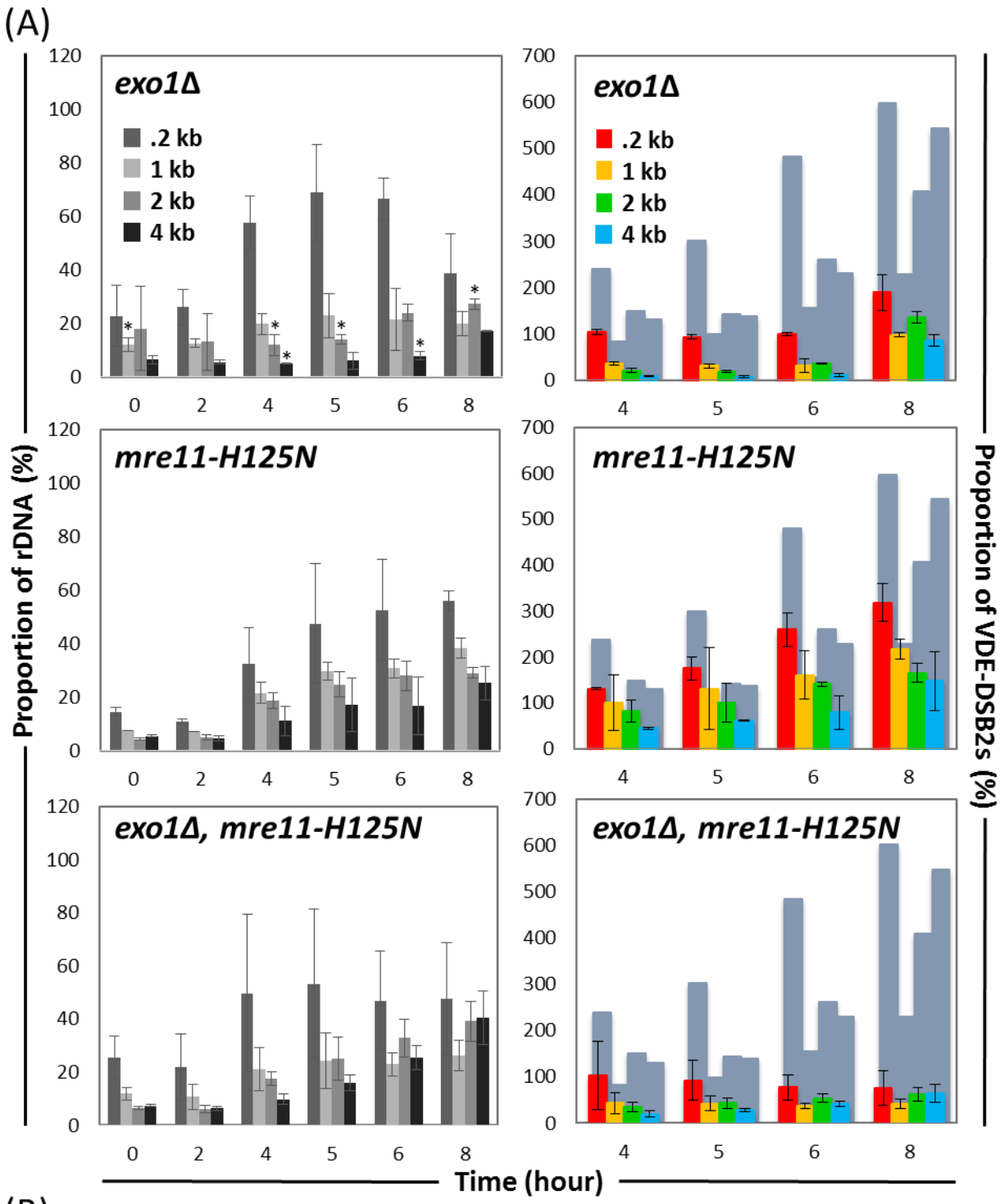


**Figure 4.5 The loss of RE site assay in the *exo1*Δ- and the *mre11-H125N*-related mutants. (A)** Quantification of the qPCR expressed as a proportion of rDNA that turns into ssDNA **(left)** and a proportion of VDE-DSB2s in a single-stranded state **(right)** at coloured-coded distances and time points shown. The grey offset bars in the right are WT for comparison. **(B)** The ratio of the longest ssDNA signal to the shortest. Each bar is the average of data from two independent experiments and all genomic DNA are from the same resource of the Southern. *, $p<0.05$ compared to WT.

Southern analysis that there is a significant delay in SSA repair in *exo1*Δ cells. Furthermore, through highlighting the ratio of the 4.0 kb to the 0.2 kb from 4 to 8 h **(Figure 4.5 B)**, it also indicates that long-range resection was severely reduced in the absence of *EXO1*, where the ratio was below 0.15 from 4 to 6 h **(Figure 4.5 B)**. The proportion of VDE-DSB2s in each single-stranded state obviously increased at 8 h compared to other time points **(Figure 4.5 A *top right*)**, consistent with our previous published data in VDE-DSB1 resection (Hodgson et al., 2011). These data fit well with the finding from Southern analysis indicating there is accelerated repair of VDE-DSBs after 6 h of meiosis induction in *exo1*Δ cells.

### 4.2.5 Mutation of the Third Phosphoesterase Domain of Mre11 Causes a Severe Deficiency in Producing ssDNA of VDE-DSB2

Through the loss of RE site assay, it showed that mutating *MRE11* as *mre11-H125N* alleles caused the impairment of producing ssDNA intermediates of VDE-DSB2 **(Figure 4.5 A *mre11-H125N*)**. As meiosis progressed and more VDE-DSB2 were created, the relative proportion of ssDNA intermediates in *mre11-H125N* cells became much less than wild-type cells **(Figure 4.5 A *middle right*)**, and the relevant ratio of the 4.0 kb to the 0.2 kb also displayed significant reduction compared to the wild-type **(Figure 4.5 B)**. This can explain what the Southern blot found in *mre11-H125N* cells, where a delay of SSA repair occurred in the late stages of the meiosis time course with a reduction of approximately half of Δdistal compared to wild-type cells **(Figure 3.5)**. Nuclease activity of Mre11 from the third phosphoesterase domain is, therefore, confirmed to play an important role in the processivity of DSB resection during meiosis, and the data from the loss of RE site assay is the direct evidence for this phenomenon, which also appeared in the VDE-DSB1 processing that has been published (Hodgson et al., 2011).

### 4.2.6 The *mre11-H125N*, *exo1*Δ Double Mutants Exhibit a Synergistic Effect on Generating ssDNA for VDE-DSB2 Resection

Doubly mutant cells, *mre11-H125N*, *exo1*Δ, showed a gradual accumulation of ssDNA intermediates throughout the meiosis time course **(Figure 4.5 A *bottom left*)**: the proportions of the *arg4-vde* chromatids being single-stranded at each target RE-site were lower than that in wild-type cells **(Figure 4.4 A)** at 4 and 5 h, especially in the long ssDNA molecules, and later became similar or even greater than wild-type cells at 6 and 8 h. However, due to the amount of VDE-DSB2s accumulating throughout meiosis in the *mre11-H125N*, exo1Δ cells **(Figure 3.8)**, the amount of ssDNA as a proportion of VDE-DSB2 present at each target RE-site in this double mutant decreased compared to wild-type cells **(Figure 4.5 A *bottom right*)**. After this normalisation, the *mre11-H125N*, *exo1*Δ double mutants also showed a much more severe reduction in ssDNA than the *mre11-H125N* single mutants **(Figure 4.5 A *right*)**. Moreover, although the ssDNA profile before 8 h was slightly better than *exo1*Δ cells, the *mre11-H125N*, *exo1*Δ double mutants displayed the most severe deficiency in producing ssDNA at 8 h **(Figure 4.5 A *right*)**. This is consistent with the Southern analysis which indicated that repair of VDE-DSB2 is most severely impaired by simultaneous mutation of *MRE11* and *EXO1* compared to its single mutants **(Figure 3.9)**. Therefore, both nucleases contribute to the processivity of VDE-DSB2 resection. Intriguingly, instead of abolishing the ability to produce ssDNA in the *mre11-H125N*, *exo1*Δ cells, there was still a small amount of ssDNA that appeared throughout the meiosis time course **(Figure 4.5 A *bottom right*)**, and the ratio of long ssDNA to short ssDNA appeared similar to wild-type **(Figure 4.5 B)**. It suggests this small amount of ssDNA intermediates might result from other nuclease factors, which do not rely on Mre11 and Exo1 proteins.

## 4.3 Discussion

Our evidence through the loss of RE site assay with qPCR have directly proved that not only Exo1 but also the nuclease function of Mre11 truly take part in processive DSB resection during meiosis. Interestingly, our Southern blot data have shown that in *mre11-H125N*, *exo1*Δ double mutants the SSA distal repair was completely abolished, while there was still a small amount of Δproximal produced. Then, the long ssDNA molecules should not be detected by our qPCR assay here. However, all kinds of ssDNA intermediates in *mre11-H125N*, *exo1*Δ cells were generated, though the signals after normalising with the present of VDE-DSB2 showed much less than wild-type cells. This small amount of ssDNA are suggested due to other nuclease factors that are independent of Exo1 and Mre11 pathways. In addition, the ratio of the longest ssDNA to the shortest at each time points was similar to the wild-type, rather than being 0:1, suggesting the distal SSA repair of VDE-DSB2 somehow is impaired in the simultaneous absence of Exo1 and Mre11 nuclease functions, although the long range of resection occurred.

# *Chapter 5*

## Verifying the Role of DNA Damage Checkpoint Kinase Tel1 in Meiotic VDE-induced DSB2 Resection

## 5.1 Introduction

Based on the mitotic assay of a single irreparable HO-induced DSB, D. Mantiero *et al*. have found that Tel1, which is one of the major DNA damage checkpoint related kinases, has a role in DSB end processing (Longhese et al., 2010; Mantiero et al., 2007). They also observed that there is a synergistic impairment of HO-DSB resection in *tel1*Δ, *exo1*Δ double mutants, thus suggesting that the involvements of Tel1 and Exo1 in DSB resection are independent of each other, i.e. acting in two different pathways. Moreover, it was proposed that the contribution of Tel1 to the HO-DSB resection is mediated by activating a nuclease that resects DSB ends, and the most probable candidate for this is the MRX complex, which participates in resection independently of Exo1, and is also required for the recruitment of both Tel1 and Mec1 to DSB ends (Mantiero et al., 2007). They also found that the signaling activity of Tel1 becomes dominant only after producing multiple DSBs (11-HO-DSBs), and the phosphorylation of Mre11 is specially related to the Tel1 function (Mantiero et al., 2007). These findings prompted us to investigate whether during meiosis (where multiple Spo11-induced DSBs have been formed), Tel1 has a role in the meiotic DSB resection and whether this is through the regulation of Mre11 function. Thus, in this chapter, the mutant strains were constructed based on the VDE-DSB2 system that the resection is able to be monitored by the detectable

VDE-DSB2.

## 5.2 Results

### 5.2.1 Tel1 Participates the Meiotic VDE-DSB2 Resection

If in meiosis Tel1 has a similar function to mitotic cells in activating Mre11 nuclease activity, the *tel1*Δ single mutants should have a phenotype similar to *mre11-H125N* cells. We found instead that deleting *TEL1* genes (dAG1636) caused a more severe meiotic VDE-DSB2 phenotype than *mre11-H125N* cells **(Figure 5.1)**. Calculating the amount of remaining unrepaired VDE-DSB2 showed the rate of the VDE-DSB2 repair in the absence of *TEL1* was similar to *exo1*Δ cells, rather than *mre11-H125N* cells **(Figure 5.1 C *left*)**. Throughout the meiotic time course neither *tel1*Δ nor *exo1*Δ single mutants have the VDE-DSB2 repair until 6 h, after which both exhibited accelerated SSA proximal repair **(Figure 5.1 C *middle*)**. The long resection repair in *tel1*Δ cells was not abolished as much as *exo1*Δ cells; instead, it resembled *mre11-H125N* cells showed **(Figure 5.1 C *right*)**. These data support the view that Tel1 indeed plays an early role in processing DSB end resection during meiosis.

### 5.2.2 Directly Monitoring the Role of Tel1 in the Process of Meiotic Resection by the Loss of RE Site Assay

To directly verify whether Tel1 has a role in meiotic DSB resection, we monitored the change of ssDNA levels by our loss of RE site assay with qPCR when *TEL1* was deleted in the VDE-DSB2 system **(Figure 5.2)**. Compared to wild-type cells, the resection rate of the VDE-DSB2 present at each RE site was less in *tel1*Δ cells **(Figure 5.2 B)**. Moreover, this ssDNA profile in *tel1*Δ cells was more similar to

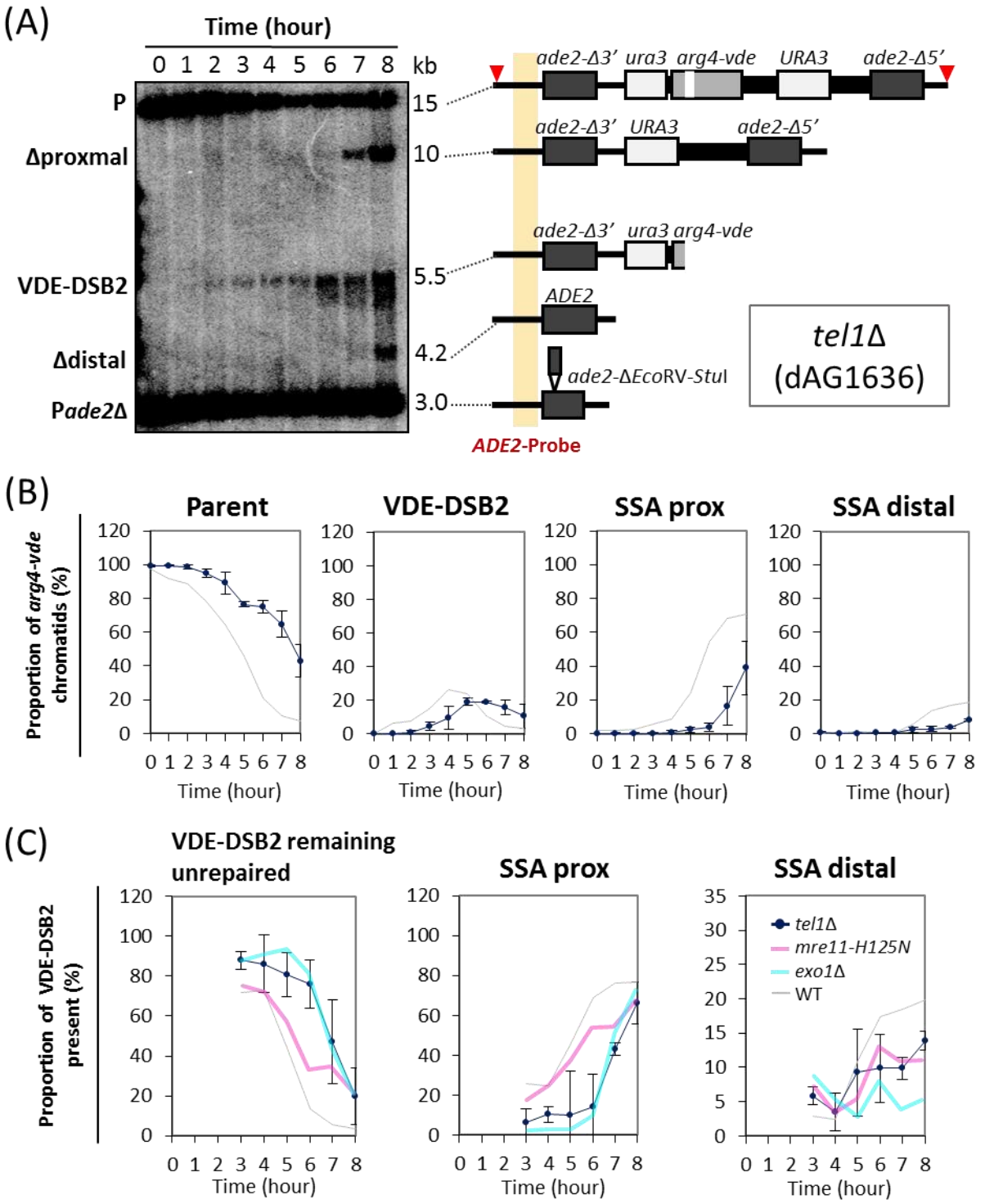


**Figure 5.1 Analysis of the VDE-DSB2 turnover in the single mutants of *tel1Δ*.** The legends of **(A)**, **(B)** and **(C)** here are same as the previous graphs (Figure 3.3 to 3.5), except the DNA here is from *tel1Δ* cells. Through the meiotic VDE-DSB2 assay, we have verified Tel1 indeed has a role in the process of resection in meiosis. Furthermore, the *exo1Δ*-like SSA proximal repair and the *mre11-H125N*-like SSA distal repair imply that Tel1 might have another role in regulating repair of the breaks. Duplicated experiment have been done (n=2). **(C. *right*)** is in different scale to others.

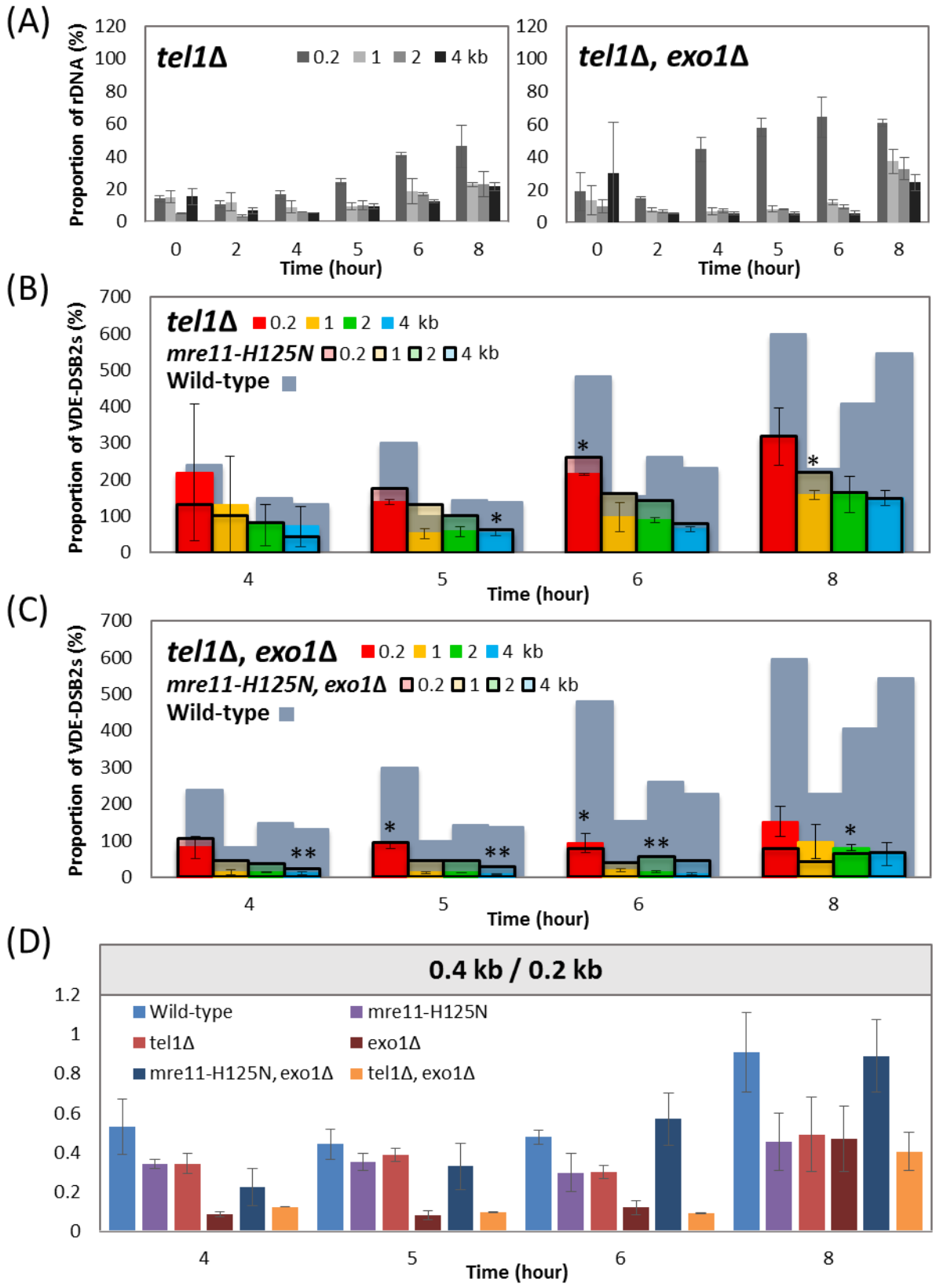


**Figure 5.2 Analysis of the ssDNA profiles in *tel1Δ* and *tel1Δ, exo1Δ* cells by our loss of RE site assay. (A)** are expressed as a proportion of rDNA turning into ssDNA at the distances we targeted and time point shown. **(B and C)** are expressed as a proportion of VDE-DSB2s in a single-stranded state at coloured-coded distances and time point shown, with comparison to the *mre11-H125N* cells and the double mutants of *mre11-H125N, exo1Δ*, respectively. **, p<0.01; *, p<0.05. **(D)** The ratio of the longest ssDNA signal to the shortest ssDNA signal. Each bar is the average of data from two independent experiments and all genomic DNA are from the same resource of the Southern.

*mre11-H125N* than *exo1*Δ cells **(Figure 5.2 B and 4.5 A *right*)**. The ratio of the longest ssDNA (4.0 kb) to the shortest (0.2 kb) from 4-8 h was also similarly to *mre11-H125N* cells **(Figure 5.2 D)**. These findings are the first direct evidence of Tel1 playing a role in processive resection during meiosis, and imply Tel1 and Mre11 might act in the same pathway for meiotic resection, which raises the possibility of Tel1 activating the nuclease function of Mre11 by phosphorylation to conduct the resection process during meiosis.

### 5.2.3 The Involvement of Tel1 in Processing VDE-DSB2 is Related to the Nuclease Function of Mre11

If Tel1 has a role in meiotic resection through targeting and regulating the Mre11 function, the phenotype of *tel1*Δ, *exo1*Δ double mutants (dAG1629) is predicted to be the same with *mre11-H125N*, *exo1*Δ cells. Indeed, these two mutant strains displayed similar phenotypes to each other **(Figure 5.3)**: both of them exhibited accumulation of VDE-DSB2 throughout the meiosis time course **(Figure 5.3 B *VDE-DSB2* and C *left*)** and there was less repair particularly via long resection, compared to wild-type cells **(Figure 5.3 B and C)**. There was some differences between the phenotypes of these two double mutant strains. The VDE-DSB2 kept accumulating and no repair was visible until 7 h in *tel1*Δ, *exo1*Δ cells, but in *mre11-H125N*, *exo1*Δ double mutants the VDE-DSB2 repair was more gradual **(Figure 5.3 C *left*)**. As by 8 h the amounts of repair product were similar for the two strains, the *tel1*Δ, *exo1*Δ cells apparently had a fast SSA proximal repair after 7 h that was not present in *mre11-H125N*, *exo1*Δ cells **(Figure 5.3 C *middle*)**. This prompts us to think whether Tel1 has more than Mre11 nucleases as targets to be regulated during the processivity of meiotic resection.

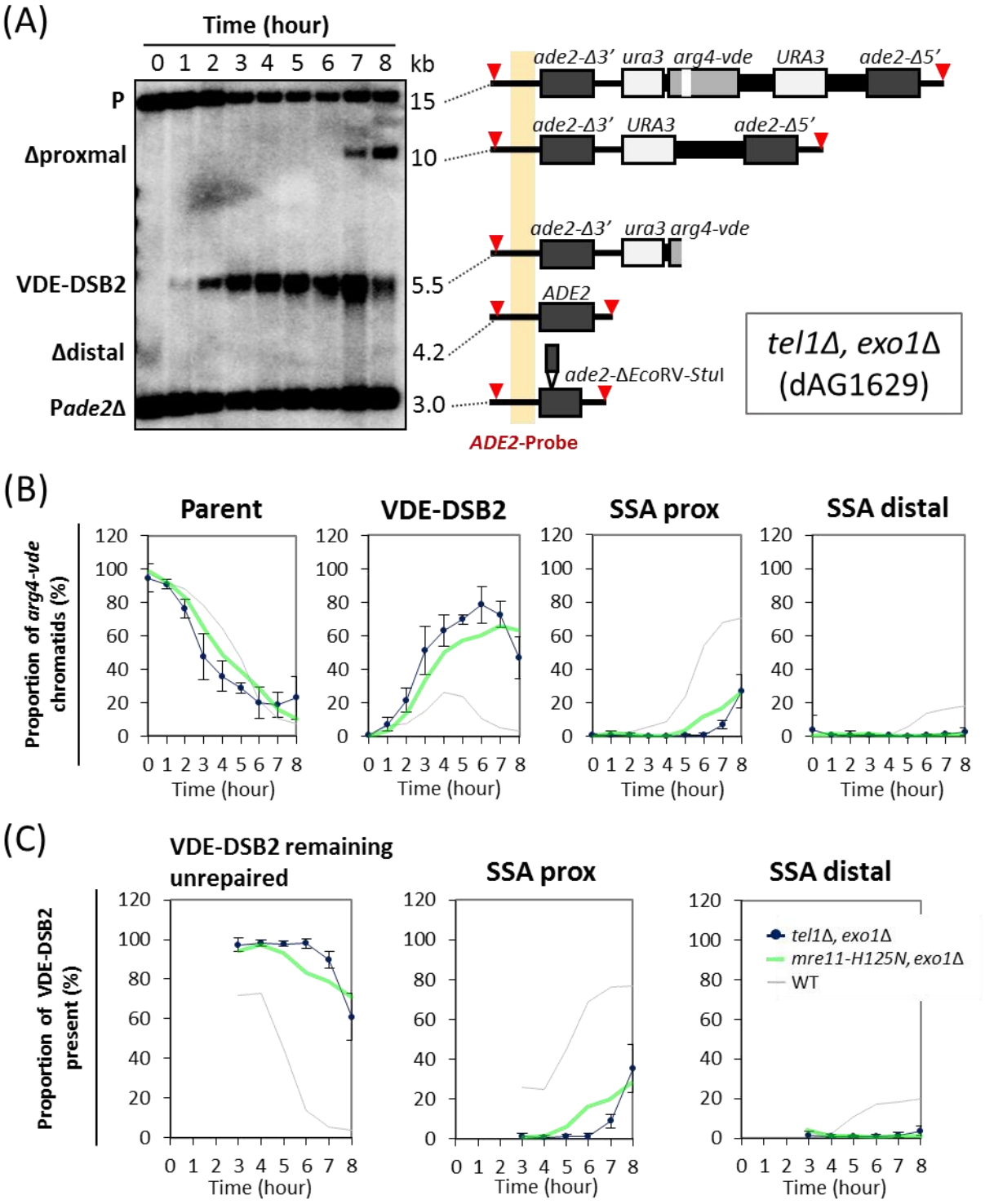


**Figure 5.3 The turnover of VDE-DSB2 in the double mutant strain of *tel1*Δ and *exo1*Δ displays a similar scenario to that in *mre11-H125N, exo1*Δ cells.** The legends of **(A)**, **(B)** and **(C)** here are same as the previous graphs (Figure 3.3 to 3.5), except the DNA here is from the *tel1*Δ, *exo1*Δ cells. Doubly mutating *TEL1* and *EXO1* alleles caused a repair phenotype of VDE-DSB2 similar to the *mre11-H125N*, *exo1*Δ cells, suggesting Tel1 participates in the process of DSB resection during meiosis, and this is presumably achieved by regulating the Mre11 nuclease function. Quintuplicated experiments have been done (n=5).

### 5.2.4 Monitoring the VDE-DSB2 Resection Tract of the *tel1*Δ, *exo1*Δ Double Mutants by the Loss of RE Site Assay

Compared to wild-type cells, deleting both *TEL1* and *EXO1* caused a dramatic drop in the amount of the *arg4-vde* chromatids becoming ssDNA intermediates before 8 h, even for the shortest resection measured of 1.0 kb ssDNA **(Figure 5.2 A *right*)**. The resection rates of VDE-DSB2s from 4-6 h were lowest in *tel1*Δ, *exo1*Δ cells **(Figure 5.2 C)** compared to their single mutants **(Figure 5.2 B, *tel1*Δ; 4.5 A *top right*, *exo1*Δ)**, though the ratio of the 4.0 kb to 0.2 kb in *tel1*Δ, *exo1*Δ cells was similar to *exo1*Δ cells **(Figure 5.2 D)**. This agrees with our Southern analysis of the synergistic effect of *tel1*Δ, *exo1*Δ cells on VDE-DSB2 repair, further confirming Tel1 indeed has a role in participating in meiotic VDE-DSB2 resection that acts independently of Exo1. We also compared the amounts of ssDNA of the *tel1*Δ, *exo1*Δ cells to the double mutants of *mre11-H125N*, *exo1*Δ. For the period 4-6 h, there was less ssDNA in *tel1*Δ, *exo1*Δ cells compared to *mre11-H125N*, *exo1*Δ cells **(Figure 5.2 C)**, further supporting that during this period Tel1 might regulate not only Mre11 but also other factors for producing ssDNA. Moreover, at 8 h, the absence of Tel1 is presumably able to release some proteins for progressing resection that causes increasing ssDNA levels at the end of meiosis time course **(Figure 5.2 C)**.

### 5.2.5 Tel1 Not Only Has an Impact on Producing ssDNA But Also Influences the VDE-DSB2 Repair

Cells lacking Tel1 caused a reduction of ssDNA levels similar to *mre11-H125N* mutants **(Figure 5.2 B)**. This should lead to a similar repair phenotype to *mre11-H125N* cells as well. In other words, since both *tel1*Δ and *mre11-H125N* cells produced similar amounts of ssDNA intermediates, then these ssDNA should be turned over into the same amount of SSA repair products, causing similar repair

phenotypes. However, according to our Southern blot results, the repair phenotype of *tel1*Δ was worse than the *mre11-H125N* cells **(Figure 5.1 and Section 5.2.1)**. This reduced propensity for repair of ssDNA in the absence of Tel1 implies that it somehow influences the SSA repair processes.

### 5.2.6 Repressing *MEC1* Expression Does Not Completely Abolish the Ability to Repair VDE-DSB2 under the *tel1*Δ, *exo1*Δ Background

In order to investigate whether the remaining SSA repair in *tel1*Δ, *exo1*Δ cells is Mec1-dependent **(Figure 5.3)**, the kinetics of generating and repairing meiotic VDE-DSB2 were monitored in cells lacking *MEC1*, *TEL1* and *EXO1*. Owing to problems with synchronizing *mec1Δ* cultures, a meiosis-specific *pCLB2-MEC1* conditional allele was constructed by replacing the native *MEC1* promoter with the *CLB2* promoter, which strongly represses its downstream gene during meiosis (Gray et al., 2013). Therefore, the triple mutant of *pCLB2-MEC1*, *tel1*Δ and *exo1*Δ with the VDE-DSB2 system was established (dAG1649). After normalising with the actual amount of broken chromatids, the rate of the meiotic VDE-DSB2 turnover in *pCLB2-MEC1*, *tel1*Δ, *exo1*Δ cells was similar to the *tel1*Δ, *exo1*Δ double **(Figure 5.4 C *left*)**. The SSA proximal repair was shown similarly to *tel1*Δ, *exo1*Δ double mutants **(Figure 5.4 C *middle*)**, but the amount of SSA distal products was increased significantly compared to *tel1*Δ, *exo1*Δ cells ($p<0.01$) **(Figure 5.4 C *right* and 5.5)**. These data verify that the induced ssDNA in *tel1*Δ, *exo1*Δ cells are not Mec1-depedent, and the higher of the long resection repair suggests the absence of Mec1 in the *tel1*Δ, *exo1*Δ genetic background might able to relieve or activate some recombinases or other proteins to improve the distributions of Δdistal products. Moreover, the resection intermediates seen as smears underlying the VDE-DSB2 bands were visible in the *tel1*Δ, *exo1*Δ double mutants but no the *pCLB2-MEC1*, *tel1*Δ, *exo1*Δ triple mutants

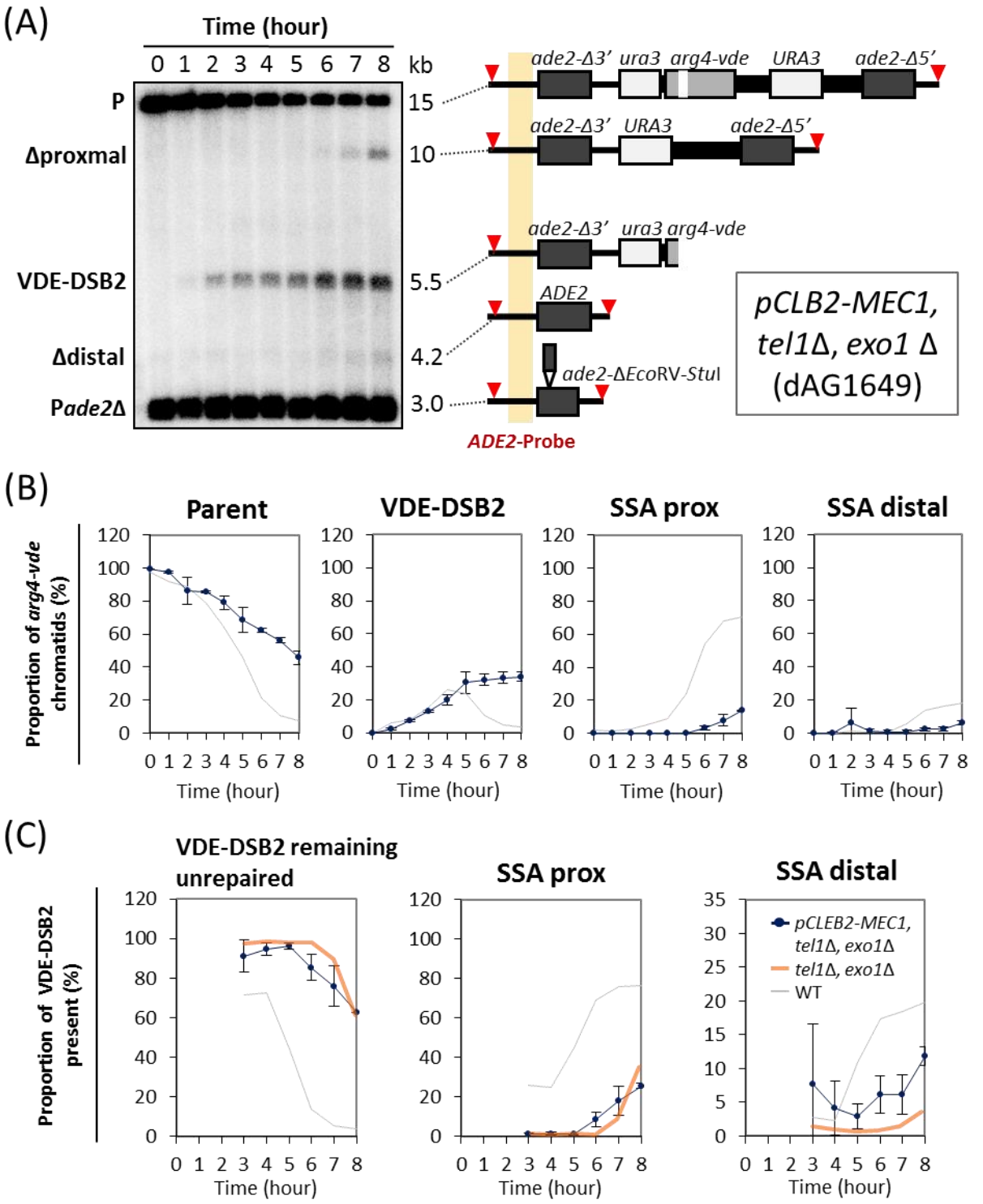


**Figure 5.4 Comparison of the VDE-DSB2 repair phenotypes with and without *MEC1* expression under the *tel1Δ, exo1Δ* genetic background.** The legends of **(A)**, **(B)** and **(C)** here are same as the previous graphs (Figure 3.3 to 3.5), except the DNA here is from the triple mutants of *pCLB2-MEC1*, *tel1*Δ , *exo1*Δ. When repressing *MEC1* expression within the *tel1*Δ, *exo1*Δ cells, the remaining SSA repairs was not abolished, indicating this remaining repair in the *tel1*Δ, *exo1*Δ cells is not Mec1-dependent. Moreover, the SSA distal repair appeared more abundant in the triple mutants. **(C. *right*)** is in different scale to others. Duplicated experiment have been done (n=2).

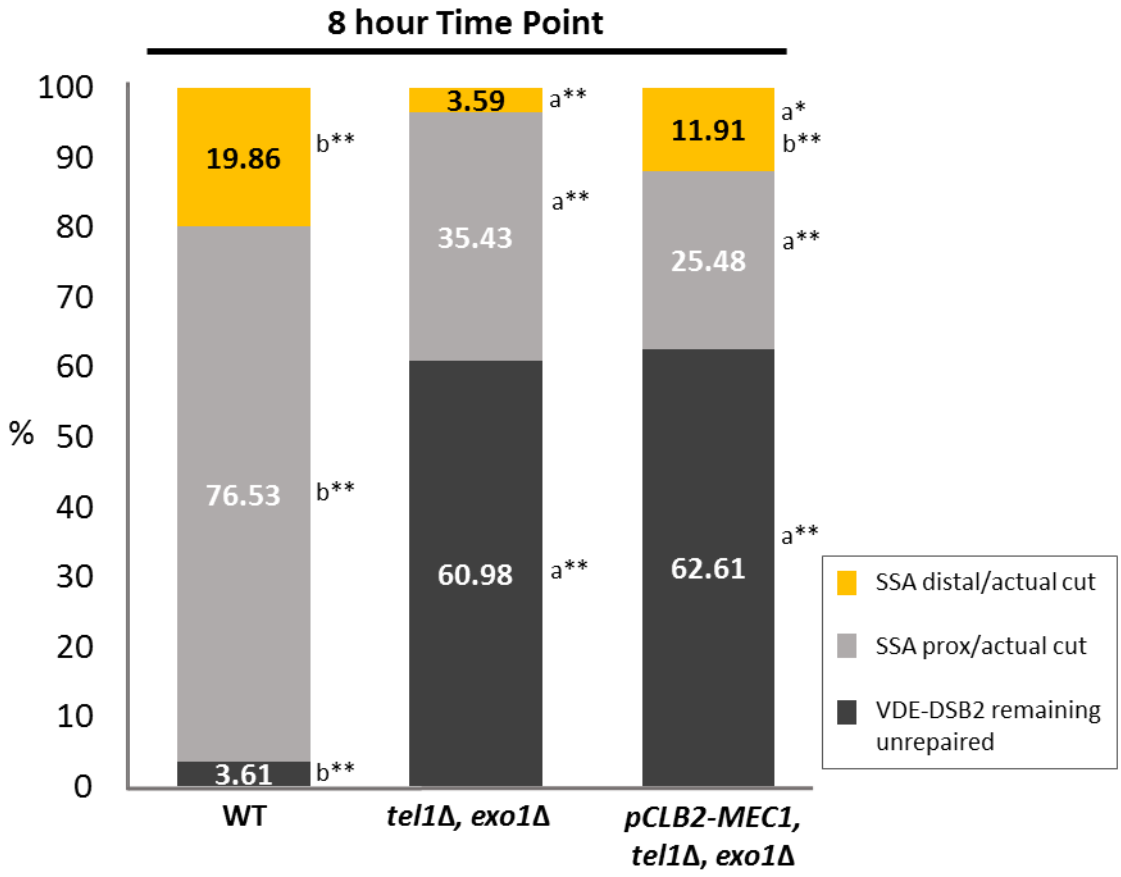


**Figure 5.5 Highlighting the VDE-DSB2-turnover phenotypes at the 8 hour meiosis time point in the *tel1Δ, exo1Δ* double mutants and the *pCLB2-MEC1, tel1Δ, exo1Δ* triple mutant cells.** At the 8$^{th}$ hour, repressing *MEC1* expression did not have significant effect on SSA proximal repair, but significantly increased the SSA distal products by around three times compared to the double mutant of *tel1*Δ, *exo1*Δ. *, p<0.05; **, p<0.01; a, compared to WT; b, compared to the *tel1*Δ, *exo1*Δ double mutant cells. Duplicated experiments have been done for WT and *pCLB2-MEC1*, *tel1*Δ, *exo1*Δ cells (n=2), and quintuplicated experiments have been done for the *tel1*Δ, *exo1*Δ cells (n=5).

**(Figure 5.3 A and 5.4 A)**. This could imply more rapid repair of the ssDNA when *MEC1* is absent.

## 5.3 Discussion

Altogether, our data have verified that Tel1 indeed has a role in the process of meiotic VDE-DSB2 resection that is independent of Exo1 but relates to the Mre11 nuclease function. This suggests Tel1 and Mre11 are in the same pathway for processing the resection of VDE-DSB2, and Tel1 might mediate through regulating the Mre11 nuclease activity, likely via phosphorylation, to achieve this process. Besides influencing the production of 3' ssDNA tails, Tel1 is likely to have another role in the process of recombination for ssDNA repair that resulted in better SSA distal repair than the proximal in *tel1*Δ cells. Through the triple mutant of *pCLB2-MEC1*, *tel1*Δ and *exo1*Δ, we have shown that the remaining ability of the VDE-DSB2 repair in *tel1*Δ, *exo1*Δ cells is not Mec1-dependent, and the improvement of SSA repairs throughout the meiosis is thought to be due to releasing or activating some recombinases or other proteins as the absence of Mec1. We also imply that there is more rapid repair of the ssDNA in the triple mutants of *pCLB2-MEC1*, *tel1*Δ, *exo1*Δ. This should be further verified by the single mutants of *pCLB2-MEC1* cells.

Comparing *tel1*Δ, *exo1*Δ cells to *mre11-H125N*, *exo1*Δ cells has shown a difference for 4-6 h that the ssDNA levels with resection tracts above 0.2 kb were much lower in *tel1*Δ, *exo1*Δ cells than the *mre11-H125N*, *exo1*Δ. This implies there are more than Mre11 nucleases as targets regulated/activated by Tel1 kinases for processing resection during meiosis. One of the possible candidates as a target of

Tel1 for processing meiotic resection could be Trm2, which is a tRNA methyltransferase and also acts as an endo/exo-nuclease with a role in DNA repair (Choudhury et al., 2007; Nordlund et al., 2000).

# *Chapter 6*

## General Discussion and Future Directions

During meiosis, recombination between homologous chromosomes is initiated at high levels of DNA double-strand break (DSB) sites that are created by the meiosis-specific protein, Spo11. Repair of these programmed Spo11-induced DSBs by interhomologue recombination is essential to achieve the formation of interhomologue joints (chiasmata; observed genetically as crossovers), which are required for establishing the correct disjunction of homologous chromosomes during meiosis I. Recently, much attention has been paid to the mechanism and the significance of 5' to 3' resection of DNA at the ends of DSBs, which is an intermediate step during the DSB repair. It is important to produce the 3' single-stranded DNA tails (3' ssDNA) through this intermediate process that are active to invade donor homologous templates, thus leading to the initiation of meiotic recombination. There are multiple proteins participating in this DSB end resection, and the aim of this research project was to characterize the roles of the nuclease proteins, Exo1 and Mre11, as well as the DNA damage checkpoint kinase Tel1 during meiotic DSB resection, and further to elucidate their relationships in this mechanism of resection based on different combinations of double mutant strains. However, because several mutants, such as *rad50S*, *mre11-nd* (nuclease dead) and *sae2*Δ cells, have been verified as failing to remove the covalently bound Spo11 from DSBs (Krogh and Symington, 2004; Mimitou and Symington, 2011), we have analyzed the meiotic resection at a DSB created by the site-specific homing endonuclease VDE (*VMA1*-derived endonuclease, also known as PI-*Sce*I) instead,

which does not form a covalent bond when making a DSB (Gimble and Thorner, 1992), thus allowing us to model the roles of our genes of interest after Spo11 would have been removed. Therefore, two VDE-DSB systems have been established and both of them contain a reporter cassette that harbors a VDE-cutsite sequence and locates within the yeast gnome for providing information of the repair process, and a *TFP1::VDE* allele for encoding a VDE endonuclease to create a VDE-DSB at the VDE-cutsite sequence. One difference between these two systems is that VDE-DSB1 can be repaired either by gene conversions (GC) or SSA due to the existence of a donor homologous template (*ura3::arg4-bgl*) in the VDE-DSB1 system, while there is no GC repair for VDE-DSB2 because the donor homology was deleted (*ade2*Δ(*Eco*RV-*Stu*I)) from the VDE-DSB2 system. Here, we focused on using the VDE-DSB2 system as a model to monitor the process of meiotic DSB resection by Southern analysis and our loss of RE site assay.

## 6.1 Verification of the Roles of Exo1, Mre11 and Tel1 in the Meiotic VDE-DSB2 Resection

Taken altogether, the Southern analysis and the direct evidence from our loss of RE site assay mediated by qPCR have indicated that not only the Exo1 protein but also the nuclease activity of Mre11 from the third phosphoesterase motif play roles in progressing the process of meiotic VDE-DSB2 resection. This is consistent with the finding in mitotic cells that the MRX complex together with Sae2 and the Exo1 nuclease are all required for the repair of HO-induced DSBs (Longhese et al., 2010). However, in opposition to the mitotic studies, our Southern meiotic data on *mre11-58S* and *mre11-H125N* resection activity from both VDE-DSB1 and VDE-DSB2

systems have revealed that the integrity of the MRX complex is not necessary for the meiotic DSB resection, and also implies that the nuclease function of Mre11 from the third phosphoesterase motif has a major impact on the resection and repair of VDE-DSB, but not the fourth one **(Table 3.1)**. Further, we introduced one of the main DNA damage checkpoint kinases, Tel1, into our meiotic resection activity assay. When deleting *TEL1* alleles within the VDE-DSB2 system, we have proved that Tel1 indeed has an impact on the process of VDE-DSB2 resection that the level of ssDNA with different lengths of resection tracts was shown to be reduced compared to wild-type cells, and the repair phenotypes in both SSA proximal and distal products were also affected.

The similar ssDNA profiles between the *mre11-H125N* and the *tel1*Δ cells, which are not as severe as in the *exo1*Δ cells, and the synergistic effects on producing ssDNA intermediates resulting from simultaneously deleting *EXO1* alleles within these single mutants have suggested that Tel1 and Mre11 are likely to act on the same pathway for generating ssDNA molecules during meiosis that is independent to Exo1, and the major player for processing VDE-DSB resection is thought to be Exo1. The relationship among our proteins of interest for the processive resection and the repair of meiotic VDE-DSB2 is further discussed in detail in the next section.

## 6.2 Revealing Relationships among Exo1, Mre11 and Tel1 during the Meiotic VDE-DSB2 Resection Based on Different Combinations of Double Mutants

### 6.2.1 The Relationship between Mre11 and Exo1

Besides verifying that Mre11 indeed plays a direct role in the progression of meiotic DSB resection, the relationship between Mre11 and Exo1 has been determined. The wild-type-like repair phenotype in *mre11-58S* cells, the mild-severe impairment of VDE-DSB repair shown in *mre11-H125N* cells, the accelerated SSA proximal repair performed in *exo1*Δ cells, and the restoration of SSA proximal repair of *exo1*Δ cells by simultaneously abolishing the Spo11 activity have inspired us to propose a model for the meiotic VDE-DSB2 processing that **(Figure 3.10)**: Mre11 proteins within the MRX complexes are considered to be sequestered at the multiple Spo11-DSBs during early meiosis; meanwhile, Exo1 proteins are available and are thought to be the major player for addressing the VDE-DSB2. The removal of Mre11 from Spo11-DSBs has been clarified it is because of the resection rather than the repair as the signal (Borde et al., 2004; Krogh and Symington, 2004). Therefore, this makes us further suggest that after the initiation of Spo11-DSB resection, the MRX complexes still could not be released from a number of Spo11-DSB sites until Exo1 proteins are recruited to commence further Spo11-DSB resection, and this recruitment is probably due to the association and integrity of MRX complexes at the Spo11-DSB sites. The released Mre11 proteins then become available for the VDE-DSB2 repair and work together with the existing or the dismissed Exo1 from the Spo11-DSBs to progress the long range of VDE-DSB2 resection. Alternatively, this could be in a different case that the suppression of the *exo1*Δ SSA proximal repair phenotype in the double mutants of *spo11-Y135F*, *exo1*Δ is perhaps because the regulation of nuclease activities is altered, rather than releasing an abundance of Mre11, in the absence of Spo11-DSB formation.

### 6.2.2 The Regulatory Role of Tel1 in Mre11 Activation

Our Southern analysis has indicated that Tel1 has a role in the meiotic VDE-DSB2 processing, and the loss of RE site assay with qPCR has directly evidenced that Tel1 indeed participates in the processive resection during meiosis. Further, according to the similar repair phenotypes of the *mre11-H125N*, *exo1*Δ and the *tel1*Δ, *exo1*Δ double mutants, we have suggested that the involvement of Tel1 in the resection and repair of VDE-DSB2 is likely related to the Mre11 nuclease function; that is, Tel1 might mediate the process by phosphorylating Mre11 so that the nuclease activity is thought to become active to accomplish the process of meiotic VDE-DSB2 resection. However, the ssDNA profiles between these two double mutants are different: during the meiosis time points of 4-6 hours the ssDNA levels with resection tracts above 0.2 kb are displayed much less in the *tel1*Δ, *exo1*Δ cells than in the *mre11-H125N*, *exo1*Δ cells. This implies that there are more than Mre11 nuclease as targets of Tel1 kinases that are likely to be activated by Tel1-phosphorylation for the processive resection. We suggest one of the possible candidates of Tel1-targets for meiotic resection could be Trm2, which is a tRNA methyltransferase and also contains dsDNA 5'-3' exonuclease and ssDNA endonuclease activities (Choudhury et al., 2007; Nordlund et al., 2000), and this provides us a new direction for the future study of the meiotic DSB resection.

### 6.2.3 Tel1 Has another Impact on the Repair of ssDNAs

Altogether, the Southern analysis and the loss of RE site assay related to Tel1 resection activity have indicated that Tel1 plays a role in producing 3' ssDNA tails during meiosis. Besides, we also found out a fascinating phenomenon that Tel1 is likely to have an impact on the process of SSA repairs, where although a small amount of ssDNA has been generated, the relative repair products are still shown much lower than expected, or even if the ssDNA levels are increased, it is still not

accompanied by a relative progress of VDE-DSB2 repair. This could be due to Tel1 affecting the repair of ssDNAs, or Tel1 might mediate the process through regulating the Sae2 function to process the metabolism of the resected DNA intermediates to the SSA repair products, according to the similar results displayed in *sae2*Δ cells (data not shown).

## 6.3 Future Directions

In the future, three major directions could be conducted to make the study of meiotic resection become more intact and fully-comprehended. These include:

*To verify the regulatory relationship between Tel1 and Mre11 more directly and in more detail.* – Through our resection assays, we have suggested that Tel1 might mediate the process by regulating Mre11 function to join the process of meiotic DSB resection, and this activation of Mre11 is likely to be via Tel1-phosphorylation. To further confirm this suggestion, we can introduce western blotting or the *mre11* mutants with abolished phosphorylation sites to our meiotic VDE-DSB2 resection assays.

*Cooperating with the platform of proteomics to reveal and identify more possible candidates involved in the process of meiotic DSB resection.* – Except Trm2, there must be a variety of proteins that could be possible candidates as targets of Tel1 kinases, or many unidentified or unexpected proteins are likely to play a role in the processive resection during meiosis. Therefore, we can apply the proteomic platform to find more possible candidates and further to make the picture of

meiotic resection more clear.

*Studying the meiotic DSB repair within the new VDE-DSB system that contains the 73-bp of mutated VDE-DSB homologous sequence (vde-VRS*), which cannot be recognized by VDE endonuclease, to see whether this homology can improve the strand invasion and thus cause the progress of VDE-DSB repair.* – According to Darpan Medhi, when the *vde-VRS** sequence was inserted into the homologous donor allele to make ~100% homology to the *arg4-vde* chromatid **(Figure A3)**, the spore viability was greatly increased. Thus, the other future direction is to introduce the new VDE-DSB system harboring this *vde-VRS** homologous sequence into different mutants to investigate whether the 100% homology between breaks and donor templates is important in VDE-DSB processing.

# *Appendix I*

*Data resources from: A. J. Hodgson et al., 2011.*

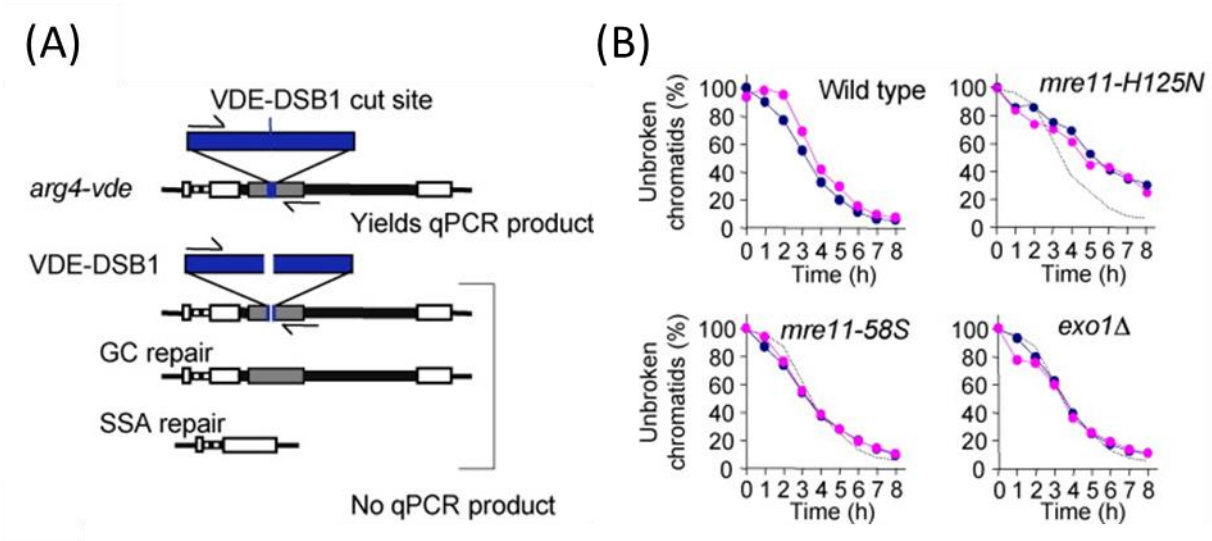


**Figure A1 The rate of VDE-DSB1 formation. (A)** Schematic of the *arg4-vde* insert at the *URA3* locus on chromosome V showing; *URA3* repeated sequences (white boxes), natural *Ty* element (stippled line), *arg4-vde* allele (greybox), vector DNA (thick black line) and relative primer positions (half arrows). In a qPCR assay to assess VDE-DSB1 formation, no PCR product can be made in chromatids after a VDE-DSB1 is formed or after repair. **(B)** Quantification of PCR product normalised to primers in rDNA. The values given show the proportion of parental *ura3::arg4-vde* chromatids remaining unbroken. Data from independent time courses are shown in different colours and the wild-type average is displayed with a grey line for comparison. The cumulative fraction of *ura3::arg4-vde* chromatids, used in later calculations, that have received VDE-DSB1 by each time point is determined by subtracting the proportion of unbroken chromatids from 100.

# *Appendix II*

*Data resources from: A. J. Hodgson et al., 2011.*

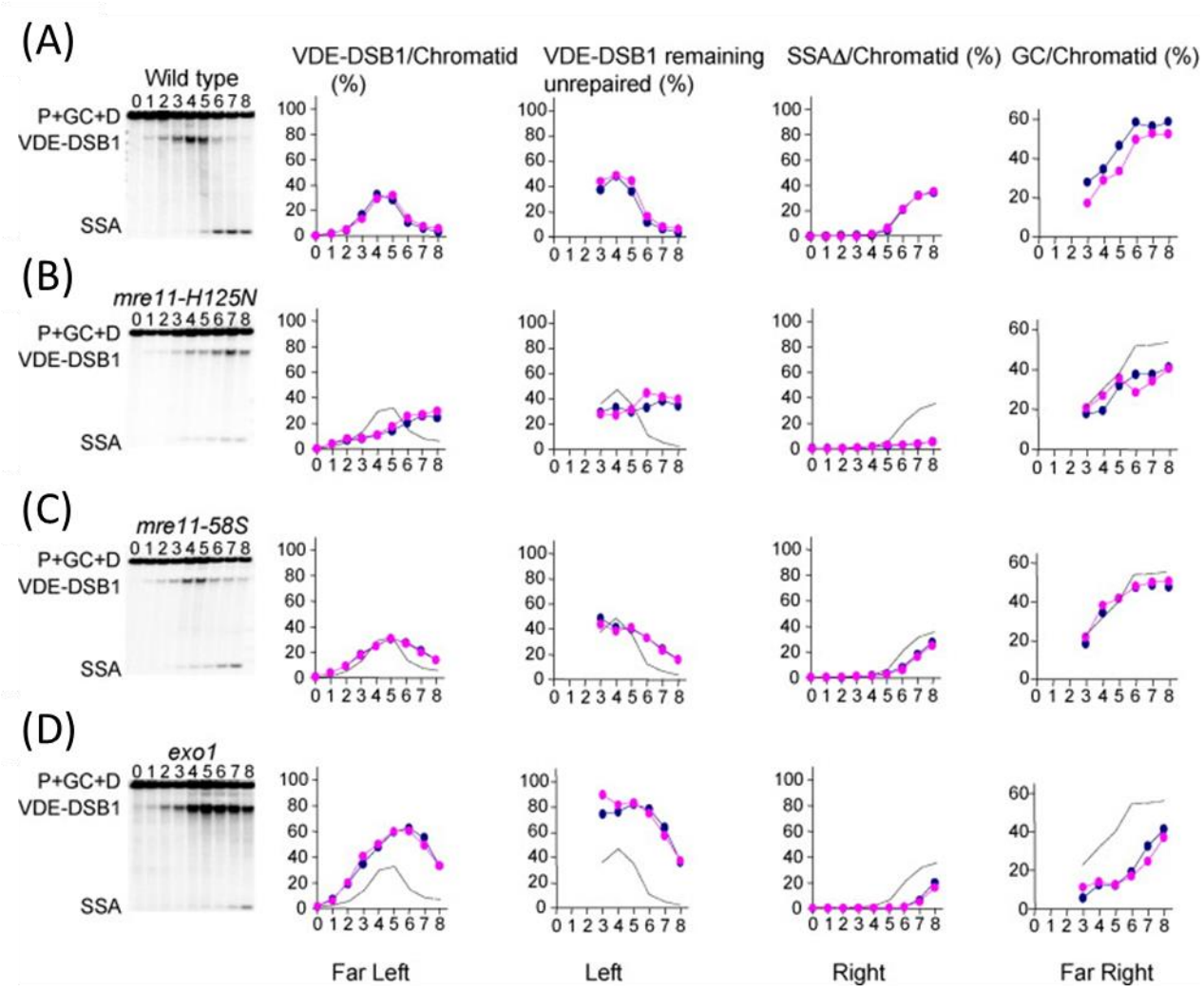


**Figure A2 VDE-DSB1 repair is delayed in *mre11* and *exo1*Δ cells. (A to D)** Southern blots reveal 3 bands as indicated in (Figure 3.2) with gene conversion products (GC) running with the parental band. The graphs are: (far left) quantification of the VDE-DSB1 band expressed as a proportion of *ura3::arg4-vde* chromatids in the population, (left) the calculated proportion of VDE-DSB1s that have been made up to the time point and remain unrepaired, (right) quantification of SSA product expressed as proportion of *ura3::arg4-vde* chromatids in the population, and (far right) calculated frequency of gene conversion expressed as proportion of *ura3::arg4-vde* chromatids in the population. All values are plotted against time of sampling (hour), duplicate experiments are indicated by the different colours and the wild-type average is displayed with a grey line for comparison.

# Appendix III

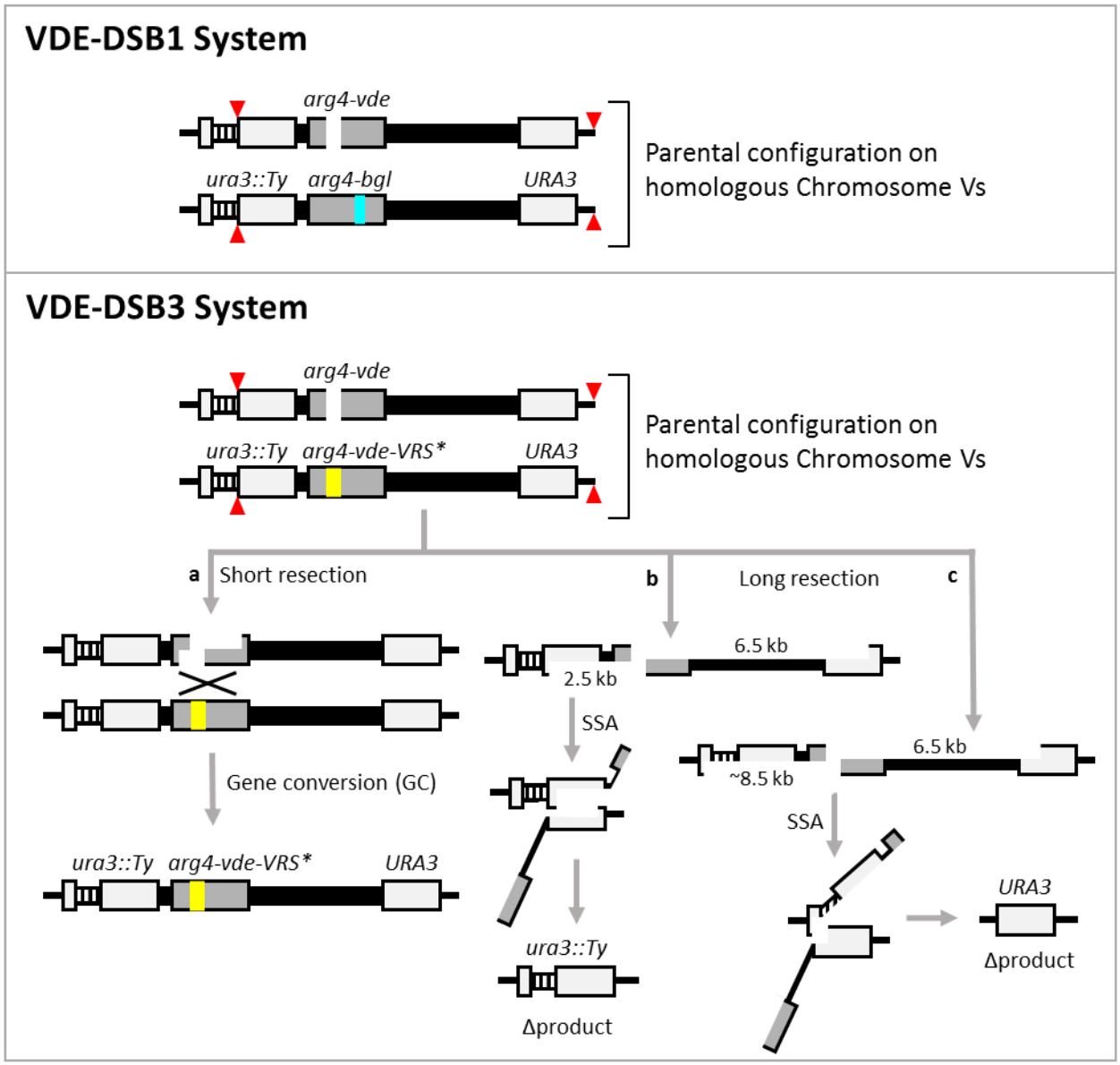


**Figure A3 The VDE-DSB1 system versus the VDE-DSB3 system.** The VDE-DSB3 system is the new construct for remodeling resection and repair of the DSBs during meiosis. This new system is based on the VDE-DSB1 system, and only differ in that the new system contains the *arg4-vde-VRS** allele, rather than the *arg4-bgl*, as the donor allele. Therefore, the VDE-induced DSB3 can be repaired by either GC or SSA same as the VDE-DSB1 repair. The *arg4-vde-VRS** allele has a 73-bp homologous sequence of the VDE recognition cut-site, but cannot be recognized by VDE nuclease, thus making almost 100% homology to the *arg4-vde* allele that might improve the repair through GC.

# *Appendix IV*

## VDE-DSB3 System_WT (dAG1684)

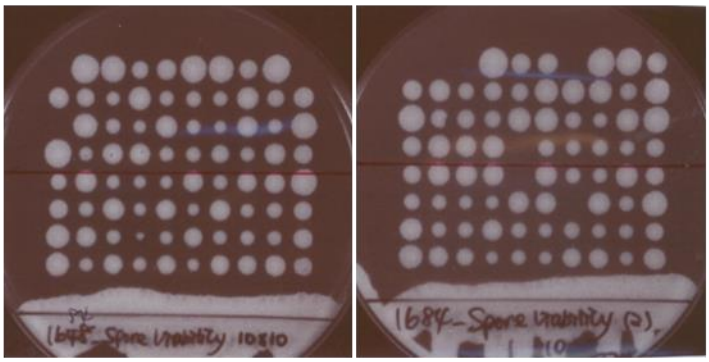

| **Spore Viability: (150/160) % = 93.75 %** |
|---|
| 0 spores survive: (0/40) % = 0 % |
| 1 spores survive: (0/40) % = 0 % |
| 2 spores survive: (1/40) % = 2.5 % |
| 3 spores survive: (8/40) % = 20 % |
| 4 spores survive: (31/40) % = 77.5 % |

## VDE-DSB1 System_WT (dAG206)

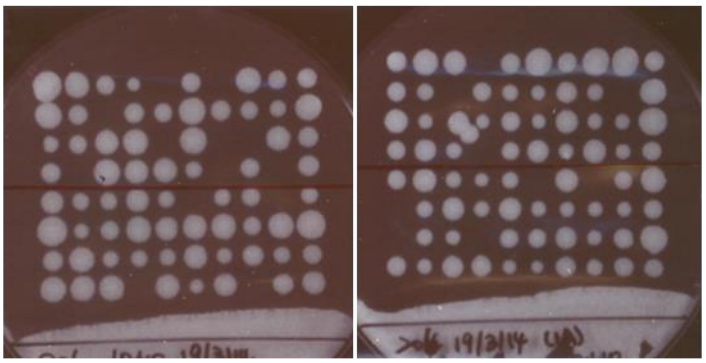

| **Spore Viability: (138/160) % = 86.25 %** |
|---|
| 0 spores survive: (0/40) % = 0 % |
| 1 spores survive: (1/40) % = 2.5 % |
| 2 spores survive: (3/40) % = 7.5 % |
| 3 spores survive: (13/40) % = 32.5 % |
| 4 spores survive: (23/40) % = 57.5 % |

**Figure A4 Comparison of spore viability between VDE-DSB3 and VDE-DSB1 systems.** Through the spore viability analysis, the VDE-DSB3 system that contains ~100% homology between *arg4-vde* and *arg4-vde-VRS** chromatids was shown to have higher spore viability than the VDE-DSB1 system. There was 77.5% of tetrads being 4 sprees viable in the VDE-DSB3 system, that is, around 1.3 fold increase compared to the VDE-DSB1 system.

# Appendix V

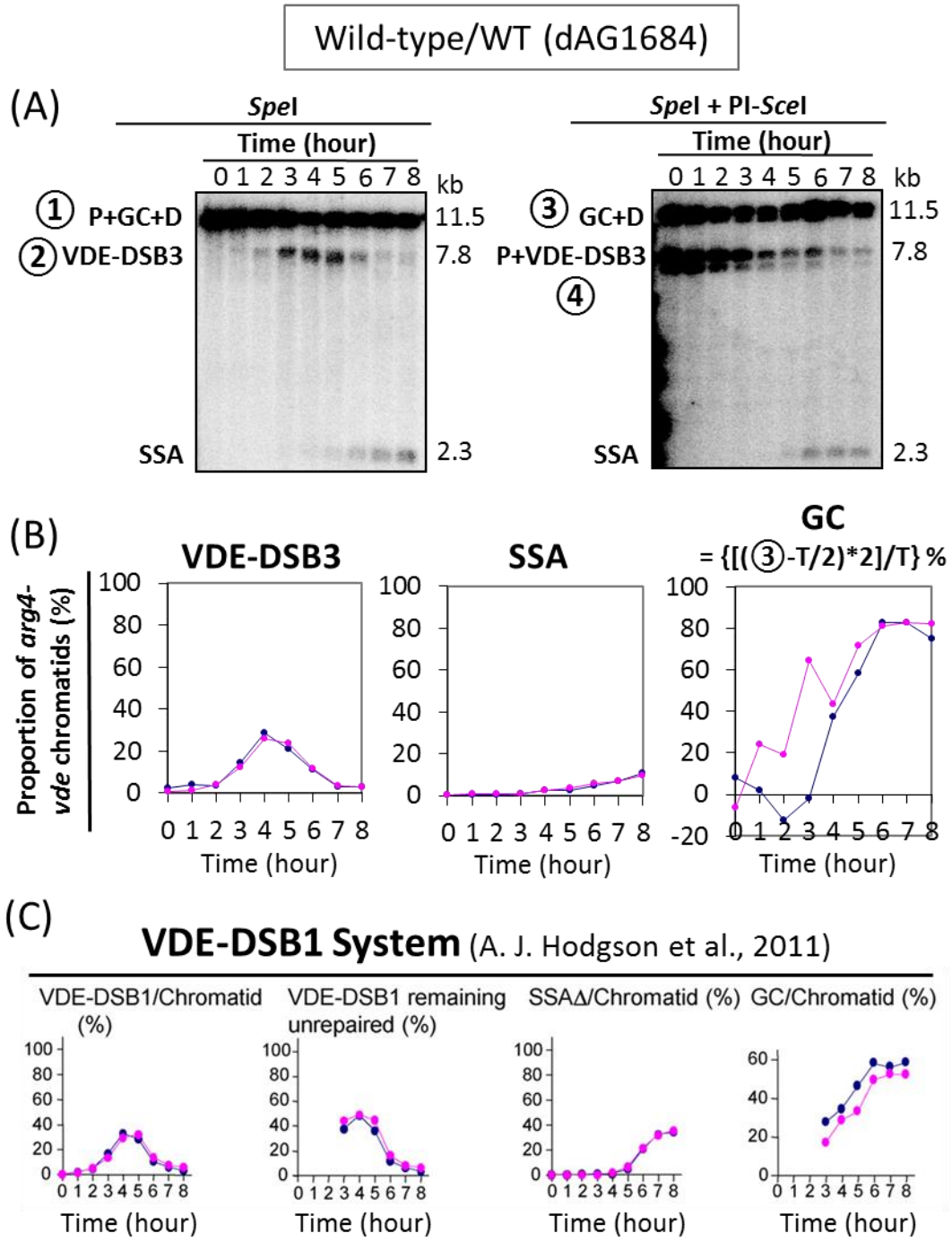


**Figure A5 Physical analysis of *arg4-vde* cleavage and repair product formation within the VDE-DSB3 system. (A)** The DNA events of *arg4-vde* during meiosis was visualized by Southern blotting, with *Spe*I digest and hybridizing with *Spe*I-probe, that showed three major fragments as expected, P+GC+D, VDE-DSB3 and SSA (left). For isolation the signal of GC bands, we used *Spe*I together with PI-*Sce*I digest and also hybridized the digested genomic DNA with *Spe*I-probe that revealed three other bands, GC+D, P+VDE-DSB3 and SSA. The proportion of GC products then were calculated by the formula shown in **(B)**. **(B)** are the proportion of *arg4-vde* chromatids in VDE-DSB3, SSA and GC fragments at each time point. **(C)** Compared to the results from the VDE-DSB1 system, most of the VDE-DSB3 repair was mediated through GC (~80% at 8h) rather than by SSA (~10% at 8h). P: *arg4-vde* chromatids, GC: gene conversion products, D: the donor homologue *arg4-vde-VRS** chromatids, VDE-DSB3: broken *arg4-vde* chromatids, SSA: SSA repair products. Duplicated experiments have been done indicated by blue and pink colours.

# Appendix VI

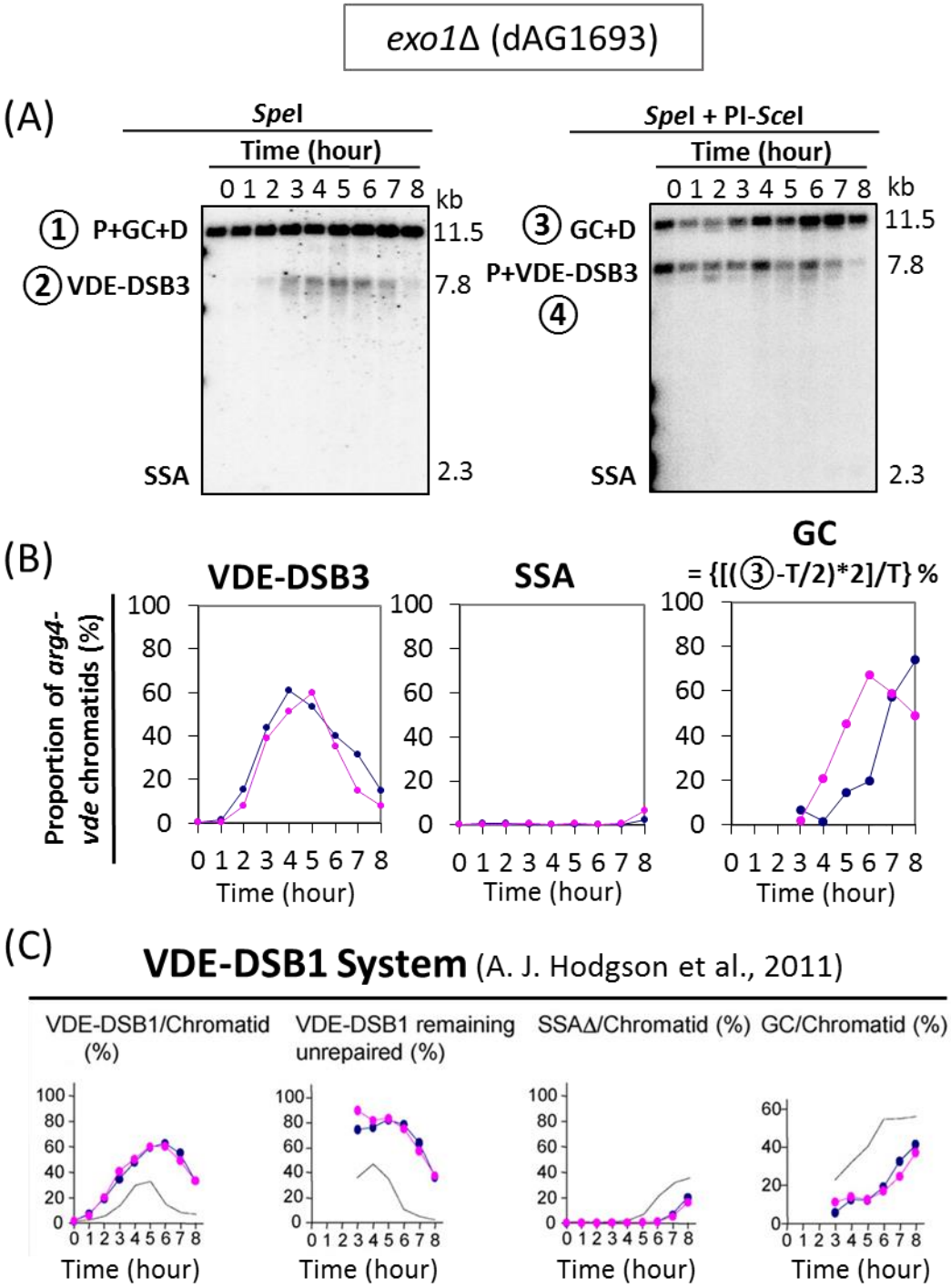


**Figure A6 Southern blot analysis of *exo1Δ* mutant cells within the VDE-DSB3 and the VDE-DSB1 systems.** The legends of **(A)**, **(B)** and **(C)** here are same as the previous (Figure A5). Deleting *EXO1* in both VDE-DSB3 and 1 systems caused continuous accumulation of the VDE-DSBs to reach a maximum of ~60% at 5h and 6h, respectively. However, most of the repair was channeled into GC through short-range resection (GC: ~61.5% and SSA: ~4.3% at 8h) in the VDE-DSB3 system, unlike VDE-DSB1 repair (GC: ~40% and SSA: ~20% at 8h). This suggests that the degree of homology between homologues chromosomes has impact on the range of meiotic resection.

# Appendix VII

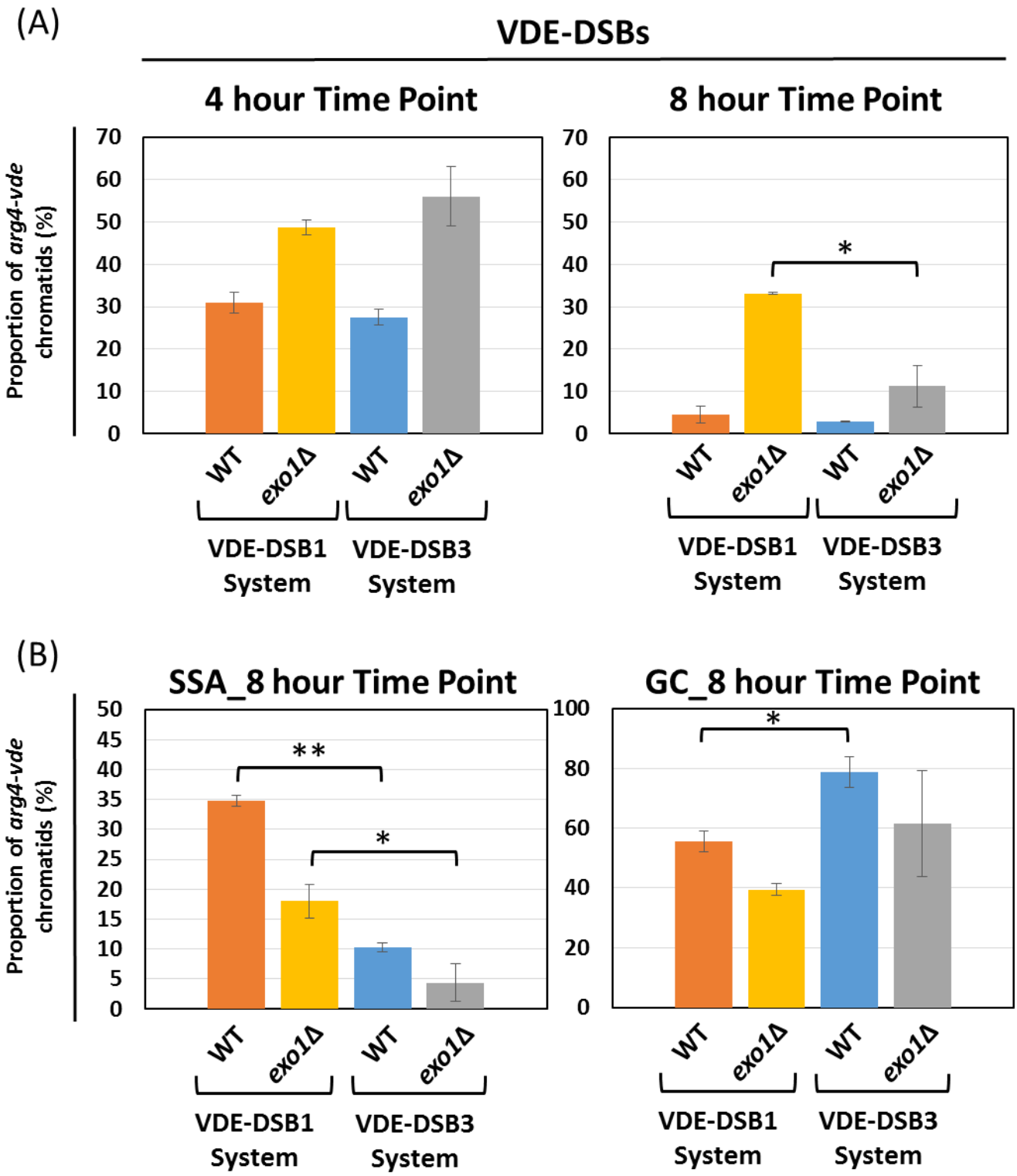


**Figure A7 Summary of wild-type and *exo1Δ* data in the VDE-DSB1 and 3 systems. (A)** Highlighting the VDE-DSB-formation phenotypes at 4h and 8h. It has shown that the VDE-DSB formation in these two systems are similar to each other, no matter under the WT or *exo1*Δ genetic backgrounds. However, the VDE-DSB1 of *exo1*Δ were accumulated more than the VDE-DSB3 at the end of meiosis time course. **(B)** Highlighting the repair products at 8h has shown that the VDE-DSB3 prefer to be repaired by short-range of resection that producing more GC products than the VDE-DSB1 repair. *, $p<0.05$; **, $p<0.01$. Duplicated experiments have been done.

# *Appendix VIII*

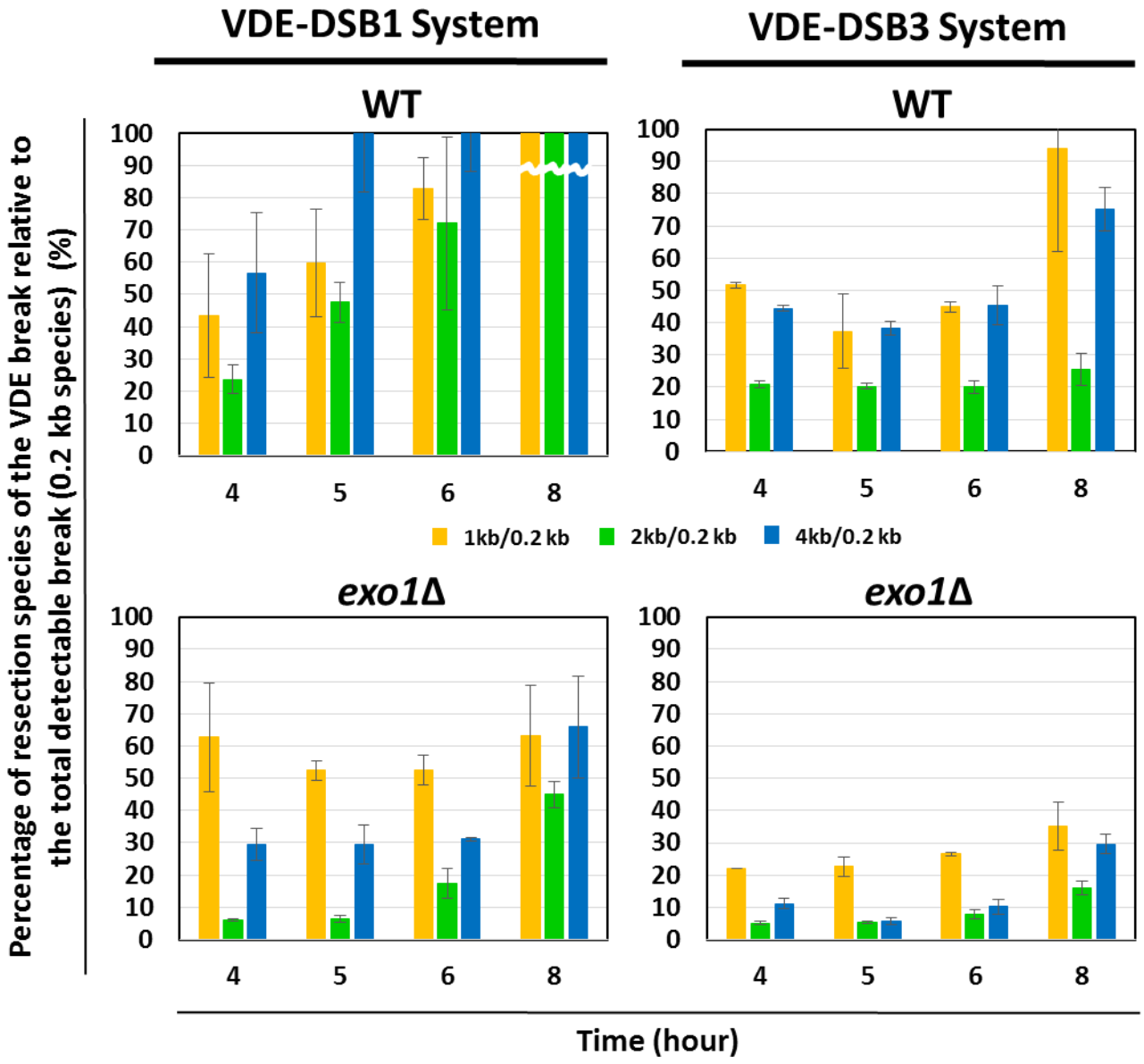


**Figure A8 Loss of RE site assay for revealing the resection tracts in both VDE-DSB3 and 1 systems.** In order to confirm whether the resection tracts of VDE-DSB3 are reduced due to the ~100% homology present between *arg4-vde* and *arg4-vde-VRS** chromatids, resulting in more GC products and less SSA products compared to the VDE-DSB1 turnover, we have calculated out the percentage of resection species of the VDE break relative to the total detectable break (0.2 kb species). In fact, the level of ssDNA with different resection tracts were decreased in the VDE-DSB3 repair compared to the VDE-DSB1 repair, no matter under the WT or *exo1*Δ genetic backgrounds. In addition, both in the VDE-DSB1 and 3 systems, *exo1*Δ mutants caused severe defect in producing ssDNA, especially the long-resected ssDNA. This is because Exo1 has an important role in resection, especially in the long range of resection. All together, these qPCR results increasing the possibility that the degree of homology between homologues chromosomes has impact on the range of meiotic resection. Duplicated experiments have been done.

# Appendix IX

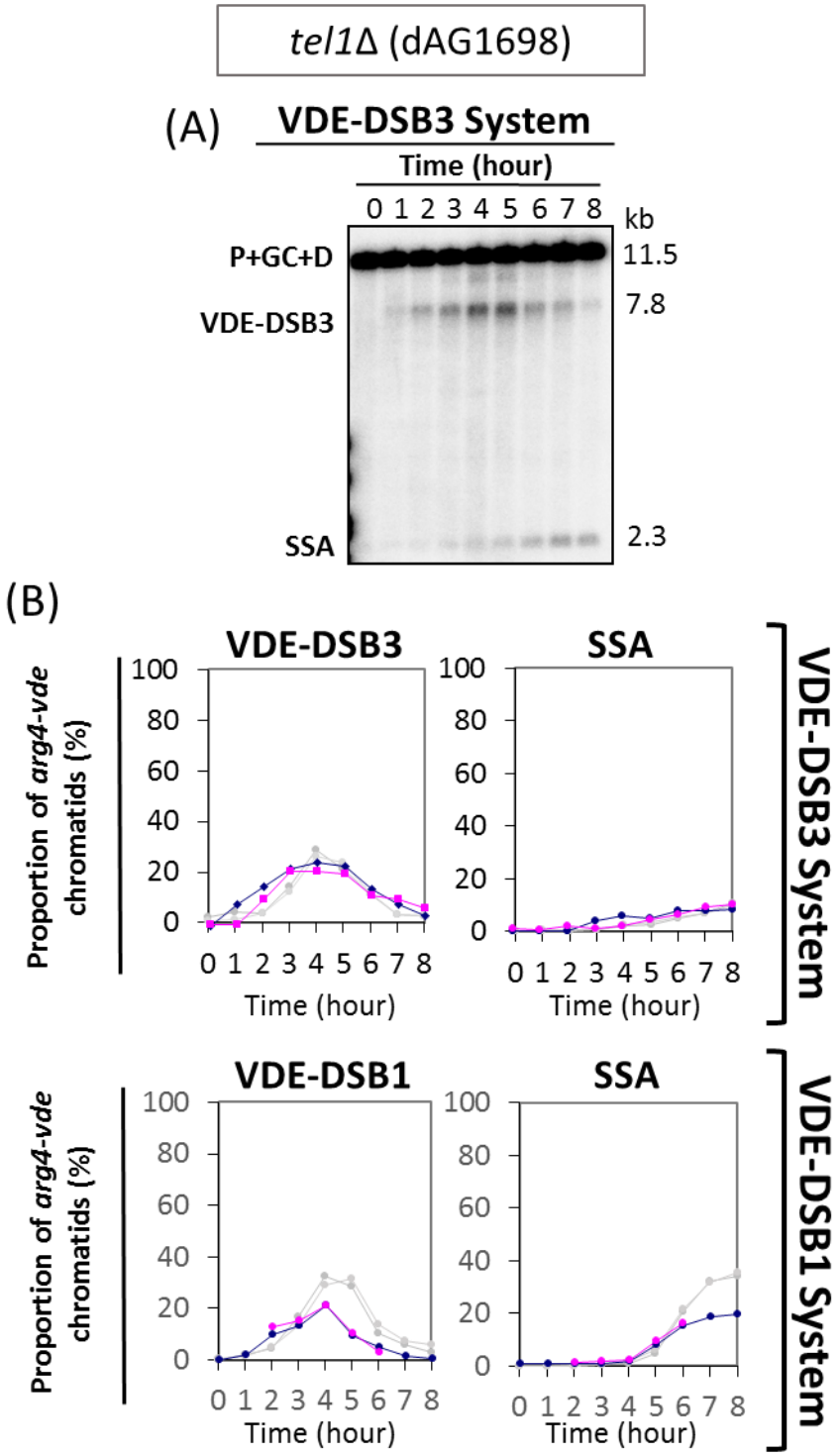


**Figure A9 Southern analysis of *tel1Δ* mutant strains within the VDE-DSB3 and 1 systems.** The legends of **(A)** and **(B)** here are same as Figure A5. The VDE-DSB3-turnover phenotype of *tel1*Δ was similar to its WT cells, whereas deleting *TEL1* in the VDE-DSB1 system caused sever effect on SSA repair, nearly a 50% of reduction compared to WT cells. This is due to lower homology present in VDE-DSB1 repair that needs longer resection to complete the DSB repair, namely by SSA. The data here further confirm the results from the VDE-DSB2 analysis that Tel1 indeed plays a role in processing the meiotic resection. Duplicated experiments have been done.

# *Appendix X*

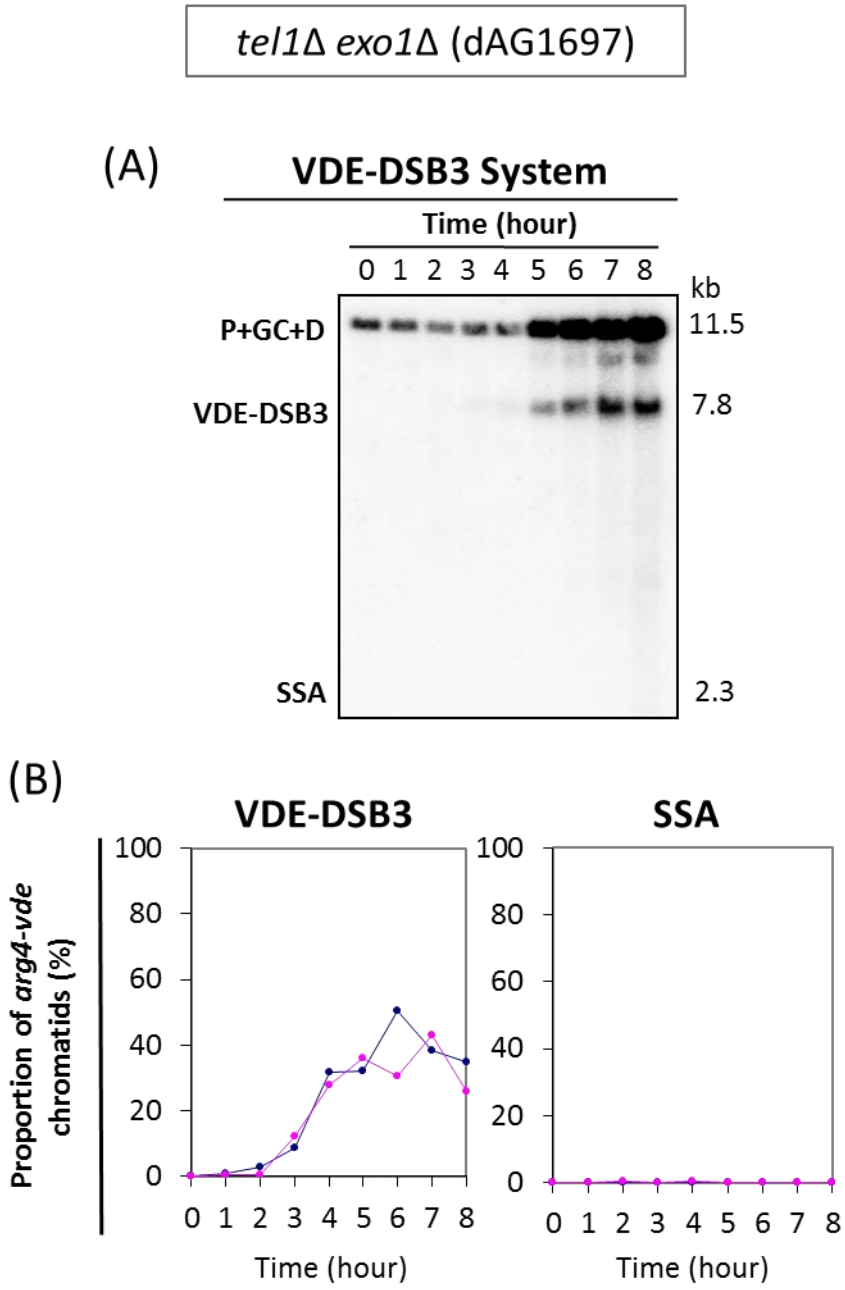


**Figure A10 Southern analysis of *tel1Δ exo1Δ* double mutant strains within the VDE-DSB3 system.** The legends of **(A)** and **(B)** here are same as Figure A5. Simultaneously deleting *TEL1* and *EXO1* genes caused the accumulation of VDE-DSB3 throughout the meiosis time course, and no SSA production. In addition, the repair phenotype of the *tel1Δ exo1Δ* double was much sever than its single mutants. It further suggests Tel1 indeed has a role in processing the meiotic resection that is independent of Exo1, and this resection process by Tel1 is presumably related to the nuclease function of Mre11. Duplicated experiments have been done.

# References

**Adams, A., Gottschling, D.E., Kaiser, C.A., and Stearns, T. (1997).** Methods in Yeast Genetics: A Cold Spring Harbor Laboratory Course Manual, 1997 Edition. Cold Spring Harbor Laboratory Press.

**Agarwal, S., and Roeder, G.S. (2000).** Zip3 provides a link between recombination enzymes and synaptonemal complex proteins. Cell *102(2)*, 245-255.

**Alani, E., Subbiah, S., and Kleckner, N. (1989).** The yeast RAD50 gene encodes a predicted 153-kD protein containing a purine nucleotide-binding domain and two large heptad-repeat regions. Genetics *122*, 47-57.

**Alberts, B., Johnson, A., Lewis, J., Raff, M., Roberts, K., and Walter, P. (2008).** Molecular Biology of the Cell, Fifth Edition. Copyright © Garland Science.

**Allers, T., and Lichten, M. (2000).** A method for preparing genomic DNA that restrains branch migration of Holliday junctions. Nucleic Acids Res *28*, e6.

**Allers, T., and Lichten, M. (2001a).** Differential timing and control of noncrossover and crossover recombination during meiosis. Cell *106*, 47-57.

**Allers, T., and Lichten, M. (2001b).** Intermediates of yeast meiotic recombination contain heteroduplex DNA. Mol Cell *8*, 225-231.

**Anderson, D.E., Trujillo, K.M., Sung, P., and Erickson, H.P. (2001).** Structure of the Rad50 x Mre11 DNA repair complex from Saccharomyces cerevisiae by electron microscopy. J Biol Chem *276*, 37027-37033.

**Aravind, L., Walker, D.R., and Koonin, E.V. (1999).** Conserved domains in DNA repair proteins and evolution of repair systems. Nucleic Acids Res *27*, 1223-1242.

**Arora, C., Kee, K., Maleki, S., and Keeney, S. (2004).** Antiviral protein Ski8 is a direct partner of Spo11 in meiotic DNA break formation, independent of its cytoplasmic role in RNA metabolism. Mol Cell *13*, 549-559.

**Ashton, N.W., Bolderson, E., Cubeddu, L., O'Byrne, K.J., and Richard, D.J. (2013).** Human single-stranded DNA binding proteins are essential for maintaining genomic stability. BMC Mol Biol *14*, 9.

**Bae, S.H., Bae, K.H., Kim, J.A., and Seo, Y.S. (2001).** RPA governs endonuclease switching during processing of Okazaki fragments in eukaryotes. Nature *412*, 456-461.

**Baroni, E., Viscardi, V., Cartagena-Lirola, H., Lucchini, G., and Longhese, M.P. (2004).** The functions of budding yeast Sae2 in the DNA damage response require Mec1- and Tel1-dependent phosphorylation. Mol Cell Biol *24*, 4151-4165.

**Baudrimont, A., Penkner, A., Woglar, A., Machacek, T., Wegrostek, C., Gloggnitzer,**

**J., Fridkin, A., Klein, F., Gruenbaum, Y., Pasierbek, P., *et al.* (2010).** Leptotene/zygotene chromosome movement via the SUN/KASH protein bridge in Caenorhabditis elegans. PLoS Genet *6*, e1001219.

**Bergerat, A., de Massy, B., Gadelle, D., Varoutas, P.C., Nicolas, A., and Forterre, P. (1997).** An atypical topoisomerase II from Archaea with implications for meiotic recombination. Nature *386*, 414-417.

**Bishop-Bailey, A. (2006).** Use of a unique reporter cassette to examine 5' to 3' resection at a site specific DMA double-strand break during meiosis. The University of Sheffield (Thesis for Doctor of Philosophy).

**Bishop, D.K., Park, D., Xu, L., and Kleckner, N. (1992).** DMC1: a meiosis-specific yeast homolog of E. coli recA required for recombination, synaptonemal complex formation, and cell cycle progression. Cell *69*, 439-456.

**Bishop, D.K., and Zickler, D. (2004).** Early decision; meiotic crossover interference prior to stable strand exchange and synapsis. Cell *117*, 9-15.

**Blat, Y., Protacio, R.U., Hunter, N., and Kleckner, N. (2002).** Physical and functional interactions among basic chromosome organizational features govern early steps of meiotic chiasma formation. Cell *111*, 791-802.

**Borde, V., Lin, W., Novikov, E., Petrini, J.H., Lichten, M., and Nicolas, A. (2004).** Association of Mre11p with double-strand break sites during yeast meiosis. Mol Cell *13*, 389-401.

**Borner, G.V., Kleckner, N., and Hunter, N. (2004).** Crossover/noncrossover differentiation, synaptonemal complex formation, and regulatory surveillance at the leptotene/zygotene transition of meiosis. Cell *117*, 29-45.

**Bremer, M.C., Gimble, F.S., Thorner, J., and Smith, C.L. (1992).** VDE endonuclease cleaves Saccharomyces cerevisiae genomic DNA at a single site: physical mapping of the VMA1 gene. Nucleic Acids Res *20*, 5484.

**Bressan, D.A., Olivares, H.A., Nelms, B.E., and Petrini, J.H. (1998).** Alteration of N-terminal phosphoesterase signature motifs inactivates Saccharomyces cerevisiae Mre11. Genetics *150*, 591-600.

**Carballo, J.A., Johnson, A.L., Sedgwick, S.G., and Cha, R.S. (2008).** Phosphorylation of the axial element protein Hop1 by Mec1/Tel1 ensures meiotic interhomolog recombination. Cell *132*, 758-770.

**Cartagena-Lirola, H., Guerini, I., Viscardi, V., Lucchini, G., and Longhese, M.P. (2006).** Budding Yeast Sae2 is an In Vivo Target of the Mec1 and Tel1 Checkpoint Kinases During Meiosis. Cell Cycle *5*, 1549-1559.

**Champoux, J.J. (2001).** DNA topoisomerases: structure, function, and mechanism. Annu Rev Biochem *70*, 369-413.

**Chen, J.M., Cooper, D.N., Chuzhanova, N., Ferec, C., and Patrinos, G.P. (2007).** Gene

conversion: mechanisms, evolution and human disease. Nat Rev Genet *8*, 762-775.

**Chen, L., Trujillo, K., Ramos, W., Sung, P., and Tomkinson, A.E. (2001).** Promotion of Dnl4-catalyzed DNA end-joining by the Rad50/Mre11/Xrs2 and Hdf1/Hdf2 complexes. Mol Cell *8*, 1105-1115.

**Cheng, Y.H., Chuang, C.N., Shen, H.J., Lin, F.M., and Wang, T.F. (2013).** Three distinct modes of Mec1/ATR and Tel1/ATM activation illustrate differential checkpoint targeting during budding yeast early meiosis. Mol Cell Biol *33*, 3365-3376.

**Choudhury, S.A., Asefa, B., Kauler, P., and Chow, T.Y. (2007).** Synergistic effect of TRM2/RNC1 and EXO1 in DNA double-strand break repair in Saccharomyces cerevisiae. Mol Cell Biochem *304*, 127-134.

**Chua, P.R., and Roeder, G.S. (1998).** Zip2, a meiosis-specific protein required for the initiation of chromosome synapsis. Cell *93(3)*, 349-359.

**Clerici, M., Mantiero, D., Guerini, I., Lucchini, G., and Longhese, M.P. (2008).** The Yku70-Yku80 complex contributes to regulate double-strand break processing and checkpoint activation during the cell cycle. EMBO Rep *9*, 810-818.

**Clerici, M., Mantiero, D., Lucchini, G., and Longhese, M.P. (2005).** The Saccharomyces cerevisiae Sae2 protein promotes resection and bridging of double strand break ends. J Biol Chem *280*, 38631-38638.

**Clerici, M., Mantiero, D., Lucchini, G., and Longhese, M.P. (2006).** The Saccharomyces cerevisiae Sae2 protein negatively regulates DNA damage checkpoint signalling. EMBO Rep *7*, 212-218.

**Connelly, J.C., and Leach, D.R. (2002).** Tethering on the brink: the evolutionarily conserved Mre11-Rad50 complex. Trends Biochem Sci *27*, 410-418.

**de Jager, M., van Noort, J., van Gent, D.C., Dekker, C., Kanaar, R., and Wyman, C. (2001).** Human Rad50/Mre11 is a flexible complex that can tether DNA ends. Mol Cell *8*, 1129-1135.

**De Massy, B., Baudat, F., and Nicolas, A. (1994).** Initiation of recombination in Saccharomyces cerevisiae haploid meiosis. Proc Natl Acad Sci U S A *91*, 11929-11933.

**Deng, C., Brown, J.A., You, D., and Brown, J.M. (2005).** Multiple endonucleases function to repair covalent topoisomerase I complexes in Saccharomyces cerevisiae. Genetics *170*, 591-600.

**Diaz, R.L., Alcid, A.D., Berger, J.M., and Keeney, S. (2002).** Identification of residues in yeast Spo11p critical for meiotic DNA double-strand break formation. Mol Cell Biol *22*, 1106-1115.

**Dong, H., and Roeder, G.S. (2000).** Organization of the yeast Zip1 protein within the central region of the synaptonemal complex. J Cell Biol *148*, 417-426.

EUROGENTEC qPCR guide.

**Falck, J., Coates, J., and Jackson, S.P. (2005).** Conserved modes of recruitment of ATM, ATR and DNA-PKcs to sites of DNA damage. Nature *434*, 605-611.

**Fishman-Lobell, J., Rudin, N., and Haber, J.E. (1992).** Two alternative pathways of double-strand break repair that are kinetically separable and independently modulated. Mol Cell Biol *12*, 1292-1303.

**Furuse, M., Nagase, Y., Tsubouchi, H., Murakami-Murofushi, K., Shibata, T., and Ohta, K. (1998).** Distinct roles of two separable in vitro activities of yeast Mre11 in mitotic and meiotic recombination. EMBO J *17*, 6412-6425.

**Garcia, V., Phelps, S.E., Gray, S., and Neale, M.J. (2011).** Bidirectional resection of DNA double-strand breaks by Mre11 and Exo1. Nature *479*, 241-244.

**Gimble, F.S., and Thorner, J. (1992).** Homing of a DNA endonuclease gene by meiotic gene conversion in Saccharomyces cerevisiae. Nature *357*, 301-306.

**Gravel, S., Chapman, J.R., Magill, C., and Jackson, S.P. (2008).** DNA helicases Sgs1 and BLM promote DNA double-strand break resection. Genes Dev *22*, 2767-2772.

**Gray, S., Allison, R.M., Garcia, V., Goldman, A.S., and Neale, M.J. (2013).** Positive regulation of meiotic DNA double-strand break formation by activation of the DNA damage checkpoint kinase Mec1(ATR). Open Biol *3*, 130019.

**Hassold, T., Hall, H., and Hunt, P. (2007).** The origin of human aneuploidy: where we have been, where we are going. Hum Mol Genet *16 Spec No. 2*, R203-208.

**Henderson, K.A., Kee, K., Maleki, S., Santini, P.A., and Keeney, S. (2006).** Cyclin-dependent kinase directly regulates initiation of meiotic recombination. Cell *125*, 1321-1332.

**Hirano, T. (2012).** Condensins: universal organizers of chromosomes with diverse functions. Genes Dev *26*, 1659-1678.

**Hirata, R., Ohsumk, Y., Nakano, A., Kawasaki, H., Suzuki, K., and Anraku, Y. (1990).** Molecular structure of a gene, VMA1, encoding the catalytic subunit of H(+)-translocating adenosine triphosphatase from vacuolar membranes of Saccharomyces cerevisiae. J Biol Chem *265*, 6726-6733.

**Hodgson, A., Terentyev, Y., Johnson, R.A., Bishop-Bailey, A., Angevin, T., Croucher, A., and Goldman, A.S. (2011).** Mre11 and Exo1 contribute to the initiation and processivity of resection at meiotic double-strand breaks made independently of Spo11. DNA Repair (Amst) *10*, 138-148.

**Hodgson, A.J. (2009).** Resection analysis of the VDE-DSB during meiosis. The University of Sheffield (Thesis for Doctor of Philosophy).

**Hopfner, K.P., Craig, L., Moncalian, G., Zinkel, R.A., Usui, T., Owen, B.A., Karcher, A., Henderson, B., Bodmer, J.L., McMurray, C.T.*, et al.* (2002).** The Rad50 zinc-hook is a structure joining Mre11 complexes in DNA recombination and repair. Nature *418*,

562-566.

**Hopfner, K.P., Karcher, A., Craig, L., Woo, T.T., Carney, J.P., and Tainer, J.A. (2001).** Structural biochemistry and interaction architecture of the DNA double-strand break repair Mre11 nuclease and Rad50-ATPase. Cell *105*, 473-485.

**Hopfner, K.P., Karcher, A., Shin, D.S., Craig, L., Arthur, L.M., Carney, J.P., and Tainer, J.A. (2000).** Structural biology of Rad50 ATPase: ATP-driven conformational control in DNA double-strand break repair and the ABC-ATPase superfamily. Cell *101*, 789-800.

**Huertas, P., Cortes-Ledesma, F., Sartori, A.A., Aguilera, A., and Jackson, S.P. (2008).** CDK targets Sae2 to control DNA-end resection and homologous recombination. Nature *455*, 689-692.

**Hunter, N., and Kleckner, N. (2001).** The single-end invasion: an asymmetric intermediate at the double-strand break to double-holliday junction transition of meiotic recombination. Cell *106*, 59-70.

**Jeggo, P.A. (1998).** Identification of genes involved in repair of DNA double-strand breaks in mammalian cells. Radiat Res *150*, S80-91.

**Johnson, R., Borde, V., Neale, M.J., Bishop-Bailey, A., North, M., Harris, S., Nicolas, A., and Goldman, A.S. (2007).** Excess single-stranded DNA inhibits meiotic double-strand break repair. PLoS Genet *3*, e223.

**Kane, P.M., Yamashiro, C.T., Wolczyk, D.F., Neff, N., Goebl, M., and Stevens, T.H. (1990).** Protein splicing converts the yeast TFP1 gene product to the 69-kD subunit of the vacuolar H(+)-adenosine triphosphatase. Science *250*, 651-657.

**Kane, S.M., and Roth, R. (1974).** Carbohydrate metabolism during ascospore development in yeast. J Bacteriol *118*, 8-14.

**Kee, K., Protacio, R.U., Arora, C., and Keeney, S. (2004).** Spatial organization and dynamics of the association of Rec102 and Rec104 with meiotic chromosomes. EMBO J *23*, 1815-1824.

**Keeney, S. (2001).** Mechanism and control of meiotic recombination initiation. Curr Top Dev Biol *52*, 1-53.

**Keeney, S., Giroux, C.N., and Kleckner, N. (1997).** Meiosis-specific DNA double-strand breaks are catalyzed by Spo11, a member of a widely conserved protein family. Cell *88*, 375-384.

**Klein, F., Mahr, P., Galova, M., Buonomo, S.B., Michaelis, C., Nairz, K., and Nasmyth, K. (1999).** A central role for cohesins in sister chromatid cohesion, formation of axial elements, and recombination during yeast meiosis. Cell *98(1)*, 91-103.

**Krejci, L., Damborsky, J., Thomsen, B., Duno, M., and Bendixen, C. (2001).** Molecular dissection of interactions between Rad51 and members of the recombination-repair group. Mol Cell Biol *21*, 966-976.

**Krejci, L., Song, B., Bussen, W., Rothstein, R., Mortensen, U.H., and Sung, P. (2002).** Interaction with Rad51 is indispensable for recombination mediator function of Rad52. J Biol Chem *277*, 40132-40141.

**Krogh, B.O., Llorente, B., Lam, A., and Symington, L.S. (2005).** Mutations in Mre11 phosphoesterase motif I that impair Saccharomyces cerevisiae Mre11-Rad50-Xrs2 complex stability in addition to nuclease activity. Genetics *171*, 1561-1570.

**Krogh, B.O., and Symington, L.S. (2004).** Recombination proteins in yeast. Annu Rev Genet *38*, 233-271.

**Lammens, K., Bemeleit, D.J., Mockel, C., Clausing, E., Schele, A., Hartung, S., Schiller, C.B., Lucas, M., Angermuller, C., Soding, J.*, et al.* (2011).** The Mre11:Rad50 structure shows an ATP-dependent molecular clamp in DNA double-strand break repair. Cell *145*, 54-66.

**Lee, S.E., Bressan, D.A., Petrini, J.H., and Haber, J.E. (2002).** Complementation between N-terminal Saccharomyces cerevisiae mre11 alleles in DNA repair and telomere length maintenance. DNA Repair (Amst) *1*, 27-40.

**Lee, S.E., Moore, J.K., Holmes, A., Umezu, K., Kolodner, R.D., and Haber, J.E. (1998).** Saccharomyces Ku70, mre11/rad50 and RPA proteins regulate adaptation to G2/M arrest after DNA damage. Cell *94*, 399-409.

**Leu, J.Y., Chua, P.R., and Roeder, G.S. (1998).** The Meiosis-Specific Hop2 Protein of S. cerevisiae Ensures Synapsis between Homologous Chromosomes. . Cell *94(3)*, 375-386.

**Lewis, L.K., Karthikeyan, G., Westmoreland, J.W., and Resnick, M.A. (2002).** Differential suppression of DNA repair deficiencies of Yeast rad50, mre11 and xrs2 mutants by EXO1 and TLC1 (the RNA component of telomerase). Genetics *160*, 49-62.

**Li, J., Hooker, G.W., and Roeder, G.S. (2006).** Saccharomyces cerevisiae Mer2, Mei4 and Rec114 form a complex required for meiotic double-strand break formation. Genetics *173*, 1969-1981.

**Lin, F.L., Sperle, K., and Sternberg, N. (1984).** Model for homologous recombination during transfer of DNA into mouse L cells: role for DNA ends in the recombination process. Mol Cell Biol *4*, 1020-1034.

**Lisby, M., Barlow, J.H., Burgess, R.C., and Rothstein, R. (2004).** Choreography of the DNA damage response: spatiotemporal relationships among checkpoint and repair proteins. Cell *118*, 699-713.

**Liu, C., Pouliot, J.J., and Nash, H.A. (2002).** Repair of topoisomerase I covalent complexes in the absence of the tyrosyl-DNA phosphodiesterase Tdp1. Proc Natl Acad Sci U S A *99*, 14970-14975.

**Liu, J.G., Yuan, L., Brundell, E., Bjorkroth, B., Daneholt, B., and Hoog, C. (1996).**

Localization of the N terminus of SCP1 to the central element of the synaptonemal complex and evidence for direct interactions between the N termini of SCP1 molecules organized head-to-head. Exp Cell Res *226*, 11–19.

**Llorente, B., and Symington, L.S. (2004).** The Mre11 nuclease is not required for 5' to 3' resection at multiple HO-induced double-strand breaks. Mol Cell Biol *24*, 9682-9694.

**Longhese, M.P., Bonetti, D., Manfrini, N., and Clerici, M. (2010).** Mechanisms and regulation of DNA end resection. EMBO J *29*, 2864-2874.

**Longhese, M.P., Guerini, I., Baldo, V., and Clerici, M. (2008).** Surveillance mechanisms monitoring chromosome breaks during mitosis and meiosis. DNA Repair (Amst) *7*, 545-557.

**Longhese, M.P., Mantiero, D., and Clerici, M. (2006).** The cellular response to chromosome breakage. Mol Microbiol *60*, 1099-1108.

**Longtine, M.S., McKenzie, A., 3rd, Demarini, D.J., Shah, N.G., Wach, A., Brachat, A., Philippsen, P., and Pringle, J.R. (1998).** Additional modules for versatile and economical PCR-based gene deletion and modification in Saccharomyces cerevisiae. Yeast *14*, 953-961.

**Lydall, D., Nikolsky, Y., Bishop, D.K., and Weinert, T. (1996).** A meiotic recombination checkpoint controlled by mitotic checkpoint genes. Nature *383*, 840-843.

**Lydeard, J.R., Jain, S., Yamaguchi, M., and Haber, J.E. (2007).** Break-induced replication and telomerase-independent telomere maintenance require Pol32. Nature *448*, 820-823.

**Majka, J., Alford, B., Ausio, J., Finn, R.M., and McMurray, C.T. (2012).** ATP hydrolysis by RAD50 protein switches MRE11 enzyme from endonuclease to exonuclease. J Biol Chem *287*, 2328-2341.

**Malone, R.E., Haring, S.J., Foreman, K.E., Pansegrau, M.L., Smith, S.M., Houdek, D.R., Carpp, L., Shah, B., and Lee, K.E. (2004).** The signal from the initiation of meiotic recombination to the first division of meiosis. Eukaryot Cell *3(3)*, 598-609.

**Manfrini, N., Guerini, I., Citterio, A., Lucchini, G., and Longhese, M.P. (2010).** Processing of meiotic DNA double strand breaks requires cyclin-dependent kinase and multiple nucleases. J Biol Chem *285*, 11628-11637.

**Mantiero, D., Clerici, M., Lucchini, G., and Longhese, M.P. (2007).** Dual role for Saccharomyces cerevisiae Tel1 in the checkpoint response to double-strand breaks. EMBO Rep *8*, 380-387.

**Maryon, E., and Carroll, D. (1991).** Characterization of recombination intermediates from DNA injected into Xenopus laevis oocytes: evidence for a nonconservative mechanism of homologous recombination. Mol Cell Biol *11*, 3278-3287.

**McKee, A.H., and Kleckner, N. (1997).** A general method for identifying recessive diploid-specific mutations in Saccharomyces cerevisiae, its application to the isolation of mutants blocked at intermediate stages of meiotic prophase and characterization of a new gene SAE2. Genetics *146*, 797-816.

**Meuwissen, R.L.J., Offenberg, H.H., Dietrich, A.J.J., Riesewijk, A., van Iersel, M., and Heyting, C. (1992).** A coiled-coil related protein specific for synapsed regions of meiotic prophase chromosomes. EMBO J *11(13)*, 5091-5100.

**Mimitou, E.P., and Symington, L.S. (2008).** Sae2, Exo1 and Sgs1 collaborate in DNA double-strand break processing. Nature *455*, 770-774.

**Mimitou, E.P., and Symington, L.S. (2009).** DNA end resection: many nucleases make light work. DNA Repair (Amst) *8*, 983-995.

**Mimitou, E.P., and Symington, L.S. (2011).** DNA end resection--unraveling the tail. DNA Repair (Amst) *10*, 344-348.

**Mockel, C., Lammens, K., Schele, A., and Hopfner, K.P. (2012).** ATP driven structural changes of the bacterial Mre11:Rad50 catalytic head complex. Nucleic Acids Res *40*, 914-927.

**Molnar, M., Bahler, J., Sipiczki, M., and Kohli, J. (1995).** The rec8 gene of Schizosaccharomyces pombe is involved in linear element formation, chromosome pairing and sister chromatid cohesion during meiosis. Genetics *141*, 61–73.

**Moreau, S., Ferguson, J.R., and Symington, L.S. (1999).** The nuclease activity of Mre11 is required for meiosis but not for mating type switching, end joining, or telomere maintenance. Mol Cell Biol *19*, 556-566.

**Moreau, S., Morgan, E.A., and Symington, L.S. (2001).** Overlapping functions of the Saccharomyces cerevisiae Mre11, Exo1 and Rad27 nucleases in DNA metabolism. Genetics *159*, 1423-1433.

**Moynahan, M.E., and Jasin, M. (2010).** Mitotic homologous recombination maintains genomic stability and suppresses tumorigenesis. Nat Rev Mol Cell Biol *11*, 196-207.

**Nagai, Y., Nogami, S., Kumagai-Sano, F., and Ohya, Y. (2003).** Karyopherin-mediated nuclear import of the homing endonuclease VMA1-derived endonuclease is required for self-propagation of the coding region. Mol Cell Biol *23*, 1726-1736.

**Nairz, K., and Klein, F. (1997).** mre11S--a yeast mutation that blocks double-strand-break processing and permits nonhomologous synapsis in meiosis. Genes Dev *11*, 2272-2290.

**Nakada, D., Hirano, Y., and Sugimoto, K. (2004).** Requirement of the Mre11 complex and exonuclease 1 for activation of the Mec1 signaling pathway. Mol Cell Biol *24*, 10016-10025.

**Nakada, D., Matsumoto, K., and Sugimoto, K. (2003).** ATM-related Tel1 associates

with double-strand breaks through an Xrs2-dependent mechanism. Genes Dev *17*, 1957-1962.

**Navadgi-Patil, V.M., and Burgers, P.M. (2009).** A tale of two tails: activation of DNA damage checkpoint kinase Mec1/ATR by the 9-1-1 clamp and by Dpb11/TopBP1. DNA Repair (Amst) *8*, 996-1003.

**Neale, M.J. (2002).** Examining the Role of Spo11-induced DNA Double-strand Breaks on the Regulation of Recombination During Meiosis. The University of Sheffield (Thesis for Doctor of Philosophy).

**Neale, M.J., Pan, J., and Keeney, S. (2005).** Endonucleolytic processing of covalent protein-linked DNA double-strand breaks. Nature *436*, 1053-1057.

**Nimonkar, A.V., Ozsoy, A.Z., Genschel, J., Modrich, P., and Kowalczykowski, S.C. (2008).** Human exonuclease 1 and BLM helicase interact to resect DNA and initiate DNA repair. Proc Natl Acad Sci U S A *105*, 16906-16911.

**Nishant, K.T., Chen, C., Shinohara, M., Shinohara, A., and Alani, E. (2010).** Genetic analysis of baker's yeast Msh4-Msh5 reveals a threshold crossover level for meiotic viability. PLoS Genet *6*.

**Nordlund, M.E., Johansson, J.O., von Pawel-Rammingen, U., and Bystrom, A.S. (2000).** Identification of the TRM2 gene encoding the tRNA(m5U54)methyltransferase of Saccharomyces cerevisiae. RNA *6*, 844-860.

**Palmbos, P.L., Wu, D., Daley, J.M., and Wilson, T.E. (2008).** Recruitment of Saccharomyces cerevisiae Dnl4-Lif1 complex to a double-strand break requires interactions with Yku80 and the Xrs2 FHA domain. Genetics *180*, 1809-1819.

**Panizza, S., Mendoza, M.A., Berlinger, M., Huang, L., Nicolas, A., Shirahige, K., and Klein, F. (2011).** Spo11-accessory proteins link double-strand break sites to the chromosome axis in early meiotic recombination. Cell *146*, 372-383.

**Perler, F.B., Davis, E.O., Dean, G.E., Gimble, F.S., Jack, W.E., Neff, N., Noren, C.J., Thorner, J., and Belfort, M. (1994).** Protein splicing elements: inteins and exteins--a definition of terms and recommended nomenclature. Nucleic Acids Res *22*, 1125-1127.

**Peters, J.M., Tedeschi, A., and Schmitz, J. (2008).** The cohesin complex and its roles in chromosome biology. Genes Dev *22*, 3089-3114.

**Petes, T.D., Malone, R.E., and Symington, L.S. (1991).** Recombination in yeast, In Genome dynamics, protein synthesis and energetics, J. R. Broach, E. Jones, and J. Pringle, eds. . New York: Cold Spring Harbor Laboratory Press, 407-521.

**Prieler, S., Penkner, A., Borde, V., and Klein, F. (2005).** The control of Spo11's interaction with meiotic recombination hotspots. Genes Dev *19(2)*, 255-269.

**Prinz, S., Amon, A., and Klein, F. (1997).** Isolation of COM1, a new gene required to complete meiotic double-strand break-induced recombination in Saccharomyces

cerevisiae. Genetics *146*, 781-795.

**Rattray, A.J., McGill, C.B., Shafer, B.K., and Strathern, J.N. (2001).** Fidelity of mitotic double-strand-break repair in Saccharomyces cerevisiae: a role for SAE2/COM1. Genetics *158*, 109-122.

**Roeder, G.S. (1997).** Meiotic chromosomes: it takes two to tango. Genes Dev *11*, 2600-2621.

**Roeder, G.S., and Bailis, J.M. (2000).** The pachytene checkpoint. Trends Genet *16*, 395-403.

**Sasanuma, H., Murakami, H., Fukuda, T., Shibata, T., Nicolas, A., and Ohta, K. (2007).** Meiotic association between Spo11 regulated by Rec102, Rec104 and Rec114. Nucleic Acids Res *35*, 1119-1133.

**Scherthan, H. (2001).** A bouquet makes ends meet. Nat Rev Mol Cell Biol *2*, 621-627.

**Schmekel, K., Wahrman, J., Skoglund, U., and Daneholt, B. (1993).** The central region of the synaptonemal complex in Blaps cribrosa studied by electron microscope tomography. Chromosoma *102(10)*, 669-681.

**Sharples, G.J., and Leach, D.R. (1995).** Structural and functional similarities between the SbcCD proteins of Escherichia coli and the RAD50 and MRE11 (RAD32) recombination and repair proteins of yeast. Mol Microbiol *17*, 1215-1217.

**Shim, E.Y., Chung, W.H., Nicolette, M.L., Zhang, Y., Davis, M., Zhu, Z., Paull, T.T., Ira, G., and Lee, S.E. (2010).** Saccharomyces cerevisiae Mre11/Rad50/Xrs2 and Ku proteins regulate association of Exo1 and Dna2 with DNA breaks. EMBO J *29*, 3370-3380.

**Shinohara, A., Ogawa, H., Matsuda, Y., Ushio, N., Ikeo, K., and Ogawa, T. (1993).** Cloning of human, mouse and fission yeast recombination genes homologous to RAD51 and recA. Nat Genet *4*, 239-243.

**Shinohara, A., Shinohara, M., Ohta, T., Matsuda, S., and Ogawa, T. (1998).** Rad52 forms ring structures and co-operates with RPA in single-strand DNA annealing. Genes Cells *3*, 145-156.

**Shuster, E.O., and Byers, B. (1989).** Pachytene arrest and other meiotic effects of the start mutations in Saccharomyces cerevisiae. Genetics *123*, 29-43.

**Solinger, J.A., and Heyer, W.D. (2001).** Rad54 protein stimulates the postsynaptic phase of Rad51 protein-mediated DNA strand exchange. Proc Natl Acad Sci U S A *98*, 8447-8453.

**Solinger, J.A., Kiianitsa, K., and Heyer, W.D. (2002).** Rad54, a Swi2/Snf2-like recombinational repair protein, disassembles Rad51:dsDNA filaments. Mol Cell *10*, 1175-1188.

**Song, B., and Sung, P. (2000).** Functional interactions among yeast Rad51

recombinase, Rad52 mediator, and replication protein A in DNA strand exchange. J Biol Chem *275*, 15895-15904.

**Stasiak, A.Z., Larquet, E., Stasiak, A., Muller, S., Engel, A., Van Dyck, E., West, S.C., and Egelman, E.H. (2000).** The human Rad52 protein exists as a heptameric ring. Curr Biol *10*, 337-340.

**Stracker, T.H., and Petrini, J.H. (2011).** The MRE11 complex: starting from the ends. Nat Rev Mol Cell Biol *12*, 90-103.

**Sugiyama, T., and Kowalczykowski, S.C. (2002).** Rad52 protein associates with replication protein A (RPA)-single-stranded DNA to accelerate Rad51-mediated displacement of RPA and presynaptic complex formation. J Biol Chem *277*, 31663-31672.

**Sun, H., Treco, D., and Szostak, J.W. (1991).** Extensive 3'-overhanging, single-stranded DNA associated with the meiosis-specific double-strand breaks at the ARG4 recombination initiation site. Cell *64*, 1155-1161.

**Sung, P., and Klein, H. (2006).** Mechanism of homologous recombination: mediators and helicases take on regulatory functions. Nat Rev Mol Cell Biol *7*, 739-750.

**Sym, M., Engebrecht, J.A., and Roeder, G.S. (1993).** ZIP1 is a synaptonemal complex protein required for meiotic chromosome synapsis. Cell *72(3)*, 365-378.

**Sym, M., and Roeder, G.S. (1995).** Zip1-induced changes in synaptonemal complex structure and polycomplex assembly. . J Cell Biol *128(4)*, 455-466.

**Symington, L.S. (2002).** Role of RAD52 epistasis group genes in homologous recombination and double-strand break repair. Microbiol Mol Biol Rev *66*, 630-670, table of contents.

**Thacker, D., and Keeney, S. (2009).** PCH'ing together an understanding of crossover control. PLoS Genet *5*, e1000576.

**Tsubouchi, H., and Ogawa, H. (1998).** A novel mre11 mutation impairs processing of double-strand breaks of DNA during both mitosis and meiosis. Mol Cell Biol *18*, 260-268.

**Tsubouchi, H., and Ogawa, H. (2000).** Exo1 roles for repair of DNA double-strand breaks and meiotic crossing over in Saccharomyces cerevisiae. Mol Biol Cell *11*, 2221-2233.

**Tsubouchi, H., and Roeder, G.S. (2003).** The importance of genetic recombination for fidelity of chromosome pairing in meiosis. Dev Cell *5*, 915-925.

**Tsukamoto, Y., Mitsuoka, C., Terasawa, M., Ogawa, H., and Ogawa, T. (2005).** Xrs2p regulates Mre11p translocation to the nucleus and plays a role in telomere elongation and meiotic recombination. Mol Biol Cell *16*, 597-608.

**Tung, K.S., and Roeder, G.S. (1998).** Meiotic chromosome morphology and behavior in zip1 mutants of Saccharomyces cerevisiae. Genetics *149(2)*, 817-832.

**Usui, T., Ogawa, H., and Petrini, J.H. (2001).** A DNA damage response pathway controlled by Tel1 and the Mre11 complex. Mol Cell *7*, 1255-1266.

**Usui, T., Ohta, T., Oshiumi, H., Tomizawa, J., Ogawa, H., and Ogawa, T. (1998).** Complex formation and functional versatility of Mre11 of budding yeast in recombination. Cell *95*, 705-716.

**Wan, L., de los Santos, T., Zhang, C., Shokat, K., and Hollingsworth, N.M. (2004).** Mek1 kinase activity functions downstream of RED1 in the regulation of meiotic double strand break repair in budding yeast. Mol Biol Cell *15(1)*, 11-23.

**Wan, L., Niu, H., Futcher, B., Zhang, C., Shokat, K.M., Boulton, S.J., and Hollingsworth, N.M. (2008).** Cdc28-Clb5 (CDK-S) and Cdc7-Dbf4 (DDK) collaborate to initiate meiotic recombination in yeast. Genes Dev *22*, 386-397.

**Wang, J.C. (1991).** DNA topoisomerases: why so many? J Biol Chem *266*, 6659-6662.

**White, C.I., and Haber, J.E. (1990).** Intermediates of recombination during mating type switching in Saccharomyces cerevisiae. EMBO J *9*, 663-673.

**Wiltzius, J.J., Hohl, M., Fleming, J.C., and Petrini, J.H. (2005).** The Rad50 hook domain is a critical determinant of Mre11 complex functions. Nat Struct Mol Biol *12*, 403-407.

**Woltering, D., Baumgartner, B., Bagchi, S., Larkin, B., Loidl, J., de los Santos, T., and Hollingsworth, N.M. (2000).** Meiotic segregation, synapsis, and recombination checkpoint functions require physical interaction between the chromosomal proteins Red1p and Hop1p. Mol Cell Biol *20(18)*, 6646-6658.

**Wood, A.J., Severson, A.F., and Meyer, B.J. (2010).** Condensin and cohesin complexity: the expanding repertoire of functions. Nat Rev Genet *11*, 391-404.

**Wu, D., Topper, L.M., and Wilson, T.E. (2008).** Recruitment and dissociation of nonhomologous end joining proteins at a DNA double-strand break in Saccharomyces cerevisiae. Genetics *178*, 1237-1249.

**You, Z., Chahwan, C., Bailis, J., Hunter, T., and Russell, P. (2005).** ATM activation and its recruitment to damaged DNA require binding to the C terminus of Nbs1. Mol Cell Biol *25*, 5363-5379.

**Zhang, Y., Hefferin, M.L., Chen, L., Shim, E.Y., Tseng, H.M., Kwon, Y., Sung, P., Lee, S.E., and Tomkinson, A.E. (2007).** Role of Dnl4-Lif1 in nonhomologous end-joining repair complex assembly and suppression of homologous recombination. Nat Struct Mol Biol *14*, 639-646.

**Zhu, Z., Chung, W.H., Shim, E.Y., Lee, S.E., and Ira, G. (2008).** Sgs1 helicase and two nucleases Dna2 and Exo1 resect DNA double-strand break ends. Cell *134*, 981-994.

**Zickler, D., and Kleckner, N. (1998).** The leptotene-zygotene transition of meiosis. Annu Rev Genet *32*, 619-697.

**Zickler, D., and Kleckner, N. (1999).** Meiotic chromosomes: integrating structure and

function. Annu Rev Genet *33*, 603-754.

**Zierhut, C., Berlinger, M., Rupp, C., Shinohara, A., and Klein, F. (2004).** Mnd1 is required for meiotic interhomolog repair. Curr Biol *14(9)*, 752-762.

**Zou, L., and Elledge, S.J. (2003).** Sensing DNA damage through ATRIP recognition of RPA-ssDNA complexes. Science *300*, 1542-1548.

**Website:**

National Human Genome Research Institute/NHGRI, last reviewed: May 16th, 2010: http://www.genome.gov/10000510#top